CHARACTERIZING CONTAMINATION TO EXPAND ASHRAE ENVELOPE IN AIRSIDE ECONOMIZATION AND THERMAL AND RELIABILITY IN IMMERSION COOLING OF DATA CENTERS

by

JIMIL MANOJBHAI SHAH

Presented to the Faculty of the Graduate School of

The University of Texas at Arlington in Partial Fulfillment

of the Requirements

for the Degree of

DOCTOR OF PHILOSOPHY

THE UNIVERSITY OF TEXAS AT ARLINGTON

August 2018

Supervising Committee:

Dr. Dereje Agonafer, (Supervising Professor)

Dr. Abdolhossein Haji-Sheikh

Dr. Prabjit Singh

Dr. Zeynep Çelik-Butler

Dr. Miguel Amaya

Acknowledgements

Thank you Lord for giving me the strength and courage through the years to achieve my dream, without you nothing would have been possible for me to accomplish. During this journey, I came to realize that only God Himself would have all the answers that the human race is seeking. Nevertheless, as an engineer, a scientist, it is my obligation to constantly challenge the laws created by man because these laws were created mostly out of desperation or limitation of human's endeavors, and should not be taken as the "Word of God"; otherwise, the human race is going to be doomed by what we believe is the inevitable truth.

I want to thank my advisor Dr. Dereje Agonafer for believing in me and giving me a chance of a lifetime. His wisdom, knowledge, and dedication to his profession have been a great example for me. I would like to thank my committee members Dr. Haji-Sheikh, Dr. Singh, Dr. Celik-Butler and Dr. Amaya for their valuable advises and their times spent reviewing my work. I would like to thank NSF IUCRC IAB committee for introducing such projects and all the mentors for their valuable feedback on my work. I would like to thank Dr. Prabjit Singh, IBM who was a torch bearer for me in this project related to contamination in data centers. Special thanks to my mentors in India, Ujjwell Trivedi, ITM and Dr. Akash Pandey, MSU for supporting me in each and every step of my life.

Most of all, I want to thank my lovely wife Diana Siddhi H. Shah, who always believes that I can rope the moon, and inspires me to achieve the impossible. I also want to thank my parents Mrs. Muktiben M. Shah and Mr. Manojbhai N. Shah for their sacrifices, my sister Dr. Preksha S. Shah, my brother-in-law Mr. Sapan P. Shah, my lovely niece Miska, my in-laws Mrs. Hinaben H. Shah and Mr. Hemantbhai C. Shah, and my brother-in-law Mr. Yash H. Shah for their unconditional love and support. I want to

thank my colleagues at the EMNSPC, the staff at the Mechanical and Aerospace Engineering Department, Sally Thompson, Flora Pinegar, Delania Gordon and Debi Barton for all their help and supports through my academic years.

August 09, 2018

I would like to dedicate my PhD Dissertation

To

My grandparents

Late Mr. Nandlal M. Shah, Late Mrs. Kamlaben N. Shah, Late Mr. Chandulal M. Shah and Mrs. Pushpaben C. Shah

who made me what I am today.

My parents

For their love, endless support and encouragement.

My role model, my Sister

Whom I always wanted to chase in the race of knowledge but after every 5 years of trying she was always 5 years ahead of me, which made me keep working hard forever in my life. This always kept me on ground reminding me there will always be someone superior than you.

My loving wife

who always stood by me in ups and downs of my life and encouraged me to achieve the point at which I'm standing.

August 09, 2018

Abstract

CHARACTERIZING CONTAMINATION TO EXPAND ASHRAE ENVELOPE IN AIRSIDE ECONOMIZATION AND THERMAL AND RELIABILITY IN IMMERSION COOLING OF DATA CENTERS

Jimil Manojbhai Shah, PhD

The University of Texas at Arlington, 2018

Supervising Professor: Dereje Agonafer

The Datacom facility which comprises rooms or closets used for communication, computers/servers or electronic equipment requires cooling unit which consumes 31% (23% HVAC cooling + 8% HVAC fans) of overall energy. The ASHRAE TC9.9 subcommittee, on Mission Critical Facilities, Data Centers, Technology Spaces, and Electronic Equipment, has suited the data center's executives by permitting brief period outings of the environmental conditions outside the prescribed temperature-humidity range, into passable extents A1-A3. To comprehend the expanding server densities and the required cooling vitality costs, data center operators are falling back on cost cutting measures. For instance, they are not firmly controlling the temperature and humidity levels as per ASHRAE recommended envelope and as a rule turning to airside economizers with the related danger of bringing particulate and gaseous contaminants into their data centers. This dissertation is a first attempt at addressing this challenge by characterizing contamination found in a real-world data center to expand ASHRAE envelope. In situ studies of contaminants found in data centers using air-side economization and corresponding ASHRAE Envelope Expansion in Airside Economization is the main objective of this PhD Dissertation. This study serves several purposes: 1.) Cumulative corrosion damage study for the correlation of equipment

reliability to levels of airborne corrosive contaminants and the study of the degree of reliability degradation, when the equipment is operated, outside the recommended range, in the allowable temperature-humidity range in geographies with high levels of gaseous and particulate contamination. 2.) Experimental description of information technology equipment reliability exposed to a data center using airside economizer operating in recommended and allowable ASHRAE envelopes in an ANSI/ISA classified G2 environment to estimate the end of the life of the components and to determine the free air cooling hours for the site. The study took place at the modular data center which uses air-side economizer located at Dallas Industrial area which falls under ISA 71.04-2013 severity level G2. 3.) The servers were removed, and qualitative study of cumulative corrosion damage was carried out. The particulate contaminants were collected from different locations of a server and material characterization was performed using Scanning Electron Microscopy (SEM), Energy Dispersive Spectrometer (EDS) and Fourier Transform Infrared Spectroscopy (FTIR). The analysis from these results helps to explain the impact of the contaminants on IT equipment reliability. 4.) To develop a precise and cost-effective technique to measure deliquescent relative humidity of particulate contaminants found in a data center utilizing airside economization. To develop an experimental technique to measure the DRH of dust particles by logging the leakage current versus %RH for the particulate matter dispensed on an interdigitated comb coupon. To validate this methodology, the DRH of pure salts like $MgCl_2$, NH_4NO_3 and NaCl is determined and their results are then compared with their published values. This methodology can therefore be implemented to help lay a modus operandi of establishing the limiting value or an effective relative humidity envelope to be maintained at a real-world data center facility for its continuous and reliable operation at its respective location. 5.) The interdigitated comb coupon is lodged with a dust solution in

the form of slurry taken from various servers in an actual modular Data Center. The results obtained, and the methodology used in this study can pioneer in standardizing the limiting %RH values for various operating conditions in real world Data Centers, and 6.) This dissertation also examines the flow path of contaminants in high density data centers to determine the most vulnerable location using the computational techniques.

Full submersion of servers in dielectric oils offers an opportunity for significant cooling energy savings and increased power densities for data centers. The enhanced thermal properties of oil can lead to considerable savings in both the upfront and operating costs over traditional air cooling methods. Despite recent findings showing the improved cooling efficiency and cost savings of cooling fluids, this technique is still not widely adopted. Many uncertainties and concerns persist regarding the non-thermal aspects of a single-phase immersion cooled data center. This study serves multiple purposes: 1.) To measure the thermal performance of a single-phase immersion cooled server at extreme temperatures for prolonged time. Thermal overstress experiment was performed on a fully immersed server and its cooling system components. This work explores the performance of a server and other components like pump including flow rate drop, starting trouble and other potential issues under extreme climatic conditions. 2.) The dissertation presents impact of form factor on a maximum junction temperature and thermal resistance at the server level. This work is to provide an insight to increase the rack density by reducing form factor of an existing server. The heat sink is a critical part for cooling effectiveness at server level. This work is to provide an efficient range of operation for heat sink with numerical and computational modelling of a third-generation open compute server for immersion cooling application. A parametric study is conducted, and the thermal efficiency has been optimized for mineral oil and EC 100. 3.) This research reviews the changes in physical and chemical properties of information

technology (IT) equipment and compatibility of materials like polyvinyl chloride (PVC), printed circuit board (PCB) and switching devices with mineral oil and EC 100 to characterize the interconnect reliability of materials. For the first time, material compatibility is being tested. Accelerated thermal degradation testing of printed circuit board, passive components and optical fibers for single phase immersion cooling systems is a significant part of this study. The study proposes a testing methodology which can be adopted by all for evaluating the reliability of electronic packages and components when immersed in a dielectric fluid. The study indicates the effect of mineral oil and EC 100 on IT equipment reliability and reliability enhancements for immersion cooled data centers and, 4.) This dissertation also includes Cup Burner Experiment as per ISO 14520/NFPA 2001 standard to determine the minimum design concentration of fire extinguishing agent for the class B hazard of heavy mineral oil and the class C hazard of electronic equipment as a part of the safety concerns for oil cooled data centers.

Table of Contents

List of Illustrations

List of Tables

Chapter 1

Introduction

Behind the scenes of the internet services (search, email, social networks, etc.) that have become so pervasive in everyday life are data centers. Data centers are facilities that house the computing, storage, and networking equipment that serve the Information Technology (IT) needs of modern society. Almost all industries, ranging from health care, finance, government, entertainment, to enterprise businesses rely on these services. Data center facilities range in size from a few hundred square feet to over one million square feet. The environment inside data centers differs from other facilities which are built for human comfort or industrial use. Rows of racks filled with IT equipment (ITE) occupy the floor space, as seen in Figure 1-1, with much higher power density than traditional spaces. Compared to typical office buildings, schools, and commercial buildings, the power (Watts) consumed per square foot of floor space in a data center can be as much as an order of magnitude higher. These high power densities present several challenges from power delivery, cooling infrastructure, and financial perspectives. Industry trends of increasing power density to maximize productivity per square foot of floor space only exacerbate these problems. With the continued increase in demand for information technology services, all of these topics are areas of active research. The focus of this work is on evaluating more energy efficient approaches for the cooling of ITE and represents a possible paradigm shift in how data centers, especially those with high power densities, are designed and operated. The first portion of this work seeks to modify and improve traditional air cooling methods of servers at the chassis and rack level. The second part involves complete immersion of ITE into an electrically nonconductive mineral oil which circulates at a low flow rate to remove heat. An initial evaluation on the possible impact of this fluid on the mechanical reliability and operability of ITE is also considered.

Figure 1-1 Typical interior floor space of a large data center

1.1 Data Center Power and Cooling Trends

Rapidly increasing demand for IT services led to a 56% increase in total electricity used by data centers globally over the five year period from 2005 to 2010 [1]. As an industry, data centers accounted for an estimated 1.7% to 2.2% of the total electricity used in the US and 1.1% to 1.5% globally in 2010 [1]. These numbers are expected to rise with the persistent growth of the industry. Such large proportions of energy consumed by a single industry have raised concerns over efficiencies and the sources from which they receive electrical energy.

The standard metric for gauging the overall efficiency of a data center is power usage effectiveness (PUE) which was developed by the Green Grid in 2008 [2] [3]. PUE determines efficiency by dividing total power consumed by the data center by the power consumed by IT load. IT load is considered the useful work of the data center facility. Mathematically, this metric is expressed as:

$$PUE = \frac{Total\ Facility\ Power}{IT\ Equipment\ Power} \quad (1)$$

The numerator of this expression can be broken down into its component parts: power delivery systems, cooling infrastructure, IT equipment power, lighting loads, and miscellaneous power consumers throughout the facility. A 2013 survey by Digital Realty of North America data center managers found an average PUE value of 2.9 [4]. A more recent survey in 2014 by the Uptime Institute of data center owners and operator found an average self-reported PUE value of 1.7 [5]. Although there is large variation between these two values, the range indicates moderate to very inefficient operation of data center facilities. It should be noted that not all data centers operate with such inefficiencies. State of the art data center designs have the opportunity to reduce their electricity use by nearly half [6] [7]. Hyper-scale cloud computing and mega data centers built by industry leading companies typically operate with the best-in-class designs. However, they only represent a very small portion (<5%) of the overall energy consumed by the data center market [8].

Typical distribution of power consumption within a traditional air-cooled data center facility is shown in Figure 1-2 [9]. As can be seen, apart from the IT equipment (the useful work), the largest energy consumer of the data center facility is the cooling infrastructure. This is the focus of the present work and presents a great opportunity to improve overall building efficiency.

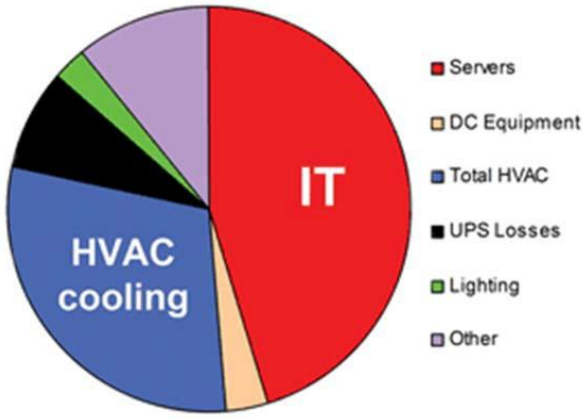

Figure 1-2 Typical energy breakdown in a traditional air-cooled data center facility [9]

The leading professional organization responsible for maintaining guidelines and standards for the data center industry is ASHRAE's Technical Committee (TC) 9.9. In addition to establishing

operating guidelines for cooling of facilities, TC 9.9 also tracks trends in IT equipment power densities. Figure 1-3, taken from projections made in 2005, indicates that over a twenty year period the power densities of ITE increased significantly, although they began to level off over the last ten [10]. As discussed above, these trends place more strain on the cooling infrastructure of the facility.

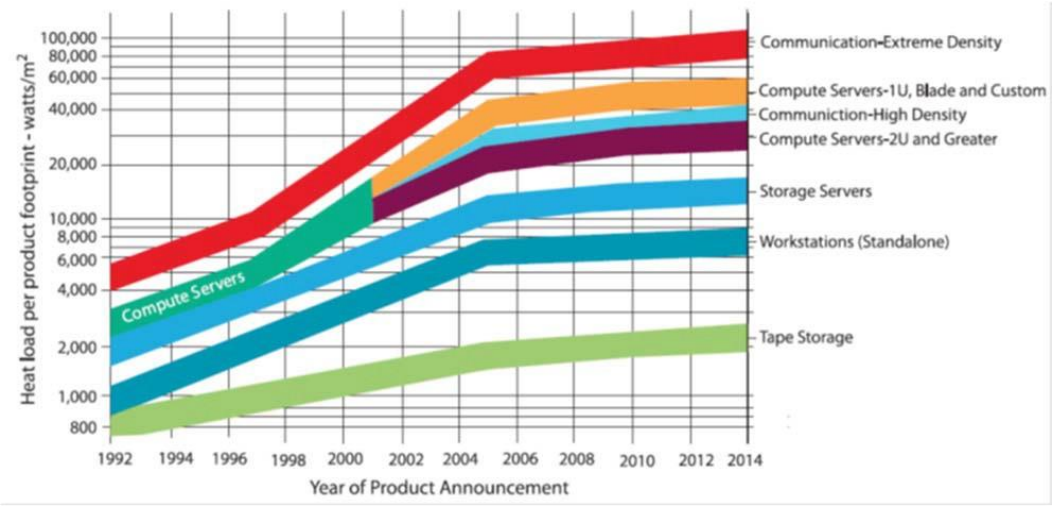

Figure 1-3 Power density trends for various types of information technology equipment (ITE) as published by ASHRAE TC 9.9 [10]

1.2 Cooling of Electronic Packages

At the heart of IT equipment are the microelectronic devices which are typically the primary sources of power consumption and heat generation. As such, these devices are the primary motivator for cooling needs within a data center. The functional limit for safe operation of silicon devices in typical commercial servers range between 85 to 105°C. At temperatures 15 to 25°C higher than this, damage to the device begins to occur [11]. This information forms the starting point for the design of thermal management solutions for ITE and around which the data center cooling system is formed.

A typical packaging architecture for a flip chip package common to today's modern microprocessors (CPUs) is shown in Figure 1-4. This simplified view shows key points in the thermal circuit which removes heat from the silicon die [12] [13]. For the sake of simplicity, it is assumed that all heat generated from the die travels in the direction opposite of the substrate. The thermal circuit consists of two main parts:

- Conduction resistance from the silicon die (T_j) to the base of heat sink (T_b) and
- Convective resistance from the extended surface of the heat sink (T_b) to the ambient fluid used for cooling (T_a).

For the context of this work, the conduction resistance is a fixed parameter dictated by the design and construction of the CPU by the manufacturer. The conduction resistance will be influenced by the pumping power and hence the flow rate of the cooling fluid.

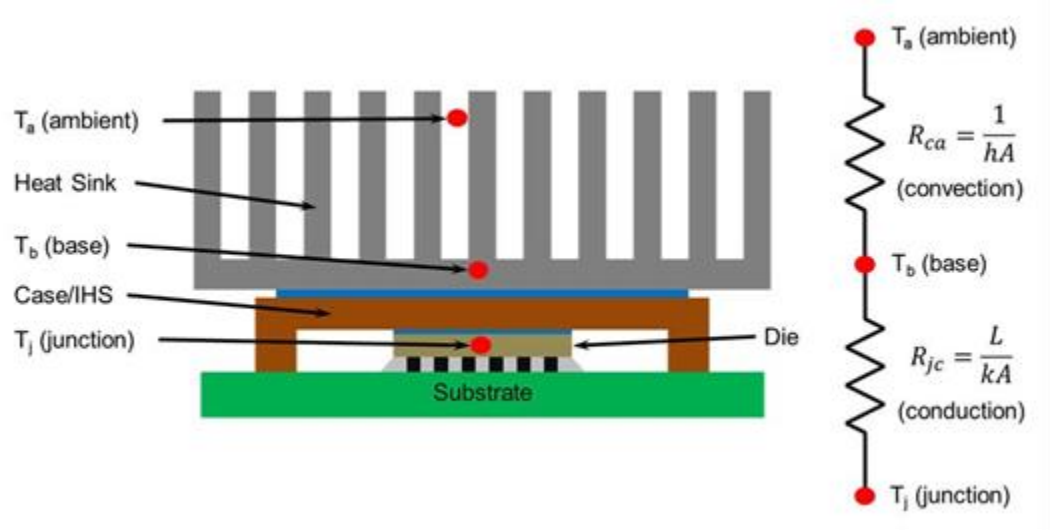

Figure 1-4 Simplified view of typical packaging architecture and thermal circuit for modern flip-chip microprocessors

1.3 Air Cooling for Data Centers

Traditional approaches to cooling data centers use air as the primary cooling medium. Heat rejected from IT hardware is absorbed by the air and either rejected to the outside ambient, mixed with incoming fresh air, or cooled through refrigeration processes. These techniques are matured fields and well documented with safe environmental conditions established by ASHRAE TC 9.9 [14]. Energy modeling of the heat transfer path, starting at the chip level then to airflow within the room and subsequent heat rejection to building HVAC equipment, provides good understanding of the overall efficiency of the facility [15] [16] [17]. The most common floor layout orients racks in a cold aisle/hot aisle arrangement to isolate cold air entering the front of ITE from the hot air exhaust out the back as shown in Figure 1-5. Cold air is supplied through an underfloor plenum from a

computer room air conditioning (CRAC) unit and the hot exhaust circulates back to the return side of the CRAC. Various alternative methods are available for distributing cold air to the inlet of racks [18] [19]. Significant work has been done to understand the physics and dynamics of airflow distribution within a data center [20] [21] [22] [23]. Best practices dictate strict separation of the cold and hot air streams to achieve the highest cooling efficiencies possible [24] [25] [26]. Any leakage, bypass, or recirculation around ITE represents wasted effort by the cooling resources. Extensive efforts to model and understand the benefits of aisle containment strategies highlight the impact of simple geometric modifications to a room on the overall thermal performance and energy efficiency of a room [27] [28] [29] [30].

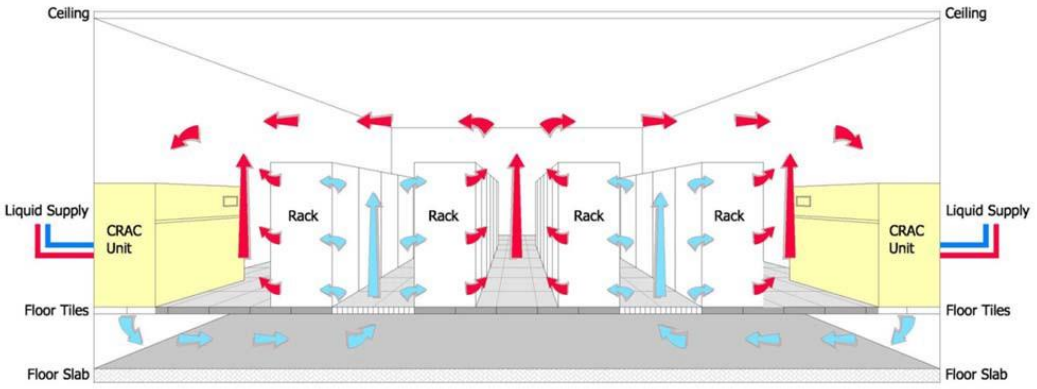

Figure 1-5 Traditional raised floor data center layout in cold aisle/hot aisle rack arrangement [10]

1.4 Limitations of Air Cooling

Data center operators have an opportunity to reduce their total cost of ownership (TCO) by increasing the density of ITE within a space [31]. However, up to a certain limit, continuing to increase heat densities of electronic components and densities at the rack level surpass the capabilities of air for efficient cooling and alternative methods should be sought [32] [33] [34]. ASHRAE TC 9.9 reports that typical air cooled rack power densities are in the range of 6 to 30 kW per rack [35]. Rack densities above this range will typically be beyond the cooling capabilities of legacy air cooling systems. Ellsworth and Iyengar showed that it is possible to cool very high density equipment (60+ kW/rack) with air cooling methods; however, the use of water cooling techniques provided anywhere from 50.1% to 92.2% operational energy savings [36]. Additional

benefits of higher computational performance at lower component operating temperatures were also seen in the study [36]. An analytical study by Saini and Webb determined the upper limit heat load for “desktop” chip packages using a parallel plate fin heat sink is roughly 95 to 100W for a 16 by 16mm heat source [37]. A white paper published by Intel shows that they are able to successfully cool heat densities of 30kW/rack with higher densities possible, but theoretical and practical limits do exist and are specific to each data center’s needs [38]. Although the precise point at which air cooling will no longer be feasible is still an area of healthy debate, it is undeniable that the research and development of alternative cooling methods will be beneficial to the industry as a whole.

1.5 Liquid Cooling for Data Centers

Both direct and indirect forms of liquid cooling offer many advantages over conventional air cooling such as higher heat capacities and lower transport energy requirements. Several liquid coolants are available and have been used in the cooling of electronic equipment with varying thermal and hydraulic properties to choose from [39] [40] [41]. Indirect methods, using water as a cooling medium through cold plates or rear door heat exchangers, demonstrate the benefits of a liquid cooling strategy [36] [42]. Direct immersion of electronic equipment offers a singular cooling solution in which the entirety of a server or other ITE may be cooled by a single fluid medium. This may provide simplicity and ease in planning and implementation of a total solution [32]. Some of the most common forms of liquid cooling for data centers are discussed below.

1.5.1 Water cooling

Water cooling allows increased efficiency through use of higher temperature fluids and possible use of waste heat for other applications [43]. Cold plates have been a long standing method of bringing water cooling to high powered devices as demonstrated by the Thermal Conduction Module (TCM) of the 80s [44]. Even today, there is continued interest in such applications and making this old approach more dynamic for the constantly changing requirements of next generation components [45]. However, the use of cold plates requires air cooling for a portion of the components within servers. Significant developments have been made to bring water cooling to a complete cooling solution (i.e. remove 100% of the ITE heat) for even the most powerful super computers [46]. Water, however, is not a dielectric fluid and as such must be

implemented in an indirect way. The additional infrastructure required within the server may influence cost considerations for this technology, although the cost per performance may still be equal or better than alternatives. Ample data and guidelines for implementing water cooled data center environments are available from sources such as ASHRAE TC 9.9 [35].

1.5.2 Immersion cooling

1.5.2.1 Fluorocarbons

A legacy approach to full liquid immersion cooling is the use of dielectric fluorocarbon refrigerants in pool boiling application. These fluids are extremely good electrical insulators and have moderate thermal characteristics [47]. Additionally, their low boiling points make them suitable for two-phase flow applications capable of removing large heat densities [48] [49] [50]. These high heat transfer rates can be further enhanced though special coatings that increase boiling rates [51] [52]. Current research in this area seeks to improve upon already available fluids by enhancing the critical heat flux for two- phase applications [53]. Full scale data center implementations of these techniques show much promise as an energy saving technique [54] [55]. However, there are additional challenges to this technology that are still to be overcome before it will see wide application.

1.5.2.2 Mineral oil

Compared to air, many mineral oils have a heat capacity roughly 1200 times greater. The increased thermal properties, along with their dielectric nature, make mineral oils a possible alternative for data center applications. Mineral oils have long been used as heat transfer fluids with especially large adoption in power delivery applications such as high voltage transformers [56]. The performance of transformer oils as heat transfer fluids may be significantly improved with the addition of nanoparticles, as recently shown by Taha-Tijerina et. al. [57]. A small fraction (<0.100% by weight) of diamond nanoparticles added to mineral oil were shown to increase the thermal conductivity of the base fluid by 40 – 70% while having minimal detrimental impact to flow properties such as viscosity.

However, when looking at the specific application of mineral oil immersion cooling for data centers, limited literature is available. Recent media attention has provided general PUE values [58]

[59], but the details of operation are absent. Pruncal provides a helpful overview of general operating benefits of oil-based data centers, mentioning the possibility to use facility chilled water up to 30°C compared to 7 – 13°C for traditional air-based systems [60]. The most thorough account is provided by Patterson and Best which showed a 36% improvement in thermal resistance of an oil immersion system compared to an air cooled counterpart with no adverse mechanical effects [61]. This worked showed successful cooling with oil temperatures up to 43°C and cooling PUEs in the 1.02 – 1.03 range; however, no discussion regarding the volume flow rates used was provided. With only limited data available, a large knowledge gap remains in the industry regarding environmental requirements to operate an oil immersion cooling facility.

A key concern regarding this technology by many industry professionals is the potential adverse impact related to the interaction of the fluid with electronic components and devices over time. Anecdotal discussions suggest there is no negative impact of mineral oil on system components; however, detailed documentation is lacking at this time [62].

Commercially available oil immersion systems are on the market and report very desirable performance of such a cooling system. One vendor showed that their system was capable of operating similarly configured servers at component operating temperatures 20 to 30°C lower than an air-cooled counterpart. Additionally, these results showed reduction in cooling costs up to 98% for their liquid cooled system [63]. Similar numbers are reported by another vendor who claims their system can reach a density of 100kW/rack and the opportunity to reduce cooling costs by 95% with mineral oil submersion cooling [64] [65]. However, the data presented by these sources is limited and the extent to which the system have been designed and optimized is unknown to the industry at large. This present work is supported by key technologists in the industry and the need for more widely available data and information regarding such systems.

1.6 Scope of Dissertation

This dissertation reviews electronic performance and reliability impacts of elevated and harsh environments – implications of free air cooling of data centers. The report provides the study on effect of relative humidity, temperature and gaseous and particulate contaminants on IT equipment reliability. The dissertation provides significant results on In Situ studies of contaminants

found in data centers using air-side economization and corresponding ASHRAE envelope expansion in airside economization. The second part of the dissertation focuses on thermo-mechanical design considerations for single-phase immersion cooling of data centers.

Chapter 2, cumulative corrosion damage study for the correlation of equipment reliability to levels of airborne corrosive contaminants and the study of the degree of reliability degradation, when the equipment is operated, outside the recommended range, in the allowable temperature-humidity range in geographies with high levels of gaseous and particulate contamination.

Chapter 3, experimental description of information technology equipment reliability exposed to a data center using airside economizer operating in recommended and allowable ASHRAE envelopes in an ANSI/ISA classified G2 environment to estimate the end of the life of the components and to determine the free air cooling hours for the site.

Chapter 4, the particulate contaminants were collected from different locations of a server and material characterization was performed using Scanning Electron Microscopy (SEM), Energy Dispersive Spectrometer (EDS) and Fourier Transform Infrared Spectroscopy (FTIR). The analysis from these results helps to explain the impact of the contaminants on IT equipment reliability.

Chapter 5, to develop a precise and cost-effective technique to measure deliquescent relative humidity of particulate contaminants found in a data center utilizing airside economization. This methodology can therefore be implemented to help lay a modus operandi of establishing the limiting value or an effective relative humidity envelope to be maintained at a real-world data center facility for its continuous and reliable operation at its respective location.

Chapter 6, the interdigitated comb coupon is lodged with a dust solution in the form of slurry taken from various servers in an actual modular Data Center. The results obtained, and the methodology used in this study can pioneer in standardizing the limiting %RH values for various operating conditions in real world Data Centers.

Chapter 7, flow path of contaminants in different types of data centers to determine the most vulnerable location of the respective data center.

Chapter 8, to measure the thermal performance of a single-phase immersion cooled server at extreme temperatures for prolonged time. Thermal overstress experiment was performed on a

fully immersed server and its cooling system components. This work explores the performance of a server and other components like pump including flow rate drop, starting trouble and other potential issues under extreme climatic conditions.

Chapter 9, the dissertation presents impact of form factor on a maximum junction temperature and thermal resistance at the server level. This work is to provide an insight to increase the rack density by reducing form factor of an existing server. The heat sink is a critical part for cooling effectiveness at server level. This work is to provide an efficient range of operation for heat sink with numerical and computational modelling of a third-generation open compute server for immersion cooling application. A parametric study is conducted, and the thermal efficiency has been optimized for mineral oil and EC 100.

Chapter 10, this research reviews the changes in physical and chemical properties of information technology (IT) equipment and compatibility of materials like polyvinyl chloride (PVC), printed circuit board (PCB) and switching devices with mineral oil to characterize the interconnect reliability of materials. The study indicates the effect of mineral oil on IT equipment reliability and reliability enhancements for immersion cooled data centers.

Chapter 11, this chapter includes Cup Burner Experiment as per ISO 14520/NFPA 2001 standard to determine the minimum design concentration of fire extinguishing agent for the class B hazard of heavy mineral oil and the class C hazard of electronic equipment as a part of the safety concerns for oil cooled data centers. This chapter also discusses the challenges related to the reliability tests for immersion cooled components.

Chapter 12, for the first time, material compatibility is being tested. Accelerated thermal degradation testing of printed circuit board, passive components and optical fibers for single phase immersion cooling systems is a significant part of this study. The study proposes a testing methodology which can be adopted by all for evaluating the reliability of electronic packages and components when immersed in a dielectric fluid.

Chapter 13 summarizes the work above and discusses opportunities and future work moving forward that can further enhance the improvements presented here.

References

1. J. Koomey, "Growth in Data Center Electricity Use 2005 to 2010," Analytics Press, Burlingame, CA, 2011.
2. The Green Grid, "Green Grid Data Center Power Efficiency Metrics: PUE and DCIE, White Paper #6," The Green Grid, Beaverton, OR, 2008.
3. The Green Grid, "PUE™: A Comprehensive Examination of the Metric, White Paper #49," The Green Grid, Beaverton, OR, 2012.
4. "North American Campos Survey Results," Digital Realty, San Francisco, CA, 2013.
5. M. Stansberry, "2014 Data Center Industry Survey Results," Uptime Institute, NewYork, NY, 2014.
6. U.S. Environmental Protection Agency: ENERGY STAR Program, "Report toCongress on Server and Data Center Energy Efficiency Public Law 109-431," 2007.
7. R. Brown, "Report to Congress on Server and Data Center Energy Efficiency: Public Law 109-431," eScholarship, 2008.
8. Natural Resources Defense Council (NRDC), "Data Center Efficiency Assessment: Scalng Up Energy Effiiency Across the Data Center Industry: Evaluating Key Drivers and Barriers," New York, NY, 2014.
9. M. Iyengard and R. Schmidt, "Energy Consumption of Information Technology Data Centers," *Electronics Cooling Magazine (Online),* 6 December 2010.
10. ASHRAE TC 9.9, "Datacom Equipment Power Trends and Cooling Applications," ASHRAE, Atlanta, GA, 2005.
11. ASHRAE TC 9.9, "IT Equipment Thermal Management and Controls White Paper," ASHRAE, Atlanta, GA, 2012.
12. R. Tummala, Fundamentals of Microsystems Packaging, New York, NY: McGraw-Hill, 2000.

13. G. Xu, B. Guenin and M. Vogel, "Extension of Air Cooling for High Power Processors," in *IEEE ITherm*, Las Vegas, NV, 2004.
14. ASHRAE TC 9.9, "2011 Thermal Guidelines for Data Processing Environments - Expanded Data Center Classes and Usage Guidance," ASHRAE, Atlanta, GA, 2011.
15. M. Iyengar and R. Schmidt, "Analytical Modeling for Thermodynamic Characterization of Data Center Cooling Systems," *Journal of Electronic Packaging,* vol. 131, no. 2, pp. 021009-1-9, 2009.
16. M. Beitelmal and C. Patel, "Model-Based Approach for Optimizing a Data Center Centralized Cooling System," Hewlett-Packard Laboratories, Palo Alto, CA, 2006.
17. T. Breen, E. Walsh, J. Punch, A. Shah and C. Bash, "From Chip to Cooling Tower Data Center Modeling: Influence of Server Inlet Temperature and Temperature Rise Across Cabinet," *Journal of Electronic Packaging,* vol. 133, no. 1, pp. 011044-1-8, 2011.
18. S. Shrivastava, B. Sammakia, R. Schmidt and M. Iyengar, "Comparative Analysis of Different Data Center Airflow Management Configurations," in *ASME InterPACK*, San Francisco, CA, 2005.
19. V. Mulay, "Analysis of Data Center Cooling Strategies and the Impact of the Dynamic Thermal Management on the Data Center Energy Efficiency," PhD Thesis, Arlington, TX, 2009.
20. S. Patankar, "Airflow and Cooling in a Data Center," *Journal of Heat Transfer,* vol. 132, no. 7, pp. 073001-1-17, 2010.
21. J. Rambo and Y. Joshi, "Modeling of Data Center Airflow and Heat Transfer: State of the Art and Future Trends," *Distributed Parallel Databases,* vol. 21, pp. 193-225, 2007.
22. A. Beitelmal and C. Patel, "Thermo-Fluids Provisioning of a High Performance High Density Data Center," *Distributed and Parallel Databases,* vol. 21, pp. 227-238, 2007.

23. P. Kumar, Y. Joshi, M. Patterson, R. Steinbrecher and M. Mena, "Cold Aisle Distribution in a Raised Floor Data Center with Heterogeneous Opposing Orientation Racks," in *ASME InterPACK*, Portland, OR, 2011.
24. The Green Grid, "Guidelines for Energy-Efficient Datacenters," The Green Grid, Beaverton, OR, 2007.
25. O. VanGeet, "Best Practices Guide for Energy-Efficient Data Center Design," US Department of Energy, National Renewable Energy Laboratory (NREL), Golden, CO, 2011.
26. The Green Grid, "Case Study: The ROI of Cooling System Energy Efficiency Upgrades (White Paper #39)," The Green Grid, Beaverton, OR, 2011.
27. V. Arghode, V. Sundaralingam, Y. Joshi and W. Phelps, "Thermal Characteristics of Open and Contained Data Center Cold Aisle," *Journal of Heat Transfer,* vol. 135, no.6, pp. 061901-1-11, 2013.
28. S. Alkharabsheh, S. Shrivastava and B. Sammakia, "Effect of Cold Aisle Containment Leakage on Flow Rates and Temperatures in a Data Center," in *ASME InterPACK*, Burlingame, CA, 2013.
29. B. Muralidharan, S. Shrivastava, M. Ibrahim, S. Alkharabsheh and B. Sammakia, "Impact of Cold Aisle Containment on Thermal Performance of Data Center," in *ASME InterPACK*, Burlingame, CA, 2013.
30. S. Shrivastava and M. Ibrahim, "Benefit of Cold Aisle Containment During Cooling Failure," in *ASME InterPACK*, Burlingame, CA, 2013.
31. M. K. Patterson, D. G. Costello, P. F. Grimm and M. Loeffler, "Data Center TCO; A Comparison of High-Density and Low-Density Spaces," Intel Corporation, 2005.
32. L. Stahl, "System Architectures and Fluids for High Heat Density Cooling Solutions," *ASHRAE Transactions,* vol. 116, no. 1, 2010.
33. P. Hughes and W. Tschudi, "Energy Efficient and Lower Capital Cost - an Alternative Data Center Cooling Strategy," in *ASHRAE Annual Conference*, Montreal, 2011.

34. H. Villa, "Liquid Cooling for Extreme Heat Densities," *ASHRAE Transactions,* vol. 113, no. 1, 2007.
35. ASHRAE TC 9.9, "2011 Thermal Guidelines for Liquid Cooled Data Processing Environments," ASHRAE, Atlanta, GA, 2011.
36. M. Ellsworth and M. Iyengar, "Energy Efficiency Analysis and Comparison of Air and Water Cooled High Performance Server," in *ASME InterPACK*, San Francisco, CA, 2009.
37. M. Saini and R. Webb, "Heat Rejection Limits of Air Cooled Plane Fin Heat Sinks for Computer Cooling," *IEEE Trans. on Components and Packaging Technologies,* vol. 26, no. 1, pp. 71 - 79, 2003.
38. M. Patterson and D. Fenwick, "The State of Data Center Cooling: A review of current air and liquid cooling solutions," Intel White Paper, 2008.
39. S. Mohapatra, "An Overview of Liquid Coolants for Electronics Cooling," *Electronics Cooling Magazine (Online),* 1 May 2006.
40. M. Ellsworth, "Comparing Liquid Coolants from Both a Thermal and Hydrualic Perspective," *Electronics Cooling Magazine (Online),* 1 August 2006.
41. S. Mohapatra and D. Loikits, "Advances in Liquid Coolant Technologies for Electronics Cooling," in *IEEE SEMI-THERM*, San Jose, CA, 2005.
42. A. Almoli, A. Thompson, N. Kapur, J. Summers, H. Thompson and G. Hannah, "Computational Fluid Dynamic Investigation of Liquid Cooling in Data Centers,"*Applied Energy,* vol. 89, pp. 150-155, 2012.
43. S. Zimmermann, I. Meijer, M. K. Tiwari, S. Parades and B. Michel, "Aquasar: A Hot Water Cooled Data Center with Direct Energy Reuse," *Energy,* vol. 43, pp. 237-245, 2012.
44. R. C. Chu, U. P. Hwang and R. E. Simons, "Conduction Cooling for an LSI Package: A One-Dimensional Approach," *IBM Journal of Research and Development,* vol. 26, no. 1, pp. 45-54, 1982.

45. J. Fernandes, S. Ghalambor, A. Docca, C. Aldham, D. Agonafer, E. Chenelly, B. Chan and M. Ellsworth Jr., "Combining Computational Fluid Dynamics (CFD) and Flow Network Modeling (FNM) Design of a Multi-Chip Module (MCM) Cold Plate," in *ASME InterPACK Conference*, San Diego, CA, 2013.
46. M. J. Ellsworth Jr., G. F. Goth, R. J. Zoodsma, A. Arvelo, L. A. Campbell and W. J. Anderl, "An Overview of the IBM Power 775 Supercomputer Water Cooling System," *Journal of Electronic Packaging,* vol. 134, 2012.
47. F. P. Incropera, Liquid Cooling of Electronic Devices by Single-Phase Convection, New York: A Wiley-Interscience Publication, 1999.
48. T. M. Anderson and I. Mudawar, "Microelectronic Cooling by Enhanced Pool Boiling of a Dielectric Fluorocarbon Liquid," *Journal of Heat Transfer,* vol. 111, pp. 752-759,1989.
49. P. Tuma, "The Merits of Open Bath Immersion Cooling of Datacom Equipment," in *IEEE SEMI-THERM Symposium*, Santa Clara, 2010.
50. B. Chan, H. Lin, S. Polzer, N. Harff, E. Daniel, B. Gilbert and P. Tuma, "Performance of Passive 2-Phase Immersion Cooling of Server Hardware," in *IMAPs ATW on Thermal Management*, Palo Alto, CA, 2010.
51. M. Arik, "Enhancement of Pool Boiling Critical Heat Flux in Dielectric Liquids by Microporous Coatings," *International Journal of Heat and Mass Transfer,* vol. 50, pp. 997-1009, 2006.
52. M. S. El-Genk, "Immersion Cooling Nucleate Boiling of High Power Computer Chips," *Energy Conversion and Management,* vol. 53, pp. 205-128, 2012.
53. P. Warrier, A. Sathyanarayana, D. V. Patil, S. France, Y. Joshi and A. S. Teja, "Novel Heat Transfer Fluids for Direct Immersion Phase Change Cooling of Electronic Systems," *International Journal of Heat and Mass Transfer,* vol. 55, pp. 3379-3385, 2012.
54. T. Cader, V. Sorel, L. Westra and A. Marquez, "Liquid Cooling in Data Centers," *ASHRAE Transactions,* vol. 115, no. 1, 2009.

55. V. Sorell, P. Tuma and L. Newcombe, "Liquid Cooling in Data Centers, Part 2," in *ASHRAE Annual Conference*, Denver, CO, 2013.
56. L. W. Pierce, "An Investigation of the Thermal Performance of an Oil Filled Transformer Winding," *IEEE Transactions on Power Delivery,* vol. 7, no. 3, pp. 1347- 1358, 1992.
57. J. J. Taha-Tijerina, T. Narayana, C. S. Tiwary, K. Lozano, M. Chipara and P. M. Ajayan, "Nanodiamond-Based Thermal Fluids," *ACS Applied Materials and Interfaces,* vol. 6, pp. 4778 - 4785, 2014.
58. P. Jones, "Data Center Dynamics," 5 September 2012. [Online]. Available: http://www.datacenterdynamics.com/focus/archive/2012/09/intel-says-liquid-andservers-do-mix. [Accessed 15 November 2013].
59. J. Rath, "Data Center Knowledge," 21 November 2013. [Online]. Available: http://www.datacenterknowledge.com/archives/2013/11/21/submergedsupercomputer-named-worlds-efficient-system-green-500/. [Accessed 22 November 2013].
60. D. Prucnal, "Doing More With Less: Cooling Computers with Oil Pays Off," *The Next Wave,* vol. 20, no. 2, pp. 20 - 29, 2013.
61. M. Patterson and C. Best, "Oil Immersion Cooling and Reductions In Data Center Energy Use," in *ASHRAE Summer Conference*, San Antonio, TX, 2012.
62. R. Miller, "Data Center Knowledge," 4 September 2012. [Online]. Available: http://www.datacenterknowledge.com/archives/2012/09/04/intel-explores-mineral-oilcooling/ 2/. [Accessed 22 November 2013].
63. A. Regimbal and R. Tufty, "Power-to-Cool: Liquid Submersion Cooled Server vs. Air-Cooled Servers," Liquid Cooled Solutions White Paper, Rochester, MN, 2013.
64. Green Revolution Cooling, "CarnotJet Submersion Cooling System Product Data Sheet," Green Revolution Cooling, Austin, TX, 2013.
65. Green Revolution Cooling, "Submerged Servers in the Data Center: Not as Scary as We All Think," Green Revolution Cooling, Austin, TX, 2014.

Chapter 2

Qualitative Study of Cumulative Corrosion Damage of IT Equipment In A Data Center Utilizing Air-Side Economizer Operating In Recommended And Expanded ASHRAE Envelope

(Journal of Electronic Packaging)

Jimil M. Shah
Mechanical and Aerospace
Engineering Department,
University of Texas at Arlington,
Arlington, TX 76019
e-mail: jimil.shah@mavs.uta.edu

Oluwaseun Awe
Mechanical and Aerospace
Engineering Department,
University of Texas at Arlington,
Arlington, TX 76019

Betsegaw Gebrehiwot
Mechanical and Aerospace
Engineering Department,
University of Texas at Arlington,
Arlington, TX 76019

Dereje Agonafer
Mechanical and Aerospace
Engineering Department,
University of Texas at Arlington,
Arlington, TX 76019

Prabjit Singh
IBM Corporation
Poughkeepsie, New York, USA

Naveen Kannan
Mestex, a Division of Mestek Inc,
4830 Transport Drive,
Dallas, TX 75247, USA

Mike Kaler
Mestex, a Division of Mestek Inc,
4830 Transport Drive,
Dallas, TX 75247, USA

Abstract

Deployment of airside economizers in data centers is rapidly gaining acceptance to reduce cost of cooling energy by reducing hours of operation of CRAC units. Airside economization has associated risk of introducing gaseous and particulate contamination into data centers, thus, degrading the reliability of IT equipment. The challenge is to determine reliability degradation of IT equipment if operated in environmental conditions outside ASHRAE recommended envelope with

contamination severity levels higher than G1. This paper is a first attempt at addressing this challenge by studying the cumulative corrosion damage to IT equipment operated in an experimental modular data center located in an industrial area with measured level of air contaminants in ISA severity level G2. This study serves several purposes including: correlating IT equipment reliability to levels of airborne corrosive contaminants and studying degree of reliability degradation when IT equipment is operated outside ASHRAE recommended envelope at a location with high levels of contaminants. Reliability degradation of servers exposed to outside air via an airside economizer was determined qualitatively by examining corrosion of components in these servers and comparing the results to corrosion of components in other similar servers that were stored in a space where airside economization was not used. In the four years of the modular data center's servers' operation, none of the servers failed. This observation highlights an opportunity to significantly save data center cooling energy by allowing IT equipment to operate outside the currently recommended and allowable ASHRAE envelopes and outside the ISA severity level G1.

2.1 Introduction

To deal with the increasing server densities and the associated cooling costs, data center operators are resorting to cost cutting measures such as allowing excursions of temperature and humidity levels outside ASHRAE recommended envelope and often turning to air side economizers which have associated risk of bringing particulate and gaseous contaminants into the data center space.

Figure 1 shows a typical power consumption by different components of a data center. A datacenter facility is comprised of rooms or closets which have computers/servers used for data processing, data communication, data storage, data transmission, et cetera, other electronic equipment, and including cooling systems. The IT equipment is cooled using cooling units which usually consume 31% (23% HVAC cooling + 8% HVAC fans) of the overall data center energy. With the change in data center operational temperature and 100% utilization of economizer, operators can save up to 74% of mechanical energy [1].

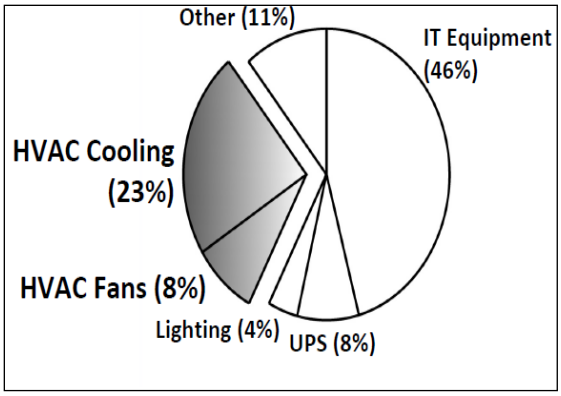

Figure 2-1: A common data center power allocation [1]

Air-side economizers get rid of mechanical cooling, but at the cost of increased risk of contamination-related to hardware failures. As an alternate source to air-conditioning/mechanical cooling, Air-side economizers bring in large amounts of outside air to cool internal loads, when weather conditions are favorable, saving a considerable amount of energy by reducing chiller operation. When the outside air is, both, adequately cool and dry no extra conditioning is required. This part of the air-side economizer control plan is called free cooling. However, the downside of air-side economization is the increased reliability risk due to the contamination that enters the data center.

Data centers are usually placed in relatively clean environments with suitable filters to reduce the entry of particulate matter. The air-side free cooling map of Figure 2 shows the distribution of the hours of free cooling operation possible across USA [2].

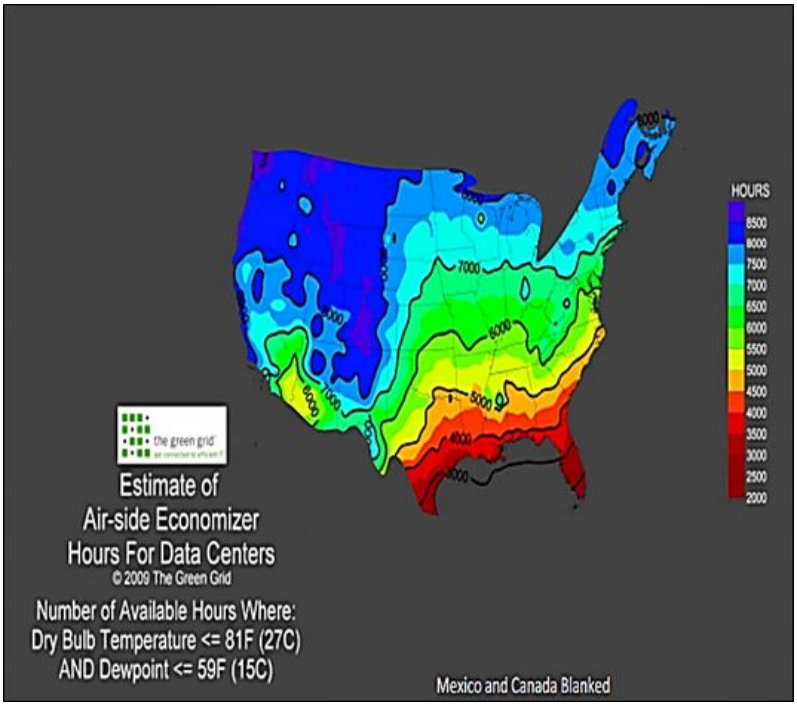

Figure 2-2: Air-side Economizer Hours for Data Centers [2]

The temperature and humidity range in which IT is recommended to operate is defined by ASHRAE [2-6] and is accepted by IT equipment manufacturers and their clients to be as follows: 18°C to 27°C (64.4°F to 80.6°F) dry bulb temperature, 5.5°C to 15°C (41.9°F to 59°F) dew point temperature, and less than 60% relative humidity. These conditions with recommended air quality levels ensure reliable operation of IT equipment.

Figure 3 shows ASHRAE recommended and allowable temperature and humidity ranges as defined in [6]. Per this guideline, brief excursions outside the recommended envelope and into the allowable A1 envelope may be acceptable. The longer an IT equipment is kept in the allowable temperature-humidity envelope and outside the recommended envelope, corrosion related component failures also increase because of gaseous and particulate contamination [6].

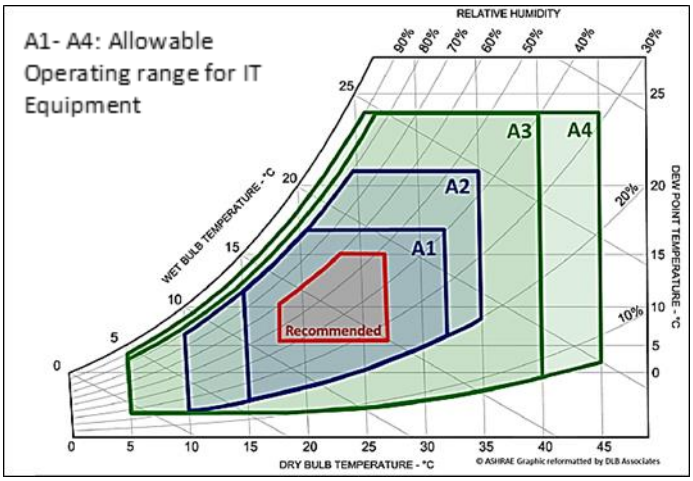

Figure 2-3: ASHRAE temperature guidelines showing the recommended and allowable ranges [6]

Continued computer performance enhancement is being accomplished by reducing the size of transistors and distance electrical signals must travel. The net impact is scaling down of electronic parts which makes them prone to contamination-related failures:

- The increased heat load per unit volume requires higher air velocities to keep equipment within acceptable temperature limits. Higher air velocities increase the rate of accumulation of particulate matter and fibrous debris on the electronic assemblies.
- The reduced spacing between features on printed circuit boards makes the electronics more susceptible to electrical shorting failures due to particulate and gaseous contamination

Environmental factors such as temperature, relative humidity, and gaseous and particulate contaminants can cause PCBs to fail in two major ways:

- Electrical open circuits occurring due to corrosion, for instance corrosion of silver terminations in surface mount segments, surface mount resistors endure open circuits because of the consumption of their silver terminations by sulfur bearing gaseous contaminants in polluted geographies. [2,3,7-10]
- Electrical short circuiting due to copper creep corrosion, by electrochemical reactions such as ion migration and cathodic-anodic filamentation [2,3,9]

In 2006, the European Union's RoHS directive banning the use of lead in solders led to changes in PCB finishes and the elimination of lead from solders. These progressions significantly expanded the PCB failure rates because of creep corrosion [2,3].

The settled, hygroscopic particulate matter contaminations reduce the surface insulation resistance between closely spaced structures on PCBs. In humid environments, it becomes very difficult to deal with the electrical short circuiting caused by the accumulated particulate matter. The difficulty arises from the intermittent electrical nature of these particles and the fact that the failure leaves no visible evidence besides the presence of deposited particulate matter. [2,3]

As more and more data centers operate outside the ASHRAE recommended temperature-humidity range for longer periods of times, it becomes important to understand the effects of temperature and relative humidity especially under the presence of gaseous and particulate contaminants. There is an urgent need to determine the reliability of IT equipment as a function of temperature, humidity and gaseous and particulate contamination so that algorithms can be generated for the most cost effective operation of data centers without adversely affecting the reliability of IT Equipment.

This undertaking addresses the IT hardware dependability issues emerging from operation in high humidity and high temperature conditions in critical situations characterized by the ISA 71.04-2013 corrosive potential severity levels G1 to G3 [11-13].

Table 2-1 ISA 71.04-2013 Severity Level Classification [11-13]

Class	Severity Level	Copper Reactivity (Å)	Silver Reactivity (Å)	Comments
G1	Mild	<300	<200	Corrosion is not a factor in determining equipment reliability
G2	Moderate	<1,000	<1,000	Corrosion effects are measurable and corrosion may not be a factor. ENIG and ImmAg PCB surface finish failures.
G3	Harsh	<2,000	<2,000	High probability that corrosive attack will occur. OSP and ImSn PCB surface finish failures.
GX	Severe	≥2,000	≥2,000	Only specially designed and packaged equipment to survive.

The current state of the components operated in a data center which uses the air-side economizer is compared with their initial state before server installation and commencement of the operation. Also, attempts are made at correlating the combined effect of the historical operating and environmental data gathered over the same period to provide insight into the reliability of IT components evaluated. The collective results of the evaluation with the historic operating and environmental conditions are discussed and presented. This is a first attempt to address these challenges by determining the negative impacts of particulate and gaseous contamination on IT equipment in real world data center where air-side economizers are implemented.

2.2 Procedure

The study considers the implications of the use of air-side economizers with ASHRAE standard filtration systems as compared to a standard CRAC-cooled data center.

The steps of the procedure are as follows:

1. Site description
2. Physical Environment: Statistical analysis of historical trend data
3. Physical Environment: Particulate and Gaseous contaminants
4. Measurement of the severity level of the site as per ISA 71.04-2013 Standard

5. Removal of the servers from both the sites regarding location and comparing of the visual images to conclude preliminary results

Here, the goal is to cover the real-world ranges of each classified parameter by different standards.

2.3 Site Description

The study includes two different experimental data center sites:

- Laboratory data center at the University with CRAC unit
- The Modular research data center located at polluted geographies of Dallas industrial area which has air-side economizer with direct and indirect evaporative cooling

Figure 4 describes the site 1 which is the laboratory data center at the University. The laboratory data center uses the 20 ton CRAC unit with standard dehumidifier. The air is filtered and assumed as ISA 71.04-2013 severity level G1 for gaseous contamination. As shown in Fig. 4, the lab data center has cold aisle/ hot aisle containment protocol to reduce the mixing of hot exhaust air with cooler room air.

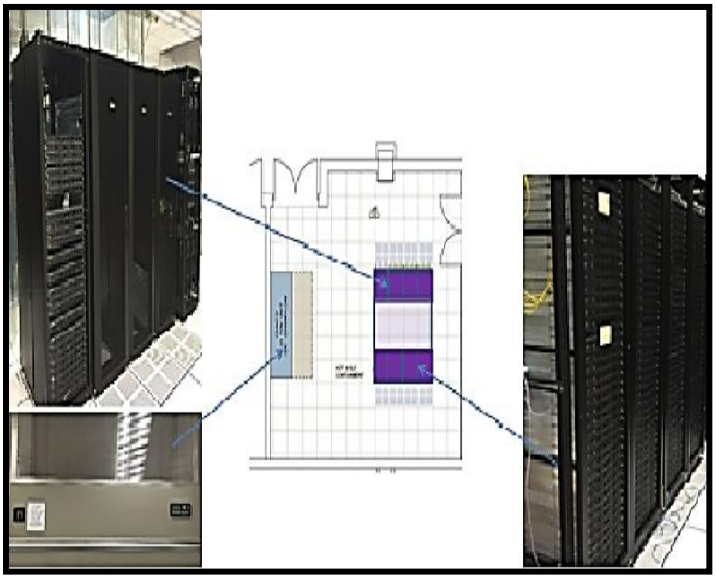

Figure 2-4: The Laboratory Data Center (Site: 1)

The computer room air conditioning (CRAC) unit contains a fan, DX cooling coil and a refrigerant compressor. The airflow protocol is front to top and rear. Cooling airflow is supplied to

the equipment racks through perforated tiles via an underfloor distribution system that is connected to CRAC units. The blanking panels are installed to prevent recirculation of hot air. The ASHRAE recommended thermal guidelines are maintained and generally, temperature is kept constant at 18°C.

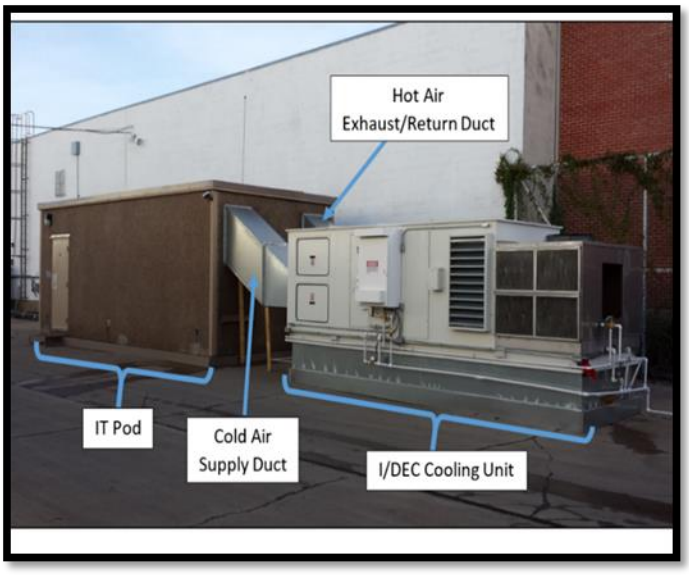

Figure 2-5 Research Modular Data Center at Dallas Industrial Area (Front View) (Site: 2) [14]

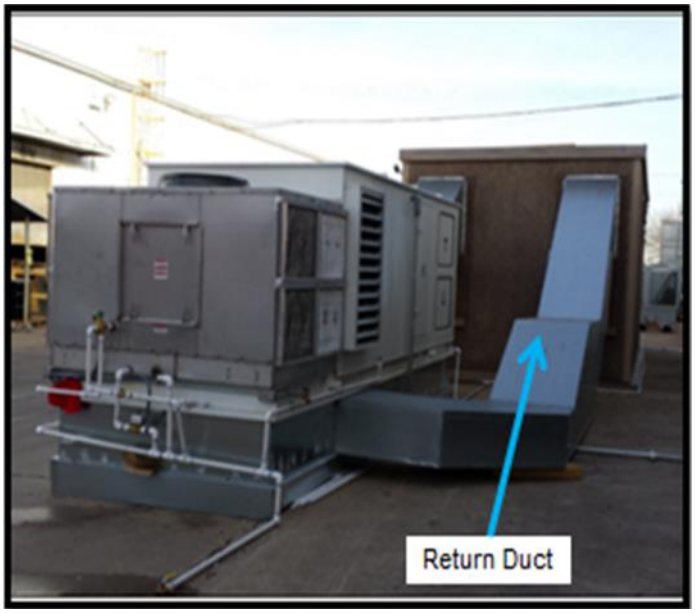

Figure 2-6: Research Modular Data Center (Side View) [14]

Figures 5 and 6 show the front and side views of the modular research data center (Site: 2) located at polluted geographies of Dallas industrial area respectively. The data center uses air-

side economizer with direct and indirect evaporative cooling. The figures show different components of IT pod and cooling unit such as cold air supply duct, hot air exhaust/return duct and I/DEC cooling Unit. The size of the research modular data center is 10ft x 12ft x 28ft [14].

2.3.1 IT Pod Configurations:

Size	:126 in X 85.5 in
IT Equipment	: HP SE1120 Servers (120 Servers)
Cabinet	: S6212B PANDUIT Rack
Flow Provisioning	: End inlet and Outlet configuration
Inlet Dimensions	: 13x27 vent with 45º Louver Angle
Outlet Dimensions	: 13x27 vent

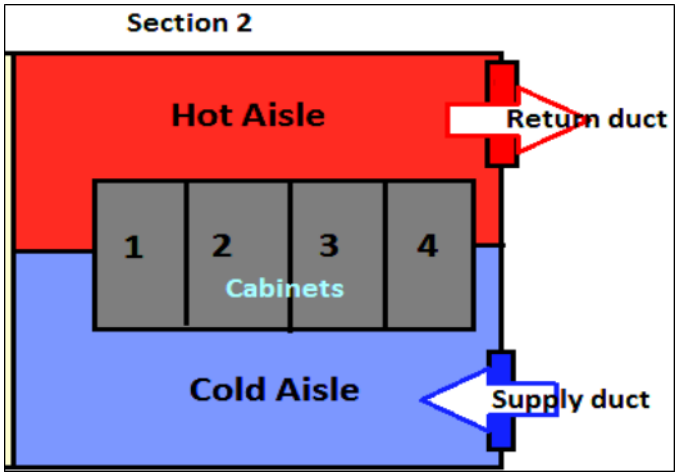

Figure 2-7: IT POD Airflow direction [14]

Figure 7 provides the information about the airflow distribution and the airflow direction inside the IT pod. The airflow (2500 - 3000 CFM) protocol is front to rear. The Fig. also provides the insight of the cold aisle/hot aisle configuration of the IT pod with the supply of cold air from the supply duct with the inlet of 45º Louver Angle inside the cold aisle and the evacuation of hot air through the return duct from the hot aisle.

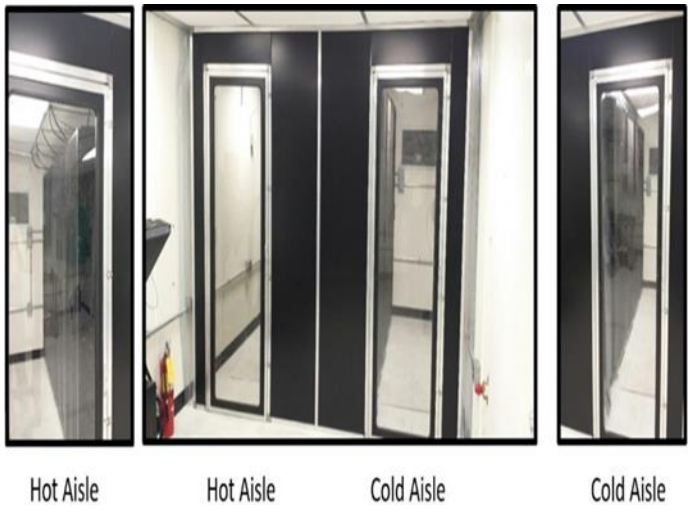

Figure 2-8: Inside the IT Pod [13,14]

The inside view of the IT Pod is presented through Figures 8 and 9. Figure 8 represents the cold aisle and hot aisle of the modular data center and figure 9 represents the model of the servers' arrangement in the cold aisle to get better thermal management of the servers positioned in four cabinets. The servers are arranged at the elevated position next to the inlet. It maintains the direction of airflow towards the servers and provides cooling properly from the front. The louver angle is responsible for the airflow pattern.

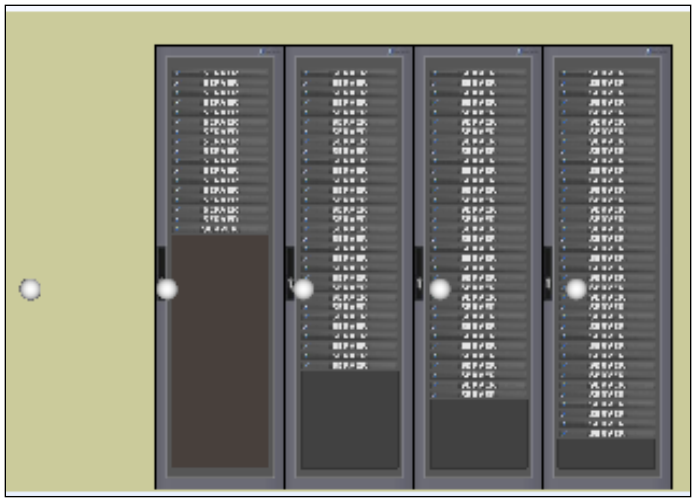

Figure 2-9: Cold aisle Rack arrangement for better air distribution [14]

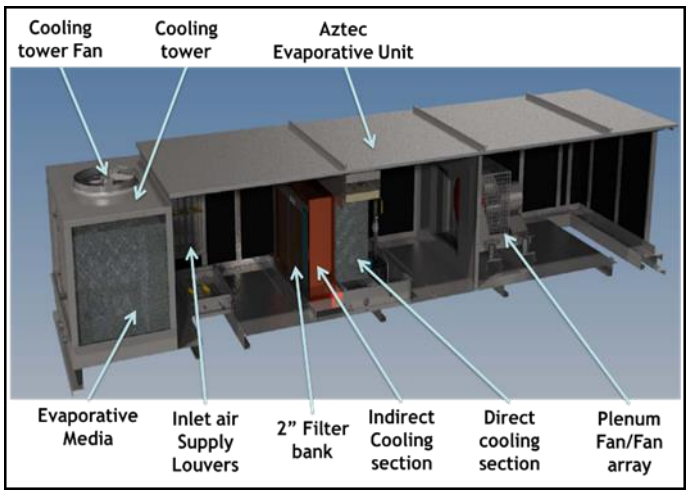

Figure 2-10: Model of the Cooling Unit [14]

The model of the cooling unit shown in Figure 10 shows the components and gives an idea about the working of the cooling unit/air handling unit deployed at the modular data center. The cooling unit is air-side economizer with direct and indirect evaporative cooling. The data center uses free air cooling in suitable environmental conditions and uses direct cooling and/or indirect cooling and/or return air and/or mixing of return air with outside air to achieve ASHRAE recommended operating conditions in the cold aisle when the environmental conditions are extreme.

2.4 Physical Environment

2.4.1 Temperature and Relative Humidity

Here, two scenarios have been discussed: including the possibility of free air cooling with and without the combination of direct and indirect evaporative cooling and statistical analysis of historical environmental data of modular data center test site.

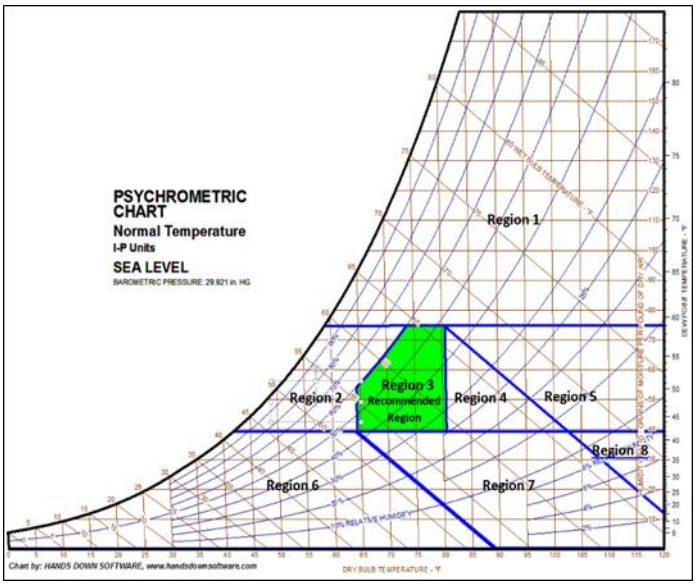

Figure 2-11 Psychrometric chart regions based on the recommended envelope [14]

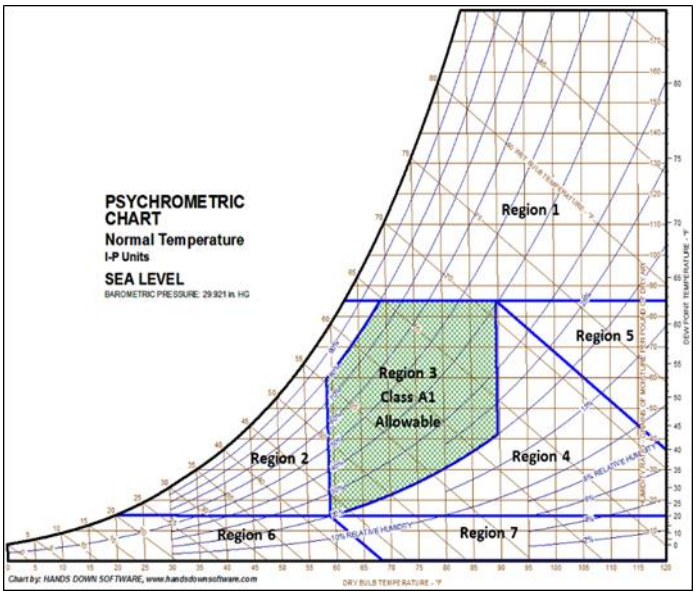

Figure 2-12 Psychrometric chart regions based on Class A1 allowable region [14]

The areas in both outline shown in Figure 11 and 12 are separated into view of the cooling capacity of the cooling unit at IT Pod to bring outside air into the target regions: Recommended or Class A1 Allowable. For both diagrams, if outside air falls into Region 1, this cooling unit can't be accustomed to bring outside air into the targeted regions since the outside air contains a lot of moisture. Maybe Dehumidifiers, DX cooling units, or multi-stage IEC units

should be utilized. For all areas, other than Region 1, the cooling unit can be accustomed to bring outside air into the objective districts. The following is an outline of how this might be accomplished if outside air falls into:

Region 2: outside air is mixed with the hot return air.

Region 3: outside air directly

Region 4: either DEC or IEC can be utilized for the chart considering the suggested envelope, however just DEC is ensured to work for the diagram in view of the Class A1 suitable envelope. It might be more effective to utilize the I/DEC mode.

Region 5: IEC should be utilized. It might be more efficient to utilize the I/DEC mode.

Region 6: blend hot return air with outside air. It might be important to run the DEC segment to add moisture.

Region 7: DEC should be utilized. It might be more effective to utilize the I/DEC mode.

Region 8: Both IEC and DEC should be utilized.

Here, we are not considering return air since our focus is mainly on determining whether it's conceivable to utilize the installed cooling unit to convey outside air to the targeted regions [14].

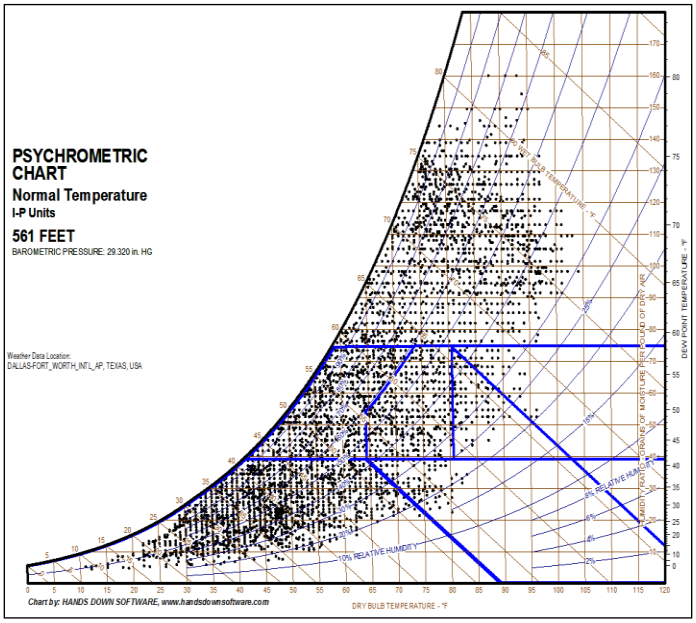

Figure 2-13 Chart I: TMY3 hourly weather data for DFW AP [14]

Figures 13 and 14 provide the analysis of hourly weather data from a nearby weather station. Typical Meteorological Year 3 (TMY3) data for Dallas/Fort Worth International Airport (DFW AP) is plotted in Chart I and Chart II, respectively. The analysis is helpful to estimate the number of hours the IT Pod which is in Dallas, TX, could use ASE and to increase the possibility of free air cooling. Percentage of hours TMY3 data fell in the regions 2 and 3 of Figure 11 are around 17% and 7%, respectively, and of Figure 12 are around 34% and 23% respectively. The results show the significant availability of outside air usage (free air cooling) at the Dallas test site during the year.

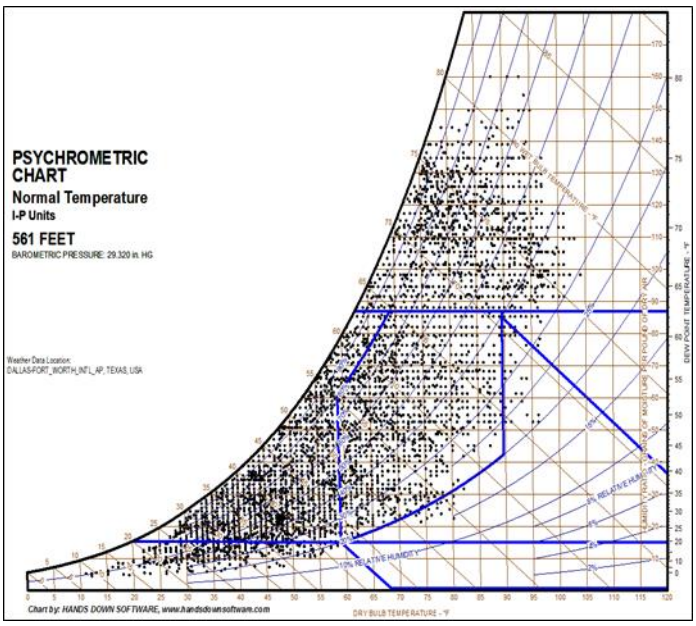

Figure 2-14 Chart II: TMY3 hourly weather data for DFW AP [14]

The below mentioned statistics demonstrations represent the environmental excursions of the last two years at the modular data center based on the trend data. The historical environmental data displays the exact operating conditions of research data center for last two years. The study of excursion of temperature and relative humidity in the data center is essential to correlate the environment of total period of operation and its implications on the reliability of the system.

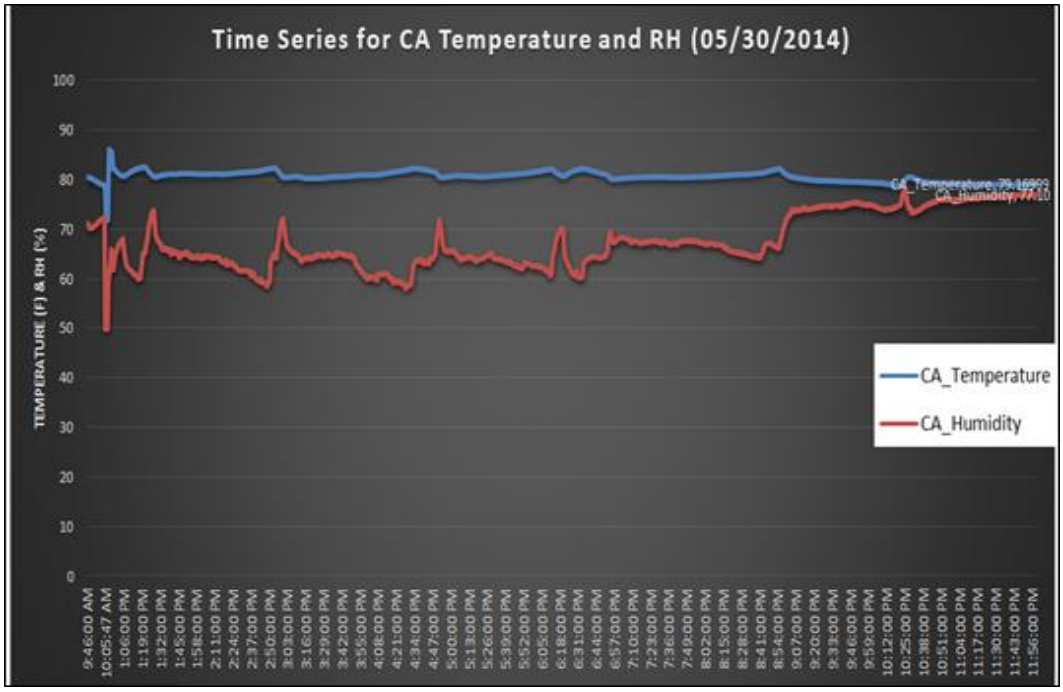

Figure 2-15 Time Series for CA Temp. and %RH (Daily) [15]

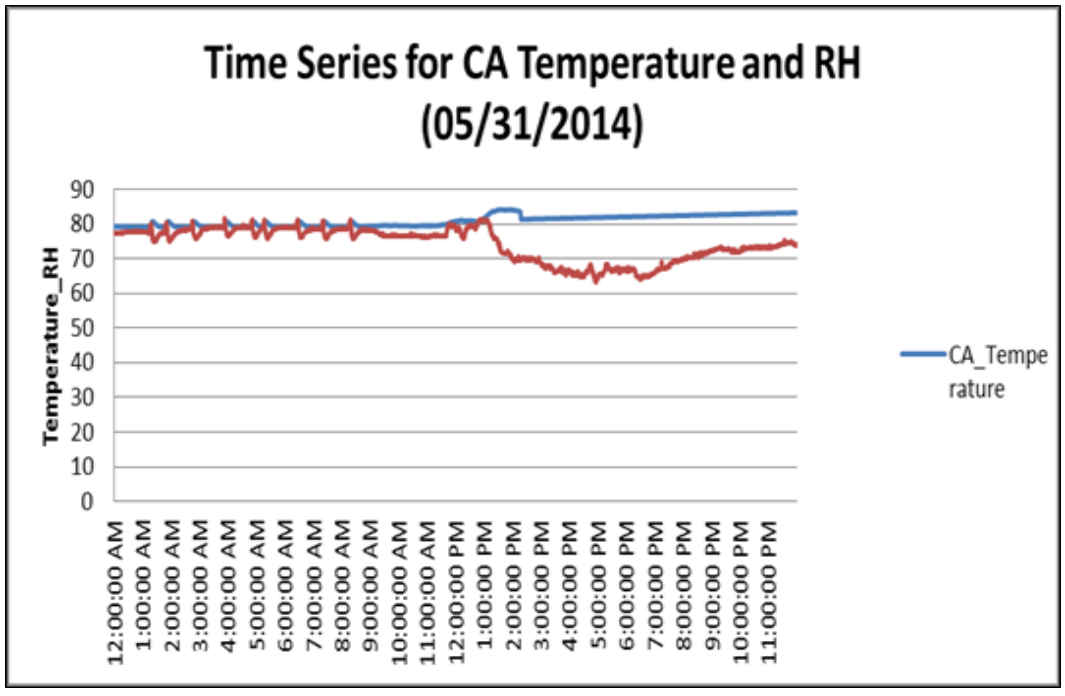

Figure 2-16 Time Series for CA Temp. and %RH (Daily) [15]

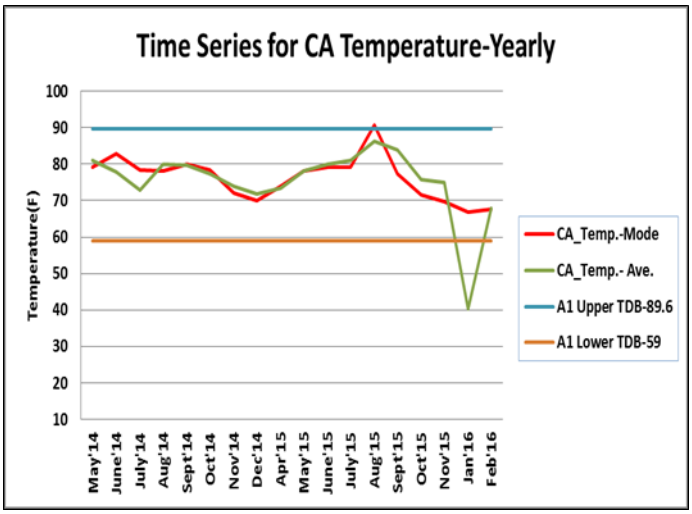

Figure 2-17 Time Series for CA Temperature (Yearly) [15]

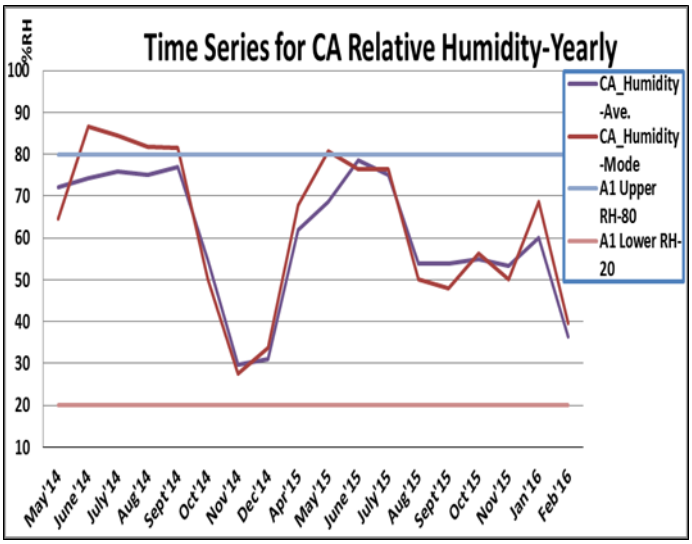

Figure 2-18 Time Series for CA Relative Humidity (Yearly) [15]

The daily statistical analysis of cold aisle temperature and relative humidity in the form of a time series chart is shown in Figures 15 and 16 for 5/30/2014 and 5/31/2014. The daily analysis was carried out for multiple days and different period during the operation. The daily analysis clearly shows that the variation in temperature is not significant for a single day for most of the time of operation. The temperature can be considered as constant for the same day. And, the variation in humidity with respect to temperature can also be supposed in a limited envelope for the same day.

Figures 17 and 18 demonstrate the time series of cold aisle temperature and relative humidity yearly basis for the last two years respectively. The statistics are shown by using the mean (average) and mode (most occurring environments) values for each parameter monthly basis. The figures also show the lower and upper limits for A1 Dry Bulb Temperature (59°F-89.6°F) and A1 relative humidity (20%-80%) respectively. It can be inferred that the data center was operated in ASHRAE class A1 allowable region for the maximum period during its tenure of the last two years.

2.4.2 Particulate Contamination

The filtration of particulates should be as outlined here:

- The room air should be continuously filtered with MERV 8 filters as recommended by ANSI / ASHRAE Standard 127-2007, “Method of Testing for Rating Computer and Data Processing Room Unitary Air Conditioners” (ASHRAE 2007)
- Air entering a data center may be filtered with MERV 11 or MERV 13 filters as recommended by the ASHRAE book titled, “Particulate and Gaseous Contamination in Datacom Environments” [ASHRAE 2014] [1-3]

Site 1 could maintain ISO 8 air quality inside the data center. Site 2 is in Dallas industrial area which is surrounded by different sources of particulate matter. In the modular data center, outside air which enters the mixing chamber from ambient passes through a set of MERV 11 filters. After the commissioning of the modular data center, the lower quality filters were used for the first six months.

Table 2-2 Particulate Matter [15]

Contaminant	Source
Zink Whiskers	Zinc Coated ICT Equipment, Steel Building Studs
Tin Whiskers	Components and products having electroplated tin
Oxide Flake Off	Magnetic Media
Natural and Artificial Fibers	Paper, Cardboard etc
Water Soluble Ionic Salt	Chemical Reactions
Sulphates, Nitrate, Sea Salts	Winds
Lime Dust with Water	Concrete Material
Dust	Farm, especially during ploughing
Toner Dust	Toner
Smoke	Cigarette, Winds
Cellulose Fragments	Traditional Ceiling Tiles and Spaces
Synthetic Rubbers	Belt Drive and Pully

Table 2 illustrates the particulate matter generally found in the nearby surroundings of industrial area like the experiment site and their sources. The modular data center is surrounded by Diesel generator, automobile exhaustion, gas welding and manufacturing process environment which are responsible for different kinds of particulate matter.

2.4.3 Gaseous Contamination

Gaseous contamination should be within the modified ANSI / ISA – 71.04-2013 severity level G1 that meets:

- A copper reactivity rate of less than 300Å / month, and
- A silver reactivity rate of less than 200Å / month [2,3,11,12]

For data centers with higher gaseous contamination levels, gas-phase filtration of the inlet air and the air in the data center is highly recommended.

Since the Restriction of Hazardous Substance (RoHS) for use in IT equipment, Lead-free components have been used, which are susceptible to corrosion than the Lead based components. This resulted in a previously non-corrosive environment experiencing corrosion-related problems.

Corrosion of IT equipment has been defined as the reaction of certain metallic parts with the environment resulting in their degradation. This corrosion accelerates with a rise in temperature (heat) and relative humidity.

The ISA Standard 71.04-1985 provides a classification system using corrosion coupon/reactivity monitoring to determine the corrosive potential for an environment towards IT equipment. It classifies environments with respect to severity of corrosion and type of contaminant [11,12]. The standard defined environments in terms of their overall potential. From this analysis, four severity levels have been established as shown in Table 1 [11-13].

2.5 Measuring Severity Level of MDC

Testing was conducted in the experimental data center located in polluted geographies to measure the severity level.

The copper and silver corrosion rates should be measured as per the AHSRAE location requirements of ¼ and ¾ heights in front of the rack.

Corrosion rates should be determined by two ways:

1. Exposing metal coupons (CCC) for a 30-days period and determining the corrosion product thickness via coulometric reduction.

2. Exposing thin metal films and tracking the real-time corrosion rates by measuring the resistance change of the films. The corrosion rates should be measured at predetermined temperatures and humidity ranging from 20 to 50°C and 30 to 90%RH [2,3].

The Corrosion Classification Coupons were utilized, as a means of obtaining data, which entailed placing corrosion coupons (Copper and silver) exposed at certain locations for a period and measuring the thickness of the corrosion film in angstroms. A Combed Coupon was also installed at the data center to study the type of Particulate contaminants and the role of deliquescent relative humidity in the data center [13].

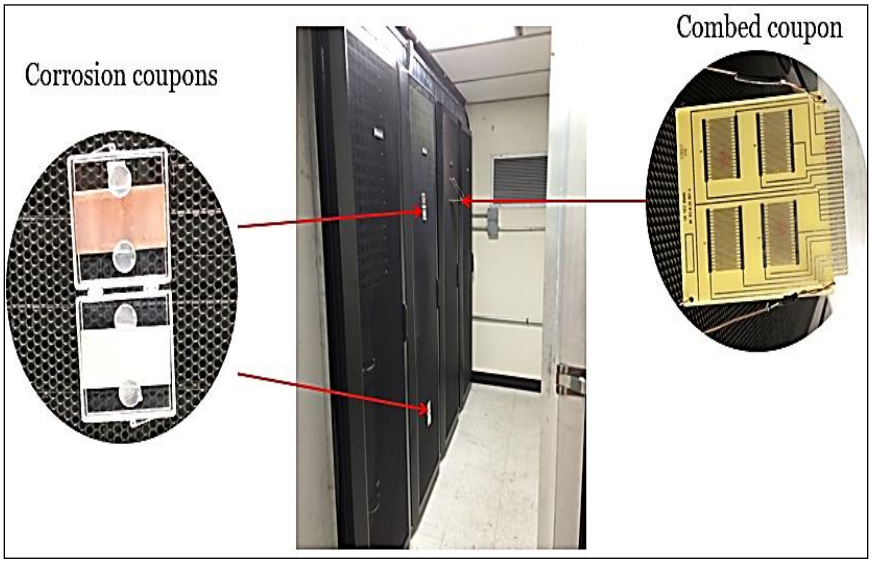

Figure 2-19 Measuring the Severity Level of MDC [13]

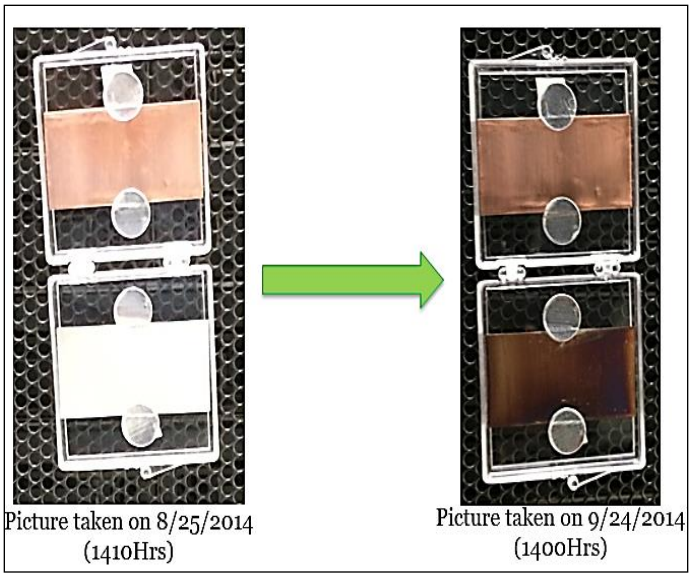

Figure 2-20 Field Exposed Corrosion Coupons [13]

Table 2-3 Corrosion Coupon Field Results [13]

Coupon	Copper corrosion product	Seconds	Thickness of corrosion product, angstroms	Exposure days	Copper corrosion rate, angstroms/month
	Cu2O	98	68		
1	CuO	94	34	30	102
	Cu2S	0	0		
	Cu20	133	92		
2	CuO	83	30	30	122
	Cu2S	0	0		
Coupon	Silver corrosion product	Seconds	Thickness of corrosion product, angstroms	Exposure days	Silver corrosion rate, angstroms/month
1	Ag2S	373	363	30	363
2	Ag2S	240	233	30	233

Table 3 clearly indicates the silver corrosion rate is higher than the copper corrosion rate, which is greater than ISA 71.04-2013 severity level G1 criteria 200Å / month. The corrosion rate was calculated by Coulometric Reduction Method at S&T Group Materials Laboratory by IBM. This indicates that the severity level of the research data center is G2 [13]. The results of combed coupon point toward the significant risk of particulate contaminants, including both fine dust and coarse dust particles.

2.6 Observations

Figure 2-21 stuck fine dust and carbon particles on hood [15]

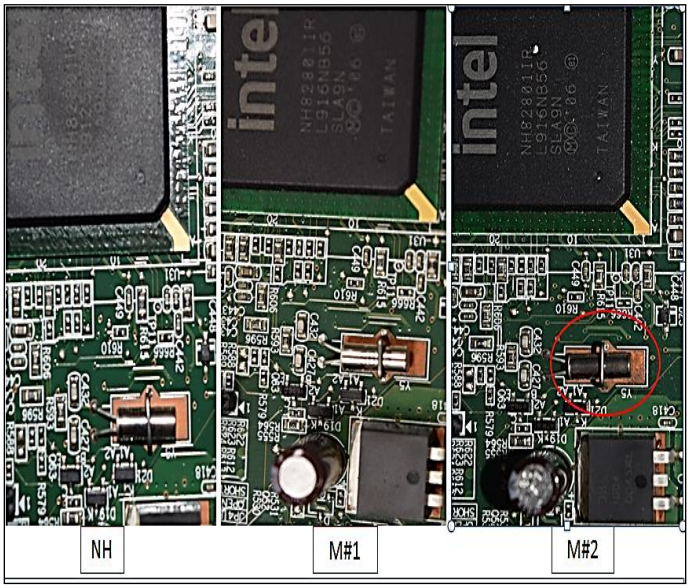

Figure 2-22 Accumulated dust on PCB and Copper [15]

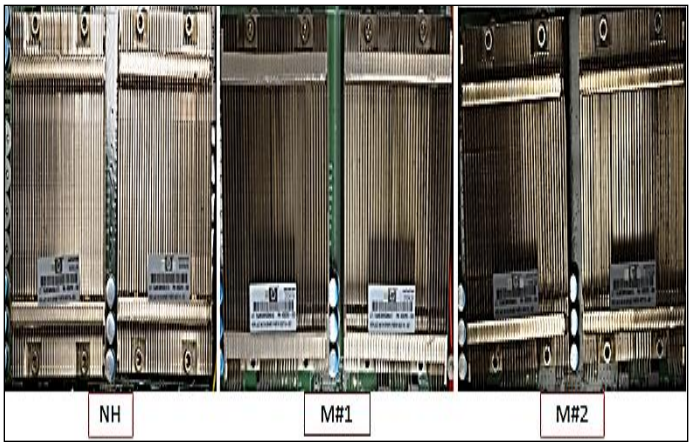

Figure 2-23 Lodged dust on heat sinks [15]

Figures 21 – 23 discuss about the implications of harsh environment and elevated temperature-relative humidity operating conditions of the last two years on the server under study from the modular data center. Here, there were three servers chosen for study. About location, servers were removed from the ¾ height of the fourth rack from the inlet of both the sites. One idle server from site 1 represented as NH and two servers from MDC (Site 2): one idle M#1 and the other used M#2 were opened and pictures were taken from different locations to observe the cumulative corrosion damage to figure out reliability challenges. The particulate contamination was found significant as shown in figures. The particulate matter was stuck and jammed at different important locations.

2.7 Discussion

The implication of found particles may be on both performance and reliability of IT equipment. Very high concentration of particulate contaminant may degrade:

- Heat sink thermal performance
- Detrimental to separable connectors and mechanical devices.

But at this level of concentration found in MDC, the critical and the deliquescence relative humidity of particulate matter are the most important factors determining the possibility of particulate matter getting wet and thereby short circuiting closely spaced features on printed-circuit boards.

- Efficiency of the filters is very less for the dust particles of size PM2.5

- PCBs in IT equipment's working in high humid situations will get wet at 50-65% relative humidity in view of the fine, clean (PM2.5) that will get accumulated on the surface of PCBs with time.
- Leakage current flow across the neighboring highlights of the PCBs due to wetting.

Properties of found Particulates that affect equipment:

Thermal Conductivity - The accumulation of solid dust particles significantly reduces the surface area allocated to dissipate the heat from the systems and creates the thermal insulating layer, which leads towards the overheating of the components. For example, the cooling fans of power electronics can be significantly insulated by surface deposits of substances such as textile fibers.

Magnetic permeability - Magnetically penetrable substances can assemble in magnetic fields: for instance, the development of power loops or galvanometer developments can be seriously limited or altogether deactivated by magnetic substances gathering in air holes of the perpetual magnets. In like manner, electrical engines can be significantly deteriorated by magnetic aggregation between rotor and stator.

Electrical conductivity- Solid substances are eventually classified into two categories, electrically conducting and highly insulated substances.

The particulate matter like metals, carbon blacks, and coal dusts has electrically conducting properties and can cause short circuiting when accumulated between terminals.

Insulating particles can settle static charges, which spoil the working of PCs and Integrated circuits. Under high relative humidity, few insulators tend to absorb moisture. This causes an expansion in conductivity and can bring about hardware failures because of electrical spillage.

Adhesiveness- This attribute causes contaminant to hold strong and collect on the surface. This strengthens undesirable impacts, for example, thermal protection, high voltage relays, and bearing failures. Adhesive qualities might be intrinsic to the contaminants, for example, tobacco smoke, which contains sticky tars.

Abrasiveness – This is a critical property in mechanical disintegration by high speed strong contaminants. It likewise adds to the quickened wear to moving parts.

Corrosivity - Airborne particulates matter changes from hard crystalline structures, for example, metallic minerals of delicate permeable structures, such as, climatic dust, fly slag, and smoke. Dust particles may ingest vaporous contaminants and moisture along these lines, and therefore, become corrosive in nature [12].

Here, there are some recommendations to deal with this challenge:

- The particulate matter in data centers must be kept clean to ISO Standard 14644-1 Class 8 (ISO 1999).
- MERV rating of 13 or higher is required to filter fine particles of size PM2.5 from the data centers.
- Deliquescent relative humidity of dust measurement as per Appendix A **[11,12]**.
- The critical relative humidity (CRH) of particulate matter must be greater than the relative humidity in the data center.
- Every effort should be made to filter out dust that has **CRH** and **deliquescent relative humidity** less than the maximum allowable relative humidity in the data center.
- Sources of particulate contamination inside data centers should be reduced.
- Both natural and anthropogenic sources of particulate matter should be controlled.

2.8 Conclusions And Future Scope

The rapid expansion of the IT equipment business and increasing pressure to reduce energy consumption, data centers with specific applications and specific geographies should move their operating conditions up to ASHRAE A1 allowable environment considering the danger of short-circuit failure mode due to particulate matter. The weather data bin analysis provides the opportunity of utilizing free air cooling for the maximum hours during a year. The correlation of historical environmental trend data with its implications supports the usage of air-side economizers for a certain period with proper measures of contamination. From an industry perspective, it should be noted that in the four years of operation in the hot and humid Dallas climate using only evaporative cooling or fresh air cooling, *we have not seen a single server*

failure in our research pod. That performance should highlight an opportunity for significant energy savings for data center operators in a much broader geographic area than currently envisioned with evaporative cooling.

It is required to determine the chemical composition and temporal and spatial variation of the gaseous contamination in real world data centers with ANSI/ISA Standard 71.04-2013 severity level G2. Gas Analyzers should be used to predict the gaseous composition of the air and simulating the same conditions in the laboratory to understand the parameters affecting the corrosion rate in depth. The test can be conducted by using copper and silver corrosion coupon and state-of-the-art test PCBs in experimental data centers with ISA severity level G2 or G3. The accelerated testing on real computers considering the self-heating effect should be carried out to understand the reliability degradation of an actual equipment due to corrosion.

It is essential to manufacture hardware robust against PCB creep corrosion /short ckts caused by settled particulate matter in humid environments and surface mount resistor open circuits by gaseous contamination. The corrosion testing should be done in real world field conditions with larger data as laboratory testing facility do not represent the environment in data centers. It is necessary to develop **a corrosion reliability model** to determine an end of life of servers.

Note: The servers used for this experiment were donated to the University. The initial stage was not thoroughly evaluated before installation. These results were compared with similar server that was donated to us but not deployed for the operation. It is recommended that new servers should be deployed in future work.

2.9 Acknowledgments

This work is supported by NSF I/UCRC in Energy-Smart Electronic Systems (ES2).

2.10 References

1. ASHRAE DOE Course: Save Energy Now Presentation Series, 2010, Dallas, TX, USA
2. Jimil M. Shah, “Reliability challenges in airside economization and oil immersion cooling”, UTA-THESIS, 2016-05-16, Shah, Jimil Manojbhai, 0000-0003-2297-7413.
3. Prabjit Singh, Levente Klein, Dereje Agonafer, Jimil M. Shah and Kanan D. Pujara, “Effect of Relative Humidity, Temperature and Gaseous and Particulate Contaminations on IT Equipment Reliability, DOI: 10.1115/IPACK2015-48176, ASME InterPACK 2015, San Francisco, CA.
4. Thermal Guidelines for Data Processing Environments, ASHRAE Datacom Series, 1st Edition, 2004, ASHRAE, Atlanta, GA, USA.
5. Thermal Guidelines for Data Processing Environments, ASHRAE Datacom Series, 2nd Edition, 2008, ASHRAE, Atlanta, GA, USA.
6. Thermal Guidelines for Data Processing Environments, ASHRAE Datacom Series, 3rd Edition, 2012, ASHRAE, Atlanta, GA, USA
7. Burnett W. H., F. S. Sandroff and S. M. D’Egidio, “Circuit failure due to fine dust mode particulate air pollution,” ISTFA ’92, The 18th Int’l Symposium for Testing & Failure Analysis, Los Angeles, CA, 17-23 Oct 1992, 329-333.
8. Cole, M., L. Hedlund. T; Kiraly, S. Nickel, P. Singh and T. Tofil, Harsh Environmental Impact on Resistor Reliability, SMTA Int’l Conf, Proc., 24 Oct 2010.
9. Directive 2002/95/EC of the European Parliament and of the Council of 27 January 2003 on the Restriction of the use of Certain Hazardous Substances on Electrical and Electronic Equipment Official Journal L 037, February 13, 2003, 19-23.
10. Fu, H., C. Chen, P. Singh, J. Zhang. A. Kurella, X. Chen, X. Jiang, J. Burlingame and S. Lee, Investigation of Factors that Influence Creep Corrosion on Printed Circuit Boards,” SMTA Pan Pacific Microelectronics Symposium, Kauai, 14-16 Feb 2012.
11. ISA-71.04-1985, “Environmental conditions for process measurement and control systems: Airborne contamination,” ISA-The Instrumentation Systems, and Automation Society, Approved 3 Feb 1986.

12. ISA-71.04-2012, “Environmental conditions for process measurement and control systems: Airborne contaminants,” ISA-The Instrumentation Systems, and Automation Society, Revised 09 October 2012.
13. Oluwaseun Awe, “The Effects of Temperature and Relative Humidity on Current and Future technology hardware, under real data center conditions in an ANSI/ISA classified G2 Environment – Results of Hardware Exposure”, UTA-DISSERTATION, 2016-08-12, Awe, Oluwaseun Michael.
14. Betsegaw Kebede Gebrehiwot, “Maximizing use of air-side economization, direct and indirect evaporative cooling for energy efficient data centers”, UTA-DISSERTATION, 2016-05-10, Gebrehiwot, Betsegaw Kebede, 0000-0002-0225-3525.
15. Shah, J. M., Awe, O., Agarwal, P., Iziren, A., Agonafer, D., Singh, P. J., Kannan, N., and Kaler, M., Qualitative Study of Cumulative Corrosion Damage of IT Equipment in a Data Center Utilizing Air-side Economizer, ASME IMECE 2016, November 11-17, 2016, Phoenix, Arizona, USA

Chapter 3

Experimental Description of Information Technology Equipment Reliability Exposed to a Data Center Using Airside Economizer Operating in Recommended and Allowable ASHRAE Envelopes in an ANSI/ISA Classified G2 Environment

Abstract

Airside economizers lower the operating cost of data centers by reducing or eliminating mechanical cooling. It however increases the risk of reliability degradation of IT equipment due to contaminants. IT Equipment manufacturers have tested the equipment performance; and guarantee the reliability of their equipment in environments within ISA 71.04-2013 severity level G1 and the ASHRAE recommended temperature-RH envelope. IT Equipment manufacturers require data centers operators to meet all the specified conditions consistently before fulfilling warranty on equipment failure. To determine the reliability of electronic hardware in higher severity conditions, field data obtained in real data centers is required. A corrosion classification coupon experiment as per ISA 71.04-2013 was performed to determine the severity level of a research data center located in an industrial area of hot and humid Dallas. The temperature-RH excursions were analyzed based on time series and weather data bin analysis using trend data for the duration of operation. After some period of operation, a failure was recorded on two PDU's located on the hot aisle. The damaged hardware and other hardware were evaluated, and cumulative corrosion damage study was carried out. The hypothetical estimation of the end of the life of the components is provided to determine the free air cooling hours for the site. There was no failure of even a single server operated with fresh air cooling in an industrial area of Dallas shows that using evaporative/free air cooling is not detrimental.

3.1 Introduction

IT equipment manufacturers are now becoming increasingly aware of the risk of contamination on their products. Their products are now tagged with information that clearly indicates environmental limits for safe operation. Nowadays, data center administrators/operators must demonstrate operation of their equipment within the acceptable environment before warranty claims can be fulfilled [1-2]. The American Society of Heating, Refrigeration and Air-

Conditioning Engineers' (ASHRAE) TC9.9 committee has specified certain recommendable and allowable envelopes for a data center operation in [2-6].

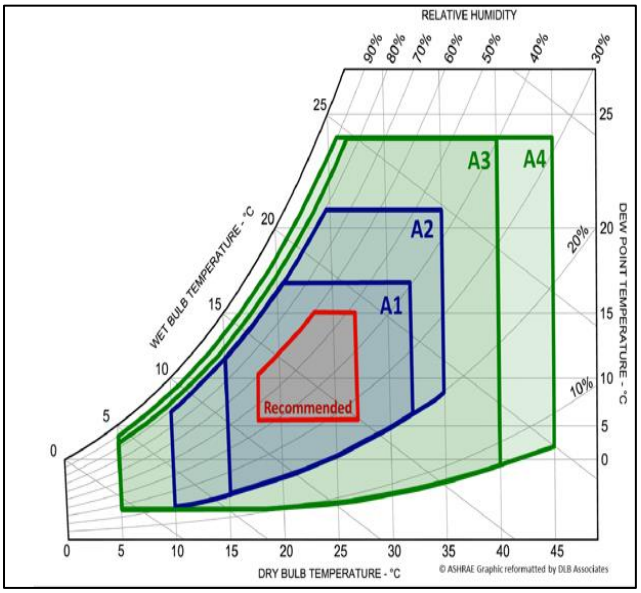

Figure 3-1 ASHRAE psychrometric chart showing the IT equipment manufacturer recommended and the allowable ranges

Psychrometric chart in Figure 1 illustrates that the recommended range for temperature and humidity is from 18°C to 27°C and up to 60% respectively. [2-6]. Air entering the data center through airside economizers outside the recommended envelope is a potential risk to IT equipment within the Data Center [6]. Major environmental factors causing failure of IT equipment are temperature, relative humidity, gaseous and airborne particulate contamination [6]. The most common source of gaseous contaminants is Sulphur-bearing gases. These gases, at the right temperature and humidity, react with copper and silver present in IT components, thereby depositing its byproducts on the surface of the components. The creep corrosion in circuit boards is the most commonly reported failure mode by gaseous contaminants. Another mode of failure is silver metallization in surface mount resistors causing open circuits in the resistors [2,3,7-10].

Corrosion of IT equipment is the reaction between certain metallic parts (specifically copper and silver) and the surrounding environment which causes deterioration of the parts. The corrosion accelerates with an increase in temperature and relative humidity.

The composition of the contaminants in the air determines the corrosivity of the environment. Determination of this composition is not a trivial task. A guide for specifying data

center environmental cleanliness has been published by ANSI/ISA-71.04-1985. The environmental classification limits adopted by ANSI/ISA uses a method called “reactive monitoring” to quantify and classify the severity level of the environment [11-12]. In reactive monitoring, analysis of corrosion product thickness and chemistry are performed on copper coupons, exposed to environment for a one-month period. Similarly, analysis on silver coupons is conducted to study environmental chemistry of sulfur-bearing gases.

Gaseous Corrosion severity level per ANSI/ISA-71.04-1985 is described in Table 1. Class G1 is a mild severity level environment such that corrosion is not a factor in determining equipment reliability. To classify the site of a data center as a G1 environment, the corrosion rate must not exceed 300 Å/month and 200 Å/month for copper and silver respectively. G2 classified environment is described as a moderate environment. Corrosion effect is significant from equipment reliability point of view in this environment. Copper corrosion rate is between 300-1000Å/month for a G2 environment. G3 is a harsh environment in which there is a high probability that corrosive attack will occur. Copper corrosion rate is between 1000-2000Å/month for this environment. A GX severe environment is an environment in which only packaged equipment are expected to survive. It has a Copper corrosion rate greater than 2000Å/month [11-13].

Table 3-1 Gaseous corrosivity levels as per ANSI-ISA-71.04-2013 [11-13,15,16]

Class	Severity Level	Copper Reactivity (Å)	Silver Reactivity (Å)	Comments
G1	Mild	<300	<200	Corrosion is not a factor in determining equipment reliability
G2	Moderate	<1,000	<1,000	Corrosion effects are measurable and corrosion may not be a factor. ENIG and ImmAg PCB surface finish failures.
G3	Harsh	<2,000	<2,000	High probability that corrosive attack will occur. OSP and ImSn PCB surface finish failures.
GX	Severe	≥2,000	≥2,000	Only specially designed and packaged equipment to survive.

Gaseous contamination is not expected to be a concern for Data center (DC) administrators when operating in an environment that is within the ANSI/ISA standard (2013) severity level G1. IT manufacturers also do not allow the environment to go outside the recommended range, into allowable ranges.

Figure 3-2 Short in adjacent solder hole and bus line as a result of creep corrosion [2]

This paper serves multiple purposes including: to determine the severity level of the research data center site as per ANSI/ISA 71.04-1985 and to provide the end of a life of IT equipment operating at a harsh environment in a real-world data center. The experiments were conducted in two parts; the first was to evaluate the environment severity of the experimental data center using the procedures specified in ASHRAE [11-13] with both, the silver and copper coupons. The second experiment was a continuous operation of the data center until a failure of any of the electronic hardware was reported.

Knowing the limits of operation of certain IT equipment hardware is helpful in providing IT equipment manufacturers with some information that might encourage them to make their equipment more robust to perform reliably even beyond the recommended environmental severity level. Based on the literature review, there are several reported laboratory and field experiments to understand the impact of corrosive environment on IT hardware. These experiments have either been performed to understand the corrosion rate of an environment, or to establish the mode of failure. Others have been too focused on the measurement techniques. This paper presents a first attempt of addressing such experiments in a real-world data center especially in a

G2 class environment. As being unacceptable, no data center administrator will allow such environment in their facilities.

3.2 Research Data Center (Rdc) Site Description

The research data center is a modular data center situated in the Dallas industrial area which is polluted due to surrounding manufacturing activities. The RDC utilizes an airside economizer with direct and indirect evaporative cooling for the thermal management. It has 4 racks with IT hardware like servers, PDUs, UPS systems, and Storage devices. Figures 3 and 4 show the front and side views of the RDC respectively.

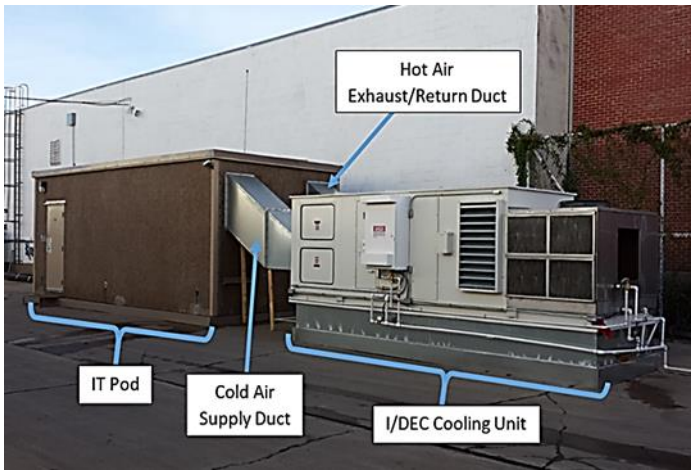

Figure 3-3 Research Data Center at Dallas Industrial Area

Figures 3 and 4 show different components of the RDC such as the IT pod and the cooling unit (which consists of the cold air supply duct, hot air exhaust/return duct, mixing chamber and I/DEC cooling Unit). The size of the research modular data center is 10ft x 12ft x 28ft [14]. The inside view of the IT pod is presented through Figure 5. Figure 5 represents the cold aisle and hot aisle of the RDC. Air enters through the supply duct into the cold aisle across the cabinet to cool the systems, then into the hot aisle from where it returns through the return duct.

3.2.1 IT Pod Configurations:

- Size: 126 in X 85.5 in
- IT Equipment: vent with 45º Louver Angle
- Outlet Dimensions:13X27 HP SE1120 Servers (120 Servers)

- Cabinet: S6212B PANDUIT Rack
- Flow Provisioning: End inlet and Outlet configuration
- Inlet Dimensions :13X27 vent [14]

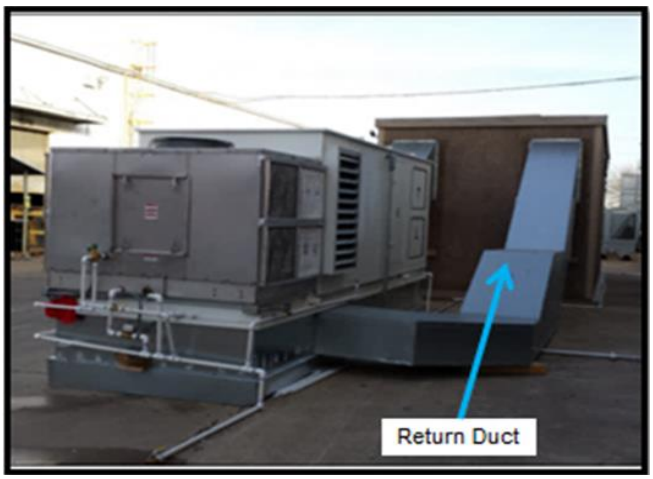

Figure 3-4 Research data center showing return duct

Figure 3-5 Experimental IT Pod Showing the Cold and Hot Aisles

The cooling unit is air-side economizer with direct and indirect evaporative cooling. The data center uses free air cooling in suitable environmental conditions and uses direct cooling and/or indirect cooling and/or return air and/or mixing of return air with outside air to achieve ASHRAE recommended operating conditions in the cold aisle when the environmental conditions are extreme.

3.2.2 Physical Environment: Temperature and Relative Humidity:

Over the course of the experiments, temperature and relative humidity readings were taken at the cold aisle and hot aisle. The physical environmental conditions of the IT pod were classified in the different regions of psychrometric chart and summarized below. The regions in figures 6 and 7 show recommended and Class A1 allowable regions of the cooling units (ASC-15-2A11) to bring outside air into the target regions. For both charts, cooling unit cannot be used for Region 1, since it brings moist air in the target regions. It necessitates the use of Dehumidifiers, DX cooling units, or multistage IEC units. For regions except Region 1, the cooling unit can be used to bring outside air into the target regions. Below is a summary of how this may be achieved if outside air falls in:

- Region 2: The cooling unit mixes hot return air with outside air
- Region 3: Directly takes outside air
- Region 4: Based on the recommended envelope either DEC or IEC can be used. However, according to the Class A1 allowable envelope, only DEC is guaranteed to work for this region. I/DEC mode can be used for more efficient results.
- Region 5: Use of IEC is must, I/DEC can be used for more efficient results
- Region 6: mix hot return air with outside air. It may be necessary to run the DEC section to add moisture
- Region 7: Must use DEC, additionally I/DEC can be used for more efficient results.
- Region 8: Both IEC and DEC must be used [14]

Various scenarios summarized above are the guidelines for operating the RDC. This was plotted on psychrometric charts overlaid with ASHRAE recommended and allowable regions as shown in figures 6 and 7.

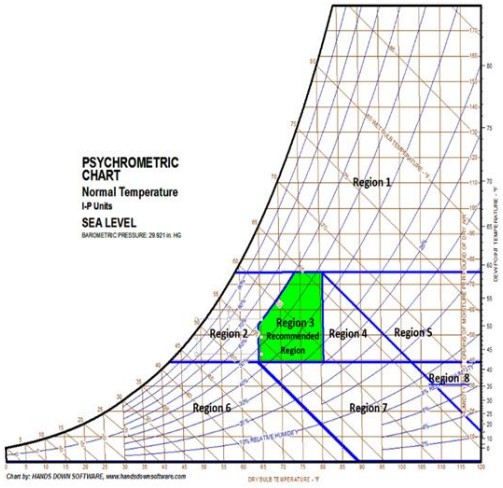

Figure 3-6 Psychrometric chart regions based on the recommended envelope [14]

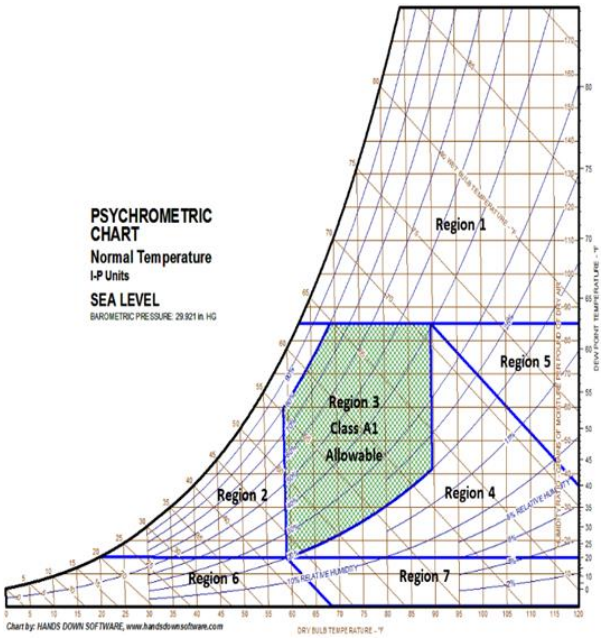

Figure 3-7 Psychrometric Chart regions based on Class A1 allowable region [14]

3.3.3 Particulate Contamination:

For data centers without airside economizers, filtration schemes have been determined to achieve a level of cleanliness of Class 8 of ISO 14644-1.

The filtration of particulates should be as outlined here:

1. Continuously filter room air with MERV 8 filters as recommended by ANSI/ASHRAE Standard 127-2007, “Method of Testing for Rating Computer and Data Processing Room Unitary Air Conditioners” (ASHRAE 2007)
2. Filter air entering data center with MERV 11 or MERV 13 filters as recommended by the ASHRAE book with title “Particulate and Gaseous Contamination in Datacom Environments” (ASHRAE 2014) [1-3]

In this research data center, MERV 11 was installed to filter off particulates that flow in with the outside air and enter the mixing chamber from the ambient.

The following table 2 illustrates the types and sources of particulate materials generally found in the industrial area, where the RDC is sited [15,16].

Table 3-2 Particulate matter and their sources

Contaminant	**Source**
Zink Whiskers	Zinc Coated ICT Equipment, Steel Building Studs
Tin Whiskers	Components and products having electroplated tin
Oxide Flake Off	Magnetic Media
Natural and Artificial Fibers	Paper, Cardboard etc
Water Soluble Ionic Salt	Chemical Reactions
Sulfates, Nitrate, Sea Salts	Winds
Lime Dust with Water	Concrete Material

Dust	Farm, especially during ploughing
Toner Dust	Toner
Smoke	Cigarette, Winds
Cellulose Fragments	Traditional Ceiling Tiles and Spaces
Synthetic Rubbers	Belt Drive and Pully

An important aspect of particulate contamination to look out for is its deliquescent relative humidity, whereby dust and/or salts of gaseous contaminants can absorb moisture, get wet, and in turn cause corrosion and/or ion migration which degrade the IT parts.

3.3.4 Gaseous Contamination:

As per ANSI/ISA-71.04-1985, gaseous contamination should be within the severity level G1 which meets the following criteria:

1. Copper reactivity rate of less than 300 Å/month
2. Silver reactivity rate of less than 200 Å/month [2,3,11,12]

For data centers that do not meet the above mentioned criteria for copper and silver corrosion, gas-phase filtration is recommended to prevent gaseous contaminants from entering the data center. The Restriction of Hazardous Substances Directive (RoHS) banned the use of Lead in the circuit boards, which led to the use of Silver as the soldering material. These circuit boards are highly susceptible to corrosion due to gaseous contaminants. The common gaseous contaminants are sulfur dioxide (SO2) and hydrogen sulfide (H2S), with other gases such as Nitrogen dioxide (NO2), chlorine, and ozone (O3), which are playing an active role in the corrosion of IT equipment.

The experiment was carried out to determine the severity level of the research data center facility as per ANSI/ISA 71.04-1985 using the corrosion classification coupons.

3.3 Coupon Testing Experiment to Measure the Severity Level of Research Data Center

Testing was conducted in the experimental data center located in polluted geographies to measure the severity level. The copper and silver corrosion rates should be measured as per the AHSRAE location requirements of ¼ and ¾ heights in the front of the rack.

Corrosion rates should be determined by two ways:

1. Exposing metal coupons (CCC) for a 30-days period and determining the corrosion product thickness via coulometric reduction.
2. Exposing thin metal films and tracking the real-time corrosion rates by measuring the resistance change of the films. The corrosion rates should be measured at predetermined temperatures and humidity ranging from 20 to 50°C and 30 to 90% RH.

For this experiment, Copper and Silver coupons were placed in front of the rack as shown in figure 6 below at ¼ and ¾ heights to check the corrosion severity level. The coupons were placed facing the incoming air into the rack and were also adjusted slightly for adequate air flow impact while entering the rack. Dead air flow spot was avoided. The coupons were left exposed for a period of 1(one) month after which the corrosion product thickness was determined via coulometric reduction [2,3].

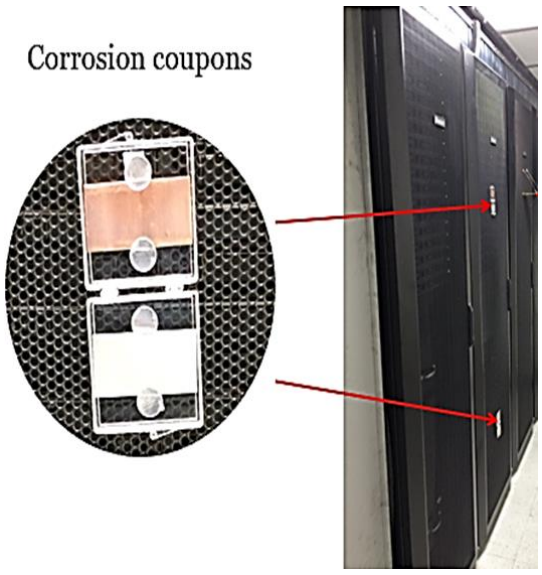

Figure 3-8 Coupon Location at the Cold Aisle section of MDC

3.4 Results and Discussions

3.4.1 Coupon Experiment Results:

For the coupons experiment, after 30 days of exposure, the coupons were retrieved and analyzed using coulometric reduction. Figure 9 below shows the state of the coupons before and after 30 days of exposure. The corrosion rate was calculated by Coulometric Reduction Method at S&T Group Materials Laboratory by IBM.

Copper coupons 1 and 2 in table 3 showed the thickness of corrosion products only for Cu_2O, CuO, and none for Cu_2S, while for corrosion thickness of products of Silver, only Ag_2S was found on both coupons. The interest of this paper is to establish the environmental class from the amount of corrosion thickness in Angstrom during the period of exposure. On both silver coupons, the corrosion thickness exceeds the G1 severity zone. This suggests that for the month, based on this information the Data Center environment can be classified as an ISA 71.04-2013 G2 severity level.

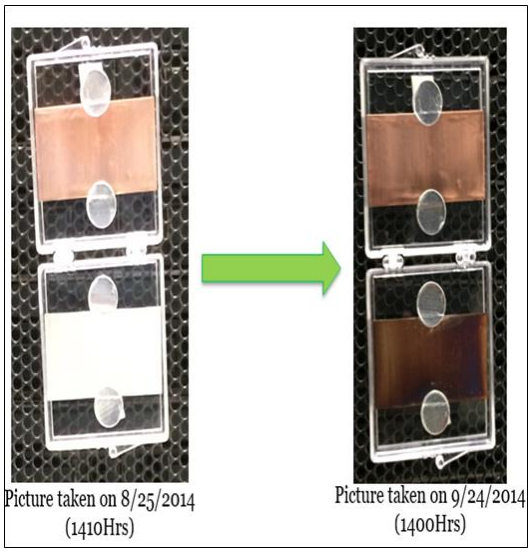

Figure 3-9 Copper and Silver Coupons before and after the 30-days exposure

Table 3-3 Coulometric Results of the Corrosion thickness on both Copper and Silver Coupons

Coupon	Copper corrosion Product	Seconds	Thickness of corrosion product, angstroms	Exposure days	Copper corrosion rate, angstroms/month
1	Cu_2O	98	68	30	102
	CuO	94	34		
	Cu_2S	0	0		
2	Cu_2O	133	92	30	122
	CuO	83	30		
	Cu_2S	0	0		
Coupon	Silver corrosion Product	Seconds	Thickness of corrosion product, angstroms	Exposure days	Silver corrosion rate, angstroms/month
1	Ag_2S	373	363	30	363
2	Ag_2S	240	233	30	233

Details of the corrosion product from coulometric evaluation are described in Table 3 above. Industrial activities around the area have higher Sulfur content in the atmosphere as you will normally not see in the US or the environs. This provides an opportunity to have a potential environment beyond G1, although there is currently no data to suggest that the same environment is possible all year around. Figures 10 and 11 describe the potential readings in Volts with the elapsed time in seconds.

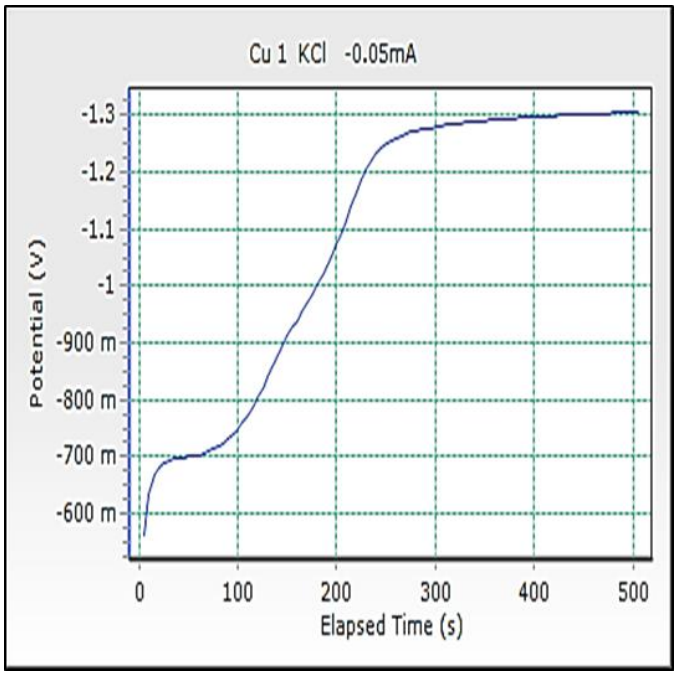

Figure 3-10(a) Cu 1 KCl -0.05mA

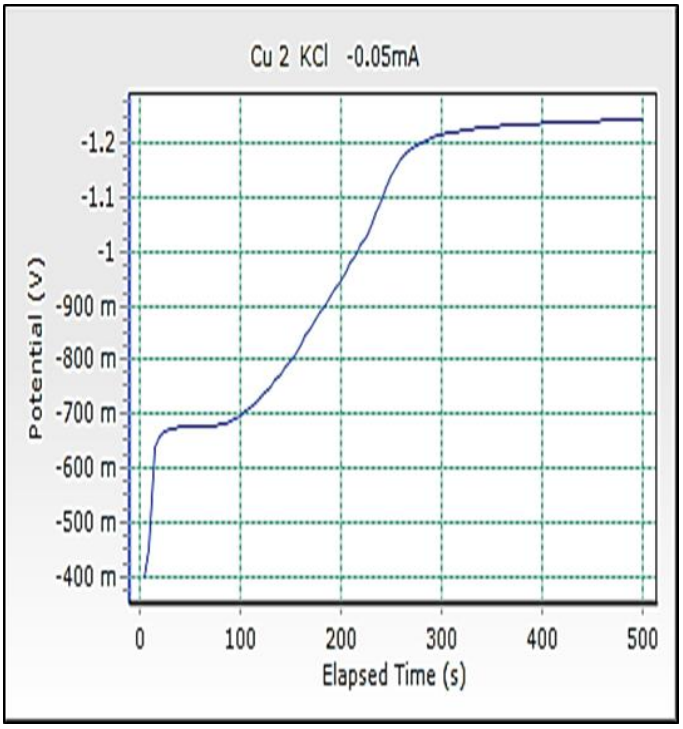

Figure 3-10(b) Cu 2 KCl -0.05mA

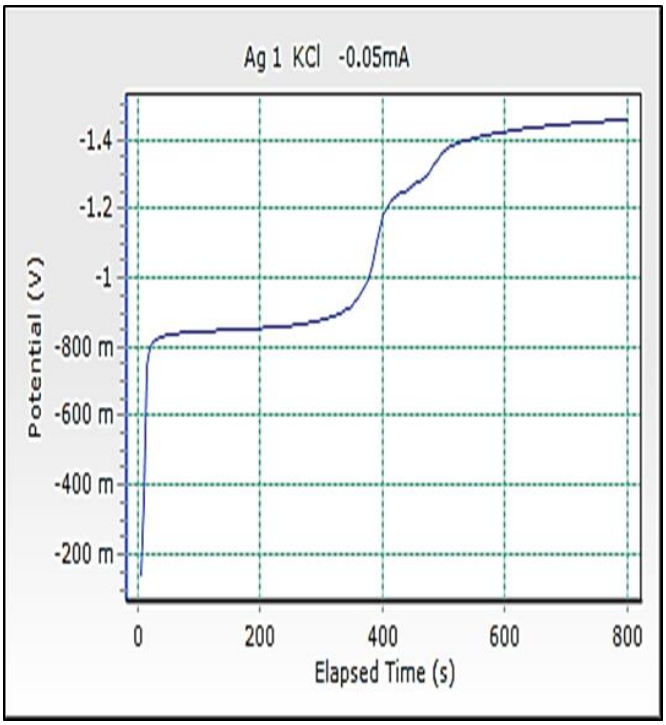

Figure 3-11 (a) Ag 1 KCl -0.05mA

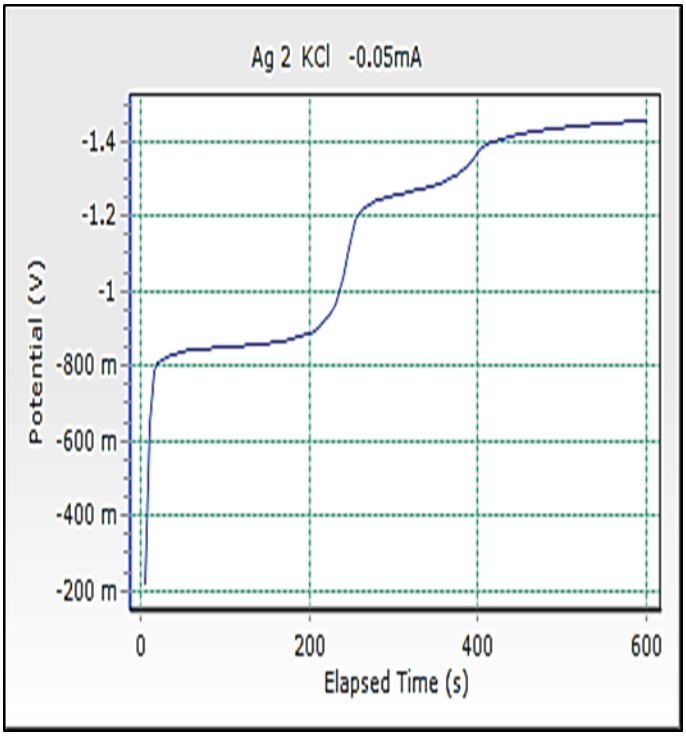

Figure 3-11 (b) Ag 2 KCl -0.05mA

In Figures 10a and 10b, the plateau at about 600 mV is due to the reduction of Cu_2O oxide to Cu metal. The other plateaus at 800 mV for CuO and at 1050 mV for Cu_2S are not dominant as Cu_2O plateau is. This means that Cu_2O is the dominant corrosion product on the copper foil. In Figures 11a and 11b, there are two plateaus: One at 820 mV for the reduction of Ag_2S to Ag. The other plateau at about 1250 mV is not associated with the reduction of any corrosion product. The dominant corrosion product on Ag is Ag_2S.

3.4.2 Weather Bin data analysis on Psychrometric Chart Regions based on Trend data of Research Data Center:

The bin data in figure 12 shows average inlet conditions for the month of April 2015 at the cold aisle. The information as plotted on the psychrometric chart with the dry and wet bulb temperatures are mostly in the A3 allowable region from ASHRAE TC 9.9 guidelines. It is an indication that our IT equipment was exposed during this period to conditions well outside the recommended zone. At allowable A3, you have an upper dry bulb temperature of 40°C.

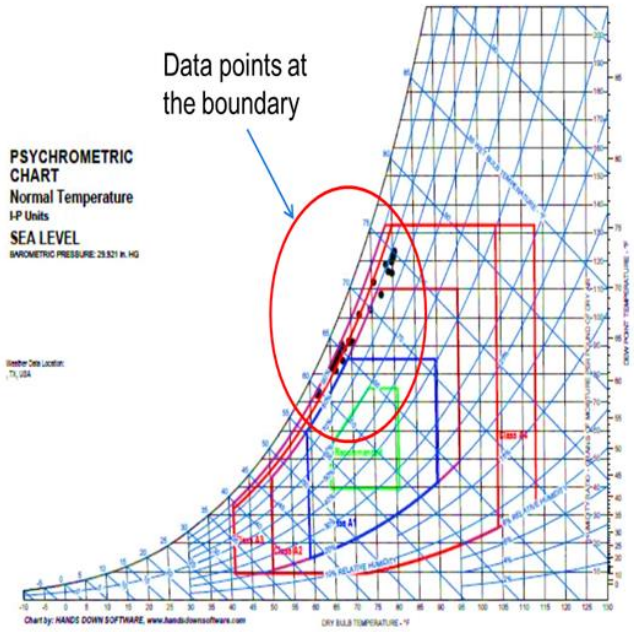

Figure 3-12 Bin Data showing average Inlet conditions for the month of April 2015

For the month of May, as shown in figure 13, there is some distribution of inlet conditions across A2 – A3. Here, some are in A1 but none are in the recommended envelope. There are slight excursions into A4 zone as well.

In the month of June as shown in figure 14 along with the distribution across A1-A4, there were excursions well outside both recommended and allowable zones. Although the percentage excursions outside the allowable zone are less than 10% in this case, the IT equipment is not rated for such environments. It might have negative implications on failed hardware.

In the month of July as shown in figure 15, the excursions outside the recommended/allowable envelope are almost the same as June and they have similar distributions.

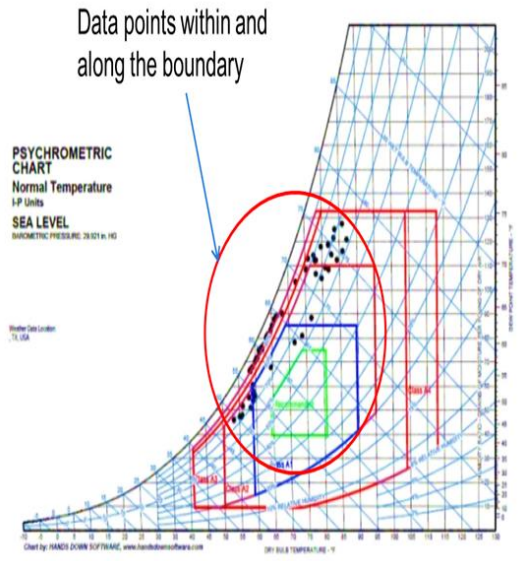

Figure 3-13 Bin data for the month of May 2015

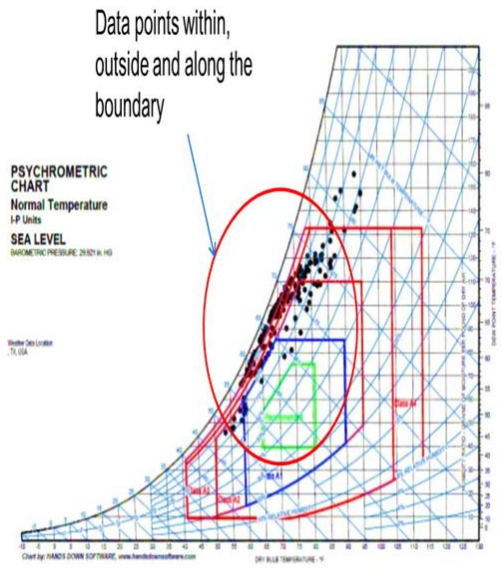

Figure 3-14 Bin data showing average inlet conditions for the month of June 2015

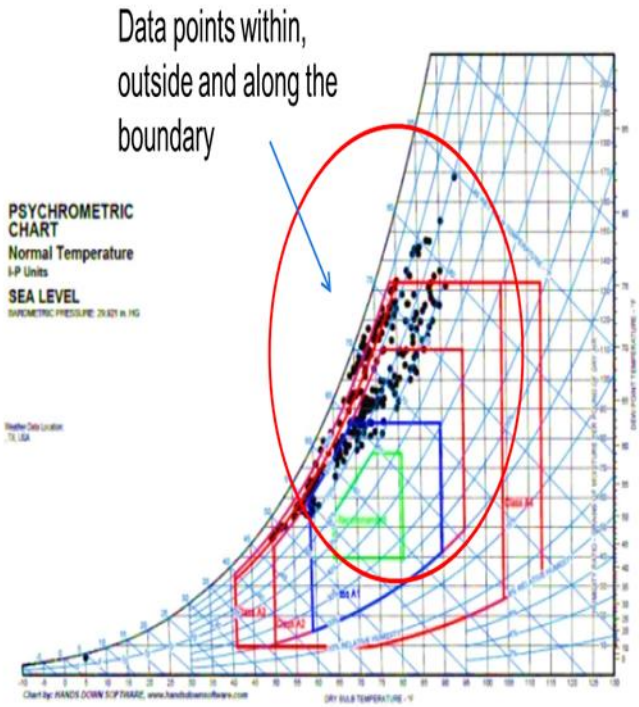

Figure 3-15 Bin data for the month of July 2015

3.4.3 Discussion on a PDU Failure:

The research data center was under operation until a failure was recorded on two PDUs at the hot aisle adjacent to the racks.

Figure 3-16 Failed PDU-1 at hot aisle

Figures 16 and 17 show failed PDUs at the **hot** aisle. Copper connectors as seen, appear to have been exposed directly to the surrounding air with the right temperature and moisture and certain levels of contaminants. As we can see from the picture, the insulator appears burnt exposing the cables to the atmosphere. Rust on the steel screw due to moisture was observed. Oxide formed on the connector after the short circuit was also found. The temperature-humidity trend data at the time of PDUs' failure were:

- Outside Air Temperature : 67 F
- Cold Aisle Temperature : 66.48 F
- Hot Aisle Temperature : 80.02 F
- Outside Humidity : 23.4%
- Cold Aisle Humidity : 87.49%
- Hot Aisle Temperature : 50.56%

This indicates the possibility of condensation in the hot aisle. The hot aisle (high temperature and high humidity air) might have caused condensation on the chassis and on the surface of power supply components. There was a rapid change in outside air conditions based on trend data and reaction of direct evaporative cooling towards humidity variations. The high temperature of hot aisle and high humidity from supply air because of evaporative cooling might have led towards shorts and damage of powered power distribution units (PDUs). However, there are 7 PDUs, out of which only two failed.

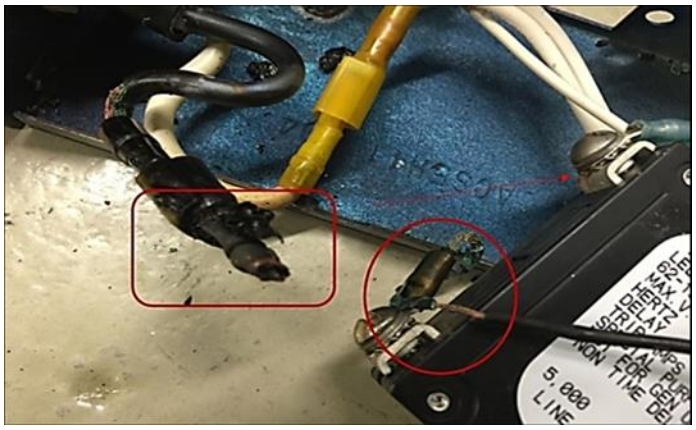

Figure 3-17 Failed PDU-2 at hot aisle

3.4.4 Qualitative Observation of Servers

In addition, the following hardware components shown in figures 18, 19 and 20 respectively are of the server under operation in the research data center, visually inspected for possible gaseous/particulate contaminants.

1. Heat Sinks
2. Server fans
3. Printed Circuit Boards

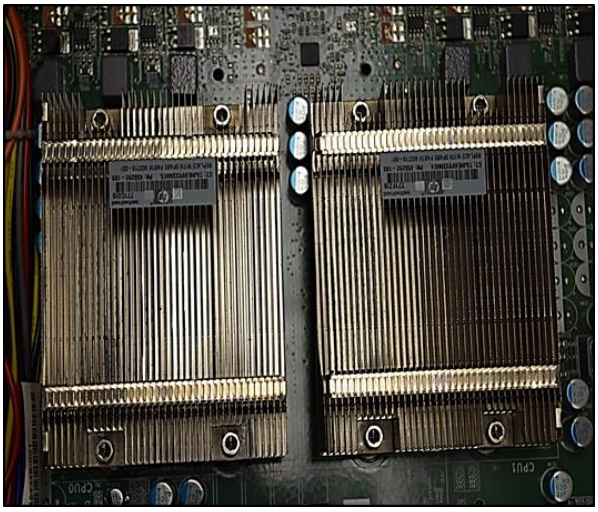

Figure 3-18 Lodged dust on heat sinks

Figure 3-19 Accumulated dust on fans

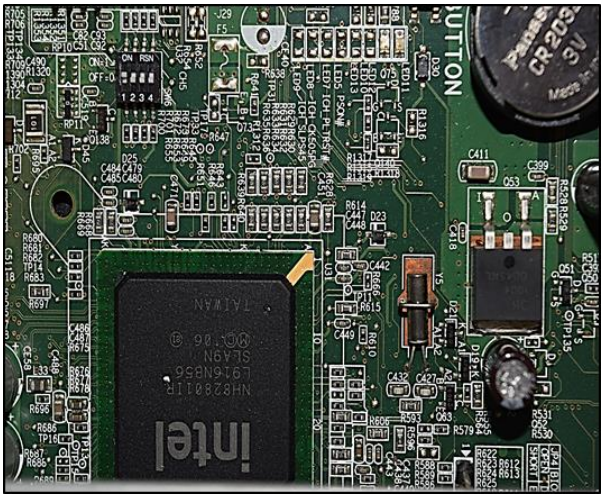

Figure 3-20 Dust on Printed Circuit Boards

No significant degradation due to corrosion was observed on the above components other than pockets of dusts around the server fans and heat sinks as shown in the above figures. This is attributed to the quality of installed MERV 11 particulate contaminant filter at the Data Center. It is extremely difficult to filter out the fine dust with such filters.

3.5 Conclusion

Table 4 shows total no. of hours of operation of an airside economizer with direct and indirect evaporative cooling during different months of years 2014 and 2015 respectively (The PDUs failed in Nov.'15) at the Research Data Center. As per Table 4, by Nov.'15 when the first PDU was reported failed (figures 21 and 22), the data center cooling unit completed the operation

of 6232.25 hours for free air cooling with direct and indirect evaporative cooling. Out of 6232.25 hours of total operation for airside economization with direct and indirect evaporative cooling, 3622 hours were for free air cooling which is way higher than the recommended no. of hours for free air cooling in Dallas. Based on the results of the above experiments, it is quite possible that air and moisture contributed to the failure of the PDUs. 2 out of 7 PDUs failed after 6232.25 hours of operation. Failure is not due to corrosion. The visual inspection of different components after 6232.25 hours of operation and temperature-relative humidity excursions outside the ASHRAE envelope showed that no failure has occurred to IT equipment, especially servers susceptible to corrosion or expected to fail under such harsh conditions. No surface mount resistor failure was reported. This effort is still ongoing, as the intent is to run until failure and thereafter evaluate and understand the contribution of corrosion on the reliability of hardware in this environment.

Table 3-4 Total Hours of operation of an airside economizer with direct and indirect evaporative cooling during different months of years 2014 and 2015 respectively

	No. of Hours of Operation	
Month	**Hours**	**Minutes**
May,2014	38	14
June,2014	337	11
July, 2014	282	47
August,2014	71	20
September, 2014	84	31
October,2014	569	1
November,2014	596	20
December,2014	93	20
April, 2015	329	22
May,2015	549	57
June,2015	611	47
July,2015	626	18
August,2015	563	23
September, 2015	600	30
October, 2015	613	10
November, 2015	265	4
Total	6232	15

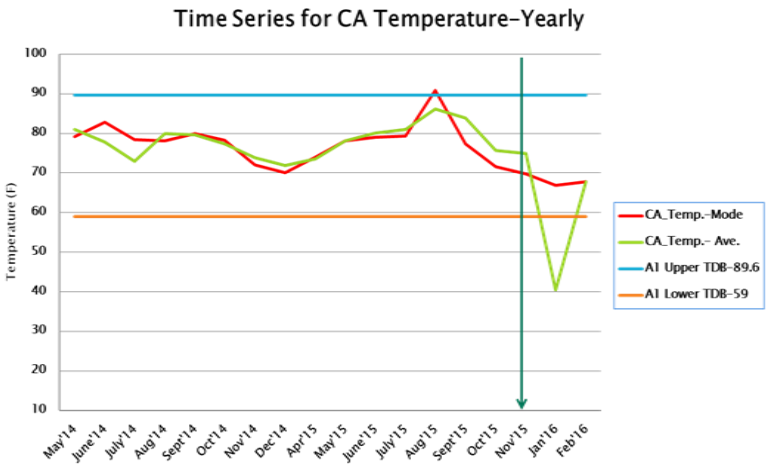

Figure 3-21 Time Series for CA Temperature (Yearly) showing the first reported failure

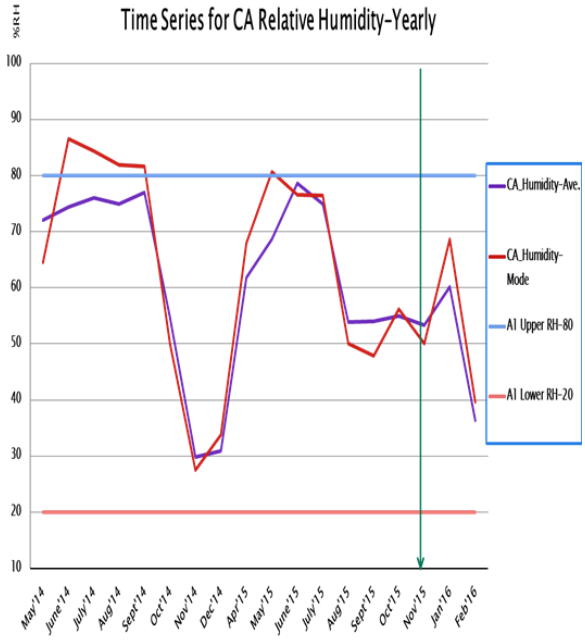

Figure 3-22 Time Series for CA Relative Humidity (Yearly) showing the first reported failure

The below mentioned statistics demonstrations represent the environmental excursions of the last two years at the modular data center based on the trend data. The historical environmental data displays the exact operating conditions of research data center for last two years. The study of excursion of temperature and relative humidity in the data center is essential to correlate the environment of total period of operation and its implications on the reliability of the system. Figures 21 and 22 demonstrate the time series of cold aisle temperature and relative

humidity yearly basis for the last two years respectively mentioning the first reported failure (2 PDUs failed) in Nov.'15. The statistics are shown by using the mean (average) and mode (most occurring environments) values for each parameter on monthly basis. The figures also show the lower and upper limits for allowable A1 Dry Bulb Temperature (59°F-89.6°F) and A1 relative humidity (20%-80%) respectively. It can be inferred that the data center was operated in ASHRAE class A1 allowable (outside recommended) region for the maximum period during its tenure of the last two years. Coupon experiment also determines the severity level G2 for the research modular data center. However, no server failure was recorded.

3.6 Future Work

This is a continuous effort to characterize the corrosion impact on IT equipment reliability. Coupon testing will be continued every month to determine if the environment is G2 all year round. The other IT hardware examined for corrosion will be continuously monitored for potential failure. It is also required to understand the environmental excursions outside the ASHRAE envelope. Later, when G2 environment is fully characterized and its corrosion impact is understood, work is then expected to continue with a higher environment G3.

Further work is planned on microscopic evaluation of any damaged IT to understand the prevailing corrosion type, i.e. due to particulate or gaseous.

3.7 Acknowledgement

This work is supported by NSF IUCRC Award No. IIP-1738811. The servers and PDUs used in this study (for the experiments) were donated to the University. The initial stage was not thoroughly evaluated before installation. These results were compared with similar servers and PDUs those were donated to the university but not deployed for the operation. It is recommended that new equipment should be deployed in future work.

3.8 References

1. ASHRAE Technical Committee 9.9, 2010, “ASHRAE DOE Course: Save Energy Now Presentation Series,” American Society of Heating, Refrigerating, and Air-Conditioning Engineers, Dallas, TX.
2. Shah, J. M., 2016, “Reliability Challenges in Airside Economization and Oil Immersion Cooling,” Master’s thesis, University of Texas at Arlington, Arlington, TX.
3. Singh, P., Klein, L., Agonafer, D., Shah, J. M., and Pujara, K. D., 2015, “Effect of Relative Humidity, Temperature and Gaseous and Particulate Contaminations on Information Technology Equipment Reliability,” ASME Paper No. IPACK2015-48176.
4. ASHRAE Technical Committee 9.9, 2004, Thermal Guidelines for Data Processing Environments (ASHRAE Datacom Series), 1st ed., American Society of Heating, Refrigerating, and Air-Conditioning Engineers, Atlanta, GA.
5. ASHRAE Technical Committee 9.9, 2008, Thermal Guidelines for Data Processing Environments (ASHRAE Datacom Series), 2nd ed., American Society of Heating, Refrigerating, and Air-Conditioning Engineers, Atlanta, GA.
6. ASHRAE Technical Committee 9.9, 2012, Thermal Guidelines for Data Processing Environments (ASHRAE Datacom Series), 3rd ed., American Society of Heating, Refrigerating, and Air-Conditioning Engineers, Atlanta, GA.
7. Burnett, W. H., Sandroff, F. S., and D’Egidio, S. M., 1992, “Circuit Failure Due to Fine Dust Mode Particulate Air Pollution,” 18th International Symposium for Testing and Failure Analysis (ISTFA), Los Angeles, CA, Oct. 19–23, pp. 329–333.
8. Cole, M., Hedlund, L., Hutt, G., Kiraly, T., Klein, L., Nickel, S., Singh, P., and Tofil, T., 2010, “Harsh Environmental Impact on Resistor Reliability,” SMTA International Conference, Orlando, FL, Oct. 24–28, Paper No. SMTAI10HE2.
9. European Union, 2003, “Directive 2002/95/EC of the European Parliament and of the Council of 27 January 2003 on the Restriction of the Use of Certain Hazardous Substances in Electrical and Electronic Equipment,” Off. J. Eur. Union, L037, pp. 19–23.

10. Fu, H., Chen, C., Singh, P., Zhang, J., Kurella, A., Chen, X., Jiang, X., Burlingame, J., and Lee, S., 2012, “Investigation of Factors That Influence Creep Corrosion on Printed Circuit Boards,” SMTA Pan Pacific Microelectronics Symposium, Kauai, HI, Feb. 14–16, Paper No. PP2012_WA1.4.
11. ISA, 1985, “Environmental Conditions for Process Measurement and Control Systems: Airborne Contamination,” ISA-The Instrumentation Systems, and Automation Society, Research Triangle Park, NC, Standard No. ISA-71.04-1985.
12. ISA, 2013, “Environmental Conditions for Process Measurement and Control Systems: Airborne Contaminants,” ISA-The Instrumentation Systems, and Automation Society, Research Triangle Park, NC, Standard No. ISA-71.04-2013.
13. Awe, O., 2016, “The Effects of Temperature and Relative Humidity on Exposure of Legacy and Future Technology Hardware, Under Real Data Center Conditions in an ANSI/ISA Classified G2 Environment,” Ph.D. dissertation, University of Texas at Arlington, Arlington, TX.
14. Gebrehiwot, B. K., 2016, “Maximizing Use of Air–Side Economization, Direct and Indirect Evaporative Cooling for Energy Efficient Data Centers,” Ph.D. dissertation, University of Texas at Arlington, Arlington, TX.
15. Shah, J. M., Awe, O., Agarwal, P., Akhigbe, I., Agonafer, D., Singh, P., Kannan, N., and Kaler, M., 2016, “Qualitative Study of Cumulative Corrosion Damage of IT Equipment in a Data Center Utilizing Air-Side Economizer,” ASME Paper No. IMECE 2016-66199.
16. Shah, J. M., Awe, O., Gebrehiwot, B., Agonafer, D., Singh, P., Kannan, N., and Kaler, M., 2017, “Qualitative Study of Cumulative Corrosion Damage of Information Technology Equipment in a Data Center Utilizing Air-Side Economizer Operating in Recommended and Expanded ASHRAE Envelope,” ASME Journal of Electronic Packaging, DOI: 10.1115/1.4036363.

Chapter 4

Identification and Characterization of Particulate Contaminants found at a Data Center Using Airside Economization

Abstract

Contamination due to the use of airside economizer has become a major issue that could cost companies revenue. This issue will continue to rise as server components become smaller, densely packed and as companies move into more polluted environments. Contaminants with small particles, usually less than 10 microns, are not noticeable, yet it is these particles those are most likely to get to areas where they can cause damage. Dust exists in suspension in air and settles on surfaces. The dust mainly contains two components: salts and metallic particles. The salts may be neutral or corrosive and the nature of the salt depends on the deliquescent humidity. For metallic particles, surveys must be performed in various data centers, which would help to determine the limits in terms of weight per unit area and particle size distribution. It is necessary to first identify those contaminants that directly affect the IT equipment in the data center. In this research, a real-world data center utilizing airside economization in an ANSI/ISA Classified G2 environment was chosen for the study. The servers were removed, and qualitative study of cumulative corrosion damage was carried out. The particulate contaminants were collected from different locations of a server and material characterization was performed using Scanning Electron Microscopy (SEM), Energy Dispersive Spectrometer (EDS) and Fourier Transform Infrared Spectroscopy (FTIR). The analysis from these results helps to explain the impact of the contaminants on IT equipment reliability.

4.1 Introduction

The effectiveness of the printed circuit board (PCBs) depends upon the atmosphere in which it is operating. The operating condition is defined by temperature, relative humidity and contaminants in the surrounding air. It is seen that the PCB components fail due to two major factors: 1.) corrosion, which results in open circuit and 2.) Short-circuit caused by creep corrosion of copper terminals. Moreover, the rate of PCB failures has increased since 2006, due to the use of lead-free solders in the PCBs enforced by European Union RoHS directive [1]. Reduction of

lead-based solders has given rise to copper creep corrosion, consequently causing electronic failures of PCBs. Similarly, corrosion of silver terminals of surface mount resistors has also given rise to the failures caused by open circuiting. Although Information Technology (IT) component manufacturers have designed equipment that overcomes these issues, however, it has been difficult to overcome the short-circuit issues caused by the settled particulate matter in humid environments. There has been no tangible evidence of failures besides the physical particles that are seen at the failure sites [2,3].

Short-circuit failure modes are generally common in IT equipment located in Asian countries. Due to a high level of fine particulate contaminants in the atmospheric air and increased use of free cooling methods, the short-circuit failure mode has elevated. The sources of the particulate matter in the ambient air are both natural as well as those caused by human activities. Particle contaminants have two categories: fine particles, which are smaller than 2.5 micrometer, while the rest are characterized as coarse.

Sources of fine particles include exhausts from motor vehicles and diesel particulate matter (DPM). Fine particles can further be divided into categories. Primary fine particles are directly emitted from sources such as forest fires, volcanoes and construction sites. On the other hand, secondary fine particles, making most of the atmospheric pollutants, are introduced through natural photochemical reactions in the atmosphere. Nitrogen oxides and sulfurs produced by power plants and industries react with fine (<0.1 micron) carbonaceous particles in complex, multistage processes, producing nitric and sulfuric acids. Ammonium salts mainly neutralize these acids. Sulfates and nitrates are found mainly in fertilizers or resulting from biological decays. Lastly, coarse particles within the range of 2.5 to 15 micrometers-including sea salts, artificial fibers and pollens result from soil and mineral erosion or biological flaking [4 - 8].

In this research, a real-world data center utilizing airside economization in an ANSI/ISA Classified G2 environment was chosen for the study. The servers were removed, and qualitative study of cumulative corrosion damage was carried out. The particulate contaminants were collected from different locations of a server and material characterization was performed using Scanning Electron Microscopy (SEM), Energy Dispersive Spectrometer (EDS) and Fourier

Transform Infrared Spectroscopy (FTIR). The data analysis of their results determines the grain size and elements in the contaminants. This data is very useful to understand the implications of contaminants on the IT equipment reliability.

4.2 Site Description

The sample for this study was collected from a research data center located in the Dallas industrial area. The data center uses airside economizer with direct and indirect evaporative cooling. The modular data center at the Dallas location has a cold aisle/hot aisle configuration. Direct/indirect evaporative cooling and/or return air and/or mixing of return air with outside air methods were used for the extreme environmental conditions, otherwise free air cooling methodology was applied if the environmental condition allowed it. The unit at the Dallas site comprised of an IT pod, which was 126 in. x 85.5 in. with 120 servers and direct/indirect evaporative cooling unit. Approximately 2500-3000 CFM volume of air was circulated through the front of the IT equipment to the rear where cold air entered the cold aisle from an inlet duct at 45° louver angle and the hot air from the hot aisle exited the pod through the return duct. The servers were arranged such that the cool inlet air entered directly towards the servers from the front to provide effective cooling. The constant direction of airflow was ensured by the louver angle. Figure 1 summarizes the airflow pattern within the IT pod [9,10].

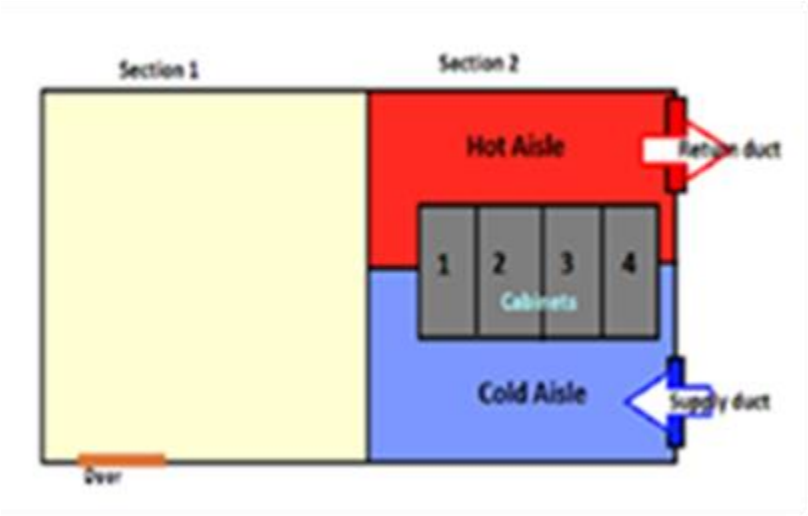

Figure 4-1 Airflow Pattern inside the IT pod

4.2.1 Physical environment: Temperature and relative humidity

Figure 2 shows the Psychrometric chart regions based on A1 allowable region as per ASHRAE environmental envelope for the cooling unit installed at the IT pod [11]. With given specifications of the unit, steps can be taken to modify outside air to the acceptable region.

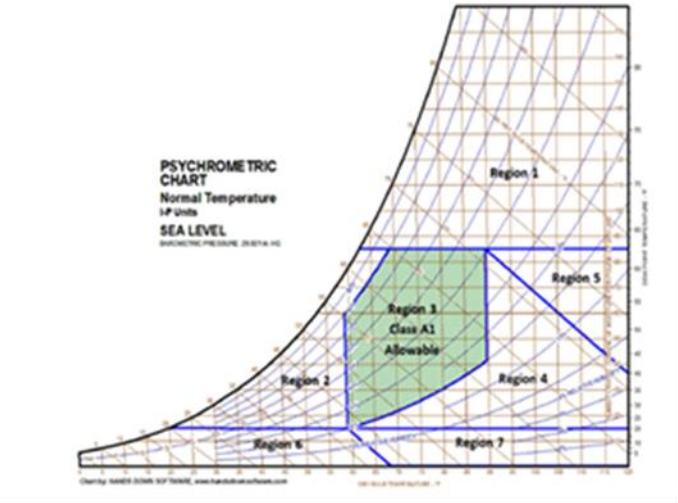

Figure 4-2 Psychrometric chart regions based on A1 allowable region [9,10]

Further, typical meteorological year 3 (TMY3) data were obtained from a nearby weather center in the Dallas/Fort Worth area. The Bin data analysis provided an estimate of the number of hours the research IT pod could use ASE allowing for the increased usage of free air cooling method. The analysis concluded that there is significant availability of outside air for free air cooling application.

Next, the operating trend data of cold aisle temperature-humidity for the previous two years was analyzed. It provided an opportunity to correlate the hours of operation and its implications on the reliability of the system. Moreover, the daily analysis of cold aisle temperature and relative humidity was carried out. The data was collected for multiple days at different periods of operations. The daily analysis concluded that there were no significant variations in the temperature and the relative humidity with respect to temperature, hence the temperature can be considered as constant for throughout the day. The analysis of the temperature and relative humidity on a monthly basis established that the unit was operated under the ASHRAE class A1

allowable region that has the lower and upper limits of A1 dry bulb temperature (59-89 ◦F) and relative humidity (20 %-80%) for the maximum period in the past two years.

4.2.2 Physical Environment: Particulate contamination

The ambient air that entered the data center was filtered using MERV 11 filters. For the initial six months, the modular data center used lower quality filters. As the data center was in the industrial area, the main sources for the contaminants were transportation exhausts and gas welding particles. Table 1 summarizes the sources of different particulates [9,10].

Table 4-1 Particulate matter and sources [9,10]

Contaminant	Source
Zink Whiskers	Zinc Coated ICT Equipment, Steel Building Studs
Tin Whiskers	Components and products having electroplated tin
Oxide Flake Off	Magnetic Media
Natural and Artificial Fibers	Paper, Cardboard, etc.
Water Soluble Ionic Salt	Chemical Reactions
Sulphates, Nitrate, Sea Salts	Winds
Lime Dust with Water	Concrete Material
Dust	Farm, especially during ploughing
Toner Dust	Toner
Smoke	Cigarette, Winds
Cellulose Fragments	Traditional Ceiling Tiles and Spaces
Synthetic Rubbers	Belt Drive and Pully

4.2.3 Physical environment: Gaseous contamination

Exposed corrosion classification coupons (copper and silver) were installed at different locations of the rack for one month and its corrosion thickness was measured. A combed coupon

was also installed to study the type of contaminants and the role of deliquescent relative humidity. Collected data was processed to compute the corrosion rate, using coulometric reduction method at the S&T Group Materials Laboratory by IBM. The analysis revealed that the corrosion rate for silver was greater than that of copper; higher than the G1 criteria for Silver of 200 Å/month, concluding that the data center was operating at G2 severity level as per ISA 71.04 – 1985 standard [12,13]. Comb coupon further revealed a high risk of particulate contamination including that by fine and coarse dust particles.

4.3 Procedure

A server was removed from the research data center; and studied qualitatively for cumulative corrosion damage. Figure 3 shows the lodged dust at the different locations of the server i.e., heat sinks, fans and server lid (inside). The dust sample was collected from those locations and different material characterization experiments (SEM, EDS and FTIR) were performed.

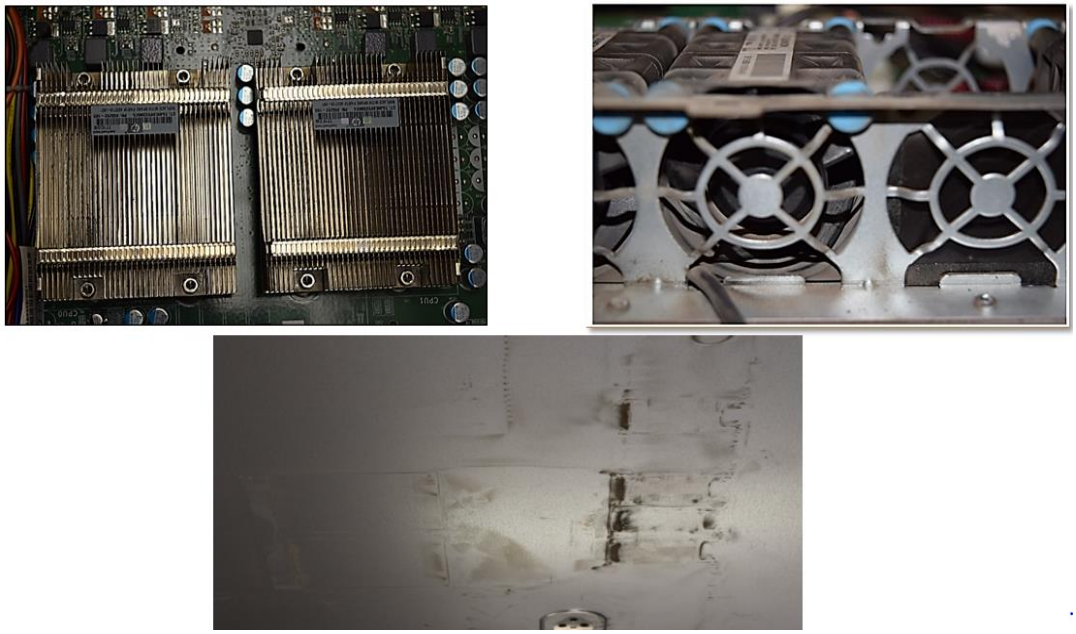

Figure 4-3 Lodged Dust

4.3.1 Scanning Electron Microscopy (SEM)

Scanning Electron Microscopy (SEM) is an advanced form of microscopy that uses high voltage electrons with the wavelength as short as 0.1Å. Though SEM technique is expensive, however, it produces images with high magnification, resolution and larger depth of field. SEM is used to obtain topographical, morphological, compositional, and crystallographic information. While both conducting and non-conducting samples can be studied using SEM, however, for non-conducting sample, tests are performed under low vacuum or the sample is coated with silver.

There are two types of signal electrons that result from elastic and inelastic scattering of electron due to the interaction of the probe electrons and the sample. The elastically scattered electrons produce Backscattering Electrons (BSEs), while the inelastic scattering produces Secondary Electrons (SEs). In this project, both SEs and BSEs were used to obtain high-resolution images.

In this project, two SEMs were used, one with a thermionic source (W gun) and the other with cold Field Emission source. The experimental procedure for each test is as follows:

4.3.2 Experimental Procedure for Hitachi S-3000N Variable Pressure SEM:

The Hitachi S-3000N Variable Pressure SEM uses a Tungsten gun for electron source. This equipment was used to obtain SE images at x500, x10k, and x20k magnificaiton, and BSE images at x10k for the COMPO, TOPO, and 3D modes.

4.3.2.1 Sample Preparation

Contaminants from a server taken at Mestex data center were collected. Since the contaminants were expected to be non-conductive, they were placed on a carbon tape and then coated with silver using the CrC 100 Sputtering System shown in figure 4. Figure 5 shows the sample holder with the silver-coated sample.

Figure 4-4: CrC 100 Sputtering System coating the non-conductive samples with silver

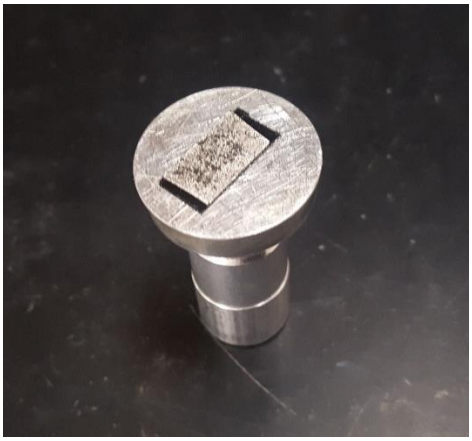

Figure 4-5: Sample holder with the silver-coated sample

After placing the sample in the SEM machine, and obtaining the desired vacuum, the following steps were conducted to obtain the images:

After the PC-SEM software was started, the desired voltage of 10kV was selected and the HV was turned on. The AFS was clicked to protect the filament. The Automatic Brightness and Contrast options were used to adjust the brilliance/sharpness of the image. The beam current was then changed to 30 nA for imaging. Next, the alignment was performed by optimizing shift and tilt of the gun to give the maximum intensity. Simultaneouly, Stigmator X and Stigmator Y were optimized to reduce the movement of the image. Lastly, the Stigmator knobs on the controller were used to correct for stigmation.

The maginification was increased (up to x30k), and the alignment and the stigmation corrections were repeated.

4.3.2.2 Backscatter Mode

For backscatter mode, the TV was first turned off and the backscatter detector was inserted from the back. From the signal setup option, the signal was changed to BSE2 and imaging was then done at slow scan window.

Since the stigmation was already corrected in the SE mode, the desired images were taken for the different BSE modes at x10k. For 3D mode, the detector was pull backward and placed in a different position.

4.3.3 Experimental Procedure for Hitachi S-4800 II FE SEM:

The same sample that was used for VP-SEM was used for the FE-SEM experiment. Since very high vacuum is required for the FE-SEM operation, gloves were worn when inserting and removing samples. After putting the sample in the intermediate chamber, the high vacuum pump was turned on. As the desired vacuum was achieved, the sample was placed in the inside chamber, and the chamber was then closed.

After the sample was placed inside, the SEM software was started. The stage was then placed on the home position. The emission current was set to 10 μA and the voltage was set to 10kV. Next, the alignment was performed using the beam alignment, aperture alignment, Stig X and Stig Y options, and then stigmation was corrected using the Stigmator knobs. Magnification was increased up to x500k, and the alignment and stigmation corrections were repeated. High resolution images were obtained at x8k, x20k, x200k, x220k, x350k, and x500k.

4.3.4 Energy Dispersive Spectrometer (EDS)

The EDS technique was used to identify the different elements found in contaminant samples. X-ray Energy-Dispersive Spectrometer (XEDS) was developed in the late 1960s and is available as an option on TEM and SEM. For this experiment, the EDS attached on the Hitachi S-3000N Variable Pressure SEM was used.

The EDS system consists of three parts: a detector, processing electronics and a multichannel analyzer (MCA) display. A charged pulse proportional to the x-ray coming from the sample is generated by the detector. The generated pulse is converted to voltage and the signal is amplified through a field effect transistor (FET). Then, it is identified electronically as an X-ray of specific energy.

To perform an EDS study, a larger field of view of the sample was needed. Thus, a lower magnification was selected (x150). After the alignment and stigmation were corrected as per the steps given under the SEM section above, the beam current 1 was increased to 60 nA. Next, TV was turned off, and the NSS software was booted on another computer. Selected parameters such as magnification, beam current, voltage, walking distance, and EDS detector position were entered under Microanalysis. After making sure the dead time did not exceed 40% (which previously was at 10%), the scan was performed to identify the elements in the sample. The "Spectral imaging" and "Quantify Spectrum" options were also used to recognize the location of the elements, and the percentage in which the elements were present.

4.3.5 Fourier Transform Infrared Spectroscopy (FTIR)

The vibration spectroscopy was used to analyze molecular structure by examining the interaction between infrared light and nuclear vibrations in molecules. Fourier Transform Infrared Spectroscopy (FTIR) detects the molecular vibrations by measuring the absorption of infrared light. Although this approach can be used to study both organic and inorganic materials, although, metallic materials cannot be studied using FTIR because of their strong reflective property.

The Thermo Nicolet 6700 FTIR spectrometer in CCMB lab along with the smart iTR accessory were used to study the powder samples collected from the server of the research data center.

First, the OMNIC software was booted. For both the transmission and absorption measurements, the following parameters were selected:

- Number of scans: 32
- Resolution: 4
- Range: 4000 – 40 1/cm

After collecting the background, the sample was placed in the FTIR machine and the data was collected.

4.4 Results and Data Analysis

4.4.1 Scanning Electron Microscopy (SEM)

4.4.1.1 VP-SEM Results

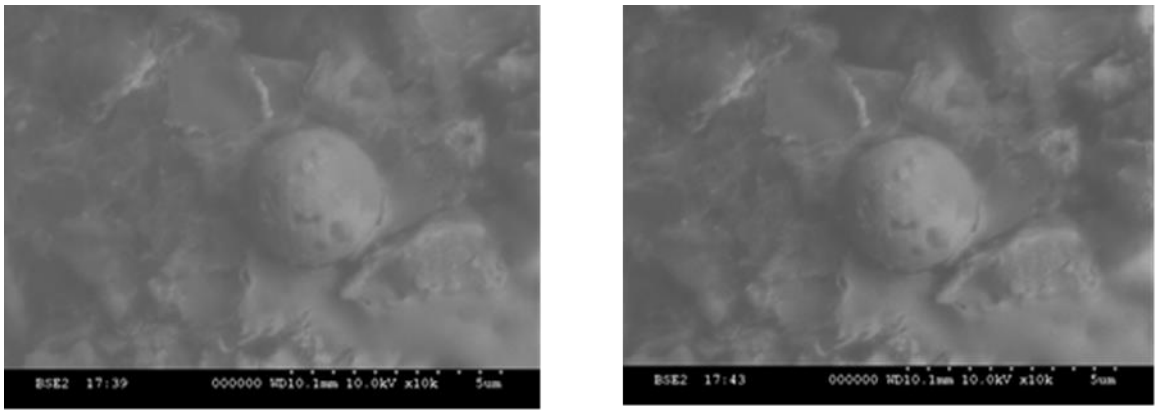

Figure 4-6: Back Scatter images in 3D mode at x10k.

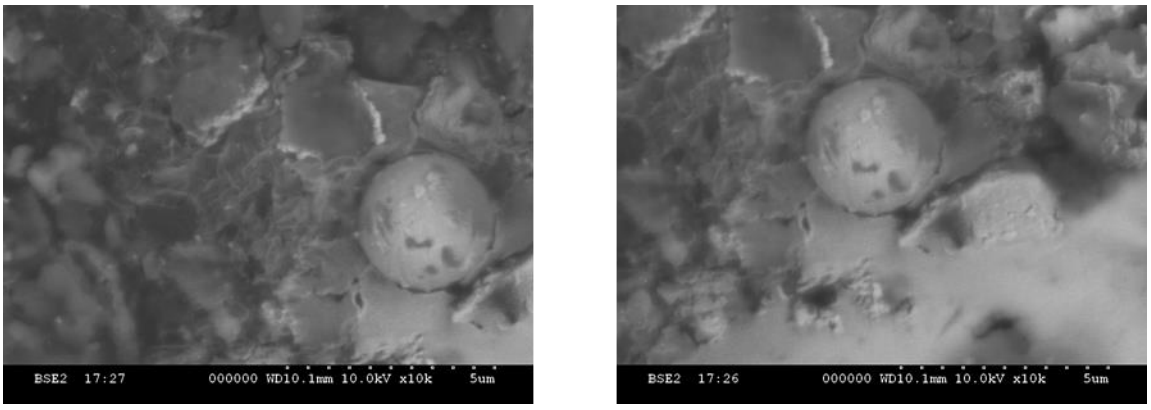

Figure 4-7: Back Scatter images in COMPO mode at x10k.

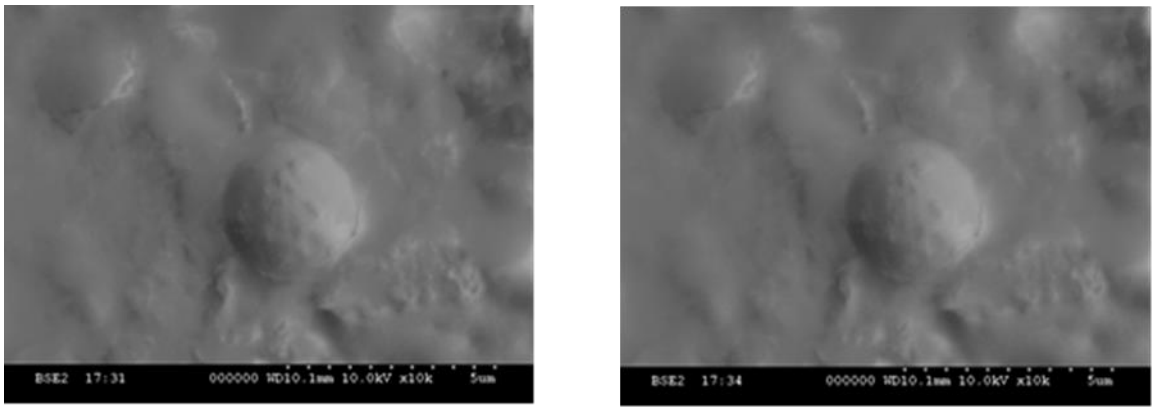

Figure 4-8: Back Scatter images in TOPO mode at x10k.

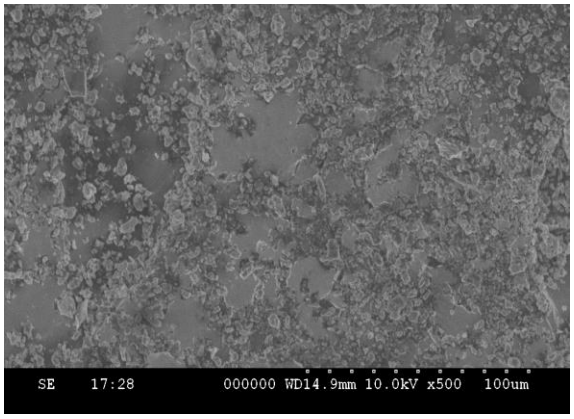

Figure 4-9: SE images x500

Figures 6, 7, 8, and 9 shown above shows the results obtained from VP-SEM.

4.4.1.2 FE-SEM Results

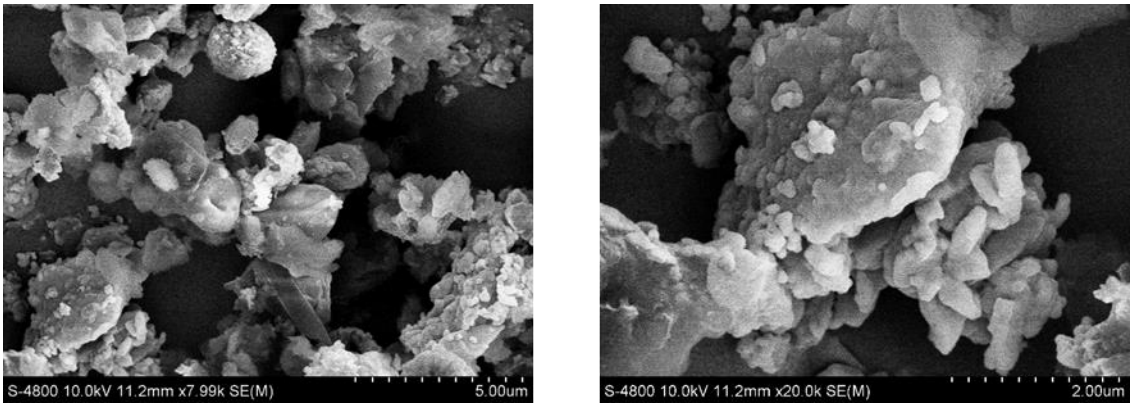

Figure 4-10: SE images at x8k (left) and x20k (right) at 11.2 mm WD.

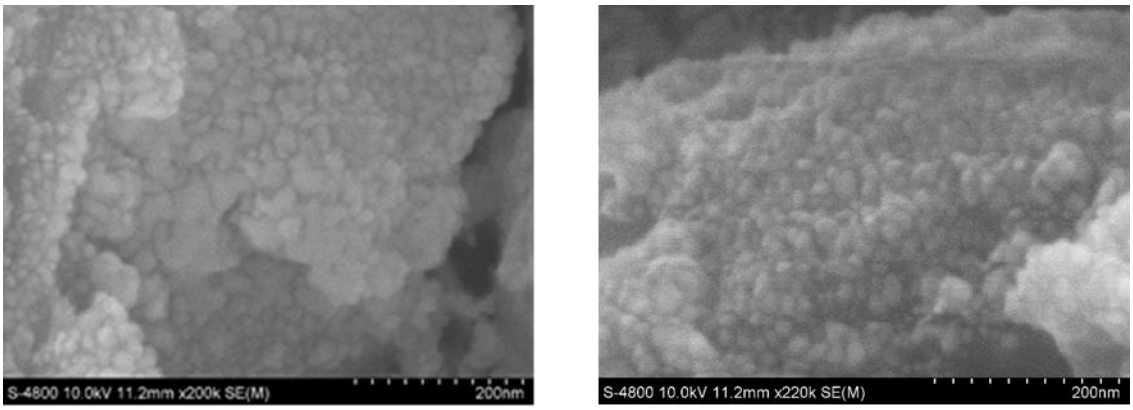

Figure 4-11: SE images at x200k (left) and x220k (right) at 11.2 mm WD.

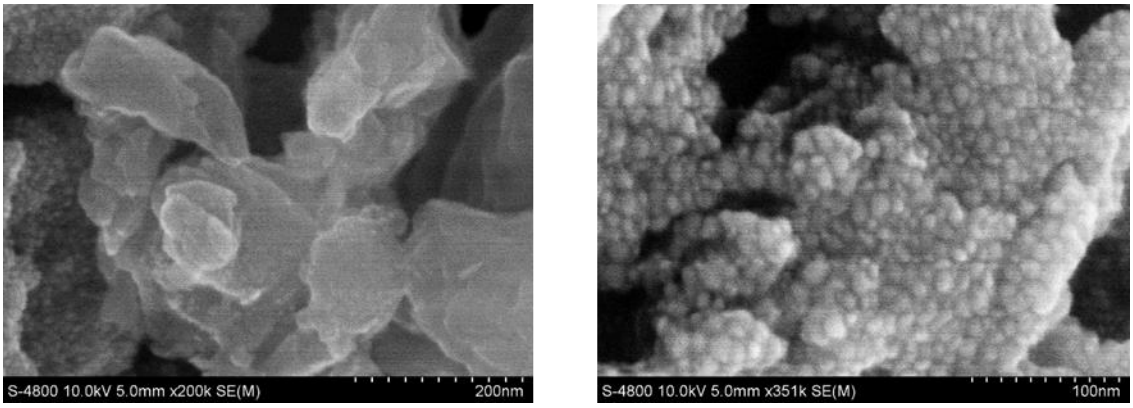

Figure 4-12: SE images at x200k (left) and x350k (right) at 5mm WD.

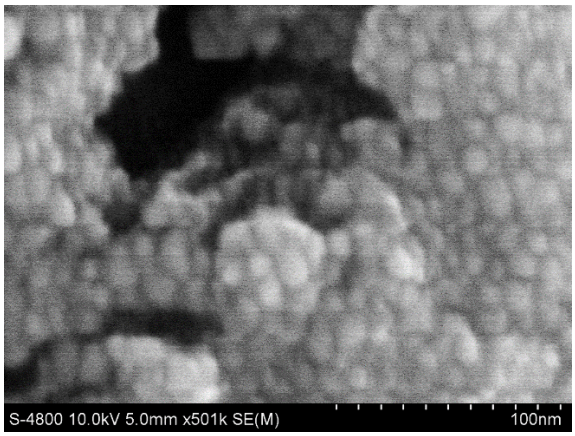

Figure 4-13: SE image at x500k at 5mm WD.

Figures 10, 11, 12, and 13 shown above shows the results obtained from FE-SEM. SEM results clearly show that the shape of found contaminants is spherical.

4.4.1.3 Data Analysis - SEM

The Scanning Electron Microscopy (SEM) data was analyzed to obtain two sets of data. First, the SEM SE images were used to obtain the average grain size for the contaminants. Second, The Energy Dispersive Spectrometer (EDS) data was analyzed to obtain the compositional analysis of the contaminants. To determine the particulate size, the image analysis tool in Matlab was used. Some of the results are given below in Figure 14:

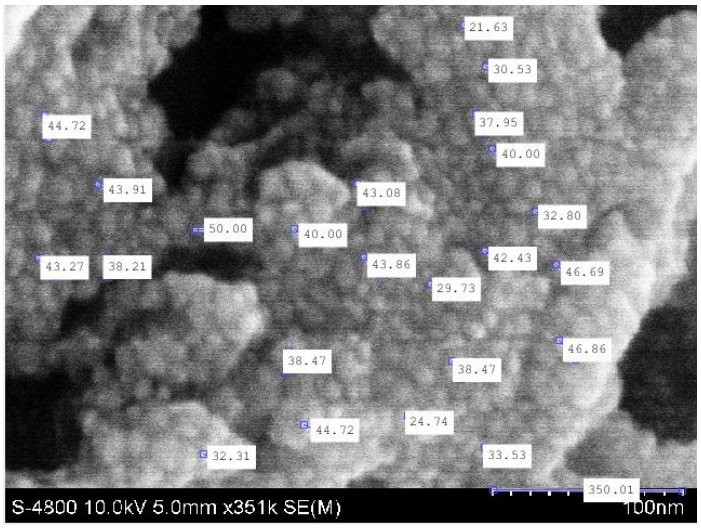

Figure 4-14: The size of the different contaminants measured using analysis tool on Matlab.

Size of the various grains identified above in figure 14 is given by: {21.63, 30.53, 44.72, 37.95, 43.91, 43.08, 40.00, 50, 40, 32.8, 3.27, 38.21, 43.86, 42.43, 46.69, 29.73, 38.47, 46.86, 44.72, 24.74, 32.31, 33.53} Using the scale in the bottom of the figure 14, the average particulate size is determined to be: 11.03 nm. The results clearly indicates that the found particulates are the ultra-fine particles.

4.4.2 Energy Dispersive Spectrometer (EDS)

4.4.2.1 Results

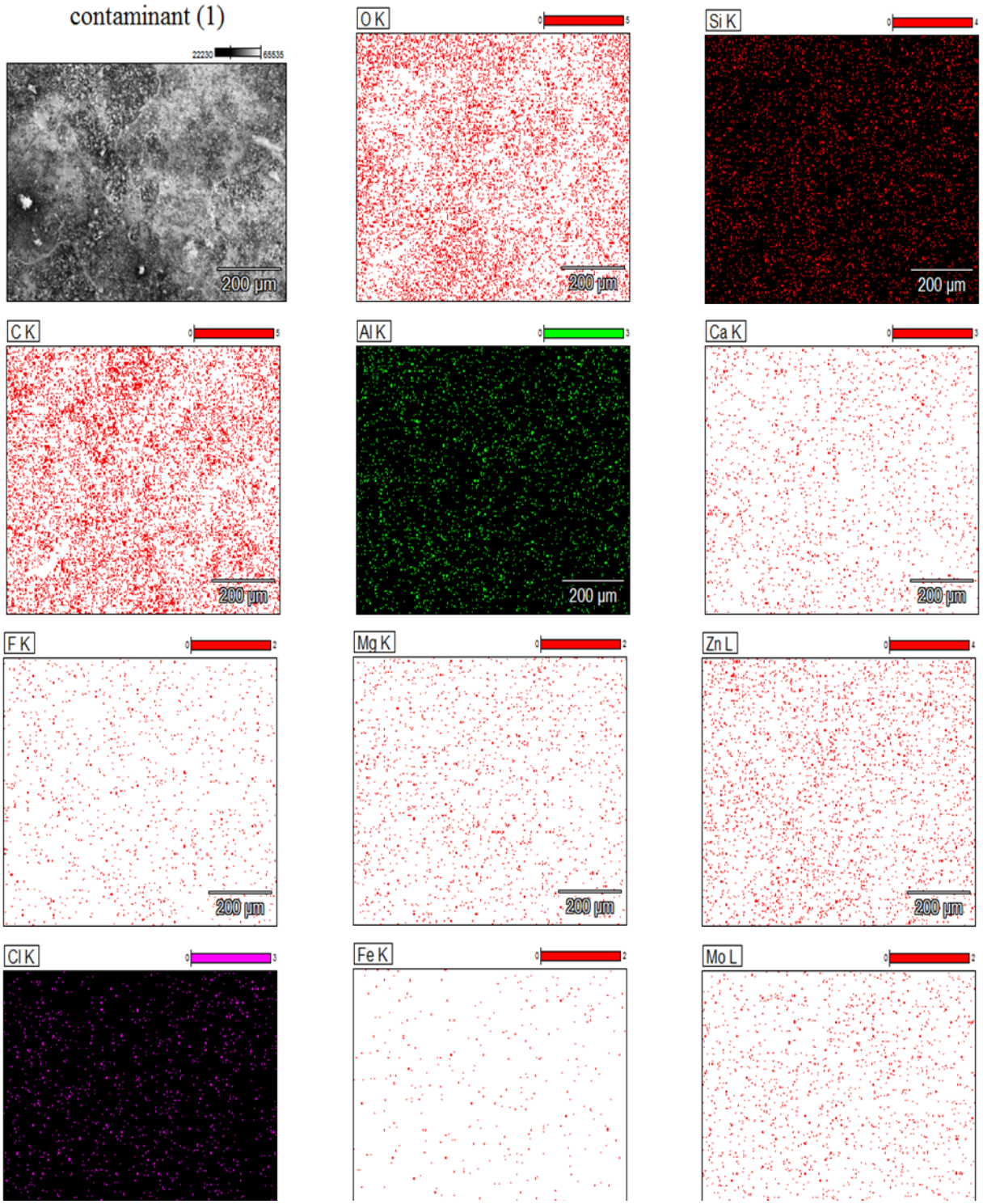

Figure 4-15: Result obtained from the Spectral Analysis showing the location of the various elements identified in one location of the sample.

Figures 15 shown above shows the results obtained from the Spectral Analysis showing the location of the various elements identified in one location of the sample.

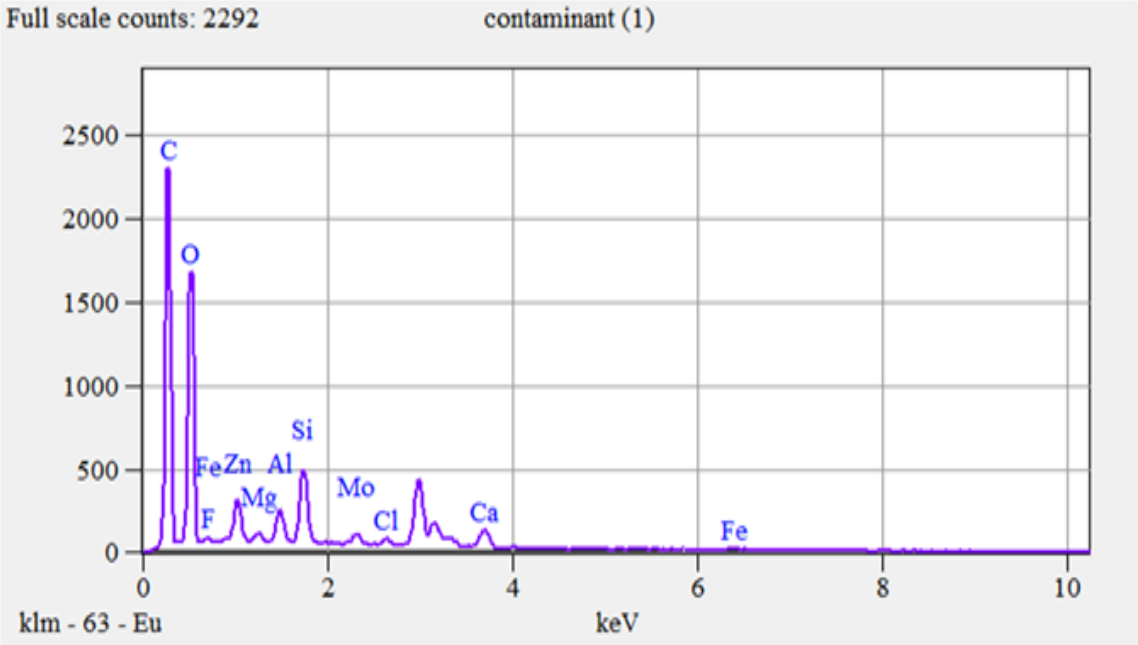

Figure 4-16: Result of the spectrum analysis of one location of the sample.

Element Line	Int. Cps/nA	Z	A	F	ZAF	Weight %	Weight % Error	Norm. Wt.%	Norm. Wt.% Err	Atom %	Atom % Error
C K	---	0.960	2.172	1.000	2.086	46.70	± 0.48	46.70	± 0.48	62.27	± 0.64
O K	---	0.984	2.673	1.000	2.629	27.11	± 0.52	27.11	± 0.52	27.14	± 0.52
F K	---	1.050	2.495	1.000	2.618	0.46	± 0.37	0.46	± 0.37	0.39	± 0.31
Mg K	---	1.037	1.293	0.998	1.339	0.47	± 0.07	0.47	± 0.07	0.31	± 0.05
Al K	---	1.072	1.172	0.997	1.254	1.94	± 0.16	1.94	± 0.16	1.15	± 0.09
Si K	---	1.045	1.108	0.998	1.155	5.22	± 0.16	5.22	± 0.16	2.98	± 0.09
Cl K	---	1.112	1.037	0.997	1.149	3.19	± 0.22	3.19	± 0.22	1.44	± 0.10
Ca K	---	1.094	1.010	1.000	1.105	5.90	± 0.20	5.90	± 0.20	2.36	± 0.08
Fe L	---	1.163	1.650	0.999	1.917	0.00	---	0.00	---	0.00	± 0.00
Zn L	---	1.213	1.278	0.999	1.550	5.81	± 0.28	5.81	± 0.28	1.42	± 0.07
Mo L	---	1.333	0.993	0.997	1.320	3.20	± 0.20	3.20	± 0.20	0.53	± 0.03
Total						100.00		100.00		100.00	

Figure 4-17: Result of quantitative analysis of one location of the sample.

4.4.2.2 Data Analysis – EDS

The EDS data was analyzed to obtain the compositional analysis of the contaminants. From the EDS measured values, the ZAF matrix corrected value for the composition of the contaminant is given in Table 2.

Table 4-2: Elements identified in the contaminant sample

Sample Location	Elements by Weight %													
	C	O	F	Mg	Al	Si	S	Cl	Ca	Fe	Zn	Mo	Sm	*Total*
1	46.70	27.11	0.46	0.47	1.94	5.22	0.00	3.19	5.90	0.00	5.81	3.20	0.00	100.00
2	40.33	30.72	0.38	0.53	2.30	6.27	1.75	2.26	7.21	0.00	8.25	0.00	0.00	100.00
3	50.55	26.61	0.00	0.42	1.37	4.21	0.00	2.77	4.93	0.80	5.62	2.72	0.00	100.00
4	53.58	25.30	0.00	0.44	1.37	3.71	0.00	3.35	4.71	0.00	5.00	2.55	0.00	100.01
5	44.17	30.12	0.00	0.53	2.33	5.89	1.47	2.19	6.06	1.01	6.21	0.00	0.00	99.98
6	50.45	25.44	0.27	0.45	1.52	4.46	0.00	4.00	5.97	0.00	4.78	2.67	0.00	100.01
Average Weight %	47.63	27.55	0.19	0.47	1.81	4.96	0.54	2.96	5.80	0.30	5.95	1.86	0.00	100.00
Average Weight (ppm)	476300.00	275500.00	1850.00	4733.33	18050.00	49600.00	5366.67	29600.00	57966.67	3016.67	59450.00	18566.67	0.00	1000000

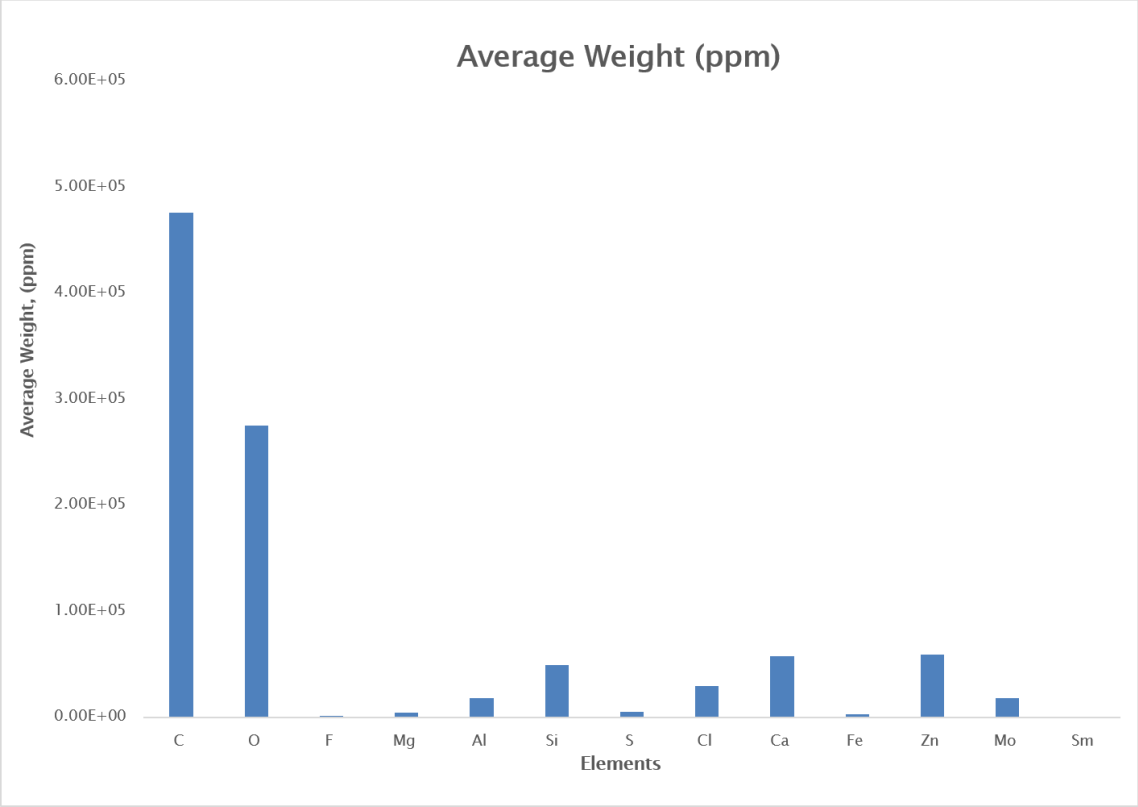

Figure 4-18: Average Weight of Elements identified in the contaminant sample in ppm

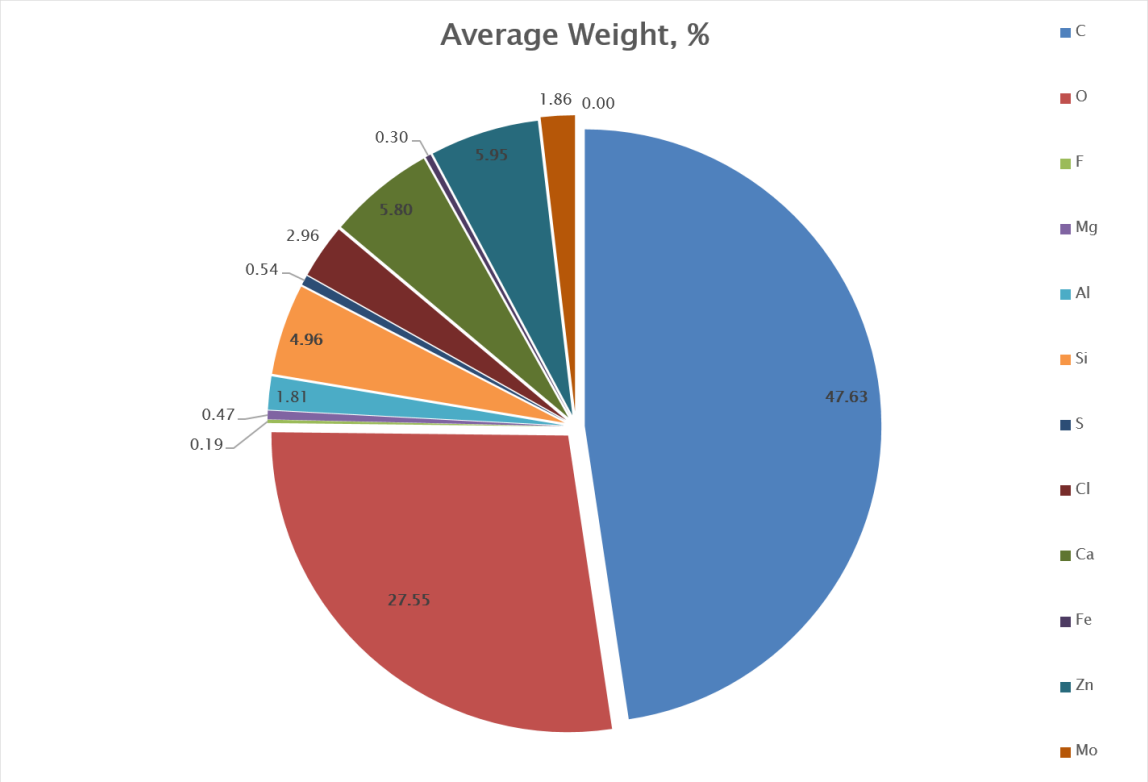

Figure 4-19: Average Weight of Elements identified in the contaminant sample in percentage

4.4.3 Fourier Transform Infrared Spectroscopy (FTIR)

4.4.3.1 Results

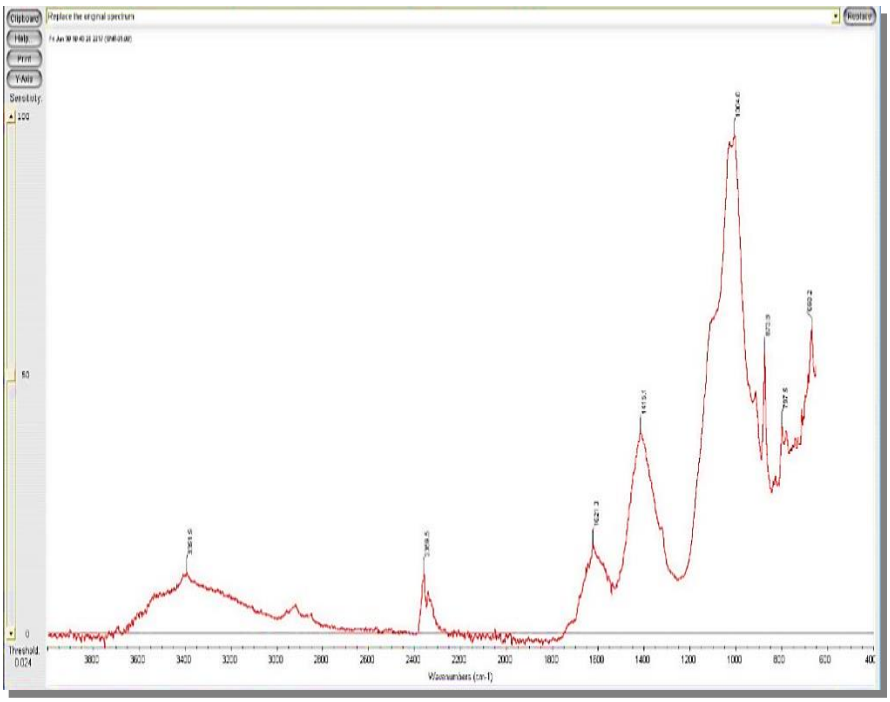

Figure 4-20: Absorbance data collected using FTIR.

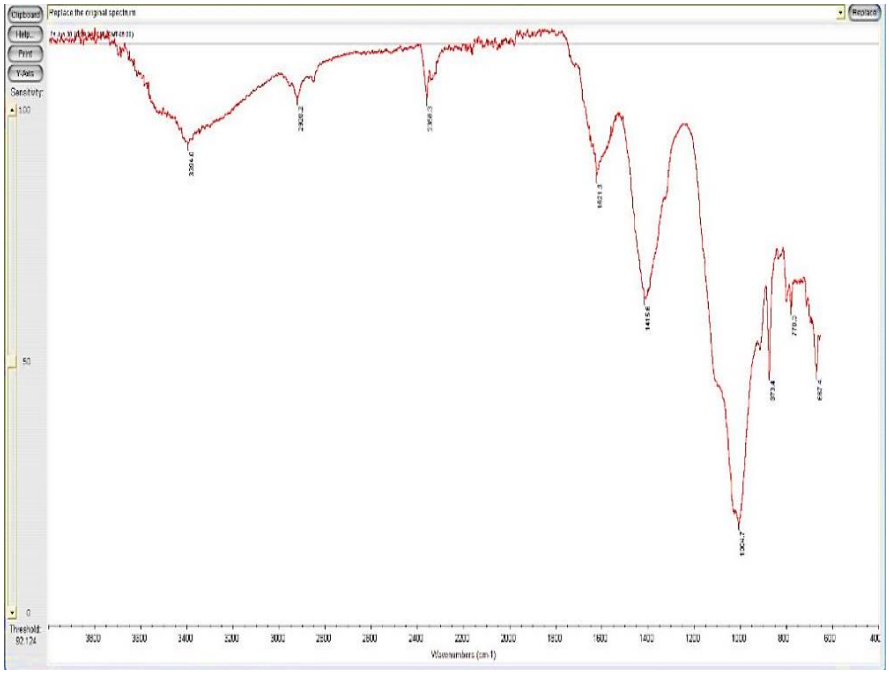

Figure 4-21: Transmission data collected using FTIR.

Figures 20 and 21 shown above show the absorbance and transmission data collected using the FTIR respectively. Figure 22 below shows the results obtained after performing the search in the FTIR database. These results are not a good match because sample contains numerous compounds.

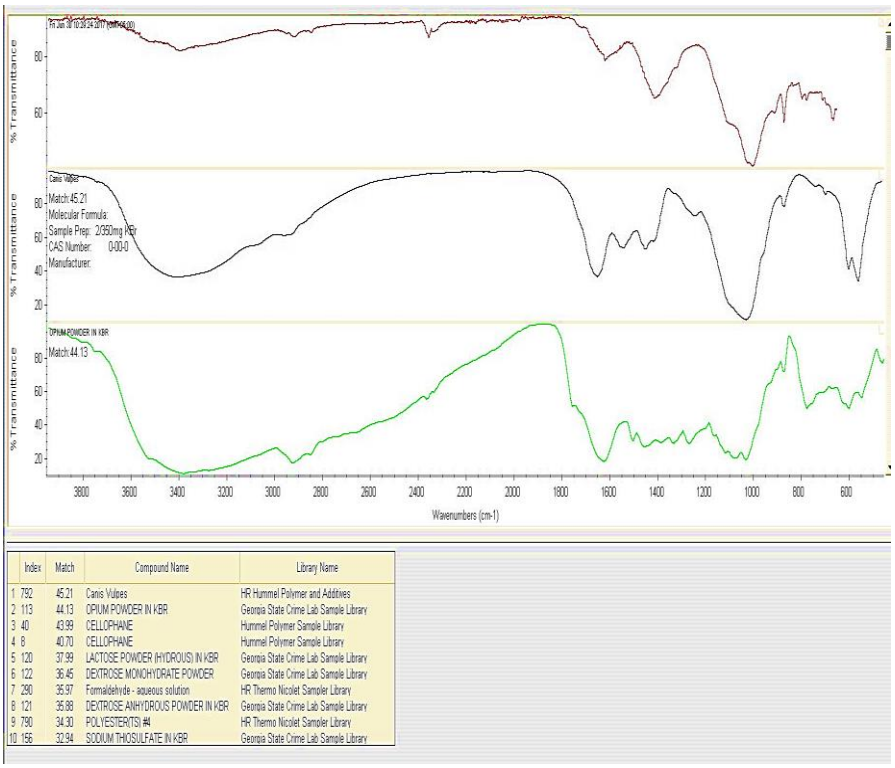

	Index	Match	Compound Name	Library Name
1	792	45.21	Canis Vulpes	HR Hummel Polymer and Additives
2	113	44.13	OPIUM POWDER IN KBR	Georgia State Crime Lab Sample Library
3	40	43.99	CELLOPHANE	Hummel Polymer Sample Library
4	8	40.70	CELLOPHANE	Hummel Polymer Sample Library
5	120	37.99	LACTOSE POWDER (HYDROUS) IN KBR	Georgia State Crime Lab Sample Library
6	122	36.45	DEXTROSE MONOHYDRATE POWDER	Georgia State Crime Lab Sample Library
7	290	35.97	Formaldehyde - aqueous solution	HR Thermo Nicolet Sampler Library
8	121	35.88	DEXTROSE ANHYDROUS POWDER IN KBR	Georgia State Crime Lab Sample Library
9	790	34.30	POLYESTER(TS) #4	HR Thermo Nicolet Sampler Library
10	156	32.94	SODIUM THIOSULFATE IN KBR	Georgia State Crime Lab Sample Library

Figure 4-22: Result obtained after performing the search in the FTIR database

4.4.3.2 Data Analysis

Fourier Transform Infrared Spectroscopy (FTIR) was performed to analyze the molecular structure and compounds of found particulates. Based on the results obtained, it can be concluded that the contaminant sample contained different compounds. Unfortunately, these compounds could not be identified from the FTIR search database. Therefore, online tools that provided chemical group classification as a function of the wavenumber were used to identify the possible chemical groups present in the contaminant sample. The sources available from *Michigan State University* and *Chemistry LibreTexts* were used to determine table 3 respectively. [14,15]

Table 4-3: Possible Functional Groups Present in the Contaminant Sample

Peaks	Wavenumber (1/cm)	Possible Group
1	3391.	**O-H (H bonded), stretching**
2	2359.5	N/A
3	1621.3	Metal-H stretching
4	1415.1	**C-O-H bending**
5	1004.0	**C-O stretching**
6	873.8	**C-H bending**
7	797.5	**=C-H & =CH2**
8	668.2	**O-H bend (out of plane)**

4.5 Discussion and Future-Plan

Particulate contamination in the data center may affect IT equipment performance as well as the reliability. This may include the performance of heat sinks, electronic and mechanical devices. Other major factors include the deliquescent relative humidity, which may humidify the particulate matter causing short-circuiting on printed circuit boards. Although filters do filter out dust particles, they are not very effective for particles of size PM2.5. Moreover, humidity conditions of about 50-65% can cause condensation on PCBs, which allows particles to settle as time goes on. Additionally, condensation causes leakage of current around PCBs, increasing the chances for short-circuits.

Particle contamination also affects the thermal conductivity of the components. Accumulated particles create an insulating layer, which reduces heat dissipation effectiveness of the server, causing components to overheat. Similarly, magnetic particles that sweep into the system may cause damage to electric components such as fans and other rotors if they come within the magnetic field generated by such components. Further, particles that have electrical conductive properties such as carbon and other metallic substances can cause short-circuits in the electrical components. Particles with insulating properties can also settle static charges, which could affect the working of PCBs and other electrical components. Some insulating particles do absorb moisture due to humid environmental conditions, consequently increasing the chances of short-circuits. Particles with adhesive properties could attract more particles to settle on the surfaces, further increasing the detrimental effects on the components. Likewise, dust

particles may become corrosive in nature by coming into contact with various contaminants, hence causing damage to components. Lastly, fast moving particles may cause erosion to the mechanical components and can cause critical damage to their surface.

4.6 Acknowledgment

This work is supported by NSF I/UCRC in Energy-Smart Electronic Systems (ES2). We would like to thank Dr. Jianchao Jiang for offering us the experiment facility in the UTA CCMB lab.

4.7 References

1. Directive 2002/95/EC of the European Parliament and of the Council of 27 January 2003 on the Restriction of the use of Certain Hazardous Substances on the Electrical and Electronic Equipment Official Journal L 037, February 13, 2003.
2. Shah, J. M., 2016, “Reliability Challenges in Airside Economization and Oil Immersion Cooling,” Master’s thesis, University of Texas at Arlington, Arlington, TX.
3. Singh, P., Klein, L., Agonafer, D., Shah, J. M., and Pujara, K. D., 2015, “Effect of Relative Humidity, Temperature and Gaseous and Particulate Contaminations on Information Technology Equipment Reliability,” ASME Paper No. IPACK2015-48176.
4. Burnett W.H., F.s. Sandroff and S.M.D ’Egidio, “Circuit failure due to fine dust mode particulate air pollution,” ISTFA ’92, The 18th Int’l Symposium for Testing & Failure Analysis, Los Angeles, CA, 17-23 Oct 1992, 329-333.
5. Litvak, A., A. J. Gadgil, and W. J. Fisk. 2000. Hygroscopic Fine Mode Particle Deposition on Electronic Circuits and Resulting Degradation of Circuit Performance: An Experimental Study, Indoor Air 2000, vol. 10, pg 47-56, 2000.
6. Fu, H., Chen, C., Singh, P., Zhang, J., Kurella, A., Chen, X., Jiang, X., Burlingame, J., and Lee, S., 2012, “Investigation of Factors That Influence Creep Corrosion on Printed Circuit Boards,” SMTA Pan Pacific Microelectronics Symposium, Kauai, HI, Feb. 14–16, Paper No. PP2012_WA1.4.
7. Comizzoli R. B. et al. “Corrosion of electronic materials and devices by the submicron atmospheric particles,” The Electrochemical Society Interface, Fall 1993, 27-33.

8. Song B., M. H. Azarisn and M. G. Pecht, “Effect of the temperature and relative humidity on the impedance degradation of dust-contaminated electronics,” Journal of The Electrochemical Society, 160 (3), 2013, C97-C105.
9. Shah, J. M., Awe, O., Agarwal, P., Akhigbe, I., Agonafer, D., Singh, P., Kannan, N., and Kaler, M., 2016, “Qualitative Study of Cumulative Corrosion Damage of IT Equipment in a Data Center Utilizing Air-Side Economizer,” ASME Paper No. IMECE 2016-66199.
10. Shah, J. M., Awe, O., Gebrehiwot, B., Agonafer, D., Singh, P., Kannan, N., and Kaler, M., 2017, “Qualitative Study of Cumulative Corrosion Damage of Information Technology Equipment in a Data Center Utilizing Air-Side Economizer Operating in Recommended and Expanded ASHRAE Envelope,” ASME Journal of Electronic Packaging, DOI: 10.1115/1.4036363.
11. ASHRAE Technical Committee 9.9, 2012, Thermal Guidelines for Data Processing Environments (ASHRAE Datacom Series), 3rd ed., American Society of Heating, Refrigerating, and Air-Conditioning Engineers, Atlanta, GA.
12. ISA, 1985, “Environmental Conditions for Process Measurement and Control Systems: Airborne Contamination,” ISA-The Instrumentation Systems, and Automation Society, Research Triangle Park, NC, Standard No. ISA-71.04-1985.
13. ISA, 2013, “Environmental Conditions for Process Measurement and Control Systems: Airborne Contaminants,” ISA-The Instrumentation Systems, and Automation Society, Research Triangle Park, NC, Standard No. ISA-71.04-2013.
14. https://www2.chemistry.msu.edu/faculty/reusch/virttxtjml/Spectrpy/InfraRed/infrared.htm
15. https://chem.libretexts.org/Core/Physical_and_Theoretical_Chemistry/Spectroscopy/Vibrational_Spectroscopy/Infrared_Spectroscopy/Infrared%3A_Interpretation

Chapter 5

Development of A Precise and Cost-Effective Technique to Measure Deliquescent Relative Humidity of Particulate Contaminants Found in A Data Center Utilizing Airside Economization

Abstract

A remarkable amount of data center energy is consumed in eliminating the heat generated by IT equipment to maintain and ensure safe operating conditions and optimum performance. The installation of ASEs bears the risk of particulate contamination in data centers, hence, deteriorating the reliability of information technology (IT) equipment. When the RH in the data center exceeds the deliquescent relative humidity (DRH) of salts or accumulated particulate matter, it absorbs moisture, becomes wet and subsequently leads to electrical short circuiting because of degraded surface insulation resistance between the closely spaced features on the printed circuit boards. Another concern with this type of failure is the absence of evidence that hinders the process of evaluation and rectification. Therefore, it is imperative to develop a practical test method to determine the DRH value of the accumulated particulate matter found on PCBs. This research is a first attempt to develop an experimental technique to measure the DRH of dust particles by logging the leakage current versus %RH for the particulate matter dispensed on an interdigitated comb coupon. To validate this methodology, the DRH of pure salts like $MgCl_2$, NH_4NO_3 and NaCl is determined and their results are then compared with their published values. This methodology can therefore be implemented to help lay a modus operandi of establishing the limiting value or an effective relative humidity envelope to be maintained at a real-world data center facility for its continuous and reliable operation at its respective location.

5.1 Introduction

ASHRAE defines an air economizer as “A duct and damper arrangement and automatic control system that together allows a cooling system to supply outdoor air to reduce or eliminate the need for mechanical cooling during mild or cold weather [1].” This efficient cooling method draws in outside air from the ambient and is then filtered using MERV 11 or MERV 13 filters to eliminate particulate contaminants before being introduced into the cold aisle of a data center [2-8]. When the temperature of the outside air is lower than the temperature of the air that is recirculated in the data center, the economizer mixes it with the exhaust air (hot air) to achieve the desired temperature and humidity range. The mixed air is then supplied to the data center with proper filtration and conditioning. The amount of enthalpy in the air is acceptable and no auxiliary conditioning is required if the outside air is both sufficiently cool and dry. This mode of cooling operation is generally termed as free cooling [9]. Free cooling is adopted by numerous data centers across the United States as displayed in Figure 1-3 which also shows the usage of airside economizers in hours per year.

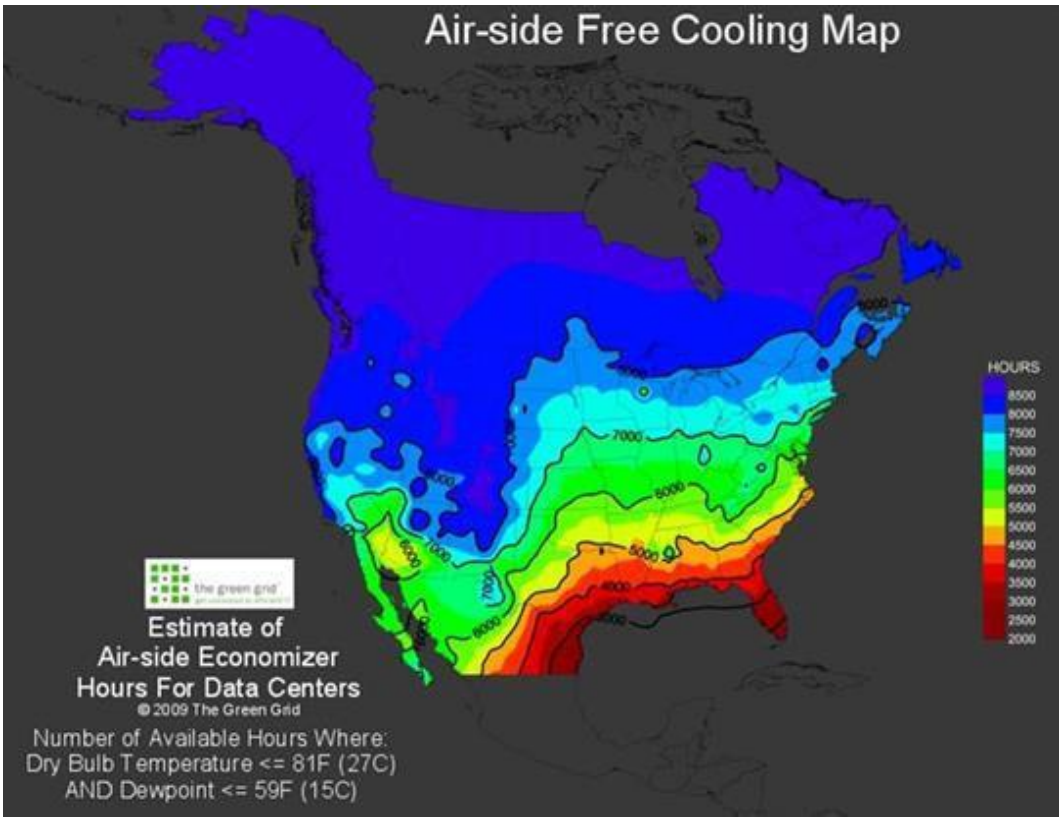

Figure 5-1 Usage hours of an airside economizer under ideal conditions

Utilization of ASEs result in the significant reduction in energy consumption of a data center in association with the cooling infrastructure. The risk that comes with the use of ASEs is that the temperature and humidity levels must be within specified ranges and more importantly is the entry of particle and gaseous contaminants that should be within allowable ranges. Direct evaporative cooling (DEC), indirect evaporative cooling (IEC), or two-stage indirect/direct evaporative cooling (I/DEC) systems could also be used to condition the outside air to increase the number of working hours of the ASE.

5.5.1 Effect of the Physical Environment on IT Equipment Reliability

The physical environment that surrounds the IT equipment is mainly defined by the temperature, relative humidity and gaseous and particulate contaminants. These factors can have adverse effects on IT equipment and can cause its failure in two ways:

- Corrosion of silver termination in surface mount components results in the formation of electrical open circuits. This type of failure mode occurs mainly in geographical areas with high levels of sulphur bearing gaseous contaminants [10]. Manufacturers have improved their hardware to tackle this failure mode.
- There are also a few other mechanisms that result in electrical short circuits. (i) In 2006, the European Union's RoHS directive banned the use of lead in solders. This led to changes in the surface finish of PCBs [11]. This also led to increased failure rates of PCBs because of creep corrosion [12,13]. (ii) Electrochemical reactions such as ion migration and cathodic and anodic filamentations [14]. (iii) Particulate matter that settles on PCBs adsorb moisture thereby reducing surface insulation resistance between the closely spaced features on PCBs.

5.2 Dust Or Particle Contamination

5.2.1 Introduction

Fine, dry particulate matter mainly composed of particles of the earth or waste material lying on the ground or on different surfaces or carried in air in defined as dust. There are numerous terms used synonymously with dust such as atmospheric dust, particulate contamination, particulate matter and airborne particles. In terms of its characteristics and compositions, dust is known to have a complex nature and understanding.

Based on their size, dust is mainly classified into two groups: fine particles and coarse particles. Fine particles are defined as particles with a diameter less than or equal to 2.5μm such as those found in diesel particulate matter (DPM), exhaust of motor vehicles, smoke and

haze. Fine particles are further classified into primary and secondary particles [15,16]. Primary particles are the fine particles that are directly emitted from a specific source, such as volcanoes, forest fires, unpaved roads, construction sites, fields, etc. Secondary fine particles are those that are formed because of photochemical reactions that take place in the atmosphere and make up most of the fine particulate pollution. These photochemical reactions occur due to the presence of oxides of sulphur and nitrogen that are emitted from automobiles and various industries. Carbonaceous material with a size of less than 0.1μm interact with nitrogen dioxide and sulphur dioxide in a multistep photochemical process to thereby result in the formation of nitric and sulfuric acids. Fertilizers generally containing ammonia, decayed biological matter and other sources neutralize these acids thereby forming ammonium sulphate, ammonium nitrate and ammonium hydrogen sulphate. Most of these secondary particles are considered anthropogenic [17,18]. On the other hand, coarse particles are those particles with a size range of 2.5-15μm. They include sea salt, natural and artificial fibres and plant pollen. Their major sources mainly include erosion of soil, flaking of biological materials and minerals [19].

Dust particles consists of both organic and inorganic substances. The inorganic substances generally outweigh the organic substances. Certain inorganic compounds are water soluble salts. Table 1 lists the relative content of the main mineral particles in dust. Methods like X-ray power diffraction (XRPD), transmission electron microscopy (TEM) and electron probe microanalysis (EPMA) have been implemented to analyze the mineral [20].

Table 5-1 Relative Content of Mineral Particles Found in Dust

Minerals	**Main Compositions**	**Relative Contents**	
		Nature dust (size < 250 μm)	**Fine particles (Size <10 μm)**
Quartz	SiO_2	1	1

Feldspar	$KAlSi_3O_8$-$NaAlSi_3O_8$- $CaAl_2Si_2O_8$	0.77	0.8
Calcite	$CaCO_3$	0.48	1.91
Mica	$SiO_2 \cdot Al_2O_3 \cdot K_2O \cdot Na_2O \cdot H_2O$	0.41	2.24
Gypsum	$CaSO_4 \cdot 2H_2O$	0.05	0.72

Fibres, carbon black and organic ions such as acetate (CH3COO-) and formate (COOH-) are the organic substances in dust [21]. These organic compounds can be analyzed by gas chromatography or mass spectrometry (GC/MS). Thermo gravimetric analysis (TGA) is used to evaluate the weight percentage of organic compounds.

When considering the impact of dust on the reliability of IT equipment, the focus is mainly imparted on the ionic content of dust particles because they have the tendency to dissolve in water and conduct electricity. When dust begins to adsorb moisture and when it eventually forms a saturated solution, the major cations and anions are Na^+, NH^{4+}, K^+, Ca^{2+}, Mg^{2+}, Cl^-, NO^{3-}, F^- and $SO4^{2-}$ [22].

In coarse particles, calcium, ammonium, sulphate, sodium, magnesium and chloride are the most common ionic components with large local variations for sodium, magnesium and chloride [23].

5.2.2 Properties of Accumulated Particulate Matter

- Thermal Conductivity: Solid dust particles that accumulate on the equipment creates a thermal insulating layer and thus minimizes the allocated area for heat dissipation. This leads to the excessive heating up of components.
- Electrical Conductivity: Solid substances can be classified into highly insulating substances and electrically conducting substances. Insulating substances aid in

accumulating static charges destroys the working on integrated circuits. When the relative humidity is considerable high, these substances can absorb moisture and can subsequently lead to their increased conductivity thus causing hardware failures.

- Abrasiveness: Particulate matter that deposit between moving parts can result in their wear and tear over time.
- Adhesiveness: This is generally defined as the ability of particulate matter to stick or hold on to the surface. This furthers leads to an increase in the thickness of the thermal layer, bearing failures and high voltage relays.
- Corrosivity: The nature of dust particles permits them to ingest moisture and vaporous contaminants and thus become corrosive [24].

Two extremely common consequences of particulate or dust contaminations on printed circuit boards are electrochemical migration and loss of impedance, i.e. the loss of surface insulation resistance, between traces and component leads. These two failure mechanisms involve the contamination by creating a path flow for leakage current.

5.3 Dust Related Failure Mechanisms

5.3.1 Surface Insulation Resistance (SIR) and Electrochemical Migration (ECM)

Accumulated particulate matter or dust drastically increases the risk of several failure modes in PCBs. Moisture sorption by hygroscopic materials in dust and the capillary action by mineral particles lead to the formation of a thick water film on the substrate of PCBs. The water-soluble salts that are present in the dust dissolve in the water film thereby causing ionic contamination. This in turn results in the reduction in surface insulation resistance (SIR) to an unacceptable limit by forming a conductive path across adjacent electrodes. In other words, SIR degradation on a printed circuit board occurs between the electrical conductors when they are connected by a substrate that is covered by an electrolyte formed by hygroscopic particulate matter or dust at elevated relative humidity conditions. The PCB includes certain metals such as

copper traces, solder materials and component leads. The ionic contamination can react with these metals on the board and can result is the dissolution of the metal which can corrode the metal. Under the influence of an electric field, certain metallic ions dissolved in the anode could migrate to the cathode to form metallic dendrites. This mode of failure is termed as electrochemical migration (ECM). An electric field is one of the main driving forces in ECM. The metal dendrites bridge the gap between adjacent conductors or features thus causing the leakage current between these conductors to increase. Permanent failures can take place if a dendrite carries current density and leads to a permanent short. When a dendrite grows, causes an electrical short and then a burn out due to high localized current density, intermittent failures occur. The propensity of ion migration also depends on the solubility of the corrosion products at the anode. Metal compounds having lower solubility give out fewer ions for migration. Corrosion and ECM are accompanied by leakage current failure that is measured as SIR degradation. PCBs that have dust settled on them might fail at an early stage due to reduction in SIR between the closely spaced features in the presence of moisturized dust (appropriate RH conditions close to the DRH), before the dendrites bridge. Figure 2 displays a schematic representation of electrochemical migration according to the ‘classical model’ [25]. The dissolved Mn+ ions at the anode migrate to the cathode. At the cathode, they are deposited by receiving electrons and reducing back to metal. This ‘classical model’ was initially demonstrated for the migration of silver [26]. It was later proved that this model could also be applied to many other metals that are used in electronics such as copper, tin and lead [27].

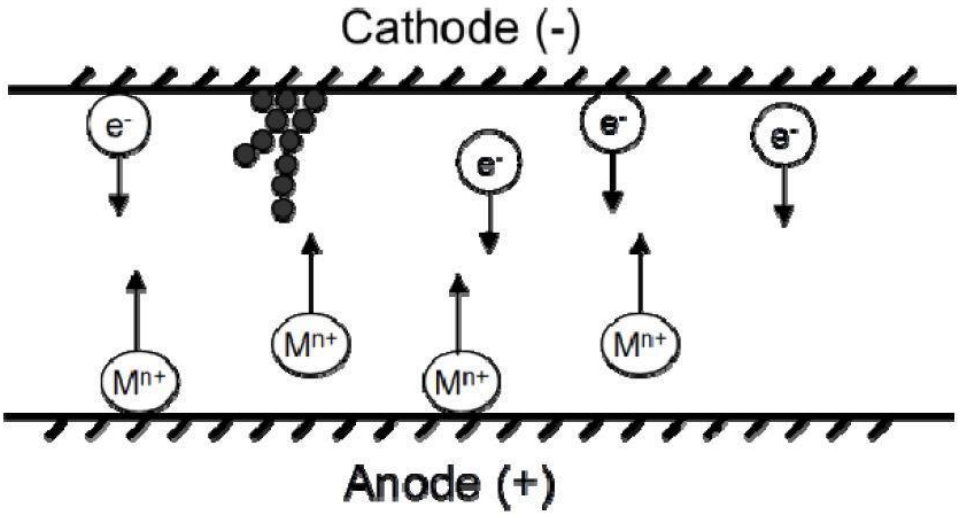

Figure 5-2 Schematic Representation of the ECM Phenomenon

The growth of dendrites take place when electrolyte bridges two electrodes and forms a path. Anodic dissolution results in the formation of metal ions. At the anode, cations are generated due to oxidation of metals and causes anodic corrosion. Under the influence of electromotive forces, the metal ions migrate through the electrolyte towards the cathode and the last step is the electrochemical metal deposition at the cathode. Dendrites or dendrite like structures may continue to grow towards the anode as more neutral metal deposits on the nuclei. When the dendrite runs through the entire gap between the two adjacent conductors and makes contact with the anode, an electrical short might occur. As a result of Joule heating, the current flowing through the dendrite could burn out a part of the dendrite. This situation can cause intermittent failures. If the dendrites that form are thick enough to withstand the current flowing through it, it can result in a permanent short [28].

5.4 Relative Humidity

5.4.1 Role of relative Humidity

Relative humidity can significantly influence IT. They are as follows [29]:

- Deteriorated performance of IT equipment through increased dissipation factor and PCB epoxy dielectric constant.
- The presence of gaseous contamination leads to enhanced corrosion.
- Decrease in the surface insulation resistance in the presence of particulate contamination.

5.4.2 Concept of CRH and DRH

In simple terms, relative humidity (RH) is defined as the amount of water vapor in the air and is generally expressed as a percentage of the maximum amount that the air could hold at the given temperature. Critical Relative Humidity (CRH) is defined as the relative humidity at which the salt or dust particles just begins to adsorb enough moisture to start becoming electrically conductive. Deliquescence Relative Humidity (DRH) is defined as the relative humidity at which the salt or dust particles begin the formation of a saturated salt solution.

When dust settles on PCBs, it can lead to an electrical short circuiting between closely spaced features when a voltage drop exists across them. This corrodes the circuit board components and metal traces. The ionic components in the dust absorb moisture from the environment and creates ionic bridges which result in the electrical short circuiting. The presence of moisture in the air and ionic components in the dust together leads to corrosion. Besides affecting the reliability of equipment by corrosion and ion migration, dust can also degrade computer reliability due to overheating by settling around electrical connectors.

When the humidity in the environment rises above the deliquescence relative humidity of the particulate matter, it is known to become wet and therefore ionically conductive and corrosive [30]. Miniaturization of electronic of electronic components, the decrease in the

feature spacing on printed circuit boards and allowing in the data center to operate in allowable temperature and relative humidity ranges in order to save energy is making electronic hardware susceptible to failure due to accumulation of particulate matter.

The plot of electrical conductivity of the particulate matter versus relative humidity can be best used to best describe the role of particulate contamination in high relative humidity environments on hardware reliability [30]. The electrical conductivity can be expressed as the leakage current through the accumulated particulate matter when a constant voltage across the particulate matter exists. Figure 3 shows an example of a graph of the log of leakage current versus relative humidity for a certain amount of particulate matter collected from IT equipment from a certain data center in India [29]. The CRH is estimated at the intersection of the lower relative humidity asymptote and the inversion line. This is the relative humidity at which the particulate matter just begins adsorbing enough moisture to start becoming electrically conductive. The intersection of the inversion line with the upper asymptote corresponds to the value of the deliquescent relative humidity (DRH) of the particulate matter. This value of relative humidity is at which the formation of a saturated salt solution begins. Particulate matter of low deliquescence relative humidity is of major concern. They could either be generated within the data center space or its source could be outside air. The fine particles and ultrafine particles that are present in the outside air are high in ionic content in the form of ammonium, sulphate and nitrate salts. Generation of particulate matter within a data center with low DRH is extremely rare. The water is high in salt content, magnesium chloride being the most damaging. In humidifiers that are poorly maintained, the salt content present in the water begins to escalate. Once the water spray droplets evaporate, they leave behind a salt residue that then becomes airborne as the air passes through the humidifier. This salt settles on IT equipment and in turn causes hardware failure in the presence of high relative humidity. The rusting of the nickel-plated steel covers on various subassemblies right above the raised floor is usually the

first indication of the presence of corrosive salts and high relative humidity. These perforated steel covers are the inlet for the cold air high in humidity. This problematic situation can be prevented by installing a reverse osmosis system in the humidifier thus keeping the humidifier water low in ionic content.

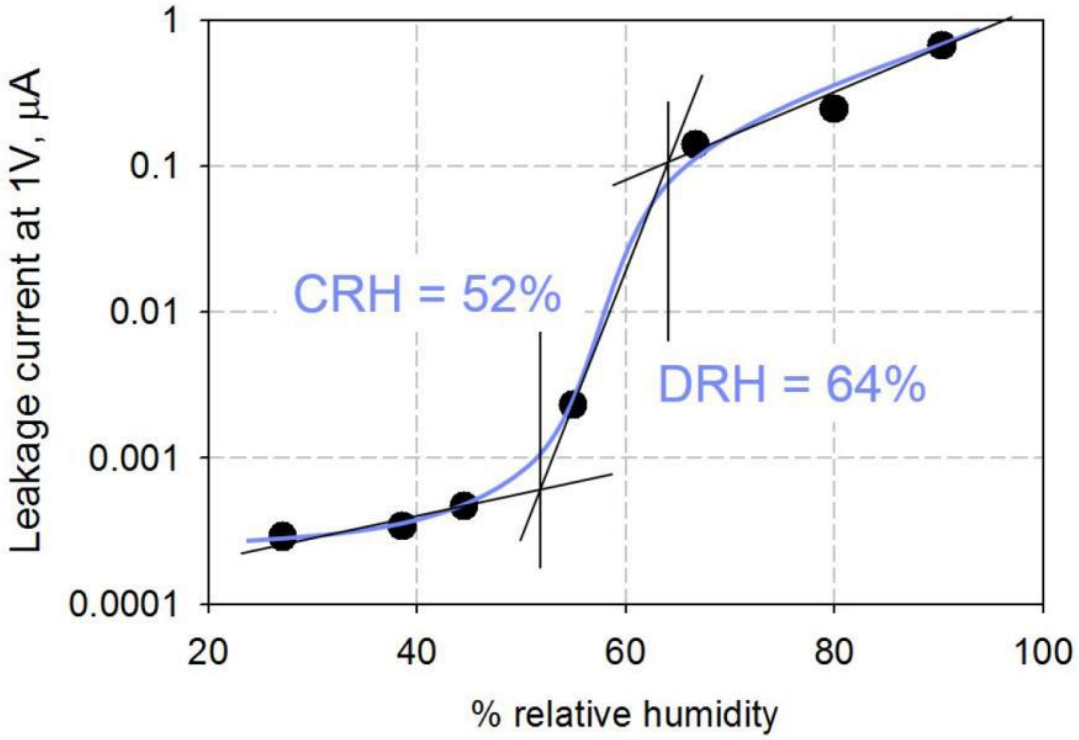

Figure 5-3 Leakage current through accumulated particulate matter as a function of relative humidity.

5.4.3 DRH Measurement Techniques

The most important parameter controlling the rate of corrosion is the relative humidity in the data center. Each salt contamination has a certain value of deliquescent relative humidity beyond which the salt will absorb moisture and become wet. Wet salts can further corrode metals. Therefore, it is imperative to develop a practical test method to determine the DRH value of the accumulated particulate matter found on PCB's.

With respect to the measurement of Deliquescent Relative Humidity of pure salts, there are two other experimental methodologies. They are:

- Gravimetric Method
- Electrical Impedance Method

5.4.3.1 Gravimetric method:

This method focuses on measuring the weight of the salt at different values of relative humidity. With a plot of the weight of the salt Vs %RH, the DRH of the salt can be determined. This plot can also be termed as a growth curve for salt particles. A microgravimetric balance is employed is measuring the weight of the salt. The ideology behind this method comes with the adsorbing nature and hence the increase in the weight of the salt sample. Thus, the value of relative humidity at which there is a sudden change in the weight of the salt is said to be its DRH value.

Certain amount of the salt sample is placed an aluminum pan and is kept in a dynamic vapor sorption apparatus at a temperature of 25^{o}C. The chamber is the evacuated to a vacuum to make sure the sample is completely dry and free of any moisture content. A mass flow controller unit is utilized to introduce water vapor into the measurement chamber until the desired value of relative humidity is obtained. The microbalance aids in monitoring the weight of the salt sample throughout the experiment. The relative humidity was varied between 0%-90% with an interval of 2%.

The following figure, Figure 4, shows the mass change or the mass uptake of a few salts (NaCl and NH_4NO_3) and varying values of relative humidity [30]. In other words, the mass uptake of the salts is compared as a function of relative humidity. Below a certain threshold relative humidity, the mass uptake of each salt is almost negligible which agrees completely with the theory as well. It can also be seen that the leakage current is also extremely low below a certain relative humidity. It is only after a certain %RH that the there is a significant rise in the

mass uptake or water adsorbed by the salt. The value of leakage current can also be seen to rise steeply beyond this threshold value. The results obtained in this method, i.e. DRH for NaCl as 73% and the DRH for NH_4NO_3 as 58% are below their published values of 75% and 62%-64% respectively.

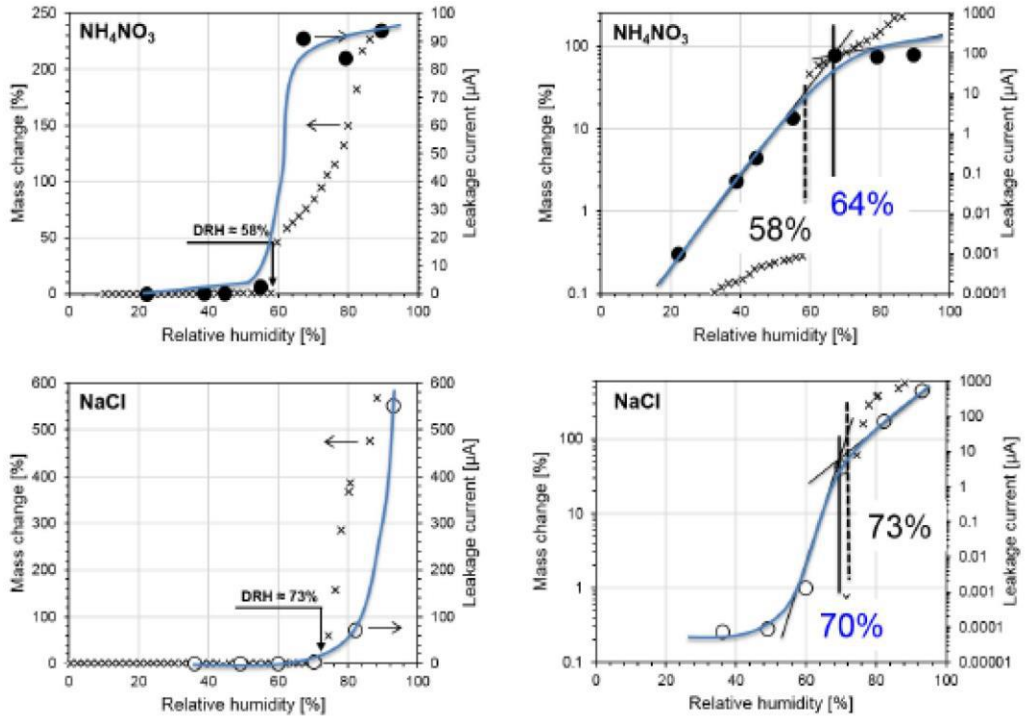

Figure 5-4 Gravimetric Method compared to the leakage current method at 25°C for NH_4NO_3 and NaCl: Linear and Logarithmic Graphs.

5.4.3.1.1 Limitations of this method

- Salts have the tendency to actively react with the environment that surrounds it. It is very important to make sure that the chamber is completely void of any moisture content at the beginning of the experiment. Since this method focuses on the mass change as a function of DRH, it is imperative to be extremely cautious with the experimental setup.

- The step range is 2% of relative humidity. Only when the change in mass over time becomes negligible for a certain value of relative humidity, the sample is considered to be in a state of equilibrium with the water vapor and only then its mass is recorded. Thus, this method would take a much longer time to give out results and thus determine the corresponding DRH of the salt.
- Despite the small step range, the intensive care of the testing equipment, incorporation of more data points and time investment, yet the results obtained by this method do not match the published values.

5.4.3.2 Electrical impedance method

The experimental setup for this method of DRH measurement is as shown in Figure 5. A conductivity cell that comprises of two platinum electrodes and a piece of porous paper is used for the DRH measurement of the salt sample. The porous paper is wetted with the salt solution to help develop an evenly distributed layer of salt crystals to form between the platinum electrodes when the relative humidity is lower than the DRH [31].

The porous paper or filtration paper is placed on a surface that is arched and that is made of polytetrafluoroethylene (PTFE). At values above the DRH of the salt, the salt adsorbs the moisture and forms a solution, the arched allows this excess liquid to drain off and thus maintain a constant thickness of the conducting layer [32]. About 0.5mL of the salt solution is carefully pipetted onto the filtration paper before starting the experiment.

A precision impedance analyzer (LCR Meter) is utilized in this experiment as a conductivity measuring meter. The alternating current voltage frequency is set at 1000Hz. At frequencies higher than 1000 Hz, poor response was noted. A data acquisition system is coupled to the LCR mater and the controller of the humidity chamber.

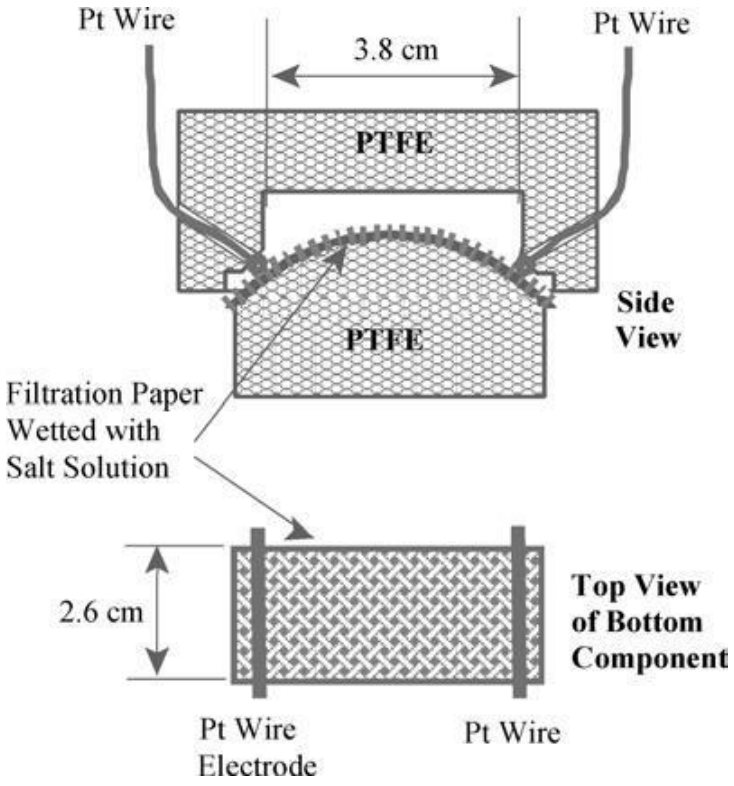

Figure 5-5 Schematic diagram of the conductivity cell for DRH Measurement

The experiment conducted in this study was used to determine the electrical impedance of the conductivity cell containing Na_2SO_4 (Sodium Sulphate). Figure 4-4 shows how the impedance of the conductivity cell varies with increasing values of %RH. The experiment was conducted at a temperature of 50^{o}C and relative humidity varying from 78%-91%. Each step is carried out an interval of 23 hours. From the graph of impedance Vs %RH, we can notice that the impedance decreases sharply as the %RH is increased from 85% to 88%. After 91%, the impedance remains unchanged. From this we can infer that the salt has reached its deliquesced state.

The sharp decrease in the electrical impedance as the %RH is increased from 85%-88% indicates that the DRH of Na_2SO_4 is between 85-88% at 50^{o}C. Another fundamental factor that this method doesn't clearly explain is that the gradual decrease in measured impedance

could also be likely due to the adsorption of water by the salt and not necessarily the deliquescence of the salt. As a result of deliquescence, an aqueous phase with a much lower impedance than that shown in Figure 6 would be formed.

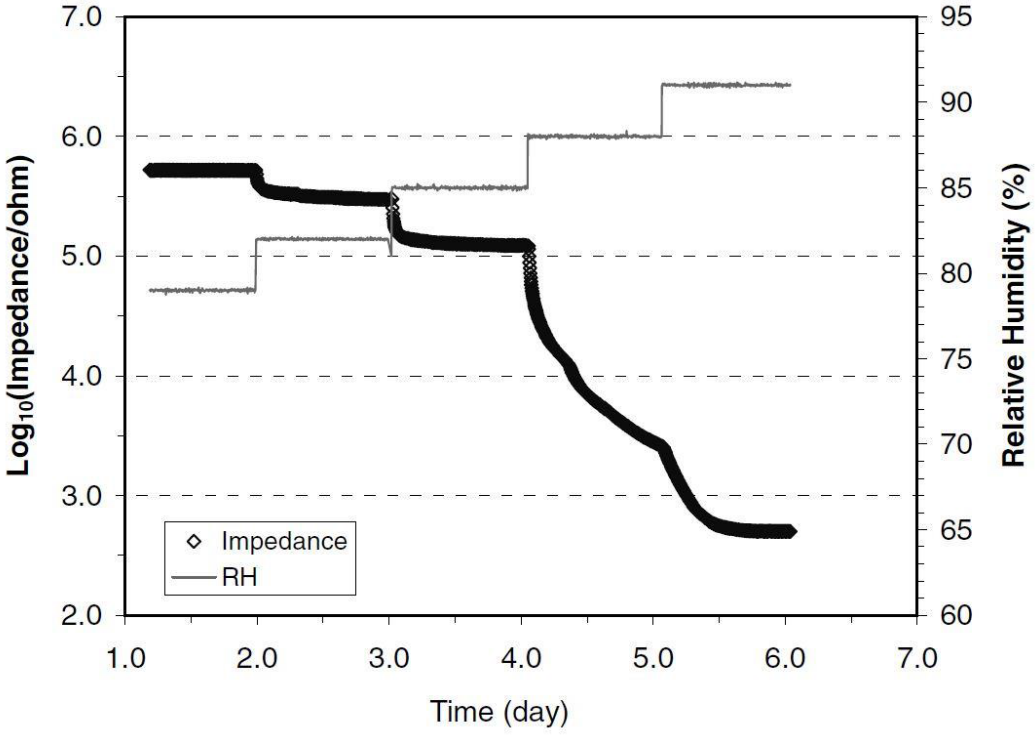

Figure 5-6 Impedance measured Vs %RH at 50°C (Na_2SO_4)

5.4.3.2.1 Limitations of this method:

- Platinum electrodes and Data Acquisition Units are used thus making this experimental setup very expensive.
- Each time step is carried out an interval of 23 hours thereby making this process time consuming.
- The setup is a complicated and should not be disturbed.
- The results obtained have to further substantiated with concrete literature to help validate the technique.

5.5 Experimental Method to Determine the DRH of Pure Salts

5.5.1 Experimental Requirements

This experiment aims at determining the deliquescence relative humidity (DRH) of pure salts. Since this experimental is the first of its kind, it is imperative to validate the experimental process by comparing the experimental results obtained with published results. This method is adopted based on the well-established relationship between the leakage current and %RH. The influence of particulate matter on the reliability of I.T. equipment can be described by a plot of the electrical conductivity of particulate matter against relative humidity.

The following items are used in order to help develop this experimental method to determine the DRH of pure salts and thus accomplish the objectives of this thesis.

5.5.1.1 Salt solutions

- Three salt solutions, namely: Sodium Chloride (NaCl), Ammonium Nitrate (NH_4NO_3), Magnesium Chloride ($MgCl_2$) are used in this experiment to determine their DRH.
- 0.1 wt% of each of the salt solution is prepared. 10mg of the salt is dissolved in 10ml of deionized water thus resulting in the 0.1 wt% concentration. The DRH of the salt is doesn't vary with its concentration.
- Deionized water is generally defined as water that is free from all charged atoms or molecules or ions. Also, deionized water is commonly used in performing this experiment because the ions found in water can affect the experiment. Incorporation of ions in the experiment, even in a small amount, can produce faulty or inaccurate results.

Figure 7 shows the three salt solutions – Sodium Chloride, Ammonium Nitrate and Magnesium Chloride respectively.

Figure 5-7 Sodium Chloride, Ammonium Nitrate and Magnesium Chloride Solution

At a temperature of 25ºC, the following are the published DRH values of each salt [33]:

- Sodium Chloride: 75.8%
- Ammonium Nitrate: 64%
- Magnesium Chloride: 32.78%

Certain information of some ions found in these salt solutions are discussed.

Chloride ions(Cl^-): One of the most detrimental materials found in dust is chloride. Chlorides accelerate the electrochemical failure mechanisms such as electrolytic corrosion and metal migration when combined with moisture in the environment and an electrical bias. The amount of chloride added by the soldering process to bare PCBs was investigated by Weekes [34]. It was shown the 3 µg/in2 was added to the bare printed circuit boards by using no-clean flux and

about 8µg/in2 was added by using water soluble flux. Ion chromatography (IC) and SIR were conducted to determine the acceptable amount of chloride on assembled boards and on bare boards. It was found that about 2.5 µg/in2 and µg/in2 were the acceptable amounts when using no clean flux when using bare boards and assembled boards respectively. When using water soluble flux, 6 µg/in2 and 8 µg/in2 were acceptable amounts.

Ammonium ions (NH_4^+): The chemical reaction of ammonia (NH_3) with hydrogen ions could result in the formation of ammonium. Ammonium (NH_4^+) is mildly acidic. Ammoium has the tendency to complex with hydroxide ions resulting in the formation of hydrogen ions thus leading to an acidic environment. Most ammonium salts are highly soluble in water. The limiting ionic conductivity of ammonium ions is 73.7 $S.cm^2/mol$ [35], making it equally conductive as the chloride and potassium ions. The presence or existence of ammonium ions can decrease the SIR of PCBs in the presence of moisture.

Sodium ions (Na^+): Since the standard electrode potential of sodium relative to the standard hydrogen electrode potential is -2.71 V, the sodium metal is highly reductive [35]. It is because of this particular reason why sodium exists in the environment never as a free element but only as a compound.

The sodium ions (Na^+) are highly stable in water. They always exist as counter ions to numerous anions, sodium chloride (NaCl) being the most abundant. The limiting value of ionic conductivity of the sodium ions is 50.11 $S.cm^2/mol$ which is two-thirds that of chloride ions (Cl^-). Thus the existence of Na^+ in the surface moisture film can lower the SIR and greatly increase the conductivity of PCBs.

5.5.1.2 Multipurpose Test Board

To specifically evaluate and understand the interactions between the solder masks, solder paste and fluxes, the Institute for Printed Circuits, also called the IPC, designed the ‘IPC-B-25A Multipurpose Test Board’ or the ‘PCB-B-25A Test Board’. Another vital function of this

test board is to evaluate the effects of moisture and insulation resistance of solder masks. The test board is normally a 0.062" FR-4. FR-4 is a NEMA (National Electrical Manufacturers Association) grade designation for the glass reinforced epoxy laminate material. This composite material is composed of woven fiberglass cloth with an epoxy resin binder that is flame resistant.

The board is a developed by a simple print and etch technique. Also, the available surfaces are bare copper, Electroless nickel immersion gold (ENIG) or hot air solder levelling (HASL) for materials qualification. It could also be any other surface finish as required.

Two comb patterns from the IPC-B-24 test board were included in the IPC-B-25A test board are designated as patterns E and F. The pattern D was included from the IPC-B-25 board, which was the older board and identical to pattern B/E. Pattern C which is the military Y pattern, was used to link to extensive qualification databases in the military.

Figure 8 shows the IPC-B-25A Multipurpose Test Board that is used in this experimental method. The comb coupons E and F are specifically used for this experiment.

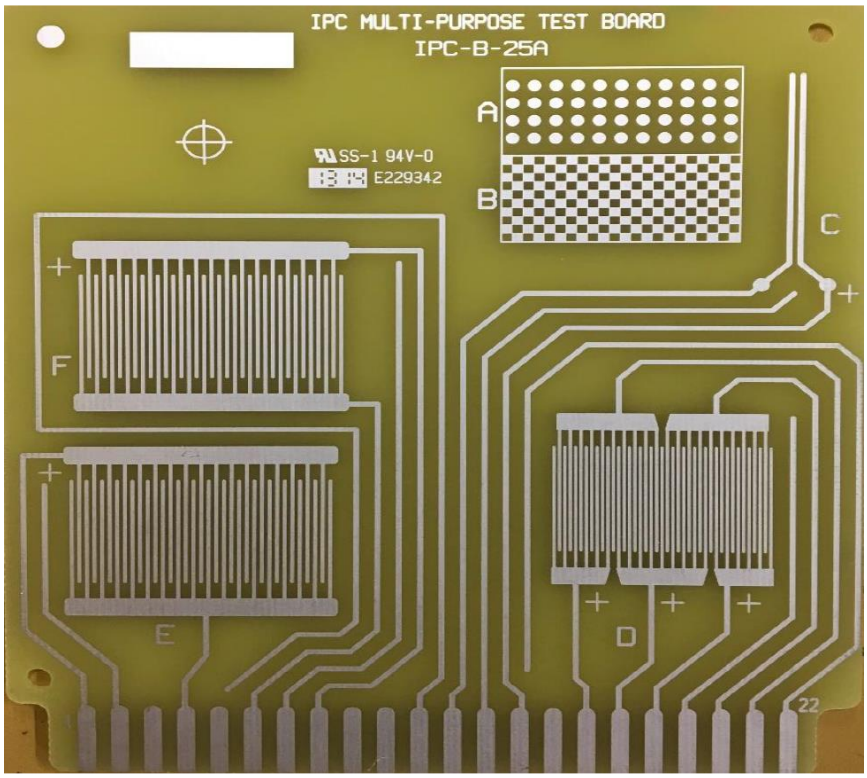

Figure 5-8 IPC-B-25A Multipurpose Test Board

5.5.1.3 Environmental Chamber

For this experiment, the temperature was maintained at 25^{o}C and the relative humidity was varied from 10%-90% at regular time intervals of 1 hour and 30 minutes between each step. In order to perform this operation, the ‘Thermotron SE-600-10-10 Environmental Chamber is used. Figure 9 shows the environmental chamber used in this experiment.

Figure 5-9 Environmental Chamber – Thermotron SE-600-10-10

The Thermotron incorporates a wide range of applications and specific compressor selections ranging from 3 to 15 Hp. It can provide rapid product temperature changes. The optimized airflow system of the Thermotron improves gradient control thereby providing greater accuracy, tighter uniformity and enhanced performance on the products.

The Thermotron is equipped with a 12" touch screen programmable controller therefore making data collection and operation of the chamber easy and reliable. With respect to the functions executed in the experiment, the following are a few chamber capabilities.

- Workspace Volume: 20.7 ft^3
- Humidity Range: 10% - 98%
- Temperature Range: -70^oC – 180^oC

5.5.1.4 D.C Power Supply

This experiment requires a very precise application of 1 volt. The ‘Agilent E3614A’ power source serves the purpose. The constant voltage (CV) mode is used to provide the desired 1V. Figure 10 shows the D.C. power source that is employed. In addition to the constant voltage and constant current modes, there also exists an adjustable over-voltage protection, front and rear output terminals, remote analog programming and remote sensing that helps in automatically compensating the voltage drops.

Figure 5-10 D.C Power Supply

5.5.1.5 INA-219 Current Sensor coupled with an Arduino Uno Board

In order to help measure the leakage current which falls in the mA range, the Adafruit INA-219 current sensor is employed. This current sensor is coupled with an Arduino Uno board. A program code as shown in Appendix A is developed to help this setup accurately measure and display the value of leakage current at each instant when voltage is applied across the ends of each comb coupon. The INA-219 board helps in obtaining solutions for all power monitoring

problems keeping the margin of error less than 1%. Figure 11 displays the current sensor with the screw terminal [36].

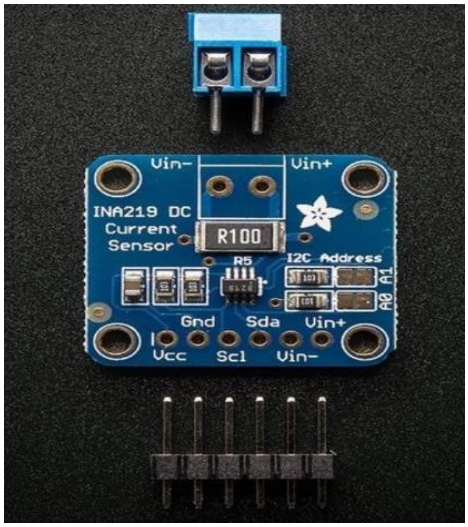

Figure 5-11 INA219 Current Sensor

Of the many Arduino boards that are currently available in the market, the Arduino Uno as shown in Figure 12, is the most commonly used open-source microcontroller board. The Arduino Uno board consists of a 16MHz quartz crystal, a power jack, a reset button, 6 analog pins and 14 digital pins that can be interfaced to various other circuits or expansion boards. The Arduino Integrated Development Environment (IDE) is used to program the Arduino Uno via a USB cable. An external 9V battery or a USB cable can be used to power the Arduino. It also accepts voltages between 7 and 20V.

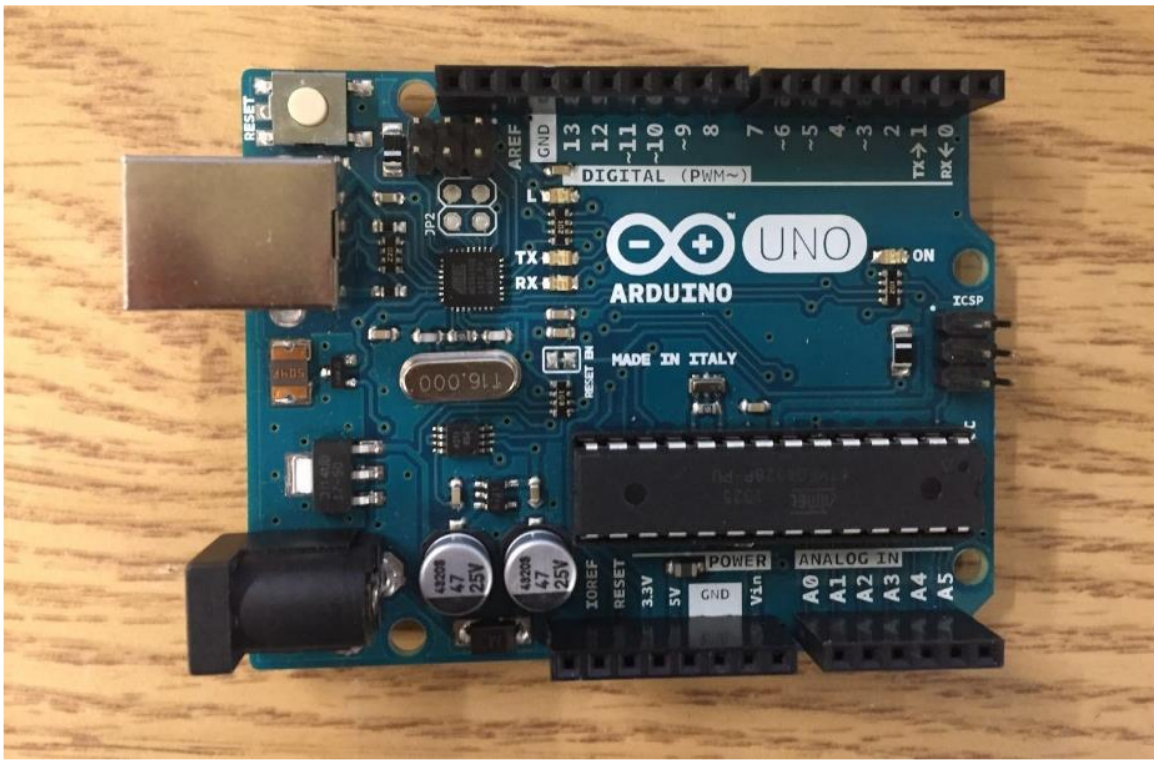

Figure 5-12 Arduino Uno

Coupling the Arduino and Current Sensor: The 5V pin on the Arduino can be used to power up the INA219 current sensor breakout board. The sensor communicates with the Arduino via the I2C. Dupont cables are used to make the interconnects between the Arduino and the INA219 current sensor thereby allowing them to freely communicate. The interconnects made are as follows:

- The GND of the Arduino is connected to the GND of the sensor.
- The 5V of the Arduino is connected to VCC of the sensor.
- The SDA of the Arduino is connected to the SDA of the sensor.
- Lastly, the SCL of the Arduino is connected to the SCL of the sensor.

The schematic representation is as shown in Figure 13.

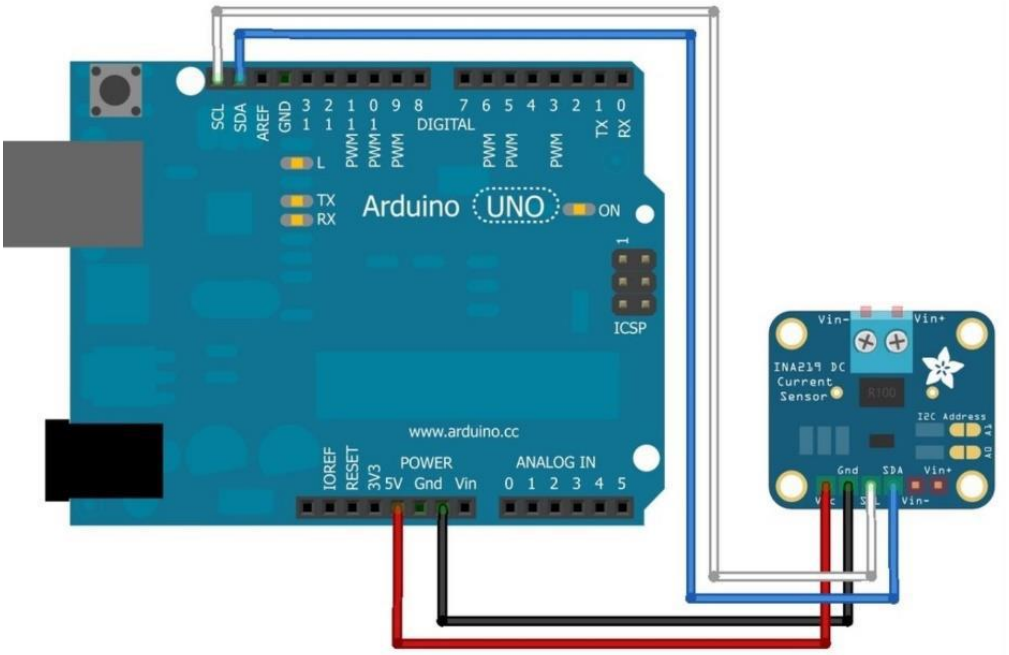

Figure 5-13 Interconnections between the Arduino and the INA219 Current Sensor

Development of the electrical circuit by assimilation of the current sensor: Figure 13 also shows a screw terminal that is connected to soldered to the INA219 current sensor. The V+ of the screw terminal is connected to the positive terminal of the Agilent power source that is used. The V- of the screw terminal is connected to the positive terminal of the load. This helps in putting the sense resistor in line with the circuit. In this experiment, the connecting wire is soldered to the positive terminal of the load. Lastly, a connecting wire from the negative terminal of the power supply is connected to the GND on the Arduino and a connecting wire from the negative terminal of the power supply is soldered to the negative terminal of the load. Figure 14 shows the coupling of the sensor to the Arduino.

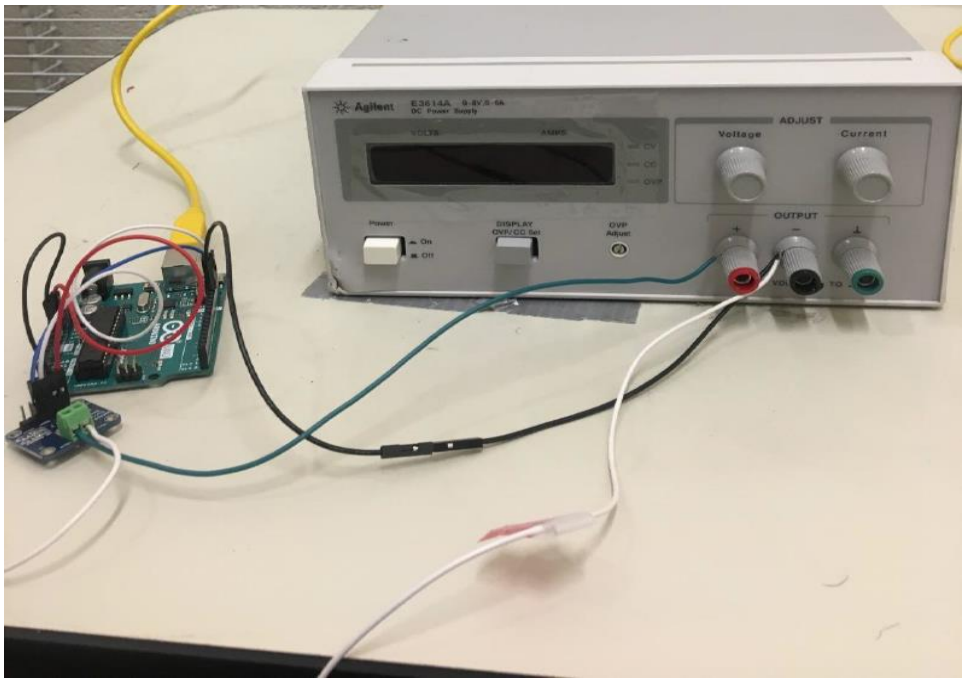

Figure 5-14 Arduino Coupled with the INA219 Current Sensor connected to the DC Power Source.

5.5.2 Experimental Procedure

- The soldering of the connecting wires and the interconnections between the Arduino and the current sensor is done as mentioned in section 5.1.5. The comb coupon is then placed in the environmental chamber as shown in Figure 15.

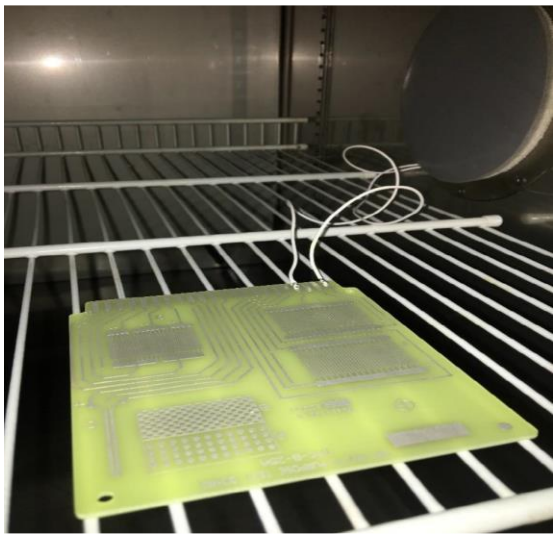

Figure 5-15 Connecting wires soldered to the positive and negative terminal of the comb coupon and place in the environmental chamber.

- 10 drops of the 0.1 wt% of the salt solution is carefully dispensed on the comb coupon using a suction syringe. A pipette can also be used. Figure 16 displays the salt solution dispensed on the comb coupon. One salt sample is tested at a time to ensure a controlled approach.

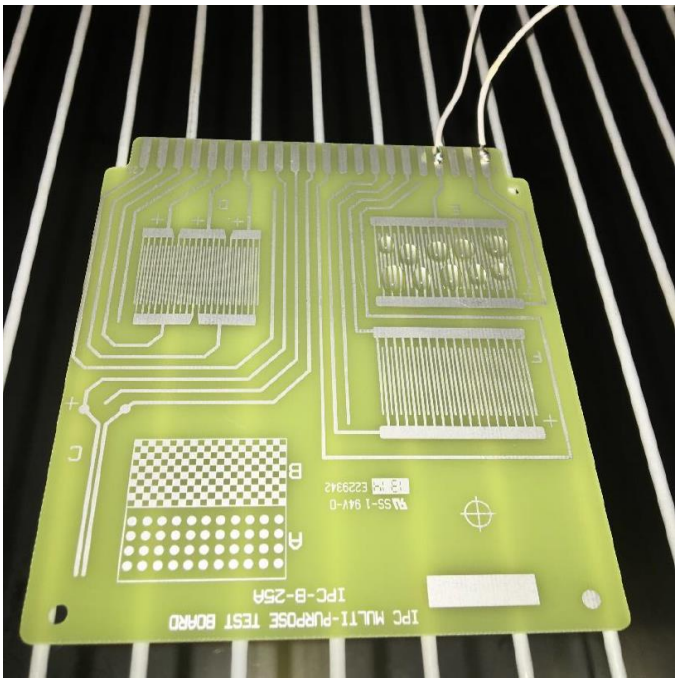

Figure 5-16 10 drops of the salt solution carefully dispensed on the comb coupon.

- It is very important to make sure that the comb coupon remains in the environmental chamber during the entire course of the experiment. The salts tend to quickly react or reach equilibrium conditions with the environment that surrounds it. Therefore, it is vital that the coupon remains untouched and undisturbed during the entire course of the experiment to obtain accurate results.
- The environmental chamber is then set to a fixed temperature of 25^{o}C and a relative humidity of 10% and is allowed to rest for a period of 12 hours. This step is performed to allow the saturated salt solution to get rid of its moisture content thereby allowing just the salt particles to settle on the coupon. At this step, the salt should be completely dry and free of moisture. Figure 17 displays the programmable monitor of the environmental chamber displaying the value of temperature and %RH in the chamber.

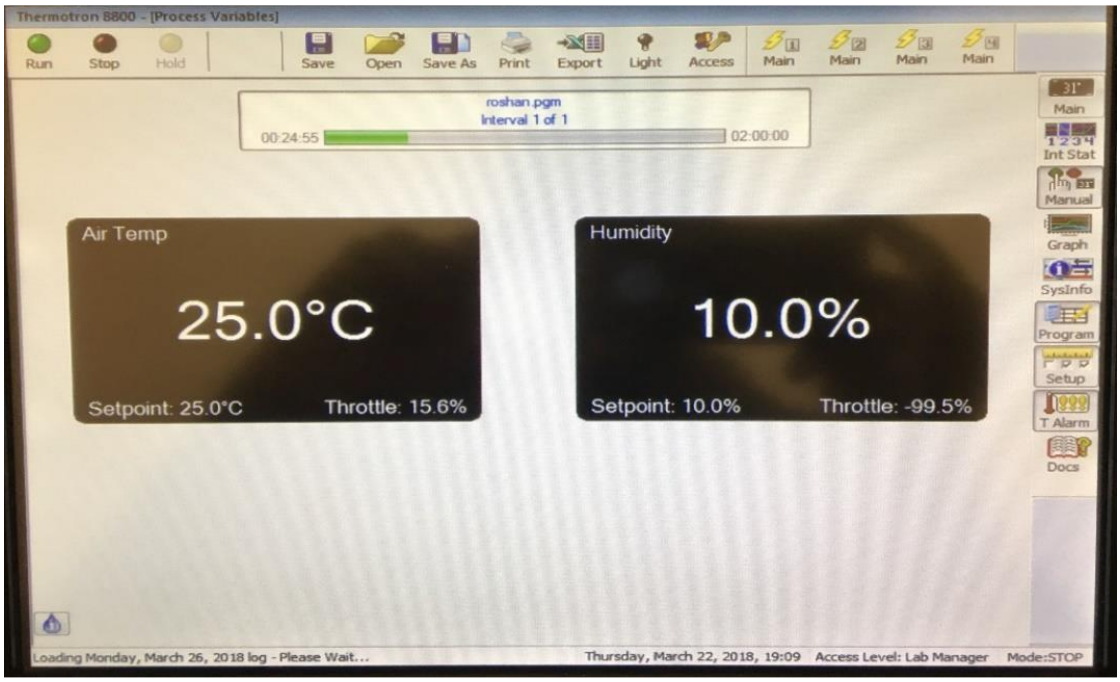

Figure 5-17 Touchscreen programmable monitor of the environmental chamber set at a temperature of 25°C and 10% RH.

- A DC voltage of +1V and -1V, each for 1-2 seconds, is passed through the comb coupon to disturb the electrochemistry of the salt that is being tested. The reason to apply the -1V immediately after the application of +1V is to neutralize or cancel the effect of the +1V on the ions of the salt.
- The application of the positive and negative voltage is carried out by switch the connecting wires at the terminals of the power supply.
- Simultaneously, at this point, the leakage current is measured across the comb coupon. The INA219 current sensor coupled with the Arduino Uno board helps in displaying the load voltage and leakage current.

- The relative humidity is gradually increased in steps of 10% for a duration of 90 minutes each. This allows the salt to attain equilibrium with the relative humidity conditions. The load voltage and leakage current is measured again.
- This process is repeated until a relative humidity of 90% is achieved.
- The values of %RH, Leakage current (in mA) and Log of leakage current are tabulated.
- A graph of the log of leakage current is plotted versus the %RH.
- This plot helps in attaining the CRH and DRH of the respective salt that is being tested.
- The experiment is repeated for the remaining salt samples.

5.6 Results And Discussions

5.6.1 Results

5.6.1.1 To estimate the DRH of Sodium Chloride (NaCl)

Table 2 displays the values of leakage current obtained at various values of %RH on the application on +1V and -1V respectively. The log of leakage current is also calculated and tabulated.

Table 5-2 Leakage current at varying values of %RH on the application of +1V and -1V (NaCl Sample)

+1 Volt			-1 Volt		
%RH	Current (mA)	Log I	%RH	Current (mA)	Log I
10	0.08	-2.52573	10	0.09	-2.40795
20	0.1	-2.30259	20	0.1	-2.30259
30	0.1	-2.30259	30	0.1	-2.30259
40	0.1	-2.30259	40	0.2	-1.60944
50	0.2	-1.60944	50	0.2	-1.60944
60	0.3	-1.20397	60	0.3	-1.20397
70	6.8	1.916923	70	8.1	2.091864
80	58.8	4.074142	80	64.6	4.168214
90	120	4.787492	90	129	4.859812

Figure 18 and 19 displays the linear plots of leakage current versus %RH when +1V and -1V have been applied respectively.

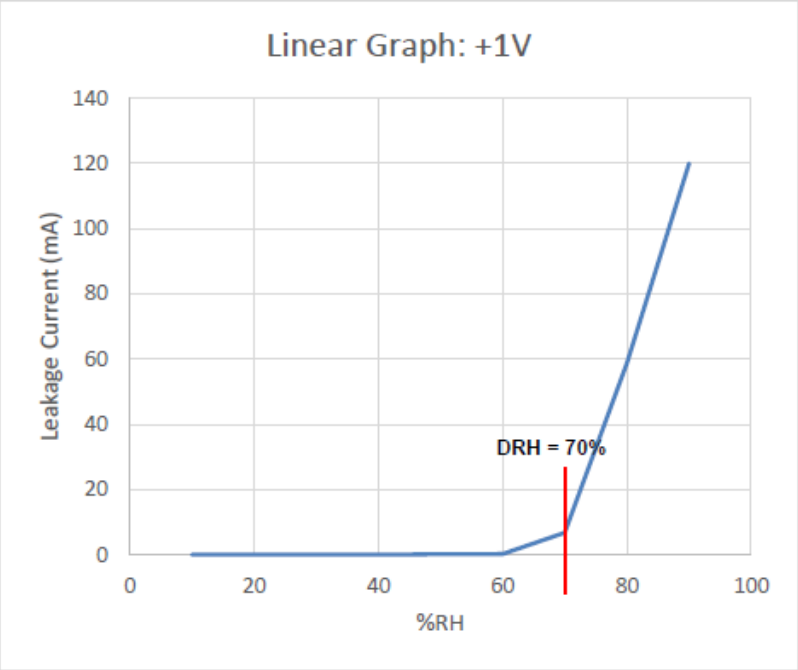

Figure 5-18 Linear plot of Leakage Current versus %RH for NaCl (+1 Volt)

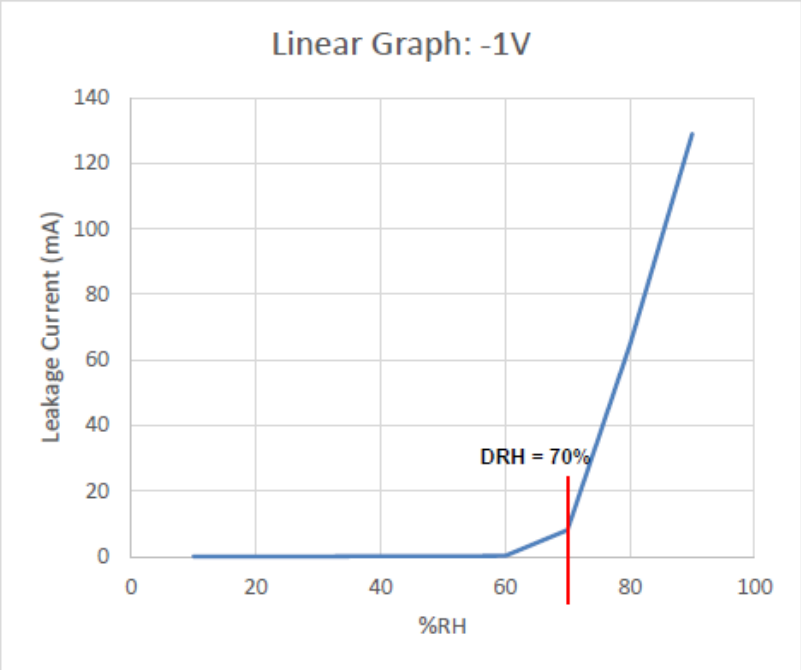

Figure 5-19 Linear plot of Leakage Current versus %RH for NaCl (-1 Volt)

Figure 20 and 21 displays the logarithmic plots of leakage current versus %RH when +1V and -1V have been applied respectively.

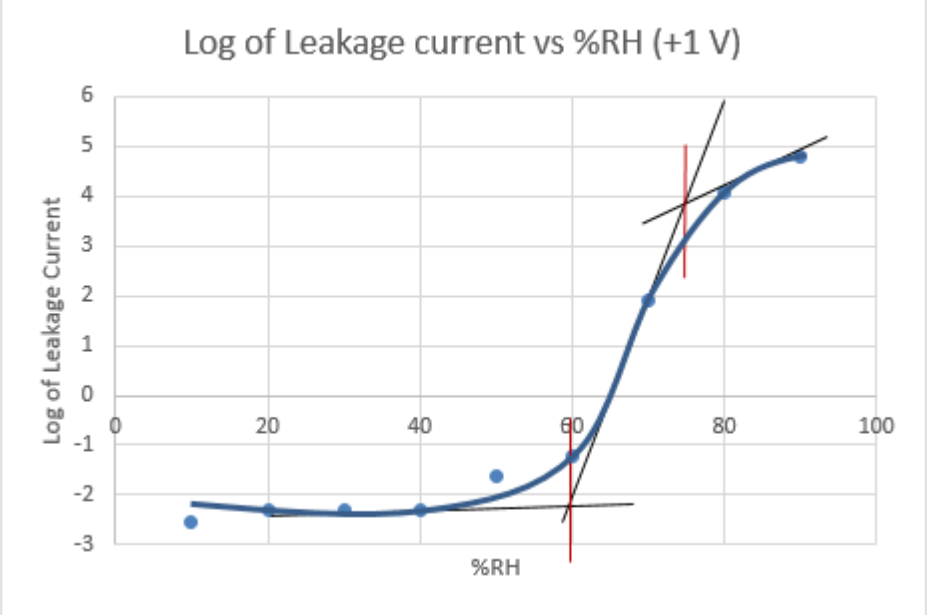

Figure 5-20 Logarithmic plot of Leakage Current versus %RH for NaCl (+1 Volt)

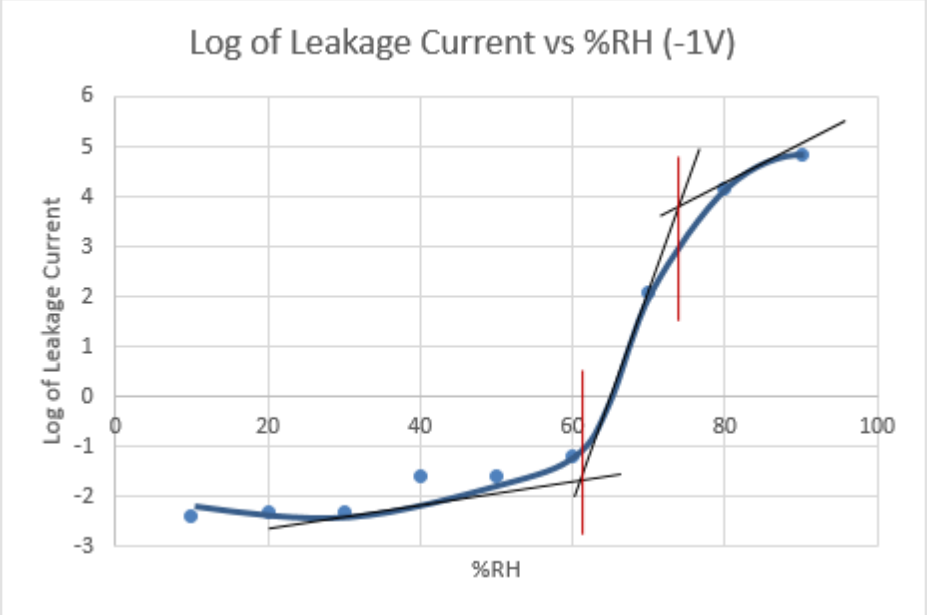

Figure 5-21 Logarithmic plot of Leakage Current versus %RH for NaCl (-1 Volt)

At the beginning of the experiment, few drops of the salt solution are dispensed on the coupon and is made to dry out completely before the stepwise increment in the %RH. During the course of the experiment, when the %RH exceeds the DRH of the salt, it begins to corrode the coupon. The before and after pictures of the comb coupon dispensed with NaCl solution is as seen in Figure 22 and Figure 23 depicts the effect of relative humidity in the presence of particulate contamination. The corrosion effects are also very evident.

Figure 5-22 Drops of NaCl dispensed on the comb coupon.

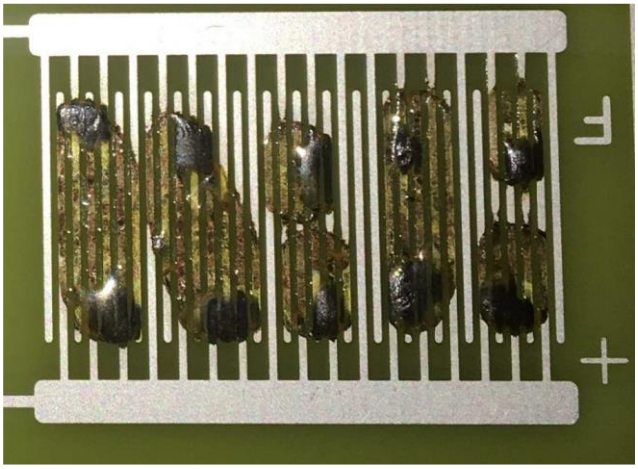

Figure 5-23 Corrosion due to the conducting nature of the NaCl salt solution at a relative humidity higher than the DRH.

5.6.1.2 To estimate the DRH of Ammonium Nitrate (NH_4NO_3)

Table 3 displays the values of leakage current obtained at various values of %RH on the application on +1V and -1V respectively. The log of leakage current is also calculated and tabulated.

Table 5-3 : Leakage current at varying values of %RH on the application of +1V and -1V (NH4NO3 Sample)

+1 Volt			-1 Volt		
%RH	I (mA)	Log I	%RH	I (mA)	Log I
10	0.07	-2.65926	10	0.08	-2.52573
20	0.09	-2.40795	20	0.09	-2.40795
30	0.1	-2.30259	30	0.1	-2.30259
40	0.2	-1.60944	40	0.1	-2.30259
50	0.2	-1.60944	50	0.2	-1.60944
60	0.4	-0.91629	60	0.4	-0.91629
70	21.1	3.049273	70	21.1	3.049273
80	38.2	3.642836	80	38.2	3.642836
90	47	3.850148	90	47	3.850148

Figure 24 and 25 displays the linear plots of leakage current versus %RH for the ammonium nitrate sample when +1V and -1V have been applied respectively.

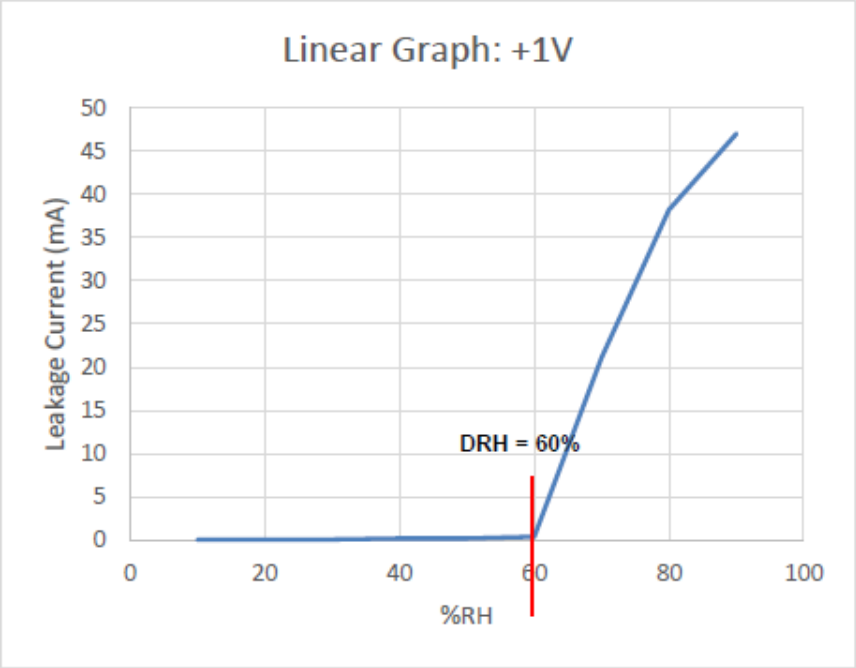

Figure 5-24 Linear plot of Leakage Current versus %RH for NH4NO3 (+1 Volt)

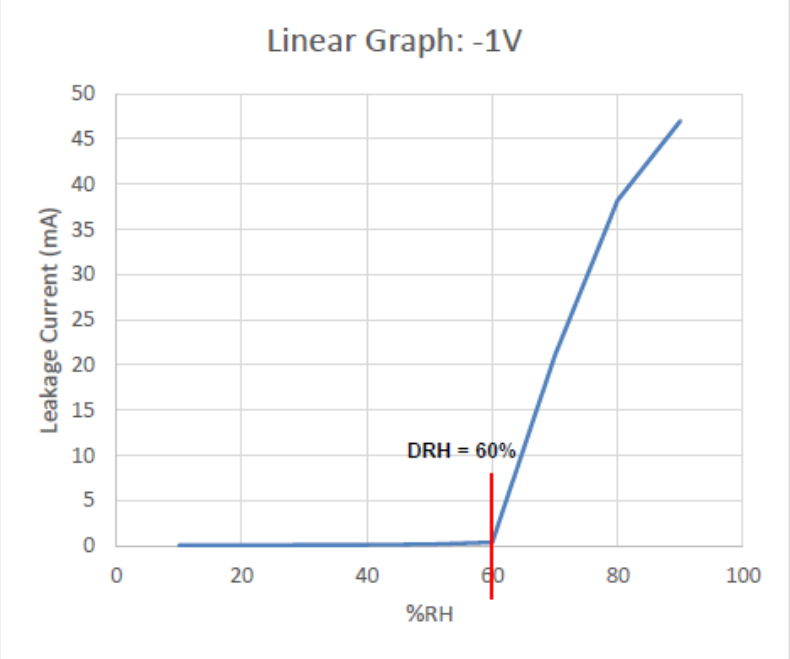

Figure 5-25 Linear plot of Leakage Current versus %RH for NH4NO3 (-1 Volt)

Figure 26 and 27 displays the logarithmic plots of leakage current versus %RH when +1V and -1V have been applied respectively.

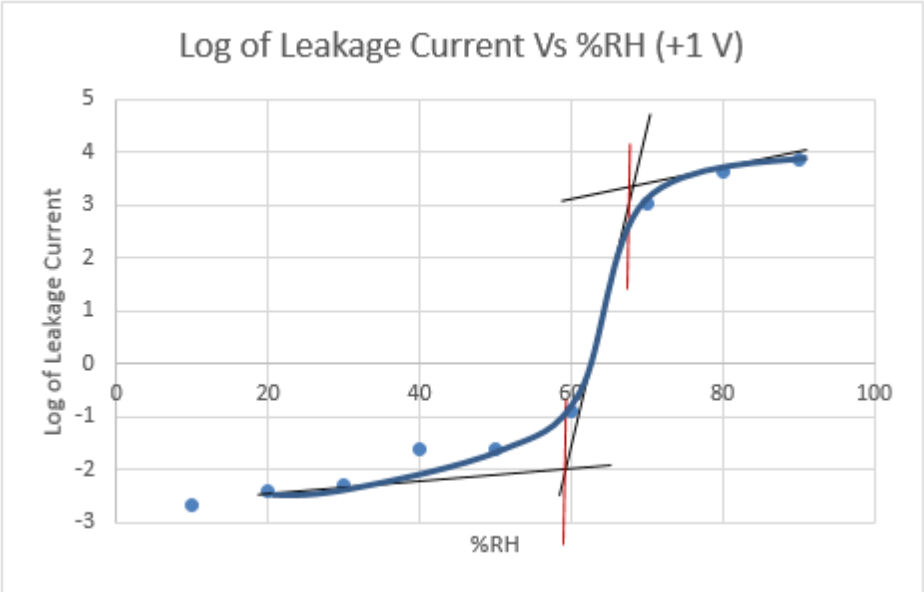

Figure 5-26 Logarithmic plot of Leakage Current versus %RH for NH4NO3 (+1 Volt)

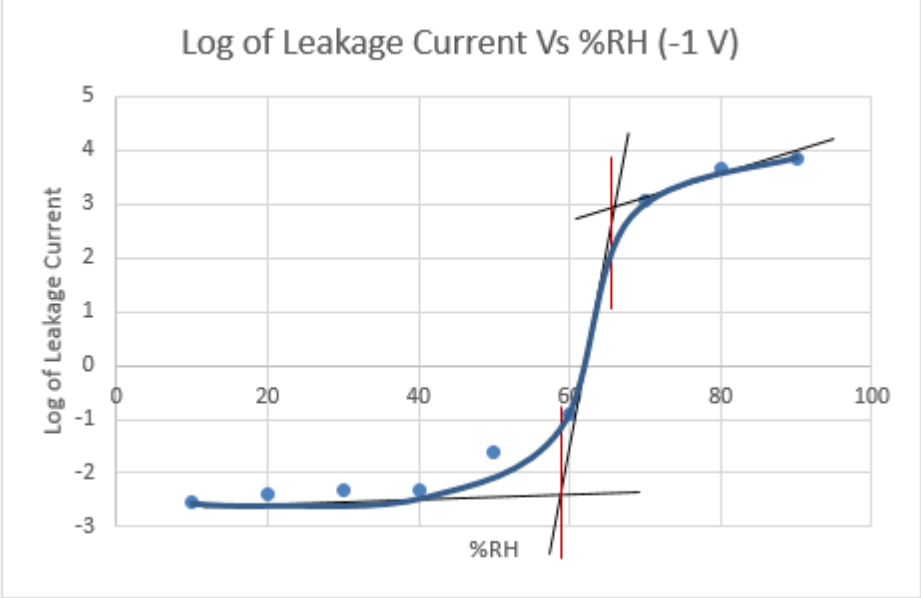

Figure 5-27 Logarithmic plot of Leakage Current versus %RH for NH4NO3 (-1 Volt)

The before and after pictures of the comb coupon dispensed with NH_4NO_3 solution is as seen in Figure 28 and Figure 29 depicts the effect of relative humidity in the presence of particulate contamination. The corrosion effects are also very evident.

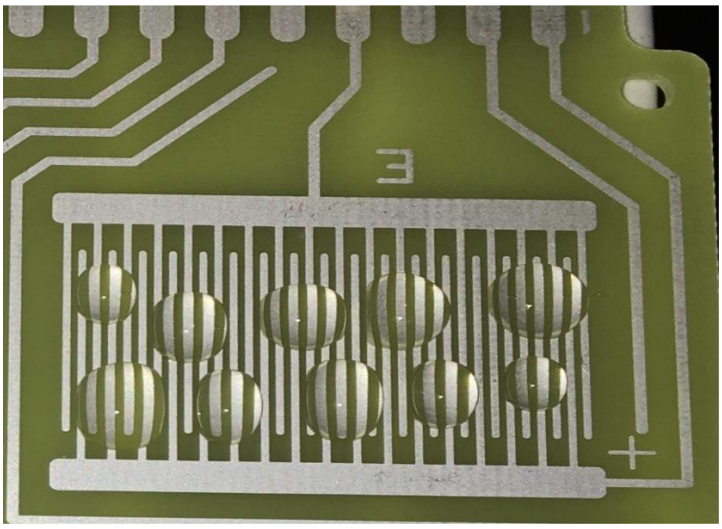

Figure 5-28 Drops of NH_4NO_3 dispensed on the comb coupon.

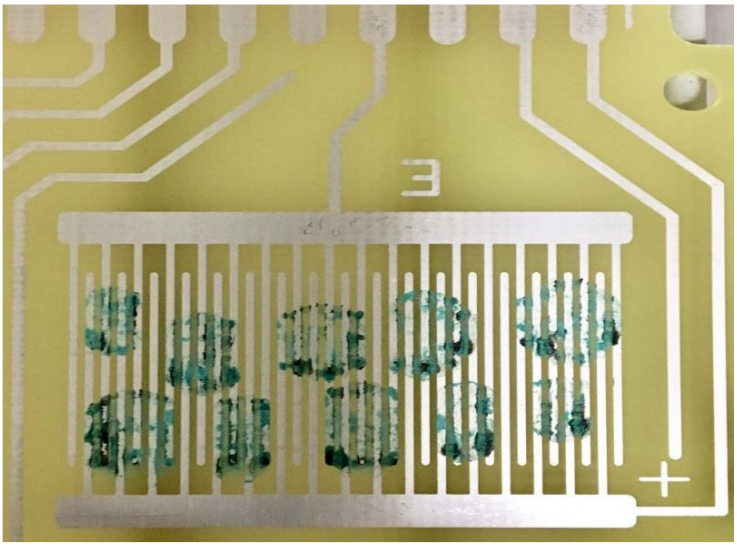

Figure 5-29 Corrosion due to the conducting nature of the NH_4NO_3 salt solution at a relative humidity higher than the DRH.

5.6.1.3 To estimate the DRH of Magnesium Chloride ($MgCl_2$)

Table 4 displays the values of leakage current obtained at various values of %RH on the application on +1V and -1V respectively to the magnesium chloride sample. The log of leakage current is also calculated and tabulated.

Table 5-4 Leakage current at varying values of %RH on the application of +1V and -1V (MgCl2 Sample)

+ Volt			-1 Volt		
%RH	I (mA)	Log I	%RH	I (mA)	Log I
10	0.1	-2.30259	10	0.1	-2.30259
20	1.3	0.262364	20	1.2	0.182322
30	5.3	1.667707	30	4.6	1.526056
40	12.8	2.549445	40	12.8	2.549445
50	18.8	2.933857	50	20.2	3.005683
60	24.7	3.206803	60	25.8	3.250374
70	33.7	3.517498	70	34.8	3.549617
80	38.8	3.65842	80	40	3.688879
90	41.3	3.720862	90	42.4	3.747148

Figure 30 and 31 displays the linear plots of leakage current versus %RH for the magnesium chloride sample when +1V and -1V have been applied respectively.

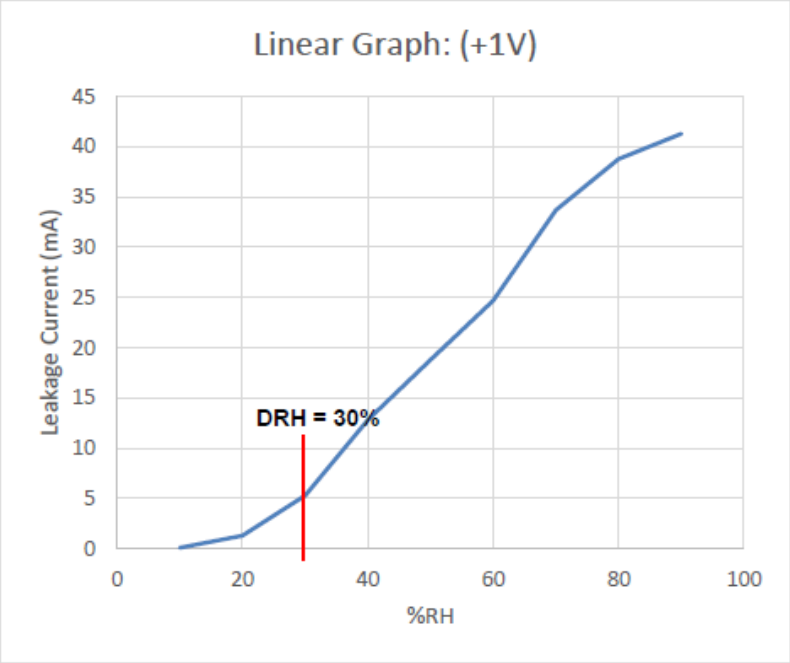

Figure 5-30 Linear plot of Leakage Current versus %RH for MgCl2 (+1 Volt)

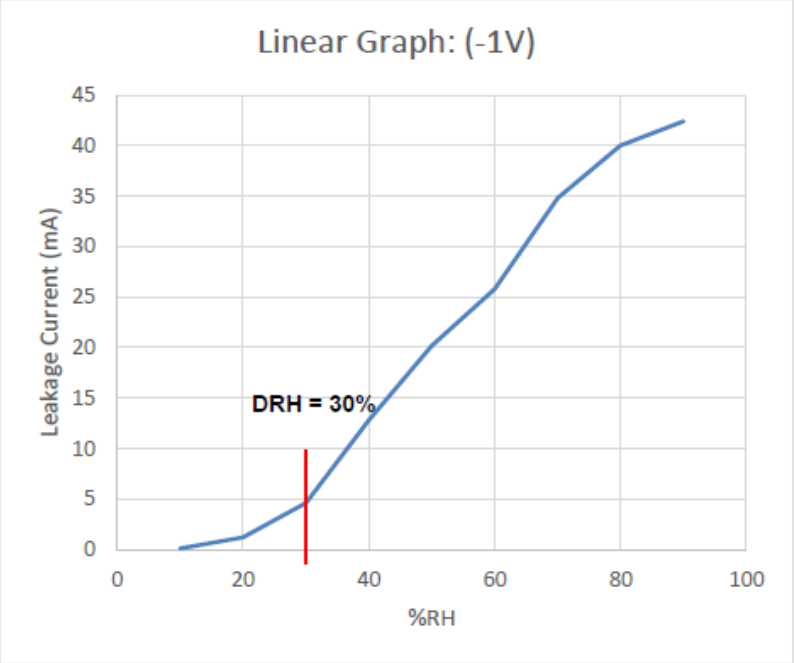

Figure 5-31 Linear plot of Leakage Current versus %RH for MgCl2 (-1 Volt)

Figure 32 and 33 displays the logarithmic plots of leakage current versus %RH when +1V and -1V have been applied respectively.

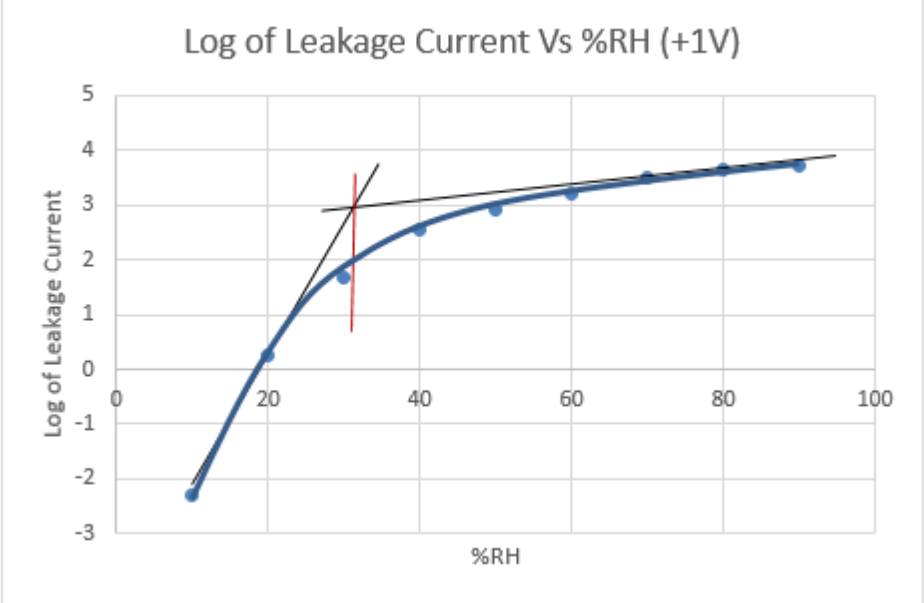

Figure 5-32 Logarithmic plot of Leakage Current versus %RH for $MgCl_2$ (-1 Volt)

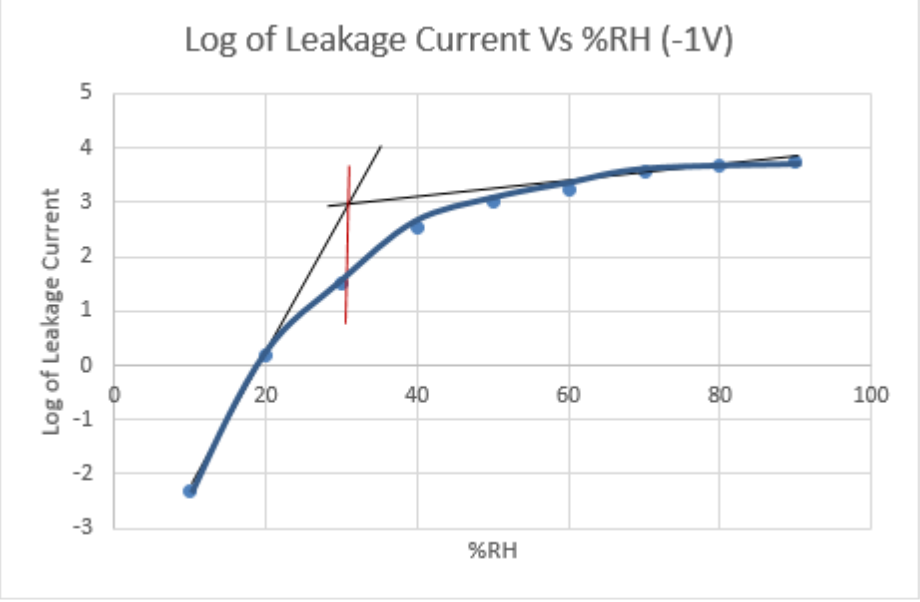

Figure 5-33 Logarithmic plot of Leakage Current versus %RH for $MgCl_2$ (-1 Volt)

The before and after pictures of the comb coupon dispensed with $MgCl_2$ solution is as seen in Figure 34 and Figure 35 depicts the effect of relative humidity in the presence of particulate contamination. The corrosion effects are also very evident.

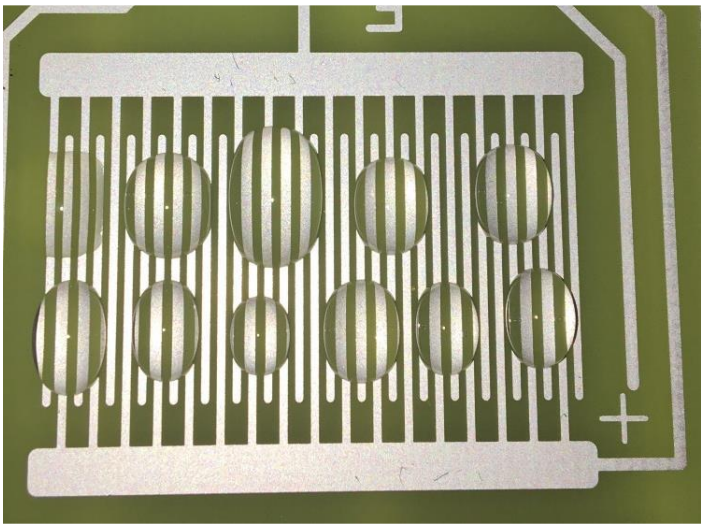

Figure 5-34 Drops of $MgCl_2$ dispensed on the comb coupon.

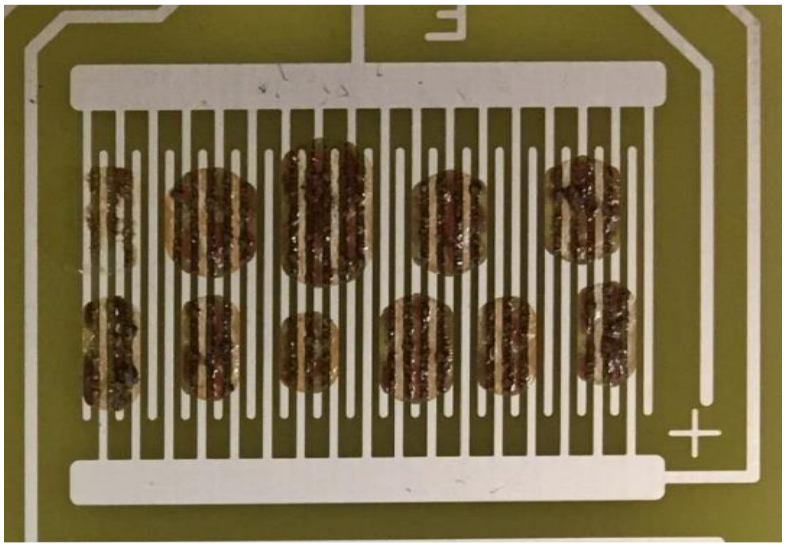

Figure 5-35 Corrosion due to the conducting nature of the $MgCl_2$ salt solution at a relative humidity higher than the DRH.

5.6.2 Discussions

From observing the linear plots for all the three salt samples Figures 18, 19, 25, 26, 31 and 32, it is rather tempting to interpret these linear plots in terms that the sudden increase in electrical conductivity (or leakage current) or the intercepts of the lower and higher humidity asymptotes being the deliquescence relative humidity of the salts. However, the main problem faced here is the obtained DRH values which are 70% for NaCl, 60% for NH_4NO_3 and 30% for $MgCl_2$ do not coincide with their published values as seen in Table 5. Also, they depend on the magnitude of the vertical scale.

Table 5-5 Comparison of experimental results with the published results by analyzing the linear plots of leakage current versus %RH

Salt	Published Values at 25oC	Experimental Values (Linear Plots)
Sodium Chloride	DRH: 75.8%	DRH: 70%
Ammonium Nitrate	DRH:64%	DRH: 60%
Magnesium Chloride	DRH: 32.78%	DRH: 30%

In order to overcome this drawback and to obtain the deliquescence relative humidity with published values, another efficient method of plotting the values of leakage current are to be discovered.

The logarithm of leakage current is plotted against %RH as seen in Figures 20, 21, 27, 28, 33 and 34. The curves which are S-shaped can then be made piecewise linear by drawing straight lines the cover the inversion region, the lower relative humidity asymptote and higher relative humidity asymptote. The intersection of the lower relative humidity asymptote and the

inversion line corresponds to the critical relative humidity (CRH) of the salt. It is at this value that the leakage current begins to rise sharply with the increase in %RH. The intersection of the inversion line with the higher relative humidity asymptote corresponds to the deliquescence relative humidity (DRH) of the salt. At lower humidity ranges, the salt is generally in equilibrium with the humidity. Thus, a small increase in the relative humidity does not considerable change the electrical conductivity of the salt as the salt stays relatively dry. There is a rapid rise in the conductivity as the salt absorbs enough moisture to start approaching the deliquescence state. This can be noticed by the high slope of the inversion region. When the relative humidity continues to rise above the DRH of the salt, the salt is completely dissolved and any further rise in the relative humidity has very little influence on the electrical conductivity of the salt solution being tested. It is logical to consider the intercept of the inversion line and higher relative humidity asymptote to be the DRH of the salt because it refers to the value of relative humidity where the salt has absorbed just the right amount of moisture to become wet and that any further absorption of water will not cause an appreciable increase in its conductivity. Table 6 shows a comparison of the DRH of salts obtained performing the experiment, using logarithmic plots, with their published values. It is seen the experimentally obtained results perfectly match the published results thereby validating this experimental approach.

At higher relative humidity ranges, the SIR between the features on the coupon drastically decrease. The salt begins to conduct electricity and the images obtained after the experiment clearly displays the corrosion that takes place. Therefore, it would be efficient and judicious to maintain the relative humidity in a data center below the CRH of accumulated particulate matter to ensure the reliable operation of IT equipment and prevent its deterioration by electrical current leakages between the closely spaced features.

Table 5-6 Comparison of Experimental Values with Published Values

Salt	Published Values at 25°C	Experimental Values (Logarithmic Plots)
Sodium Chloride	CRH: 61% DRH: 75.8%	CRH: 61% DRH: 75.5%
Ammonium Nitrate	CRH: 59% DRH: 63%-64%	CRH: 59% DRH: 63%
Magnesium Chloride	DRH: 32.78%	DRH: 32.5%

Accumulated particulate matter with low deliquescence relative humidity is of major concern. It could either be generated in the data center space or outdoor air. In certain areas with poor air quality, most of the particulate matter obtain entry into the data center by the ventilation air that is driven through the HVAC (Heating, Ventilation and air-conditioning) systems.

Coarse and fine particulate matter in semi-urban and urban areas come from the exhaust of motor vehicles. The most polluting ones being those that are generated in diesel fueled vehicles. Diesel particulate matter, also known as DPM, is a particulate component of the diesel exhaust that released into the atmosphere, it can take the form of singular or individual particles. They are known as ultrafine particles because most of them are in the invisible submicron range of 0.1μm and are not visible to the naked eye. DPM includes diesel soot, aerosols such as ash particulates, sulphates, silicates and metallic abrasion particles.

ASHRAE Standard 52.2-2012 defines MERV as minimum efficiency reporting value [37]. MERV 8 and MERV 13 air filters are used to remove coarse and fine dust particles respectively from the outside air that is entering the data center. The control of DPM require MERV 16 or higher [37]. Data center that utilize CRAC units, the minimum filter that is required is MERV 8.

Fine and ultrafine particles that are present in the outdoor air or ambient have very high ionic content. The ionic content is in the form of ammonium salts, nitrate and sulphate [38-41]. Concerns with respect to fine dust with low deliquescence relative humidity on PCBs is well documented but cases of IT equipment failure due to fine dust have not been published yet.

5.7 Conclusion

- To reduce power consumption and due to rapid expansion of the IT equipment business, data center operators should allow data centers to run using ASEs and also allow data centers to operate in the ASHRAE A1 allowable environment.
- The use of ASEs risks the entry of particle contaminants, both natural and anthropogenic, and should be controlled.
- Salts or dust has the tendency to absorb moisture, become wet and start conducting if the relative humidity in the data center rises above its DRH.
- In this study, an effective method to determine the DRH of dust is brought to light. The experiment is validated by determining the CRH and DRH of pure salts i.e NaCl, NH_4NO_3 and $MgCl_2$ and then comparing it with their published values.
- This method also proves to be an effective method in determining the CRH and DRH of salts and overcomes the limitations of the other measuring techniques.
- The current sensor can accurately measure upto 0.01mA making this a high precision technique.
- The entire setup is cost effective, very reliable and easy to handle.
- The process is also time efficient and one can obtain the DRH value of salts or dust quickly.
- This methodology can therefore be implemented to help lay a modus operandi of establishing the limiting value or an effective relative humidity envelope to be maintained at a real-world data center facility for its continuous and reliable operation at its respective location.

5.8 References

1. ASHRAE, “2015 Supplement Energy Standard for Buildings Except Low-Rise Residential Buildings,” vol. 8400, 2015.
2. Shah JM, Awe O, Gebrehiwot B, et al. Qualitative Study of Cumulative Corrosion Damage of Information Technology Equipment in a Data Center Utilizing Air-Side Economizer Operating in Recommended and Expanded ASHRAE Envelope. ASME. J. Electron. Packag. 2017;139(2):020903-020903-11. doi:10.1115/1.4036363.
3. ASHRAE Technical Committee 9.9, 2010, “ASHRAE DOE Course: Save Energy Now Presentation Series,” American Society of Heating, Refrigerating, and Air-Conditioning Engineers, Dallas, TX.
4. Jimil M. Shah, "Reliability challenges in airside economization and oil immersion cooling", *The University of Texas at Arlington*, May 2016
5. Thermal Guidelines for Data Processing Environments, ASHEAE Datacom Series, 3rd Edition, 2012, ASHRAE, Atlanta, GA, USA.
6. J. Dai, D. Das, and M. Pecht, “Prognostics-Based Risk Mitigation for Telecom Equipment under Free Air Cooling Conditions”, Applied Energy, Volume 99, November 2012, pp 423–429.
7. Intel Information Technology, “Reducing data center cost with an air economizer”, IT@Intel Brief; Computer Manufacturing; Energy Efficiency; Dec, 2008.
8. R. P. Frankenthal, D. J. Siconolfi and J. D. Sinclair, “Accelerated Life Testing of Electronic Devices by Atmospheric Particles: Why and How”, J. Electrochemical Soc., Vol. 140, pp. 3129-3134, 1993
9. "Air-Side Economizer," Energy Star, [Online]. Available: www.energystar.gov/index.cfm?c=power_mgt.datacenter_efficiency_economizer_airside

10. Cole, M., L. Hedlund. T; Kiraly, S. Nickel, P. Singh and T. Tofil, Harsh Environmental Impact on Resistor Reliability, SMTA Int'l Conf, Proc., 24 Oct 2010.
11. Directive 2002/95/EC of the European Parliament and of the Council of 27 January 2003 on the Restriction of the use of Certain Hazardous Substances on Electrical and Electronic Equipment Official Journal L 037, February 13, 2003, 19-23.
12. Fu, H., C. Chen, P. Singh, J. Zhang. A. Kurella, X. Chen, X. Jiang, J. Burlingame and S. Lee, Investigation of Factors that Influence Creep Corrosion on Printed Circuit Boards," SMTA Pan Pacific Microelectronics Symposium, Kauai, 14-16 Feb 2012.
13. Fu, H., C. Chen, P. Singh, J. Zhang. A. Kurella, X. Chen, X. Jiang, J. Burlingame and S. Lee, Investigation of Factors that Influence Creep Corrosion on Printed Circuit Boards, Part 2, SMTAI 2012.
14. Jud Ready W.,1 L. J. Turbini, R. Nickel and J. Fischer, A Novel Test Circuit for Automatically Detecting Electrochemical Migration and Conductive, Journal of ELECTRONIC MATERIALS, Vol. 28, No. 11, 1999 Anodic Filament Formation
15. Song B., M. H. Azarisn and M. G. Pecht, "Effect of temperature and relative humidity on the impedance degradation of dust-contaminated electronics," Journal of The Electrochemical Society, 160 (3), 2013, C97-C105.
16. Seinfeld J. H. and S. N. Pandis, "Atmospheric Chemistry and Physics," John Wiley & Sons, Inc, New York, NY.
17. Zhao P. et al. "Characteristics of concentrations and chemical compositions for PM2.5 in the region of Beijing, Tianjin and Hebei, China," Atmos. Chem. Phys. Discuss., Vol. 2013, 863-901.
18. U. S. Environmental Protection Agency. AIRTrends 1995 Summary – Nitrogen Dioxide (NO2). ONLINE. 2014. Available: http://www.epa.gov/airtrends/aqtrnd95/no2.html [07 Oct. 2014].

19. Comizzoli R. B.et al. “Corrosion of electronic materials and devices by submicron atmospheric particles,” The Electrochemical Society Interface, Fall 1993, 27-33.
20. Y.N.Liang, J.G.Zhang and J.J.Liu, “Identification of inorganic compounds in dust collected in Beijing and their effects on electric contacts”, 43rd IEEE Holm Conference on Electric Contacts, Philadelfia, PA. USA. Oct.20-22,1997, 315-327
21. Christofer Leygraf, Thomas E. Graedel, “Atmospheric corrosion”, John Wiley & Sons, Inc., ISBN 0-471-37219-6, 2000
22. J.W. Wan, J.C. Gao, X.Y. Lin and J.G. Zhang, “Water-Soluble Salts in Dust and Their Effects on Electric Contact Surfaces”, Proceedings of the International Conference on Electrical Contacts, Electromechanical Components and Their Applications, Jun., 1999, 37-42
23. P-E Tegehall, “Impact of Humidity and Contamination on Surface Insulation Resistance and Electrochemical Migration”, IVF Industrial Research and Development Corporation, http://www.europeanleadfree.net/
24. ISA, 2013, “Environmental Conditions for Process Measurement and Control Systems: Airborne Contaminants,” ISA-The Instrumentation Systems, and Automation Society, Research Triangle Park, NC, Standard No. ISA-71.04- 2013.
25. A DerMarderosian, "The electrochemical migration of metals," Proc. Int. Society of Hybrid Microelectronics, p.134, 1978.
26. G. T. Kohman, H. W. Hermance, and G. H. Domes "Silver migration in electricalinsulation," Bell System Technical Journal vol. 34, pp. 11-15, 1955.
27. G. Ripka and G. Harshyi, "Electrochemical migration in thick-film ICs," Electrocomp. Sci. Technol., vol. 11, p. 281, 1985.
28. M. V. Coleman and A E. Winster, "Silver migration in thick-film conductors and chip attachment resins," Microelectronics Journal, No. 4, p. 23, 1981

29. Singh P, Klein L, Agonafer D, Shah JM, Pujara KD. Effect of Relative Humidity, Temperature and Gaseous and Particulate Contaminations on Information Technology Equipment Reliability. ASME. International Electronic Packaging Technical Conference and Exhibition, *Volume 1: Thermal Management* (): V001T09A015. doi:10.1115/IPACK2015-48176
30. Singh, P. P. Ruch, S. Saliba and C. Muller, Characterization, Prevention and Removal of Particulate Matter on Printed Circuit Boards, IPC APEX, San Diego, Feb 2015.
31. Yang L., R. T. Pabalan and M. R. Juckett, “Deliquescence relative humidity measurements using an electrical conductivity method,” Journal of Solution Chemistry, Vol. 35. No. 4, April 2006, 583-604
32. L. Yang, R. T. Pabalan, and L. Browning, Experimental Determination of the Deliquescence Relative Humidity and Conductivity of Multicomponent Salt Mixtures, in *Scientific Basis for Nuclear Waste Management XXV*, P. McGrail and G. A. Cragnolino, Eds. *Mater. Res. Soc. Symp. Proc.* 713, 135–142 (2002).
33. Wexler A. and S. Hasegawa, Relative humidity-temperature relationships of some saturated salt solutions in the temperature range.
34. M. Weekes, “PWB Contamination & Reliability DOE”, Proceedings of SMTA International Conference, Chicago, IL, September 2001.
35. C. H. Hamann, A. Hamnett, and W. Vielstich, *Electrochemistry*, New York: Wiley- VCH, 1998.
36. Adafruit INA219 Current Sensor Breakout [PDF File].
37. ASHRAE Standard 52.2-2012, Method of testing general ventilation air-cleaning devices for removal efficiency by particle size, Atlanta, GA, USA.
38. Harrison R.M., et al. “Airborne Particulate Matter in the United Kingdom.” Third Report of the Quality of Urban Air Review Group, May, 1996.

39. Husar R., “Properties of Particulate Matter,” Washington University, St. Louis, 1999.
40. Harrison R. and J. Yin, “Characterisation of Particulate Matter in the United Kingdom,” Report produced for Defra, the National Assembly for Wales, the Department of the Environment in Northern Ireland and the Scottish Executive, The University of Birmingham, March 2004.
41. Čupr P., Z. Flegrová, J. Franců, L. Landlová, and J. Klánová, “Mineralogical, chemical and toxicological characterization of urban air particles,” Environment International 54 (2013), 26–34.
42. Thirunavakkarasu. G, Saini. S, Shah J.M., Agonafer. D, "Air Flow Pattern and Path Flow Simulation of Airborne Particulate Contaminants in a High-Density Data Center Utilizing Airside Economization", ASME INTERPACK 2018, San Francisco, California.
43. Gautham Thirunavakkarasu, "Air Flow Pattern and Path Flow Simulation of Airborne Particulate Contaminants in a Cold-Aisle Containment High-Density Data Center Utilizing Airside Economization", *The University of Texas at Arlington,* May 2018.

Chapter 6

Determination of the operating relative humidity of a data center utilizing an airside economization by estimating the Deliquescent Relative Humidity of found particulate contaminants in a data center and Salts present in the facility water

6.1 Sample Preparation

The samples of the particulate contaminants were collected from servers located in the Research Modular Data Center in Dallas, Texas. The samples were collected with the help of deionized water and stored carefully in air tight test tubes. To collect the samples, four servers were removed from the center of the racks and the interior of the servers was exposed by removing the top cover. Then, deionized water was poured to the server board and chassis to generate sample solution with contaminants in the form of a slurry shown in Figure 1. The sample solutions were collected in a test tube and then closed with an air tight rubber bush for safe storage. A total of five different samples were collected including one sample of the facility water and four samples from different servers as shown in Figure 2.

Figure 6-1 Collecting samples using Deionized water

Figure 6-2 Samples from four servers and facility water

6.2 Test Procedure

- The first step of the experiment is soldering the connecting wires that will be attached to the current sensor on the Arduino and INA219 current sensor to the positive and negative terminals on the multipurpose test board. Then, the solder flux was removed using Iso-Propyl Alcohol.
- The coupon is then placed in the environmental chamber shown in figure 3 and 10 drops of contaminated slurry, which is carefully stored in air tight test tubes, taken from the server in the first rack of the RDC with the help of a sanitized suction syringe.

Figure 6-3 Environmental Chamber – Thermotron SE-600-10-10

- The connecting wires from the chamber are routed to the dc power supply and the current sensor. As outlined in the experimental setup, the connections are made, and the chamber door is then shut.
- A steady temperature of 25ºC is maintained throughout the cycle and a rest period of 12 hours at 10% Relative Humidity is allowed. This is done to evaporate the moisture from the contaminated solution which leaves only dust particles on the test board and to create an equilibrium with 10% RH.
- Once the first cycle is complete, a dc voltage of +1 volt is applied across the test coupon and the leakage current is monitored using a JAVA script on an Arduino software tool.

- After taking the reading at +1 volts, a voltage of -1 volt is passed immediately across the test coupon. This helps in neutralizing the effect of the positive voltage on the ions that might be present in the dust.
- The RH% is then increased by 10% for the next cycle keeping the ambient temperature of the chamber the same as previous cycle and leakage current is measured in a similar manner as in previous step.
- The above three steps are repeated till a %RH of 90% is reached.
- The obtained values of leakage current are logged in a table against the RH% values and a graph are plotted between RH% and leakage current.
- The values of DRH and CRH are obtained from this graph.
- The above steps are repeated for the remaining samples from the servers and the facility water.

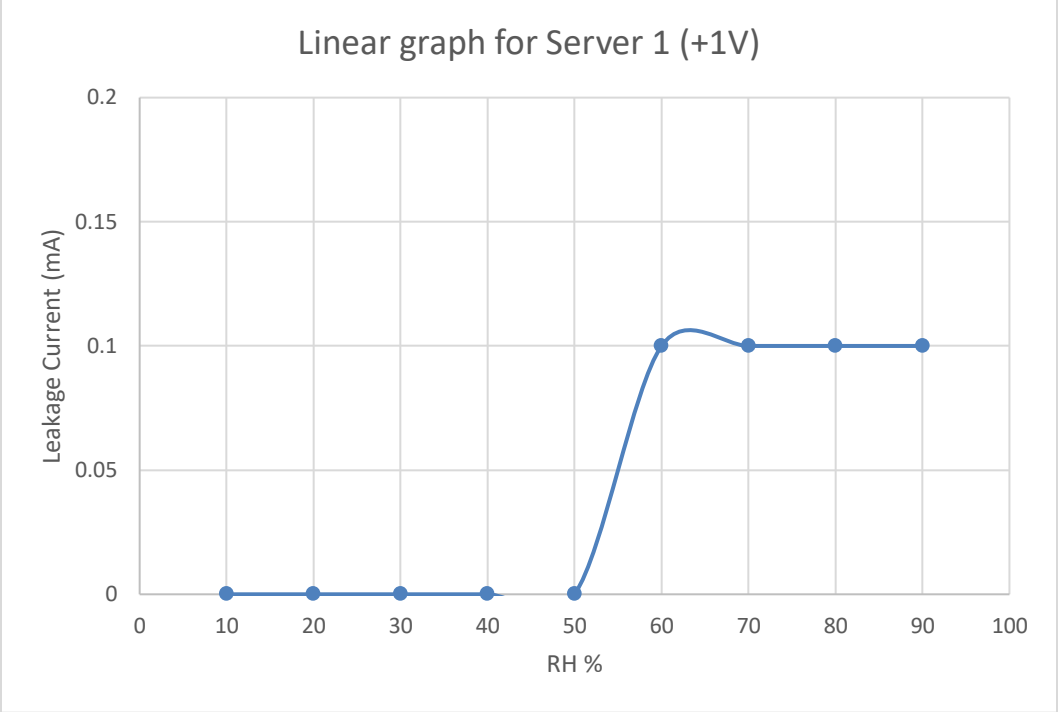

Figure 6-4 Linear plot of Leakage Current versus %RH for server 1 (+1 Volt)

The above graph shows the values of leakage current obtained from the current sensor against the increasing value of %RH for +1 volts. As evident from the linear graph, we can see a sudden increase in the value of leakage current at %RH of 60%. The sudden increase in leakage current attributes to the fact that there is an increase in electrical conductivity at the test board. This happens when the salts present in the contaminated slurry absorb moisture enough to form an aqueous solution and become conductive. For Server 2, Server 3 and Server 4, the linear plot shows that the leakage current value increases suddenly at %RH of 50% as well. As for the facility water, the linear graph shows that the experimental value of DRH is 80%. To get the exact values of the DRH the logarithm of the leakage current can be plotted against the RH% values. The before and after pictures of the comb coupon dispensed with the solution

from the server is shown in Figures 5 and 6 depicts the effect of relative humidity in the presence of particulate contamination.

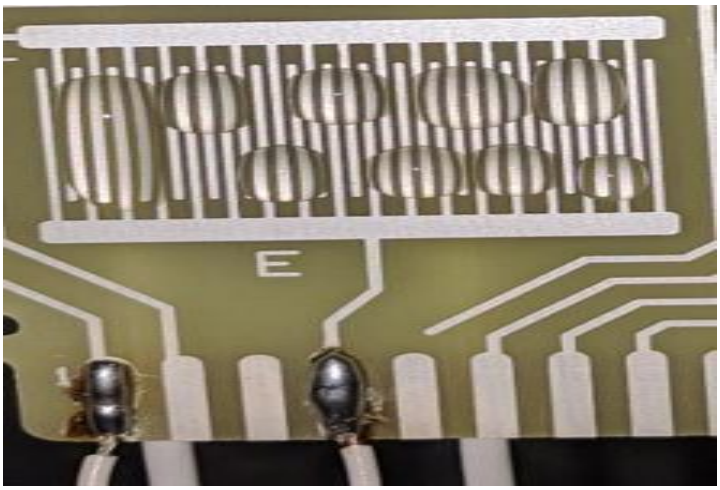

Figure 6-5 Drops of samples dispensed on the comb coupon.

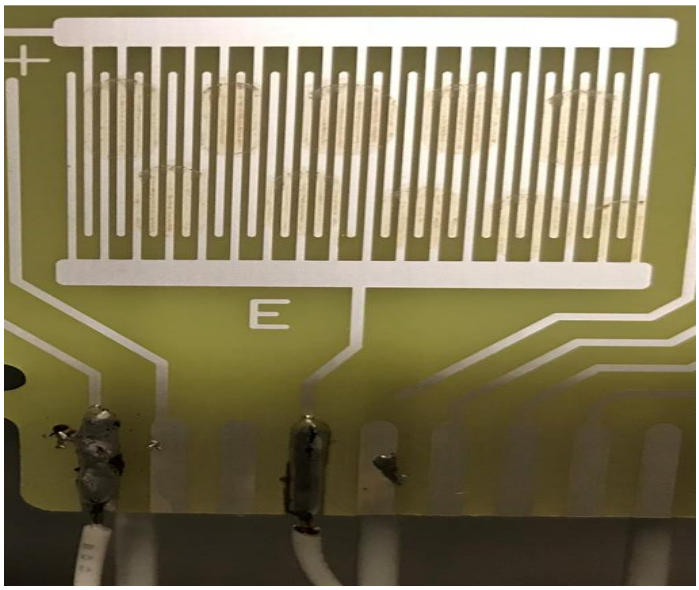

Figure 6-6 Corrosion due to the conducting nature of the salt solution at a relative humidity higher than the DRH.

Figures 7,8,9 and 10 display the linear graph of leakage current versus %RH when +1V have been applied for servers 2,3,4 and facility water respectively.

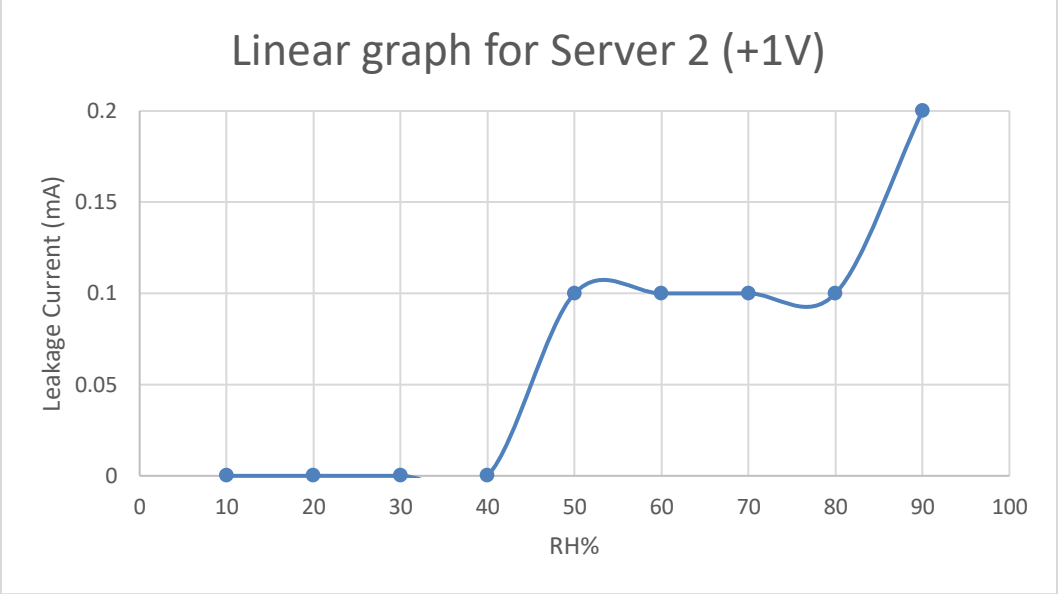

Figure 6-7 Linear plot of Leakage Current versus %RH for server 2 (+1 Volt)

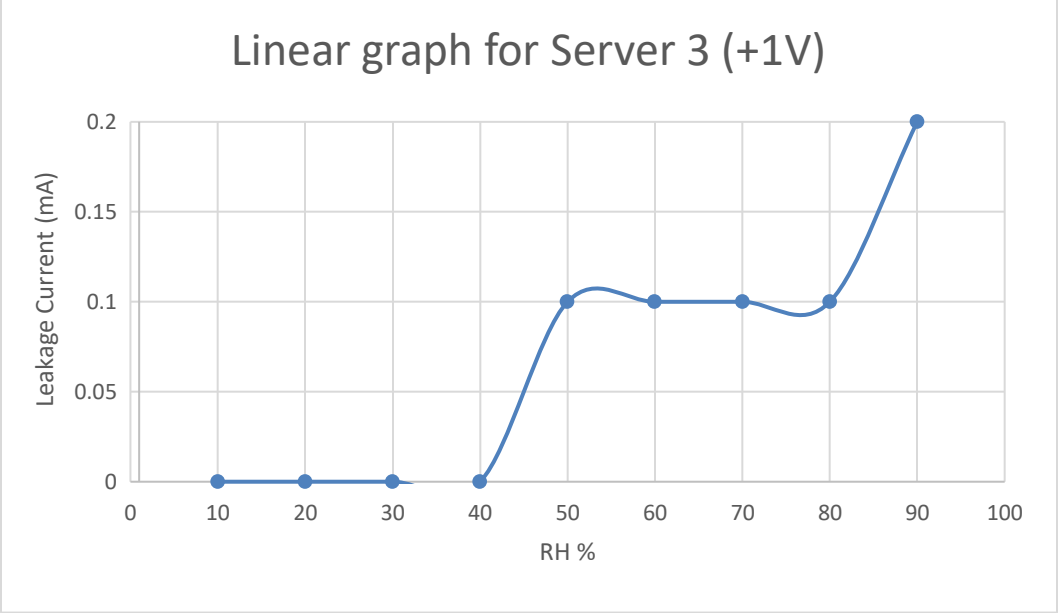

Figure 6-8 Linear plot of Leakage Current versus %RH for server 3 (+1 Volt)

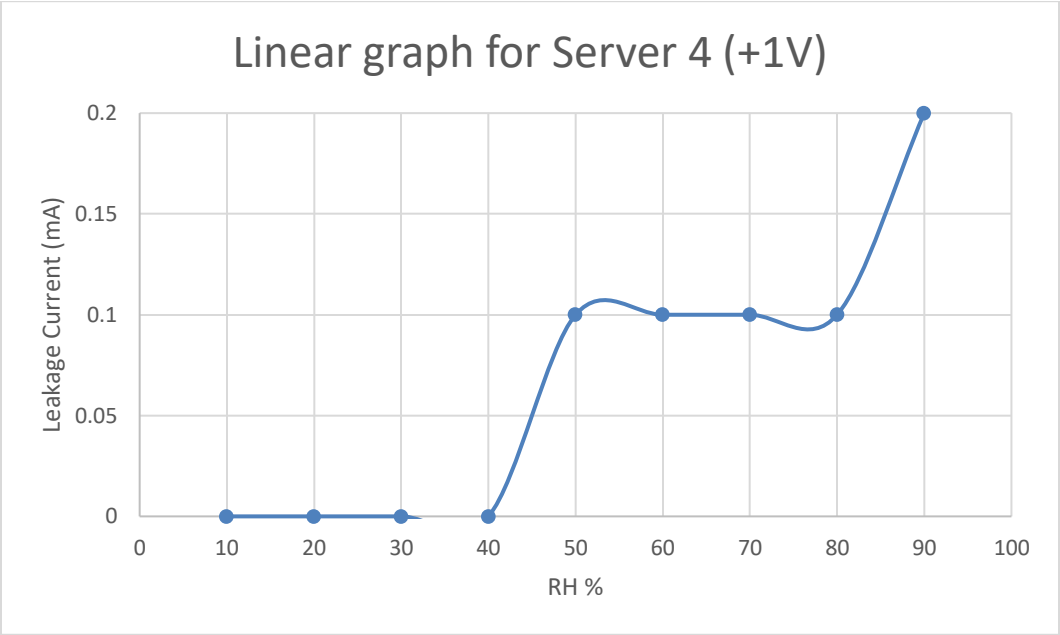

Figure 6-9 Linear plot of Leakage Current versus %RH for server 4 (+1 Volt)

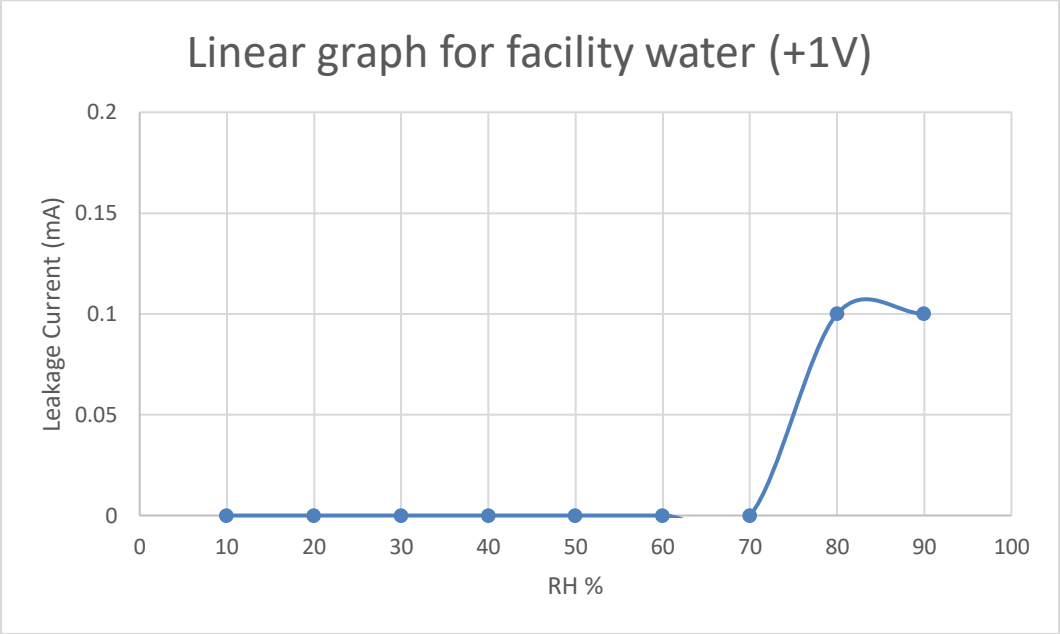

Figure 6-10 Linear plot of Leakage Current versus %RH for Facility water (+1 V)

Chapter 7

Air Flow Pattern And Path Flow Simulation of Airborne Particulate Contaminants In A High-Density Data Center Utilizing Airside Economization

Gautham Thirunavakkarasu[1], Satyam Saini[1], Jimil M. Shah[1*] and Dereje Agonafer[1]
[1]University of Texas at Arlington
P.O. Box 19023
Arlington, TX, United States, 76013
[*]**Corresponding Author:** jimil.shah@mavs.uta.edu

Abstract

The percentage of the energy used by data centers for cooling their equipment has been on the rise. With that, there has been a necessity for exploring new and more efficient methods like airside economization, both from an engineering as well as business point of view, to contain this energy demand. Air cooling especially, free air cooling has always been the first choice for IT companies to cool their equipment. But, it has its down- side as well. As per ASHRAE standard (2009b), the air which is entering the data center should be continuously filtered with MERV 11 or preferably MERV 13 filters and the air which is inside the data center should be clean as per ISO class 8. The objective of this study is to design a model data center and simulate the flow path with the help of 6sigma room analysis software. A high-density data center was modelled for both hot aisle and cold aisle containment configurations. The particles taken into consideration for modelling were spherical in shape and of diameters 0.05, 0.1 and 1 micron. The physical properties of the submicron particles have been assumed to be same as that of air. For heavier particles of 1 micron in size, the properties of dense carbon particle are chosen for simulating particulate contamination in a data center. The Computer Room Air Conditioning unit is modelled as the source for the particulate contaminants which represents contaminants entering along with free air through an air-side economizer. The data obtained from this analysis can be helpful in predicting which type of particles will be deposited at what

location based on its distance from the source and weight of the particles. This can further help in reinforcing the regions with a potential to fail under particulate contamination.

Nomenclature

ACU	Air Conditioning Unit
Cc	Cunningham correction factor
CD	Drag Coefficient
CAC	Cold Aisle Containment
CFM	Cubic Feet per Meter
d_p	Diameter of Particle
ε	Dissipation
Fbi	Component of Brownian force in x_i direction
F_{drag}	Component of drag force in x_i direction
Fgravi	Component of Saffman lift force in xi direction
gi	Component of gravitational acceleration in xi direction
IT E	Information Technology Equipment
k	Turbulence Kinetic Energy
mp	Particle mass
MERV	Minimum Efficiency Reporting Value
ρ	air density
ρp	particle density
σ	Boltzmann constant
∆t	Time step
˙u	Fluid velocity
$\dot{v}$	Particle velocity

u_i	Component of filtered fluid velocity in x_i direction
u_j	Component of filtered fluid velocity in x_j direction
v_i	Component of particle velocity in x_i direction
v_j	Component of particle velocity in x_j direction
v	Fluid viscosity
ζ	Gaussian Random Number Generator

7.1 Introduction

With the booming era of information technology, there is a steep rise in the growth in number and size of data centers. Since information is transferred continuously in the world, the need for ensuring zero downtime is of paramount importance. This rapidly accelerating demand for data center is presenting the industry to explore thermal management techniques to deal with the energy supply problem. A significant challenge being faced is the cooling of data centers due to the rapid increase in power consumption and the increasing load of the IT (Information Technology) equipment in the data center. Most of the energy requirements in the data center are towards the IT hardware and cooling requirements. With the current world circumstances, the IT load is expected to increase with improved semiconductor technologies while optimizing the cooling requirements is be- coming an important factor and can be achieved in several ways. One of the most efficient techniques being used and developed is the free cooling technique, air-side economization. Typically, a data center operates in tightly controlled environmental parameters (dew point, temperature and relative humidity) and possesses very efficient filtration system. In many emerging countries, for energy saving interests a small number of data center operate using free air, where available, to cool the data center white space. To allow this efficient method, American Society of Heating, Refrigeration and Air Conditioning Engineers (ASHRAE) recommend an envelope to define the limits under

which IT equipment would operate most reliably, particularly with the goal of reducing energy consumption, while still achieving reasonably energy-efficient data center operation [1]. The CRAC (Computer Room Air Conditioning) units in the data center usually supply cold air through raised floor tiles and the cold air passes through the server racks to cool the electronic equipment and emerges from the back of the server as hot air stream, which is them re-circulated and this continuous cycle follows. By using air-side economization, the run-time of CRAC is reduced by allowing for filtered free cool air to flow into the data center space, allowing for huge savings on operational cost. However, there is a predictive risk of server failures due to particulate and gaseous contaminants entering the data center environment. From field study, the servers in the racks act as re-circulation units which lead to the failure of circuit boards from both types of contamination. The objective of this paper is to deal only in the effect of concentration of airborne particulate contaminants on the wall surface of the servers at different rack heights in a cabinet column. The airborne particulate contaminants considered here are fine dust particulates which have their source from mineral, biological corrosion and fibrous dust. In this study, we focus on usage of air-side economizers using free air cooling for the IT hardware and issues of particulate contaminant concentration are specifically discussed. The aim is to make it possible to analyse the flow path of airborne contaminants in the data center white space. The method and procedure of this study is as follows. First, a basic model of a data center is modelled in a cfd analysis data center software and the air flow distribution in the server environment is simulated. Analyzing the air flow path, particulate contaminant trajectory and their location of deposition are the most important aspect of this paper. Second, for this purpose of particulate contamination, spherical shaped sub-micron particulates are taken into consideration. To analyse the flow path inside the data center space, 6SigmaRoom, a data center cfd simulation package is used. The layout of the servers utilizing CRAC units as air-side economizers and air-flow rate is simulated for a model data center. Third, by using

different particulate sizes and their concentration in outside free air, a simulation of their flow path is considered to identify surface faces of the server racks, which are most susceptible to accumulation of contaminants. Last, a proposal of mitigation strategies is outlined to efficiently operate a data center using air-side economization, thereby accomplishing the primary energy saving interest.

7.2 Literature Review

The air flow path and its modelling have progressed significantly over the last two decades. This has specifically allowed for accurate prediction of air flow and temperature distributions in large air-conditioned spaces, as detailed in [2] where illustrations of the technique of air flow movement in large waiting halls have been explained in depth. Many researchers have contributed their study to room air flow modelling, however, this addresses only the flow path and temperature distributions in data centers but fail to address the impact of free cooling and its risk on IT equipment reliability due to contamination. The literature on air-flow management in data centers is rather scarce and it has been discovered as a strong scientific interest only in the past couple of years.

This section presents the extensive background study which was done on airflow and thermal analysis of Data Centers and other such ventilated spaces. Temperature and airflow distributions were predicted by Awbi and Gan [3], where they used a CFD program to calculate thermal comfort and airflow in naturally and mechanically ventilated offices. Schmidt [4] in one of his studies described the flow rate and temperature measurements in an actual Data Center. The objective of this study was to fully describe the thermal environment that exists in a Data Cen- ter. Measurements for equipment power consumption, airflow through the CRAC and its power usage, ITE inlet air temperature, etc., were recorded. These values were then presented and compared with the CFD results airflow through perforated tiles; Gugaru [5] et al., through their study reported the best practices to design a Data Center. The study reports the

importance of analytical and simulation tools to improve the energy efficiency of the Data Center. This was done by performing a flow analysis of raised floor and then deciding the layout based on the flow distribution results. A CFD model of the Data Center was thendeveloped to verify the required cooling airflow characteristics. Patankar and Karki [6] state in their research about the airflow distribution and cooling in a raised floor Data Center. The study illustrated the effect of various parameters that effect the airflow distribution in such a configuration like floor height and tile open area. In another study by Karki [7] they have used CFD analysis for calculating the flow rate through perforated tiles in a raised floor configuration Data Center. The study used k-εmodel of turbulence and a finite volume method approach to calculate airflow rates through the perforated tiles, assuming pressure distribution to be uniform in the Data Center space above the raised floor.

It is also discussed by Patankar [8], that the archival literature available on airflow in data centers only discuss on temperature flow distributions in various large engineering buildings. To highlight, the only research author who has prescribed a method to mitigate contamination is by Seymour [9] where a method of application of CFD was used to calculate the trajectory of air- borne organisms being produced either by a patient coughing or sneezing in a hospital space. This modelling helped to simulate the motion of droplets carrying the bacteria and minimize its transmission by exposing it to ultraviolet irradiation. By ap- plying a very similar logic, this paper describes the air flow simulation of similar micron sized fine particulates to be extended to simulate its trajectory inside the data center space and mitigating the rate of failure of IT equipment in data centers where free cooling is frequently used, thereby, allowing for savings on operational costs.

7.3 Role Of CFD Simulation

CFD modelling is the process of representing a fluid flow problem by mathematical equations based on the fundamental laws of physics, and solving those equations to predict the

variation of velocity, pressure and temperature, and other variables such as turbulence parameters and concentrations which are disussed by Jone [10]. Eulerian or Lagrangian approaches are one of the most popular methods for flow visualization and particle tracking. The difference in both the methods is that the Eulerian method treats the particles as continuum and the Lagrangian methods focuses on the particle frame of reference, treating each particle individually. Two studies which closely relate to the type of particle transport model with the present study were by Chen and Zhang [11] which evaluate the flow using RANS (Reynolds-Averaged Navier Stokes) and LES (Large Eddy Simulation). The other study by Seymour [9] used Lagrangian approach, where the assumption that the volume fraction of particles is very less than that of total airflow and the particles do not influence the flow of air. This describes, more closely, the exact behavior of particulates in the Data Center space. The fundamental equations that depict the airflow can be expressed as:

$$\sum F_i = \frac{d(m_p v_i)}{dx} \tag{1}$$

Momentum force is transferred between air and particles through inter-phase drag and lift forces, which can be divided into, but not limited to, the following parts: the drag force, pressure gradient force, unsteady forces which include Basset force and virtual mass force, Brownian force, and body force, such as gravity force and buoyancy force discussed by Clayton in [12]

$$\sum F_i = F_{drag\,i} + F_{gravi} + F_{saf\,i} + F_{bi} \tag{2}$$

The drag force on the particle is expressed as,

$$F_{dragi} = -C_D \frac{\pi}{8} \rho {d_p}^2 |\vec{u} - \vec{v}|(v_i - u_i) \tag{3}$$

The drag coefficient, C_D in this equation depends on the particle shape as well as flow parameters like flow velocity, turbulence level, Reynolds number etc., The particle Reynolds number is expressed as:

$$Re_p = \frac{|\vec{u} - \vec{v}|d_p}{v} \tag{4}$$

The buoyancy and gravity forces on the body in a fluid are given as,

$$Fgrav_i = (\rho_p - \rho)\frac{\pi}{6}d_{p^3}g_i \tag{5}$$

The Saffman lift force on the body is given as:

$$F_{safi} = K\frac{\pi}{3}\sqrt{v}d_p^2\rho\frac{d_{ij}}{(d_{l_k d_{kl}})^{1/4}}(u_j - v_j) \tag{6}$$

After substituting these values in the equation (2) and dividing both sides by particle mass mp, the complete equation for the particle motion becomes:

$$\frac{dv_i}{dt} = -\frac{3}{4}\frac{\rho C_D}{d_p\rho_p}\left|\vec{u} - v(v_i - u_i) + (\rho_p + \rho)\frac{\pi}{6}d_p^3 g_i + \left(1 - \frac{\rho}{\rho_p}\right)g_i + \left(\frac{2K\rho\sqrt{v}d_{ij}}{\rho_p d_p\left(d_{l_k d_{kl}}\right)^{\frac{1}{4}}}\right)(u_j - v_j)\right| \tag{7}$$

For particle size less than 1μm, the Brownian force can also be included to calculate the diffusion:

$$F_{bi} = \zeta_i\sqrt{\frac{216\rho v\sigma T}{\pi\rho_p^2 d_p^5 C_c\Delta t}} \tag{8}$$

Where ζ, is the Gaussian random number given by,

$$u_i = \zeta\sqrt{\frac{2k}{3}} \tag{9}$$

Some other popular models that are used for modelling air flow inside closed environment include RANS (Reynolds Averaged Navier-Stokes) model which gives mean values of parameters like velocities, temperature and solves only the mean components. Large Eddy Simulations (LES) separates the flow into small and large eddies and solves flow motion based on Navier Stokes and mass continuity equations. The primary objective of the current study is the simulation and analysis of the airflow inside the data center. An elaborate background study has been done on the physics that controls and affects the flow of gases and particles inside the ventilated rooms like Data Centers. Computational Fluid Dynamics, when applied to air flow distribution within data centers have the potential to predict the velocity and temperature distributions. It is also possible to predict the spatially and temporally varying distribution of particulate contamination within the space and hence, evaluate IT equipment reliability. [10] To perform air flow path calculations in the data center space, it is necessary to define the boundary conditions, which is necessary for each of the turbulence transport equation to be solved. By specifying the geometry of the data center and overlaying with a mesh of control volumes, it is then necessary to identify on the mesh the locations of any supply and return terminals, the flow rates of the supply and the return air, the velocity and temperature of the supply air, the heat transfer process occurring at surfaces and within the space, and, if required, the location and release rates of any indoor air pollutants. The complex iterative nature of the calculation methods and solving the equations needed to represent a reasonably detailed description of the flow distribution in the room means that a substantial computing power and time duration is needed. Realistically, this is interpreted and analyzed using graphics-based postprocessor. The CFD package 6SigmaRoom is used as the simulation tool and the technique of simulating the air flow distribution in a high-density data center with both hot/cold-aisle configuration is used to illustrate its capability.

7.4 Data Center Modelling

Many commercial CFD packages are available which can effectively predict the flow pattern of air which are induced by mechanical devices and thermal sources. Most of them, including 6SigmaRoom [13] can be executed on personal computers.

6SigmaRoom, by Future Facilities, can predict the air flow and heat transfer explicitly for Data Center using CFD techniques. It provides a fast mean of predicting the indoor data center environment as an alternative or supplement to the physical model. It acts as an easy tool which allows the user to generate a virtual facility model that is used to assess and compare new designs, to model and troubleshoot existing facilities and to provide a basis for ongoing change management; this practice is known as predictive simulation.

Applications including design, ventilation and air-conditioning system for data centers of all types and sizes, from small to high-density data centers. The approach is very similar to that of a field model for predicting the turbulent convective air flow path within the data center space.

7.5 Data Center Environment

An IT server in a data center can be closely related to the fundamental functioning of a standard home-based PC (personal computer) unit. It produces a very unusual and concentrated head load and when running at high computing speeds, it requires some air conditioning to handle the heat load concentration. When scaling this comparison to a data center, the size of server rooms and the load of heat dissipated is very large and the need for cooling is also very large. The IT hardware equipment are very sensitive to changes in temperature and humidity, and with the introduction of free air cooling, standard design conditions would strain the operations of a data center using air-side economizations. Tackling the increasing costs because of high energy expenditures has forced data center engineers and professionals to come up with strategies which can minimize these costs. Aisle containment is one of these strategies which has become a proven measure for building energy efficient Data

Centers. To relate our results closely and more accurately with the conditions in a real-life Data Center, both configuration of HotAisle (HAC) and Cold Aisle (CAC) configuration were considered for the study.

The rack-mounted servers are designed to draw in cool air at the front and exhaust it out at the back of the unit. They are positioned in such a way that their back sides are facing to form hot aisles, while the front sides, which receive cool air from the perforated floor tiles, form the cold aisles. This set-up divides the draw air and the exhaust air of the IT equipment into separate hot-aisle and cold-aisle containments. The best standard practice observed is to configure the data center room into alternating hot and cold aisles. Containment of the hot and/or cold aisle can be configured to best suit the operational standards. Cold aisles contain the floor tiles or diffusers and the racks stacked with server fronts (intake) facing the cold aisles. This practice of having all rows arranged in a similar manner allows for easy configuration of air distribution throughout the entire data center space. Many large data centers have the practice of implementing the air inlets and outlets of the servers at separate locations for effective cooling. Figure 1 shows the cold aisle configuration of the IT server alignment considered for the study and Figure 2 shows the hot aisle configuration of the IT server alignment.

7.6 Data Center Description

In this paper, the data center model investigated is adopted from the one that has been used as a standard representation for data centers across the market. From this standard model, the data center was modelled in 6SigmaRoom. Its 3-D representation of the physical data center combined with the CFD solver allows for safe simulations of data center physical capacity and cooling efficiency. The layout of the data center is as follows. The through row orientation is chosen for simple design model of the data center space, followed with four rows for the hotaisle and cold-aisle containment configurations housing a cabinet power limit of

5.6KW, making our model a high-density data center design. The layout of the cabinets in the model data center considered in the present study is tabulated in Table 1.

The data center has a total of 486 servers which are distributed into four rows of each unit in both the hot -aisle/coldaisle configuration . There are four CRAC (Computer Room Air Conditioner) units placed along the perimeter of the server room. These units supply cooling air at 12.80 °C from the pressurized 2 foot raised floor plenum. The modelled data center was designed using the best practice of hot and cold aisle arrangements.

7.7 Hot-aisle and Cold-aisle Containment

As discussed earlier, hot aisle-cold aisle arrangement in raised floor concept prevents mixing of hot and cold flows. In addition to this, the containment of these hot or cold aisles also results in significant reduction in cooling costs. The main advantages of containment systems as discussed in a white paper by John Neimann [14] et al. are:

Table 7-1 Layout of the Cabinets in the Data Center

Object Description	**Hot Aisle Configura-tion**	**Cold Aisle Configura-tion**
Row Orientation	Through	Through
Number of Rows	4	4
Cabinets per Row	7	6
FIrst Aisle	Cold	Hot
Cold Aisle Width	2	2
Cabinet Power Limit	5.6kW	5.6kW
Server Type	2U-600W	2U-600W

- Uniformity in supply air temperature form CRAC to inlet at the racks
- Increase in economizer hours
- Humidification and dehumidification costs are reduced due to elimination of flow mixing

CAC: a cold aisle containment system is one in which the cold aisle is enclosed, and the rest of the Data Center becomes a hot air return space. The aisle maybe separated from the rest of the Data center by means of plastic curtains, plastic or plexi-glass doors.

HAC: In a hot aisle containment system the hot aisle is enclosed, and all the hot return air is channeled towards the roof through ducts and roof panels, back to the CRAC return.

After careful analysis of the background studies, it was observed that HAC is more efficient of the two.

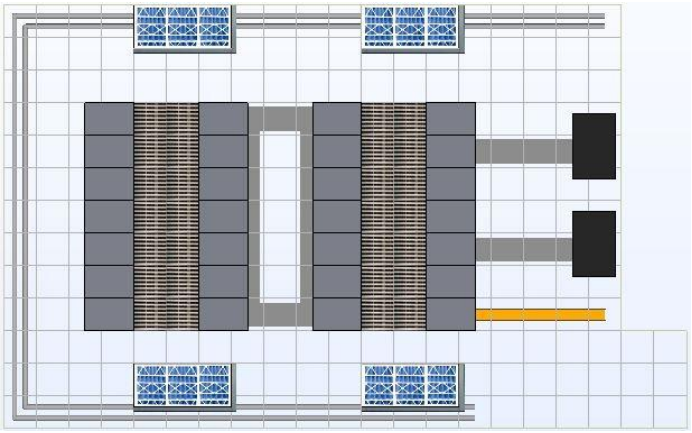

Figure 7-1 Cold-Aisle Containment Configuration

Figure 7-2 Hot-Aisle Containment Configuration

Since, the CAC makes all of the Data Center space a hot aisle plenum, it becomes difficult for Data Center personnel to carry out regular maintenance tasks. Although both type of containment have cooling efficiency benefits, the study by Neimann, reports that HAC can generate up to 40% savings when compared to 13% when there is no containment configuration. The only drawback for HAC is that it has added costs which include complex building design for false ceiling, return air ducts, roof panels etc.

7.8 Cooling Airflow in Raised Floor

The need for data center cooling in server racks arise from the facts that these servers consume electrical energy and in turn dissipate a large amount of heat. To maintain proper functionality of the servers, they must be maintained under optimum operating temperature range, exceeding which may lead to equipment malfunction or even failure in some cases.

The traditional way server cooling works in Data Centers is that the cold air through the ACU (Air Conditioning Unit) enters the server racks from the front face, flows over the hot ITE (Information Technology Equipment) and, exits from the rear face. This technique although is limited to rooms with small area. In larger Data Center spaces, raised floor concept is used where the server racks are cooled by the air coming out from perforated tiles placed next to them. The cool air enters the plenum and forces its way out through the perforated tiles, thus cooling the equipment inside the racks. For efficient execution of this concept the ITE racks are arranged in cold aisle-hot aisle/hot aisle- cold aisle configuration.

Table 7-2 Particulate Matter

Contaminant	Source
Zinc Whisker	Zinc Coated ICT equipment,steel building studs
Tin Whiskers	Components and products having electroplated tin
Oxide flake off	Magnetic Media
Natural and Artificial Fibers	Paper, cardboard, etc.,
Water-soluble ionic salt	Chemical Reaction
Sulfate, nitrate, sea salts	Winds
Lime dust with water	Concrete material
Dust	Farms, especially during plowing
Toner dust	Toner
Smoke	Cigarette, winds
Cellulose fragments	Traditional ceiling tiles and space

A hot aisle is the region between the rear sides of two ITE racks and conversely, cold aisle is the re- gion from where the cold air enters the ITE racks from perforated tiles. The main advantage of such an arrangement is that it pre- vents mixing of hot and cold flows.

The airflow rate,CFM (Cubic Feet per Meter)can be approximated using one of the following formulas:

$$CFM = 1.78 * \frac{equipment\ power\ (w)}{temperature\ difference\ (C)} \quad (10)$$

$$CFM = 3.2 * \frac{equipment\ power\ (W)}{temperature\ difference(F)} \quad (11)$$

7.9 Particulate Contaminants

The trend of intermittent, short-circuit failure mode in servers of data centers have increased since their rapid pace of being established in regions where there is a presence of high levels of fine particulate matter in the ambient air and with the in- creased using of free cooling methods (air-side economization), these failures are mainly due to particulate matter.

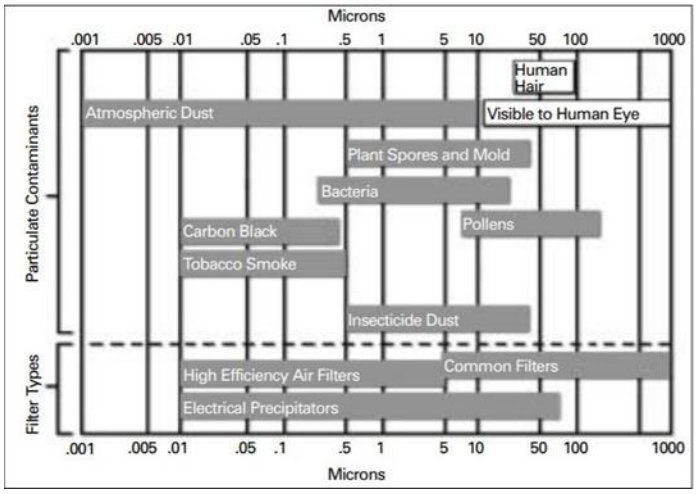

Figure 7-3 Particulate Contaminants [15]

It is explained by Prabjit.S [16] that the source of particulate matter is both nat- ural and anthropogenic. In terms of size, the contaminants can be classified into two distinct categories: fine and coarse particles.

Fine particulates (< 2.5µm), are found in motor vehicle exhaust, diesel particulate matter, smoke and haze, which are further classified into primary and secondary types. Primary

particulates are emitted from a source, such as forest fire, volcanoes, construction sites, unpaved roads, fields or smokestacks. Secondary fine particulates, which make up for the most of the fine particulate contamination, are a result of photochemical reactions in the atmosphere. Table 2, as explained by Jimil. M, [17] illustrates the particulate matter generally found in the nearby surroundings of industrial area similar to the experiment site and their sources. The experiment test site data center was surrounded by Diesel generator, gas welding and manufacturing process environment which are responsible for different kinds of particulate matter as detailed in Figure 3 [15]

As explained by Seymour, M.J. [9] that in any contamination control applications, the particles are of sub-micron level and at this size, there is little slip relative to the air in which they are situated. As a result, the particulates are considered as completely airborne and treated as if they are gaseous.

By using this as a base assumption, our study uses the physical properties of air (molecular weight of 28.9 kg/mol and density equal to 1.19 kg/m3) for 0.05µ and 0.1µ particles. To simulate the flow of 1µ particles, we assumed the properties of VOC (volatile organic compounds) like carbon black particulates which are among the prominent particulate contaminants. The considered sub-micron particulates are approximated as a concentration which excludes the particle slip. This allows for the assumption that the particles are of low concentration (10000ppm) where the air flow affects their motion, but their presence is insignificant to the flow path of air. This intake air is filtered as per ASHRAE standard which has been outlined in the Indoor Air Quality Guide [18]. The filtration of particulates is as outlined: ISO 14644-1 has become the dominant, worldwide standard for classifying the cleanliness of air in terms of concentration of airborne particles (ISO 1999).

Table 7-3 : ISO 14644-1 air cleanliness classifiction vs. maximum particle concentrations allowed(particles/m3) [17]

Maximum Number of Particles in Air			
Particle Size	**0.05µm**	**0.1µm**	**1µm**
Class 1	10		
Class 2	100	4	
Class 3	1000	35	8
Class 4	10000	352	83
Class 5	100000	3520	832
Class 6	1000000	35200	8320
Class 7		352000	83200
Class 8		3520000	832000

Table 3 provides maxi- mum concentration levels for each ISO class (ASHRAE 2009b). ASHRAE recommends that data centers be kept clean to ISO Class 8 with the strictness of the 95% upper confidence limit. For data centers with economizers, the ISO class 8 cleanliness levels may be achieved simply by specifying the following means of filtration:

- The room air may be continuously filtered with MERV 8 fil- ters as recommended by ASHRAE Standard 127 (ASHRAE 2007). [19]
- Air entering a data center may be filtered with MERV 11 or MERV 13 filters as recommended by ASHRAE (2009b). [20]

For data centers utilizing free air cooling or air-side econ- omizers, the choice of filters to achieve ISO class 8 level of cleanliness depends on the specific conditions present at that

data center. In general, air entering a data center may require use of MERV 11 or, preferably, MERV 13 filters [21].

7.10 Simulation Methodology

The CFD solver of 6SigmaRoom is a powerful and easy to use tool with a myriad of post processing options available for accurately simulating the flow conditions. The CFD solver automatically adapts to generating the meshing scheme depending on the complexity and detailing of the model. It uses the k- ε model of turbulence to model the airflow, since it most closely depicts the flow that exists inside a Data Center. Contaminants in 6SigmaRoom can be used to specify pollutants in the model, they can be created from projects, environments or vents. These pollutants can be attached to a vent, ACU, generator or environment, and specify the concentration of that contaminant as a percentage of the total air flow. In the present case study, the ACU has been chosen as the source of contaminants to simulate free air cooling during economizer hours. To show that the CFD results are converged, the default termination criteria that 6Sig- maRoom uses for executing results is that it specifies a degree of acceptable error in the calculation to end the simulation. The default value of this factor is 1. Once the CFD residuals have reduced to this factor, the solver executes the simulation.

7.11 Results and discussion

The contour plots and the streamline plots show the concentration of the contaminants in the room at a height of 1 meter off the raised floor. The number of particles per million (ppm) of the contaminants is chosen to be 10000 particles for 0.05µm and 0.1µm and 900 particles for 1µm, for a transient time period of 10 minutes.

7.11.1 0.05 µm Particulate Contaminant

The Figure 4 shows the streamline plot for the particulate contaminant 0.05µm in the hot-aisle containment model. Figure 5 shows the comparative results for the same 0.05 µm particulate contaminant in the cold-aisle containment model. Both the simulation results were

run for a transient time duration of 10 minutes and during this time period the migration of the particulates are observed either as streamline trajectories or concentration plots. When examining the streamline trajectories of the hot- aisle model, the maximum concentration is found to be around the first three cabinets on either side of the hot-aisle, as observed in Figure 6. Similarly, for the cold-aisle model, the concentration plot reveals the maximum accumulation of particulates at the far end of the ACU, i.e., the last row in the first aisle of the model, as observed in Figure 7.

7.11.2 0.1µm Particulate Contaminant

The sub-micron size particulates of size 0.1µm are specified when simulating the contamination in the hot/cold-aisle models. Since, their physical properties, both 0.05µm and 0.1µm, are the same as that of air, it is observed that they display similar trajectories as seen in both the streamline plot, as seen in Figure 8 and Figure 9 and the concentration plot as seen in Figure 10 and Figure 11. The maximum concentration observed in the con- centration plot is similar to the concentrations observed for the 0.05µm particulate.

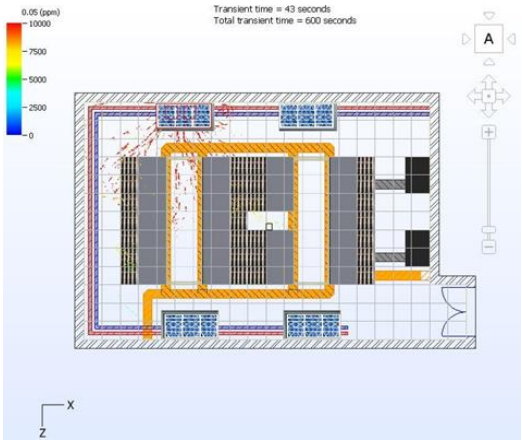

Figure 7-4 Streamline Trajectory for 0.05µm particulate contaminant in hot-aisle containment

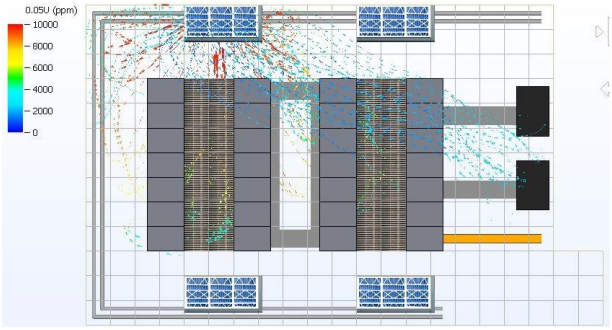

Figure 7-5 Streamline Trajectory for 0.05µm particulate contaminant in cold-aisle containment

7.11.3 1µm Particulate Contaminant

To simulate the flow of heavier particles, the amount of particles entering the white space is restricted to 900ppm, to keep the volume fraction of the particles far less than that of air. This in agreement to our assumption based on Lagrangian approach. From Figure 12 and Figure 13, the streamline trajectories and the concentration plots from Figure 14 and Figure 15 for the 1µm are very similar to that of the sub-micron particulates but the number of trajectories are reduced, accounting to the amount of particulates which enter the data center space.

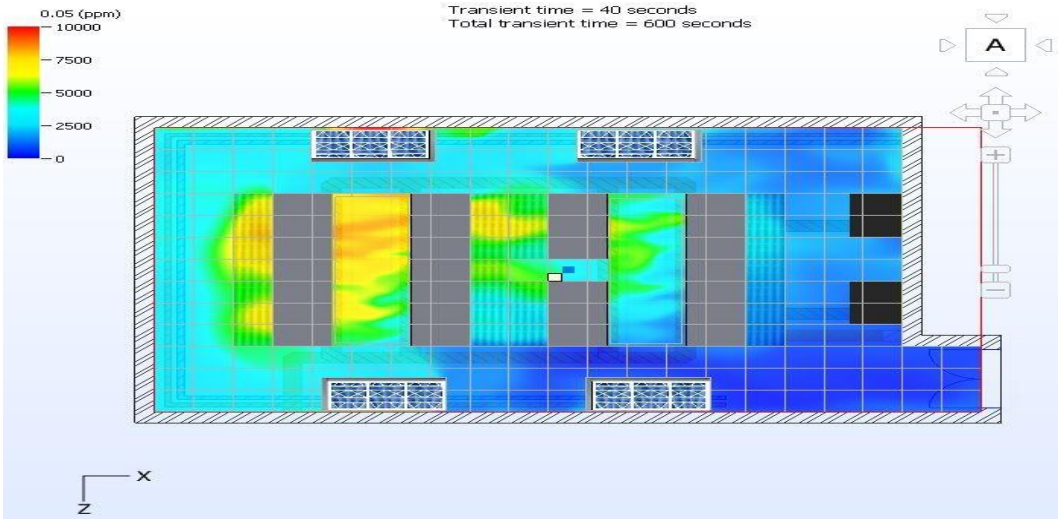

Figure 7-6 Concentration plot for 0.05µm particulate contaminant in hot-aisle containment

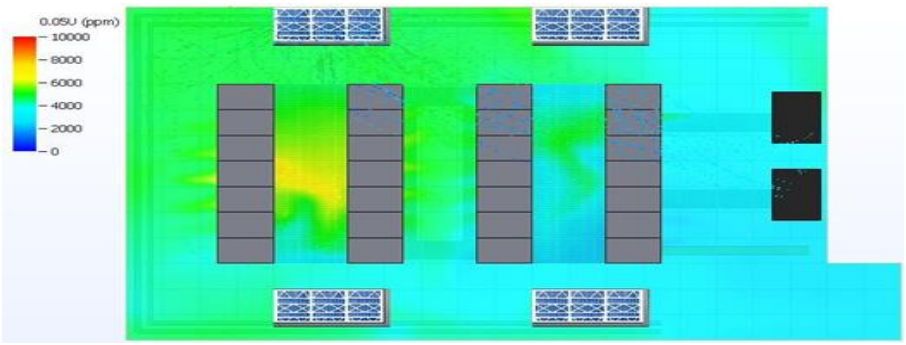

Figure 7-7 Concentration plot for 0.05µm particulate contaminant in cold-aisle containment

7.12 Differences and Challenges

The main challenge that was encountered during this study was lack of any previous literature on flow analysis of particulate contaminants inside a data center. This study is the first of its type, and the results presented in the study can be of great importance for designing more efficient Data Centers. The complexity of Data Center architecture is one of the main challenges that have been encountered to develop an efficient CFD model to validate the results from simulation numerically. Among these challenges is to accurately develop a set of boundary conditions which will represent a realistic Data Center. Also, to tackle the lack of availability of literature, a future study of flow visualization in ANSYS Fluent will be pursued to corroborate the CFD results from both software packages.

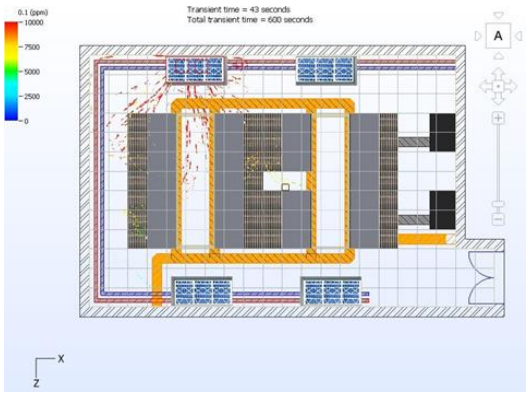

Figure 7-8 Streamline Trajectory for 0.1µm particulate contaminant in hot-aisle containment

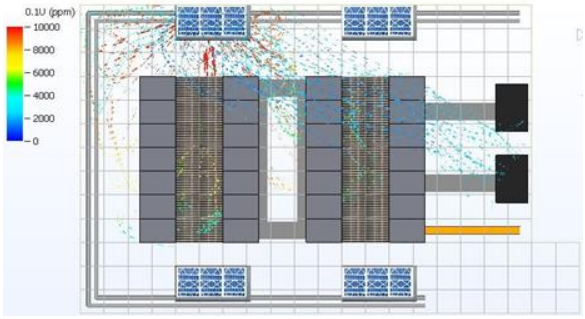

Figure 7-9 : Streamline Trajectory for 0.1µm particulate contaminant in cold-aisle containment

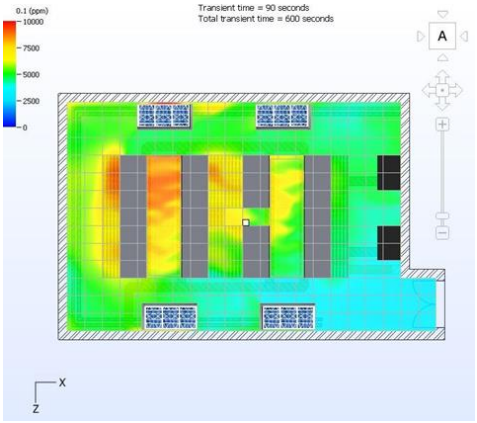

Figure 7-10 : Concentration plot for 0.1µm particulate contaminant in hot-aisle containment

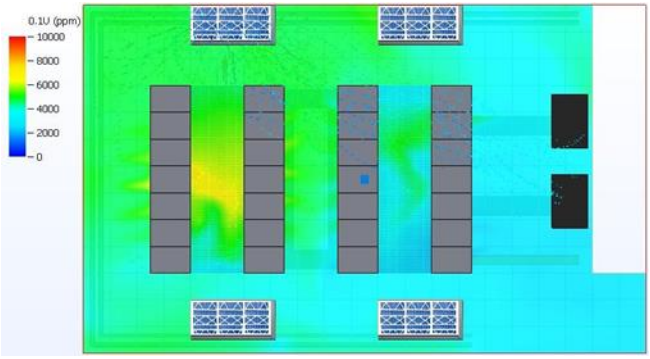

Figure 7-11 : Concentration plot for 0.1µm particulate contaminant in cold-aisle containment

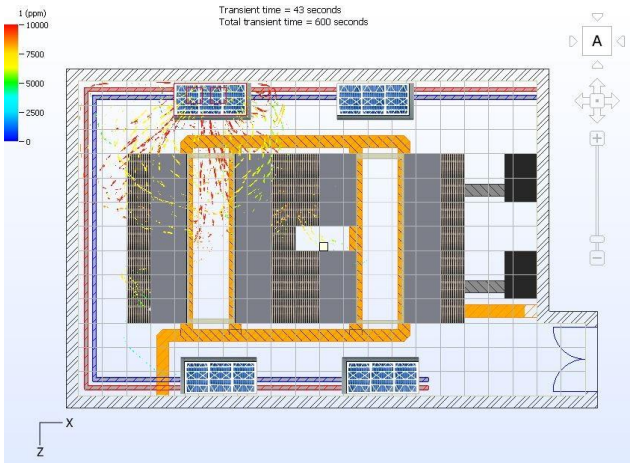

Figure 7-12 Streamline Trajectory for 1µm particulate contaminant in hot-aisle containment

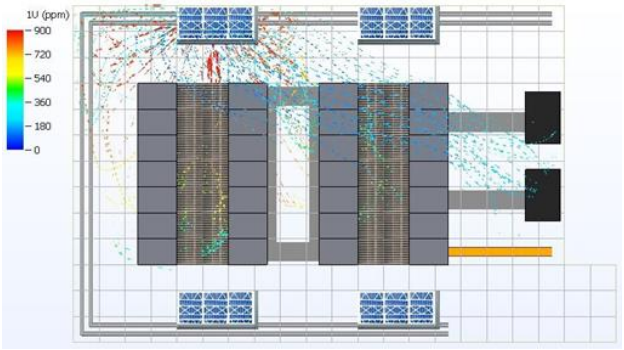

Figure 7-13 : Streamline Trajectory for 1µm particulate contaminant in cold-aisle containment

7.13 Conclusion

The flow-path and concentration plots were obtained for three different sizes of the contaminants. The CFD results are obtained for transient analysis for cold-aisle and hot-aisle containments and were compared.

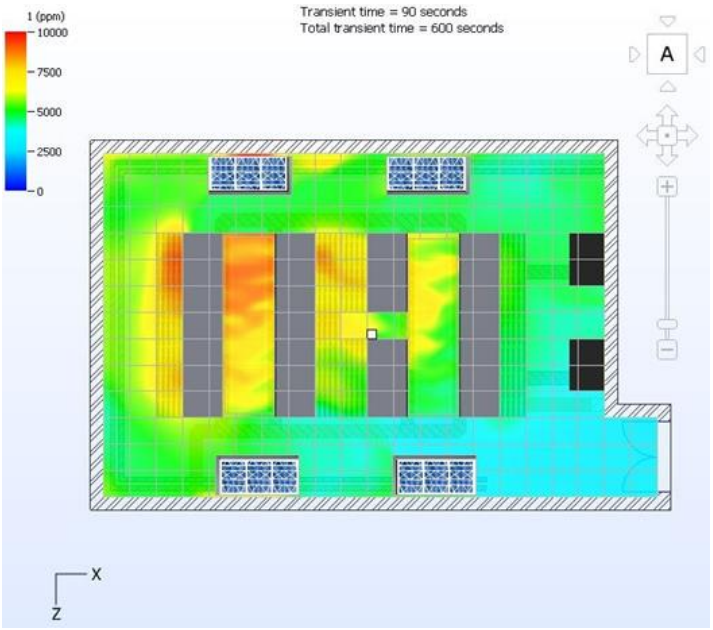

Figure 7-14 : Concentration plot for 1µm particulate contaminant in hot-aisle containment

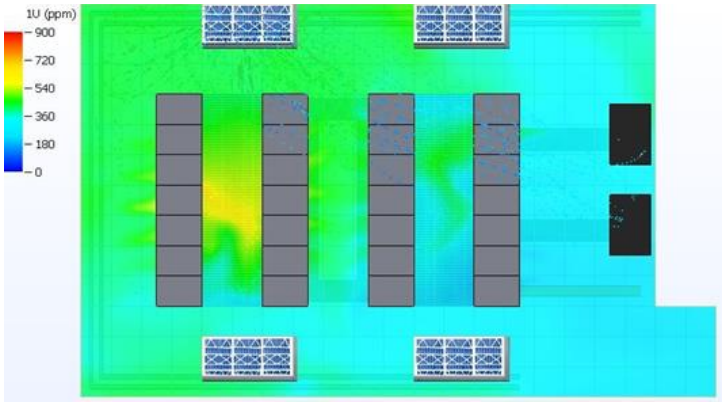

Figure 7-15 : Concentration plot for 1µm particulate contaminant in cold-aisle containment

From the simulations and the result plots obtained, the following conclusions were drawn:

- As assumed, the particles of size 0.05 and 0.1 followed the same path as of air since they have the same physical properties as air.
- The streamline plots obtained show the velocity vectors of the particles emanating from the ACU and entering the Server racks which describes the flow pattern and path. The concentration plots, which is a plane at 1m height in the room, shows the region of the most particle concentration. Result animations show that the most affected area are the first three cabinets on either side of the aisle in the hot-aisle containment model. Similarly, for the cold-aisle containment model, the most affected area are the far end cabinets in the cold aisle.
- The sensor plot, as seen in Figure 16 for contamination per- centage is obtained by placing 6 sensors at 0.5 m height from the raised floor on 3 cabinets on either side of hot aisle de- scribe the variation of contamination with increasing time at that height. It was also observed that the contamination level reduced with increasing height in both CAC and HAC.

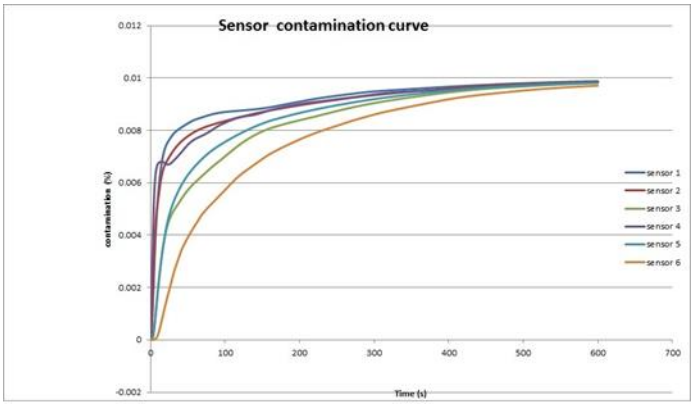

Figure 7-16 Sensor concentration graph

As we know, that while containment systems are proven to reduce cost expenditure on ITE cooling, they may also be helpful in preventing the contamination of the ITE. Firstly, the CAC might prevent the direct entry of contaminants from human sources in the Data center facility. As this study assumes that the sub-micron particles have similar properties to that of air, based on the streamline plots obtained for HAC, it is proved that these particles rise up with hot return air. This return air can be then filtered with filters of appropriate efficiency, like filters with rating above MERV 13.

There are several strategies that can be used to prevent important servers and other IT equipment using the results obtained from such simulations. If the most vulnerable locations of particle contamination are known for a given Data Center, depending on the critical use and utilization of servers, the servers can be placed accordingly in the regions where the least amount of contamination is predicted. Another way is adding an obstruction to the flow near the critical ITE, based on the knowledge of the results from simulation, to alter the flow-path of contaminants away from the cabinets.

7.14 Acknowledgment

This work is supported by NSF IUCRC Award No. IIP- 1738811. The authors would also like to extend their gratitude to Future Facilities Ltd, for promptly helping in simulations in 6SigmaRoom CFD Solver.

7.15 References

1. ANSI/AHRI, 2007. “Method of testing for rating computer and data processing room unitary air conditioners”. Ameri- can Society of heating, Refrigeration and Air-Conditioning Engineers, ANSI/ASHRAE Standard 127-2007.
2. W.K.Chow, 1995. “Ventilation design: Use of computa- tional fluid dynamics as a study tool”. The Chartered Insti- tution of Building Services Engineers, 16(2), pp. 63–76.
3. Awbi, H., and Gan, G., 1994. “Prediction of airflow and thermal comfort in offices”. ASHRAE Journal, 362, pp. 17–21.
4. Schmidt, R., 2004. “Thermal profile of a high-density data center - methodology to thermally characterize a data cen- ter”. ASHRAE Trans., 1102, pp. 635–642.
5. Guggari, S., A. D. B. C., and Stahl, L., 2003. “A hy- brid methodology for the optimization of data center room layou”. ASHRAE Trans., pp. IPACK2003–35273.
6. Patankar, S., and Karki, K., 2004. “Distribution of cool- ing airflow in a raised-floor data center”. ASHRAE Trans., 1102, pp. 629–635.
7. Karki, K.C., R. A., and Patankar, S.V., ., 1992. “Distri- bution of cooling airflow in a raised-floor use of compu- tational fluid dynamics for calculating flow rates through perforated tiles in a raised-floor data centers”. HVAC&R, Res.92, pp. 153–166.
8. Patankar, S., 2010. “Airflow and cooling in a data center”. ASME. J. Heat Transfer., 132(7), pp. 153–166.
9. Seymour, M.J., A. A. M. A., and Jiang, J., 2000. “Cfd based airflow modelling to investigate the effectiveness of control methods intended to prevent the transmission of airborne organisms”. Air Distribution in Rooms, (ROOMVENT 2000).
10. Jones, P., and Whittle, G., 1992. “Computational fluid dy- namics for building air flow prediction- current status and capabilities”. Building and Environment, 27(3), pp. 321–338.

11. Chen, Q., and Zhang, Z., 2005. “Prediction of particle transport in enclosed environment”. China Particuology, 3(6), pp. 364–372.
12. Clayton, T.Crowe, J. D. S. S. M., and Tsuji, Y. “Multiphase flows with droplets and particles,”. CRC Press, 3(ISBN).
13. Facilities, F., 2018. 6 Sigma Room Version 12, latest ed. Future Facilities.
14. Neimann, John., B. K. A. V., 2010. “Hot-aisle vs cold-aisle containment for data center(white paper)”. CRC Press, 3, p. 135.
15. ASHRAE. “Indoor air quality: A guide to understanding ashrae. standard 62-2001”.
16. Singh, P., R. P. S. S., and Muller, C., 2010. “Character- ization, prevention and removal of particulate matter on printed circuit boards”. p. 135. See also URL
17. Shah, Jimil Awe, O. . A. P. . A. I. . A. D. . S. P. . K. N. . K. M., 2016. “Qualitative study of cumulative corrosion damage of it equipment in a data center utilizing air-side economizer.v010t13a052. 10.1115/imece2016-66199”.
18. Shah J, M, A. O. A. P. e. a., 2010. “Qualitative study of cu- mulative corrosion damage of it equipment in a data center utilizing air-side economizer.”. [ASME],International Mechanical Engineering Congress and Exposition, 10. Micro and Nano-Systems Engineering and Packaging.
19. ASHRAE, 2007. “Method of testing for rating computer and data processing room unitary air conditioners (ansi ap- proved)”. American Society of Heating, Refrigeration and Air-Conditioning Engineers, Inc.
20. ASHRAE, 2009. “Particulate and gaseous contaminants in data center environments.”. American Society of Heating, Refrigeration and Air-Conditioning Engineers, Inc, 10.
21. ASHRAE, 2011. “2011 gaseous and particulate contamination guidelines for data centers”. American Society of Heat- ing, Refrigeration and Air-Conditioning Engineers, Inc.

Chapter 8

Measurement of the Thermal Performance of a Single-phase Immersion Cooled Server at Extreme Temperatures for a Prolonged Time

Abstract

The next radical change in the thermal management of data centers is to shift from conventional cooling methods like air-cooling to direct liquid cooling (DLC) to deal with high thermal mass. The past few years have consistently seen wider adoption of the most recent technology of direct liquid cooling which has been incorporated in data centers because of its simplicity and high heat dissipation capacity. Passive single phase engineered fluid immersion cooling has several other benefits like better server performance, even temperature profile and higher rack densities. This paper presents various parameters about the performance of a fully single-phase dielectric fluid immersed server over wide temperature ranges in an environmental chamber. The server was placed in an environmental chamber and was applied extreme temperatures ranging from -20°C to 55°C at constant 50% relative humidity for extended durations. Thermal overstress experiment was performed on a fully immersed server and its cooling system components. This work explores the performance of a server and other components like pump including flow rate drop, starting trouble and other potential issues under extreme climatic conditions. The possibility of connector seals observing reduced performance upon accelerated temperature cycling is addressed. Throttling limit for a server and a pump, and server power draw for different temperatures are examined to assess pump performance. Pumping power consumption is directly related to the operating cost of a data center. The experiment was carried out till the core temperature reaches to the maximum junction temperature. This experiment helps to determine the threshold capacity and the robustness of the server for its applications in extreme climatic conditions.

Key words: single phase dielectric immersion cooling, extreme temperature, engineered fluid

8.1 Introduction

In this fast-growing world, there is a continually increasing demand for information technology (IT) applications and services has provided sustained growth and interest in data centers. Many large and medium enterprises access and store online content on the World Wide Web. Because of this ever-increasing demand, the data center cooling costs are constantly on the rise as they need large amounts of energy for the cooling purpose. Due to this vast energy consumption by data center facilities, operators have placed a significant emphasis on the energy efficiency of the building's overall operation. Cooling typically accounts for 40% of a data center's total energy bill [1]. Traditionally, data centers use air as the primary cooling medium where the rejected heat from IT hardware is absorbed by the air. This heat is either rejected to the outside ambient, mixed with incoming fresh air, or cooled through refrigeration processes. With increase in heat densities of electronic components, removing heat constantly from the data centers is the biggest concern as air is less capable of efficient cooling due to its low thermal conductance. Because of the above inadequacy of traditional air-cooling, many discussions are focused on the new immersion cooling technology.

Submerging servers and IT equipment in a dielectric medium for cooling provides substantial energy savings as it accommodates heavy energy loads and density [1], [2], [3] as its heat capacity by volume is 1120-1400 times greater than air [1], [2], [3]. It also helps to keep the temperature constant irrespective of changes in server workload which means that the server is in a good isothermal environment. Single-phase immersion cooled servers are simple, easy to manufacture and inexpensive as it provides simplicity and ease in planning as only one medium is used for cooling purpose which in turns keep the server hygiene. In traditional air-cooling with airside economization, some dust and dirt particles enter the facility. These dirt and

dust particles get accumulated inside the chassis with the computers and lead towards the mechanical failure. Immersion cooling also minimizes and eliminates many common operational issues like solder joint failures, oxidation or corrosion of electrical contacts. Other advantages are no moving parts like fans, no sensitivity to humidity or any temperature condition. Operating expense of this equipment is exceptionally low [2].

One of the major causes of electronic failures is due to thermally induced stresses and strains caused by excessive differences in coefficients of thermal expansion (CTE) across the materials. This experiment focuses on thermal cycling and thermal aging process which determine the performance and efficiency of servers in extreme environmental temperature ranges for prolonged periods in an environmental chamber. It analyzes the effects of extreme temperatures on a single-phase dielectric fluid submerged server, which provides a helping hand to validate the ruggedness and robustness of the server.

The performance of a server and other components like pump and connectors sealing were observed at different temperature cycles typically between -20°C to 55°C (extreme temperatures than the operating temperatures typically found in air cooling based on ASHRAE Thermal Guidelines) at 50% RH. Some additional relations and properties of different components, examined like power draw vs chamber temperature, average core temperature vs chamber temperature. This research helps to determine the threshold limit of a server at extreme temperature and qualifies the robustness of the system for its reliability and performance.

8.2 Server Configuration

In this experiment, the server is fully immersed in a single-phase dielectric fluid. The server comprises a motherboard and an internal submerged pump in place of fan, which circulates cooling medium i.e. dielectric fluid through the system. Two passive heat exchangers transfer heat from the system to the surrounding environment. Two rugged hoses to conduct the

cooling liquid between the enclosure and the heat exchanger. Specifications of the server and the fluid are as follows:

- Server dimensions: 2.3” (H) x 8.1” (W) x 15.3” (L).
- Server Specification: Windows i7 5th Gen with Quad core processor.
- Storage: NVME SSD, 1 x mSATA III SSD, SATA SSD

  Pump Specification:
- Dimensions (WxDxH) of the pump is 90x62x38mm.
- Motor have electronically commuted ball bearing.
- Nominal voltage and power consumption: 12V DC and 18W.
- Maximum flow rate and system temperature: >900l/h and 60°C.
- Materials in contact with the coolant: Stainless steel 1.4571, PPS-GF40, EPDM O-Rings, Aluminum oxide.

Pump in the server is maintained at its maximum rpm, which is 6000 rpm. Pumps rpm does not change with the load of the server. Server have rugged seal enclosure and waterproof I/O connectors, which is IP67 Rated. Electronics are protected from air particulates, moisture contaminants and other contaminants [8]. Customized heat sink is used in the server. It is EKWPs vertical impingement heat sink where fluid can flow in both directions.

8.2.1 Software used

- Prime 95

Prime95 is one of the most popular CPU stress-testing program. It tests the computer for stability issues by stressing CPU to its maximum limit. Prime95 runs Lucas-Lehmer iteration indefinitely and only terminates a stress test when it encounters an error and informs the user that the system may be unstable. Prime95's stress test feature can be configured to test various system components by changing the Fast Fourier Transform (FFT) size. There are three pre-set

configurations available. First, one is Small FFTs primarily tests FPU and CPU caches. Second is In-Place FFTs gives maximum power consumption and tests FPU and CPU caches, some part of RAM and the last one Blend which tests everything including RAM. In this experiment small FFTs option is been used since it tests FPU at maximum stress and system operates in more stable condition.

- Core temp:

Core Temp is a compact program to monitor CPU temperature. It displays real time temperatures of each individual core (core temperature) in each processor when the load of the server varies. Core Temp is completely motherboard independent. The temperature readings are very accurate as the software is collecting the data directly from a Digital Thermal Sensor (or DTS). DTS is located near the hottest part of each core. This sensor does not rely on an external circuit located to report temperature, all core temperature values is stored in the processor. Core temp software can access and provide real time reading. This method eliminates any kind of inaccuracies [4].

- Dielectric fluid:

The server is fully submerged in a single-phase dielectric fluid. The properties of the dielectric fluid (Opticool 872552) are given in the Table (1). Flash point of the dielectric fluid is 185°C. Dielectric fluid provides great cooling efficiency, safety and thermal stability at a low cost. It is designed to use in circulating systems, which includes both heating and cooling systems of electrical applications [9].

Table 8-1 Property Table

Temp °C	Kinematic Viscosity (cSt)	Dynamic Viscosity (poise)	Specific Heat (kw-s/kg-K) (J/g/K)	Thermal Conductivity (W/m/K)
0	18.8	0.1519	2.054	0.1381
10	12.5	0.1002	2.092	0.1375
20	8.82	0.0701	2.129	0.1369
30	6.52	0.0514	2.167	0.1364
40	5.00	0.0397	2.204	0.1358
50	3.96	0.0307	2.242	0.1352
60	3.22	0.0247	2.280	0.1346
70	2.69	0.0205	2.2317	0.1341
80	2.27	0.0171	2.355	0.1335
90	1.95	0.0146	2.392	0.1329
100	1.70	0.0126	2.430	0.1323

8.3 Experimental Setup

8.3.1 Environmental chamber

Thermatron SE-600-10-10 environmental chambers figure (2) provide versatility in testing environments. In other words, Thermotron Environmental chamber provides the user to change its environment as per user fed values. Chamber consist of an onboard condenser which is water-cooled, and airflow rate is 1000 CFM. Temperatures and humidity in chamber ranges from -70°C to 180°C (-94°F to 356°F) and 10% to 98% respectively. In this experiment, the server is kept inside a Thermotron SE 600-10-10 Environmental chamber, and the thermocouples were attached at various locations on the server as shown in figure (6).

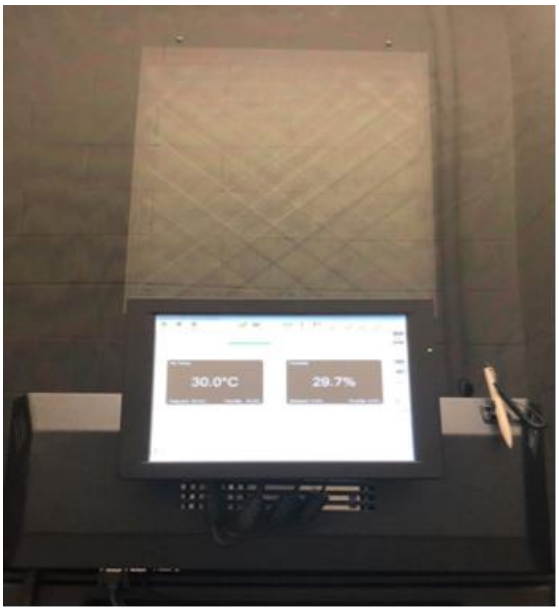

Figure 8-1 Thermatron SE-600-10-10 Environmental Chamber

8.3.2 Thermocouple

In the experiment T-Type thermocouples were used. The Type T is a very stable thermocouple and is often used in extremely low temperature applications such as cryogenics or ultra-low freezers [5]. The type T has excellent repeatability between –380°F to 392°F. Temperature Range of Type T is from -454°F to 700°F (-270°C to 370°C) and Standard Accuracy is +/- 1.0C or +/- 0.75% [5].

8.3.3 DAQ and Multiplexer

In this experiment, Agilent 34972A DAQ system was used to log the temperatures of the thermocouples. DAQ's capability of combining the precision measurement with various signal connections makes this instrument very versatile and reliable. It also has three module slots into the rear of the instrument to accept any combination of data acquisition component or multiplexer (MUX). All the data were recorded directly in the through its pre-installed Agilent

34901A software in the system. This software gives more flexibility for logging data as user desire.

8.3.4 Power meter

The Power meter used in this experiment was Watts Up Pro (Figure 2). It is one of the efficient, precise, and accurate power measuring devices. This device logs data at any interval defined by the user. It measures total server power and not only power but also voltage, current, cost, watt-hour, power factors, duty and power cycle etc.

Figure 8-2 Power meter

8.4 Methodology

8.4.1 Positions of thermocouples

T-type thermocouples attached on the server at eight different locations. Figures (3 and 4) show the precise locations of the thermocouples on the server. Nomenclatures are as follows:

- Ch-1: Top of the server

- Ch-2: Left of the server
- Ch-3: Right of the server
- Ch-4: Inlet of the server
- Ch-5: Outlet of the server
- Ch-6: Connector of two radiators
- Ch-7: Calibrator Front (Air)
- Ch-8: Calibrator Back (Air)

8.4.2 Calibration of thermocouples

Before attaching the thermocouples on the server, the thermocouples need to be calibrated. For calibration the thermocouple was attached to Agilent 34901A 20 Channel Multiplexer Module and Agilent 34972A DAQ system. The free end of the thermocouple was kept in the ice water beaker with a thermometer. Individually, the thermocouple value was checked from the DAQ system and compared with the thermometer value. The variation between the thermocouple measured temperatures and the temperature in the environmental chamber was only -/+ 1 °C.

After, first calibration the thermocouples were attached on server. The server was placed in the environmental chamber and before starting the actual experiments, the thermocouples were calibrated again. Calibration was done in following order:

1. Environmental chamber was programmed to set at ambient temperature (25°C).
2. Once temperature was set, the thermocouples were checked through the DAQ systems. The variation between the thermocouple measured temperatures and the temperature in the environmental chamber was only -/+ 1 °C.

After calibration of the thermocouples, the server was started, and 100% load was given by Prime 95 software. The temperature of the chamber was set to 25°C with 50% RH.

The experiment was performed for 4 hours. The voltage, current, power and all four core temperatures were logged at the interval of 15 minutes by the power meter and software Core Temp respectively. Temperatures of the thermocouples were logged by Agilent software.

After 4 hours, the chamber was stopped and opened, inspection was done on the server to check for any leakage from the connectors, abnormal noise, and condensation on the radiators. After inspection, the server was kept idle for 4 hours allowing it to reach to its normal state and the next experiment was performed. After initial check, the server was tested at low temperature. For the first experiment, the temperature of the chamber was kept at 20°C with 50% RH. The experiment was performed for 4 hours and readings of core temperature, power, voltage and current were taken at every 15 minutes of interval. Four hours later, chamber was stopped to inspect the server for any leakage or any abnormal noise. This procedure was repeated and performed at 10°C, 0°C, -5°C, -10°C, -15°C and -20°C.

The procedure, which was used for low temperature experiments, same was used for high temperature. The server was tested at different chamber temperatures of 30°C, 35°C, 40°C with 50% RH for 4 hours and all the parameters were recorded. For 45°C, 50°C and 55°C, the same experiment was performed but for a longer period i.e. for 8 hours with 50% RH. Temperatures of thermocouples and core were recorded at every 30 minutes by the systems. After above experiments, the server was tested at 45°C for 144 hours. This experiment was performed for detailed analysis of server performance. Core temperature were recorded at every 2 hours of interval, inlet and outlet temperature of the fluid and power was recorded at every 4 hours of interval. Longer duration experiments were performed at higher temperature to check the reliability and performance issues of the server.

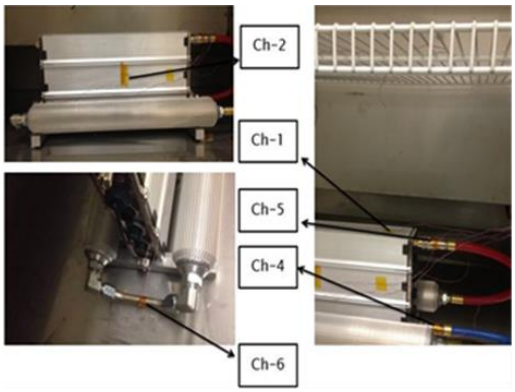

Figure 8-3 Front side of the server

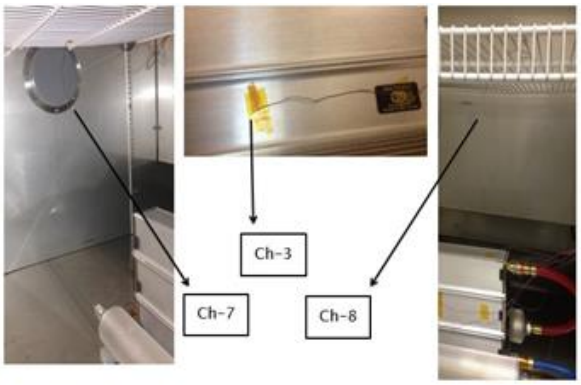

Figure 8-4 Backside of the server

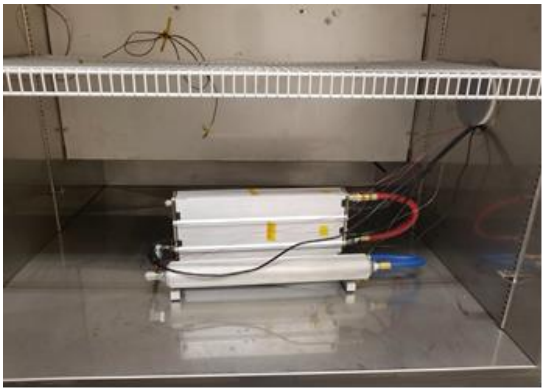

Figure 8-5 Experimental Setup in the environmental chamber

8.5 Results and Discussion

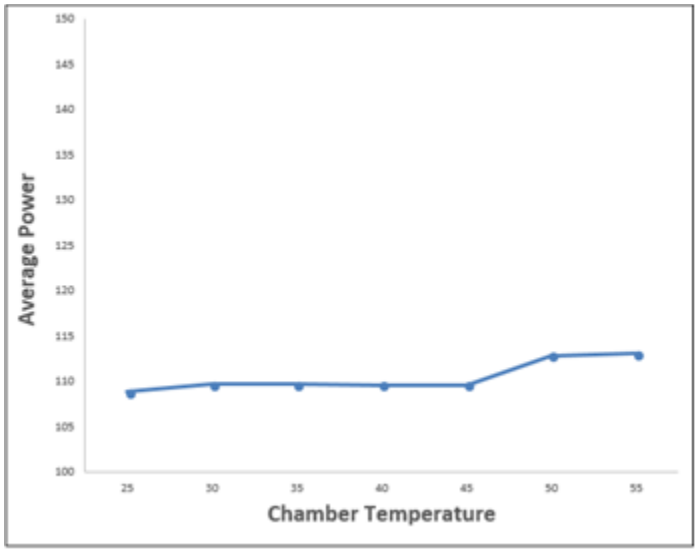

Figure 8-6 (a) Average power (W) vs Temperatures (°C) graph (High Temperature)

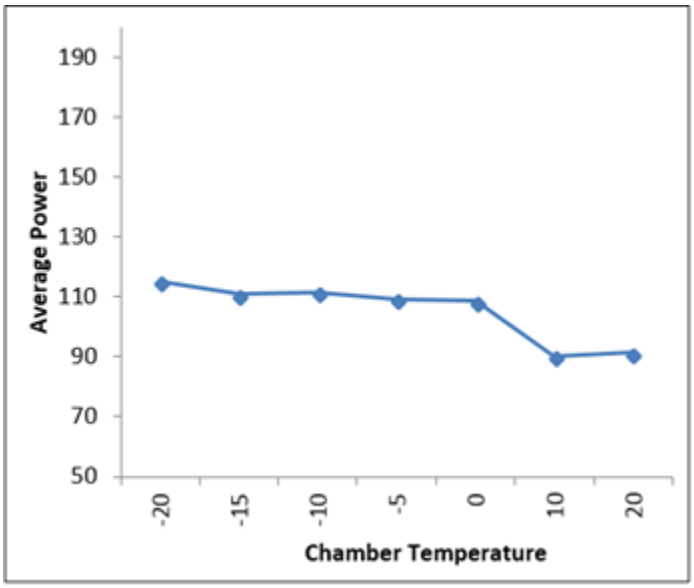

Figure 8-6 (b) Average power (W) vs Temperatures (°C) graph (Low Temperature)

Figure 6(a, b) shows the variation of average power with respect to environmental chamber temperature. Figure 6(a) shows that at 25°C, the power consumption of the server is 109.1 Watts, which steps up to 109.6 Watts at 30°C and remains constant until 45°C. After

45°C, it rises to 112.8 Watts and 113.2 Watts for 50°C and 55°C respectively. The power increase at the higher temperature is due to decrease in pump power and increase in leakage current of the pump. This is because of the low viscosity of the fluid at the higher temperature. Figure 6(b) shows that the power consumption of the server is constant around 91.5 Watts at 20°C and 10°C and rose up to 110 Watts and 110.9 Watts at 0°C and -20°C respectively. This rise in power consumption at extreme low temperature is due to increasing viscosity of the fluid. Pump drove more power to maintain the flow rate of the fluid.

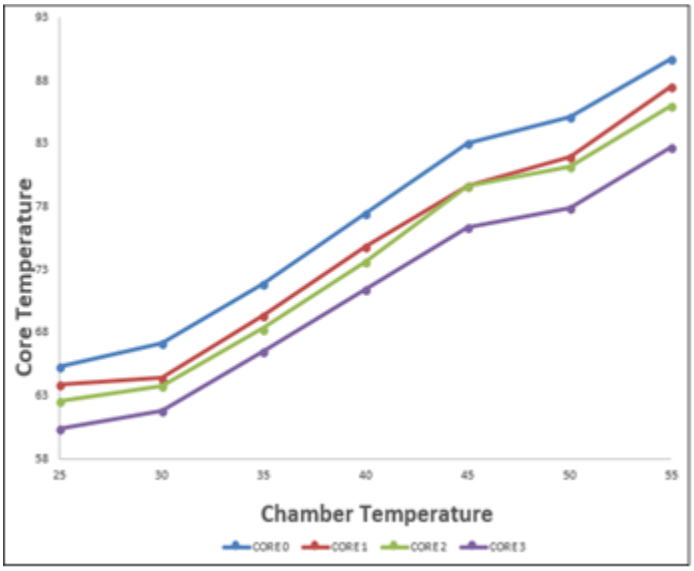

Figure 8-7(a) Average Core temperature (°C) vs Chamber temperature (°C) (High Temperature)

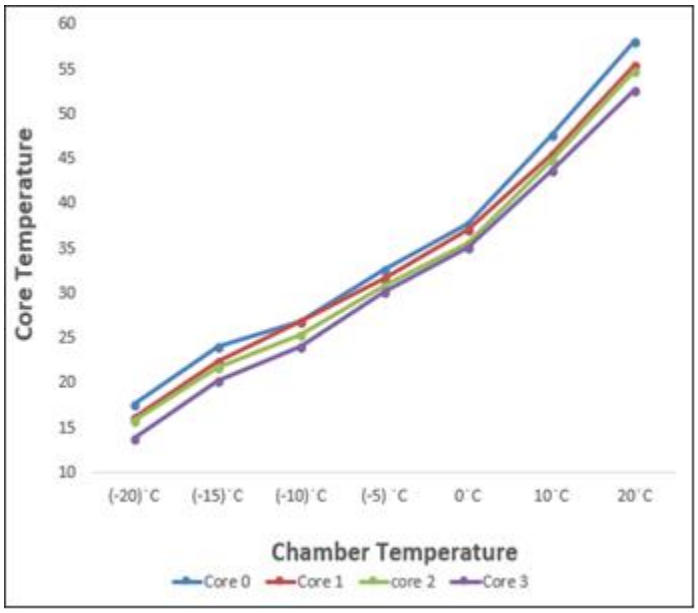

Figure 8-7(b) Average Core temperature (°C) vs Chamber temperature (°C) (Low Temperature)

Figure 7(a, b) shows the average core temperature of server with respect to the changing chamber temperature. Figure 7(a) shows that at 25°C, all core temperatures were below 65°C. It is noticeable that average core temperature is increasing drastically with the rising chamber temperature. At 55°C, core 0 temperature almost reached the Maximum Junction Temperature (T_j) of the system. The set junction temperature of the system is 92°C. Same pattern observed for all other core temperatures. In figure 7(b), the temperature of all cores dropped down with decreasing chamber temperature. At 20°C and -20°C, the temperature of the primary core (Core 0) is 59°C, and 18°C respectively. Even at low surrounding temperature, the efficiency and performance of the server was the same. There was no abnormal noise and leakage from the server.

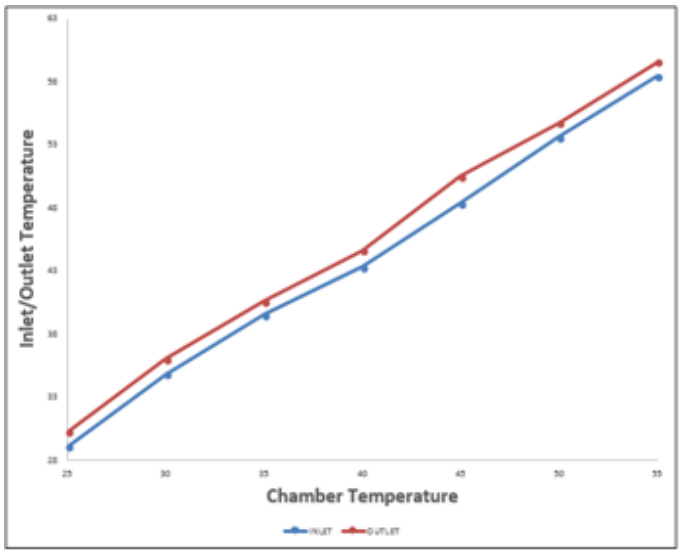

Figure 8-8(a) Average Inlet and Outlet temperatures (°C) vs Chamber temperatures (°C) (High Temperature)

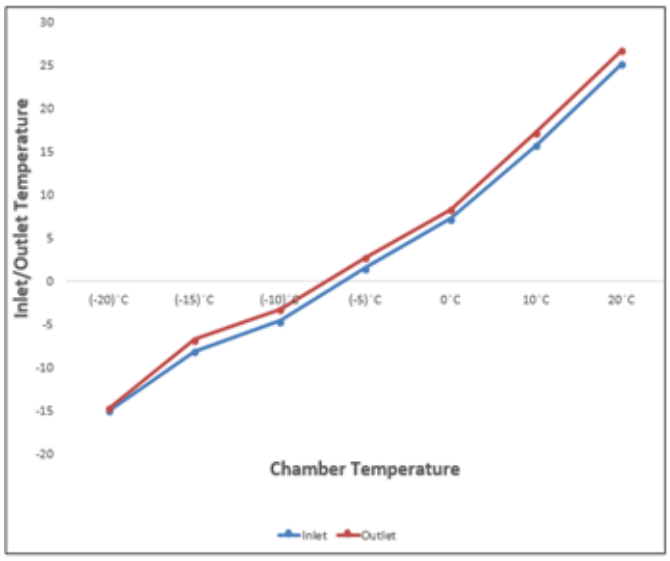

Figure 8-8(b) Average Inlet and Outlet temperatures (°C) vs Chamber temperatures (°C) (Low Temperature)

Figure 8(a, b) shows average Inlet/Outlet temperatures of the server with respect to the environmental chamber temperature. It is evident that there is almost 1°C difference between

inlet and outlet temperature of the server. Inlet and outlet temperatures are the temperatures of a coolant entering and exiting the server respectively as shown in Figure 3. The difference in temperature is almost the same from -20°C to 55 °C.

Figure 9, 10, 11 are the results of the experiment which was performed at 45°C for 144 hours. At every 2 hours of interval, core temperature reading was recorded. Similarly, inlet and outlet temperature of fluid and power was recorded at every 4 hours of interval.

Figure 10 shows core temperature of the server with respect to time. Server core temperatures was almost constant in the cycle. Maximum range of temperature for the all core is around 4 °C. It is evident that the average core temperature of all core is almost same as shown in Figure 7.

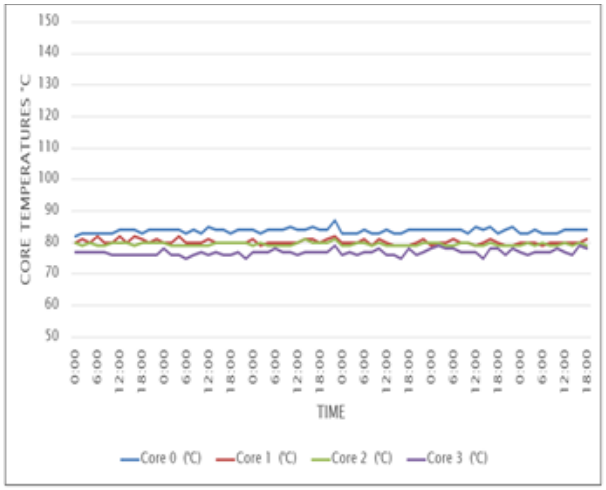

Figure 8-9 Core temperature (°C) vs Time (Hours)

Figure 10 shows Inlet/Outlet temperatures of the server with respect to time. The pre-installed Agilent software did data logging at every 4 hours of interval. The difference between inlet and outlet temperature was around 3°C. Figure 8 shows the temperature difference of 1°C for all the environment (ambient) temperature of the server.

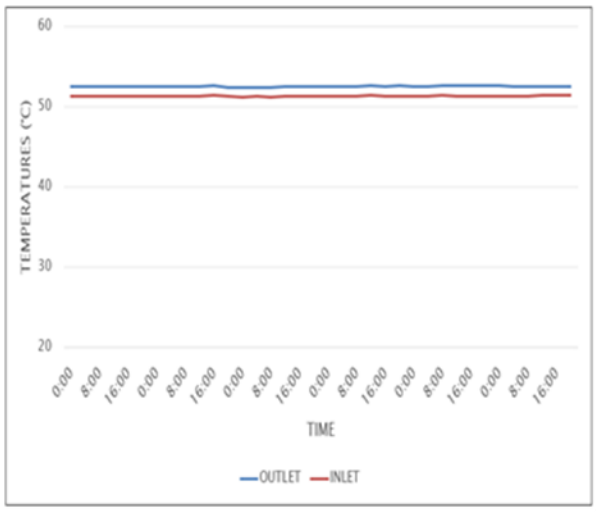

Figure 8-10 Inlet/Outlet Temperature (°C) vs Time (Hours)

Figure 11 shows server power with respect to time. It is evident that the average power consumption of the server at 45°C is around 109W, which is same as shown in Figure 6. The power consumption of the server was almost constant for the whole cycle (144 hours).

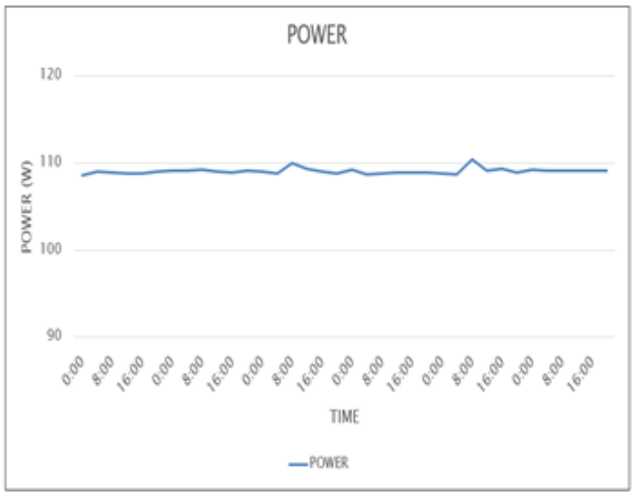

Figure 8-11 Power (W) vs Time (Hours)

8.6 Conclusion

From the experiment results, it can be inferred that the fully submerged server can be used in extreme weather conditions. As there is no direct contact with the surrounding

environment the reliability of the server increased. At extreme temperatures, the server was performing efficiently without compromising its reliability. From above results, hereby we can conclude that the server can perform efficiently at - 20°C and threshold temperature is 55°C as the core junction temperature reached its maximum temperature limit, which is 92°C. There was no leakage through any connectors and no abnormal noise from the server. The server is robust and can withstand the harsh environment. From 144 hours of experiment, it is evident that the performance of passive heat exchanger was very efficient. This server can be adapted in military and industrial applications as its performance was very efficient and showed very promising results in high temperatures. The waste heat from the server can be reclaimed thus the thermal efficiency can be increased further. Since the server is compact the size of racks can be reduced which will further reduce the initial capital cost.

8.7 Acknowledgement

This work is supported by NSF IUCRC Award No. IIP-1738811.

8.8 References

1. Almoli, A. Thompson, N. Kapur, 1. Summers, H. Thompson and G. Hannah, "Computational Fluid Dynamic Investigation of Liquid Cooling in Data Centers," Applied Energy, vol. 89, pp. 150-155, 2012.
2. Jimil M. Shah, Richard Eiland, Ashwin Siddarth and Dereje Agonafer "Effects of Mineral Oil Immersion Cooling on IT Equipment Reliability And Reliability Enhancements To Data Center Operations" 10.1109/ITHERM.2016.7517566
3. R. Eiland, J. Fernandes, M. Vallejo, D. Agonafer and V.Mulay, "Flow Rate and Inlet Temperature Considerations for Direct Immersion of a Single Server in Mineral Oil," in IEEE ITHERM, Lake Buena Vista, FL, 2014.
4. http://www.alcpu.com/CoreTemp/howitworks.html
5. https://www.thermocoupleinfo.com/thermocouple-types.html
6. C. Tulkoff and C. Boyd, "Improved Efficiency & Reliability for Data Center Servers Using Immersion Oil Cooling," in Electronic System Technology Conference & Exhibition, Las Vegas, NV, 2013
7. J. Shah, ET. al., "Critical non-thermal consideration for oil cooled data-center", IMAPS ATW 2015, Los Gatos, Ca, 2015.
8. Jimil M. Shah and Dereje Agonafer, "Issue on Operational Efficiency for Oil Immersion Cooled Data Centers", Session Co- Chair and Presenter for ASME Panel On "ThermalManagement Challenges in Energy Conversion & Conservation", ASME IMECE 2015, November 13-18, Houston, Texas.
9. http://dsiventures.com/
10. http://www.liquidcoolsolutions.com/
11. https://mfvl.home.xs4all.nl/prime/readme.txt

Chapter 9

Computational Analysis of Form Factor Study, Study of Impact of Thermal Shadowing and Customization of Heat Sink for Single-Phase Immersion Cooled 3rd Generation Open Compute Server

9.1 Introduction

In this study, we have used white mineral oil and synthetic fluid Electro Cool 100 (EC-100). The physical properties of different types of fluids are mentioned below.

Table 9-1 Properties of different fluids

Type of Fluid	Heat Capacity (KJ/Kg K)	Density (Kg/m^3)	Kinematic viscosity (X 10^{-6} m^2/s)	Heat Conductivity (W/m K)
Air	1.01	1.225	0.016	0.02
Water	4.19	1000	0.66	0.58
White Mineral Oil	1.67	849.3	16.02	0.13
Synthetic fluid (EC-100)	2.165	803.78	13.22	0.1378

It is clear from the Table1 that the Thermal mass (Density x Heat Capacity) of Di-Electric liquids is high compared to air. Although the thermal mass of water is the highest, water is a conductive fluid and servers cannot be immersed in water directly.

9.2 Specification of the Server

9.2.1 Server Description

The server considered for the study is a “Third Generation Open Compute Server”. It comprises of four DIMM blocks each having four DIMMS of 8GB memory. It consists of two

microprocessors with design power density of 115 W each. It has two CPU's each having a dimension of 50mm X 50mm. The length and width of the chassis are 166.2mm and 511mm, and the height varies for different form factors are as follows.

Table 9-2 Height of the chassis for rack unit and open rack unit

	RACK UNIT	**OPEN RACK UNIT**
1U	44.5	48
1.5U	66.5	72
2U	89	96

The Open Compute Server taken under study has a form factor of 2 Open rack unit and with the dimensions of 166.2mm x 511mm x 96mm. The server is enclosed with a top cover on the chassis body. The top view of the server is shown in the figure 1.

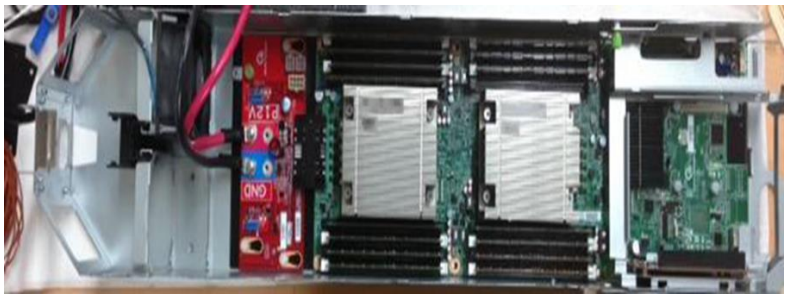

Figure 9-1 Top view of Open Compute Server

9.2.2 Baseline Air Cooled Server Specifications

The baseline air cooled server has the same dimensions as considered for the study. But the power of each CPU is 95W instead of 115W. Ducting system is provided at the top of the server to manage the air flow.

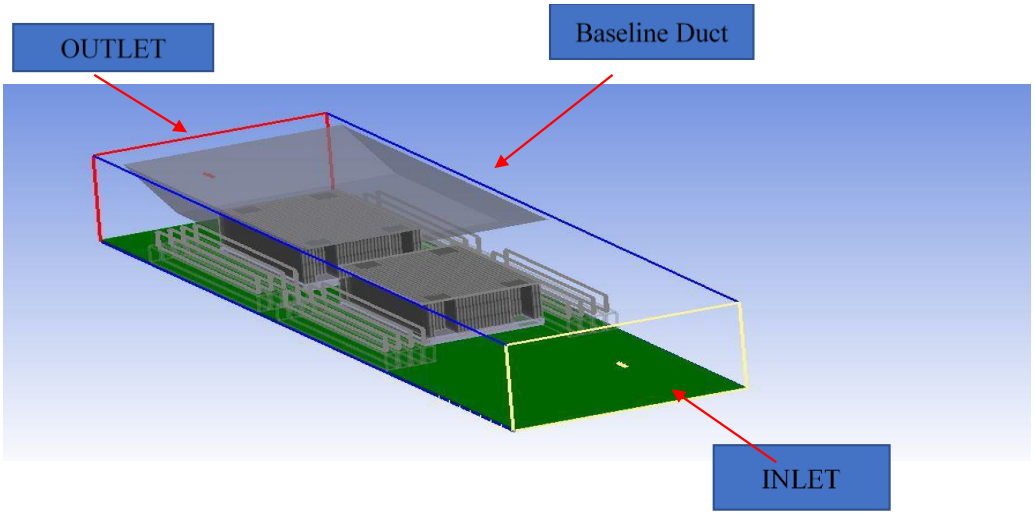

Figure 9-2 CFD model of Baseline Air Cooled Server

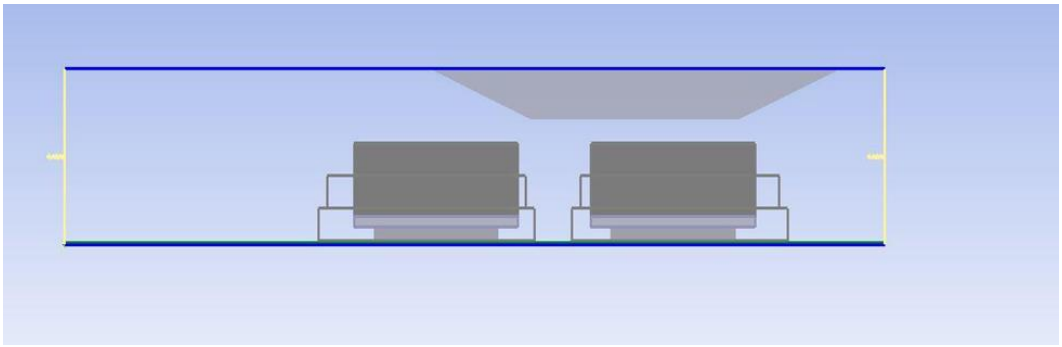

Figure 9-3 Side view of Baseline Air Cooled Server

The CFD model has been developed using the Computational tool called ANSYS ICEPAK and duct geometry has been imported from the modelling tool SOLIDWORKS. The baseline duct is made of aluminium. From the Fig 2, we can see that one end is considered as inlet and the other as outlet. Experiment on air cooling was performed by previous master's

student Divya Mani. The baseline single server had been tested experimentally and computationally at various inlet velocity and varying the processor usage.

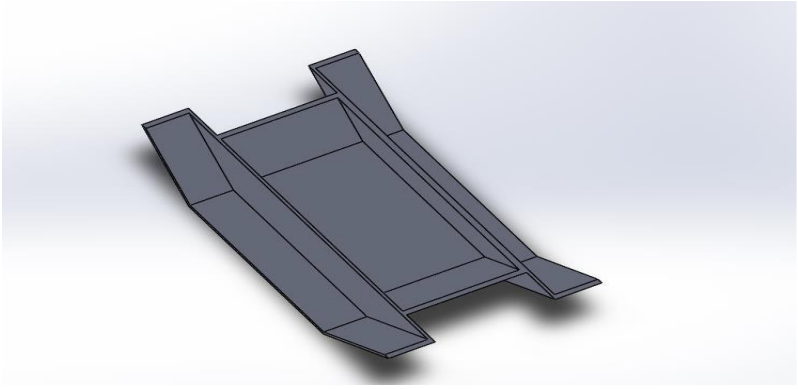

Figure 9-4 Baseline Duct

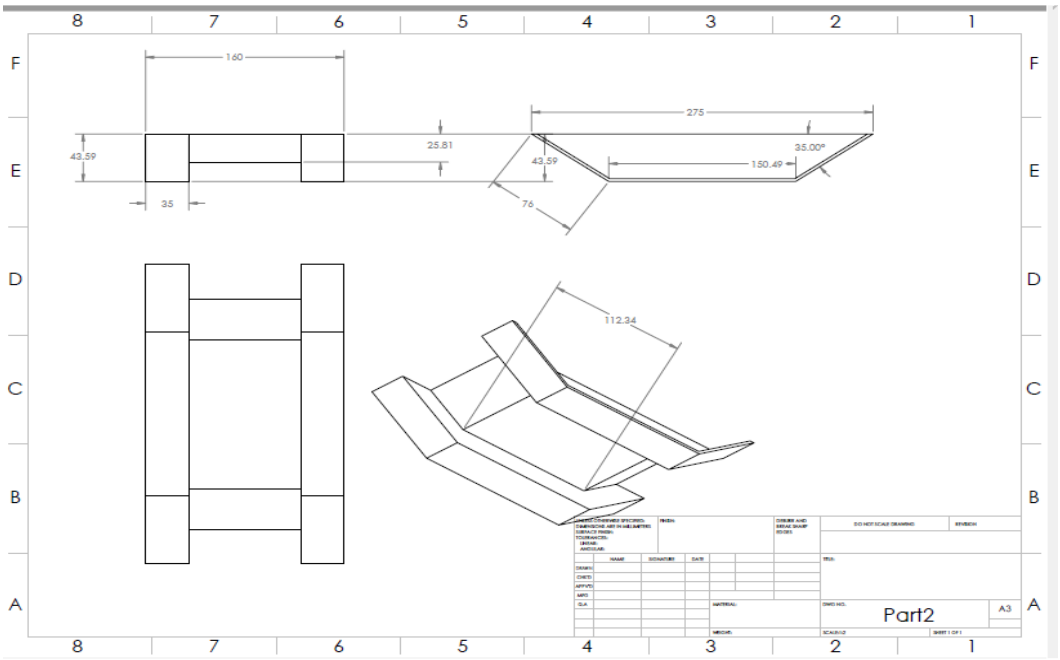

Figure 9-5 Dimensions of baseline duct

9.2.3 Baseline Oil Cooled Server

The baseline oil cooled server has been developed using the computational tool ANSYS ICEPAK. Server dimensions were kept same as the baseline server except the duct

and fans were removed. In this geometry, Cabinet max y is the inlet and min y is the outlet for the flow of fluid.

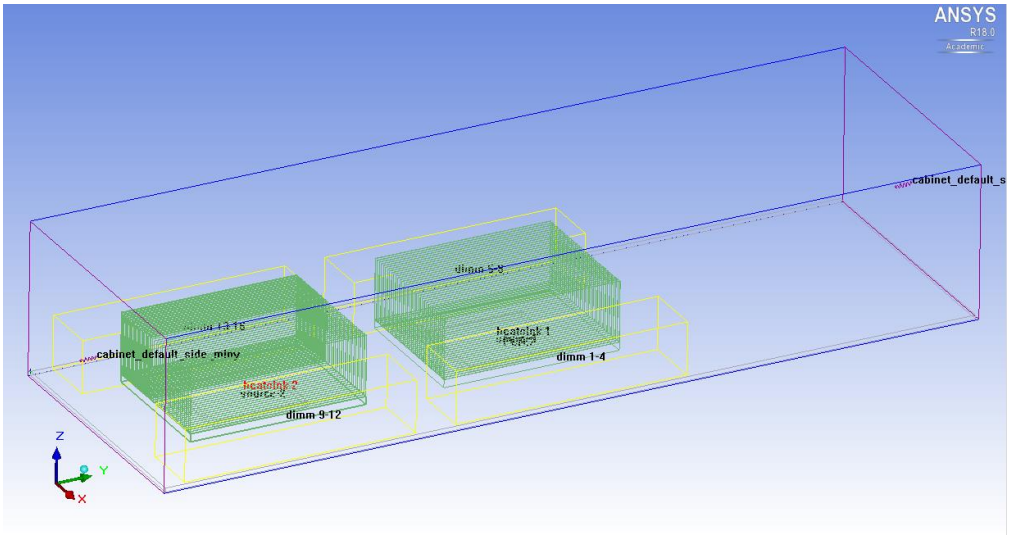

Figure 9-6 CFD model of a Baseline Oil Cooled Server

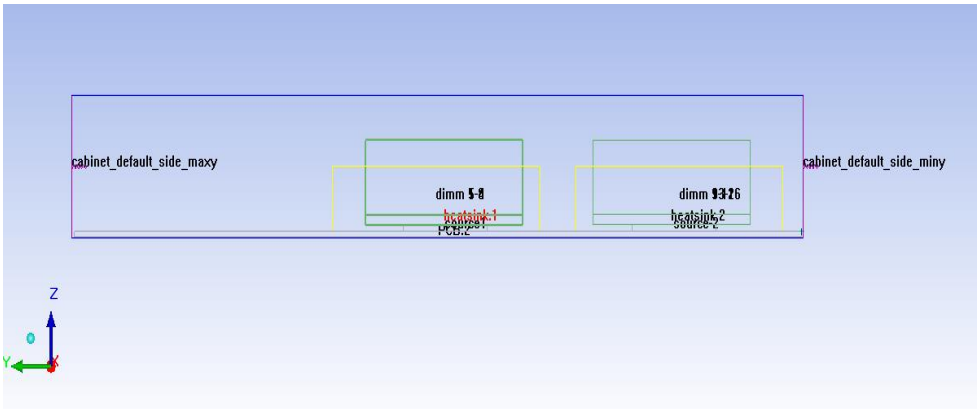

Figure 9-7 Orientation of serve in the Positive X-Direction

9.2.4 Area Calculation for Different Form Factors

The area for the different open rack unit servers has been calculated by using the following formula:

$$\text{Area} = \text{Length x Height} \quad (1)$$

The dimensions and the areas calculated for the different open rack unit servers have been tabulated as below:

Table 9-3 Area calculation

Open Rack Unit Server	Length (mm)	Width(mm)	Height(mm)	Area(m^2)
1 ORU	166.2	511	48	7977.6×10^{-6}
1.5 ORU	166.2	511	72	11966.4×10^{-6}
2 ORU	166.2	511	96	15955.2×10^{-6}

9.2.5 Volumetric Flow Rate Conversion

In this study we consider volumetric flow rate of 0.5 Litres Per Minute (LPM) to 2 LPM. These values in m^3/sec are tabulated as follows:

Table 9-4 Volumetric Flowrate conversion

LPM	$\mathbf{m^3/sec}$
0.5	8.33×10^{-6}
1	1.6667×10^{-5}
1.5	2.5×10^{-5}
2	3.333×10^{-5}
2.5	4.1667×10^{-5}

9.2.6 Velocity Calculation

The velocity of the fluid changes whenever the volumetric flow rate and cross-sectional area changes. So we need to change the velocity while running simulations for different flow rates. It can be calculated using the formula,

$$\text{Volume flow rate} = \text{Area x Velocity} \quad (2)$$

$$\text{Velocity} = \text{Volume flow rate}/\text{Area} \quad (3)$$

Table 9-5 Velocity Calculation

LPM	m^3/sec	1 Open Rack Unit	1.5 Open Rack Unit	2 Open Rack Unit
0.5	8.33×10^{-6}	0.0010442	0.00069639	0.00052209
1	1.6667×10^{-5}	0.0020896	0.0013928	0.0010448
1.5	2.5×10^{-5}	0.0031337	0.002089	0.00156689
2	3.333×10^{-5}	0.00417795	0.002785	0.0020889
2.5	4.1667×10^{-5}	0.005223	0.003482	0.0026115

9.3 Reynolds Number Calculations

For validation of the oil cooled server, some material properties must be specified. The material property of the server component will remain same as an air-cooled server, but fluid properties must be changed in place of air. There are different types of Dielectric Fluids, but in this study, White Mineral Oil and Synthetic Fluid EC100 are used. Flow condition is kept same as that of an actual experiment. Inlet oil temperature is taken as 30˚C, volume flow rate is kept constant of 1 LPM. 2 Open Rack Unit Server cross section in this case is considered as 511mm x 166.2mm x 96mm.

The formula below can calculate Hydraulic Diameter,

$$D = \frac{2\ b\ h}{(b + h)} \quad (4)$$

Where,

b= channel width = 511 mm

h= channel height = 96 mm

D = (2 x 511 x 96) / (511 +96)

= 161.6 mm

= 0.1616 m

9.3.1 Reynolds number calculation for White Mineral Oil

There are some physical properties of white mineral oil that should be considered for computational analysis.

Density – 851.515 Kg/m^3

Thermal conductivity – 0.13 W/m K

Specific heat – 1680 J/kg k

Thermal Diffusivity – 9.166E-8 m^2/s

Molecular Weight–150 Kg/ K Mol

Overall heat transfer co-efficient – 50-30 W/ $\mathrm{m}^2\ K$

At 30℃, the Dynamic Viscosity (μ) of White mineral oil is 0.01405 Kg/m s

The Kinematic Viscosity (v) is 1.65E-05 m^2/s

Reynolds number can be calculated using the below formula

$$Re = \frac{\mathrm{V\,D}}{\nu} \qquad (5)$$

Where Re is the Reynolds number, V is the Velocity, D is the Hydraulic Diameter, and v is the Kinematic Viscosity.

Substituting Hydraulic Diameter, Velocity and Kinematic Viscosity in eq 5,

Re= (0.0010448 x 0.1616) / (1.65E-05)

Re = 10.23

Prandtl number can be calculated using the below formula

P= $\frac{\mu\, C_P}{\lambda}$ = (0.01405 X 1670) / 0.13

P= 180.488

Table 9-6 Change in properties of White Mineral Oil due to Temperature

Temperature (℃)	Dynamic Viscosity (kg-m/s)	Kinematic Viscosity (m^2/s)	Reynold's Number	Prandtl Number
30	0.01405	1.65E-05	10.23	180.488
40	0.01046	1.23E-05	13.72	134.37
45	0..00909	1.07E-05	15.77	116.77
50	0.00794	9.35E-06	18.05	101.99

9.3.2 Reynolds number calculation for Synthetic Fluid

The properties that must be considered for the calculation of Reynold's number for synthetic fluid, EC 100 are as follows:

Density – 803.78 Kg/m^3

Thermal conductivity – 0.1378 W/m K

Specific heat – 2165.9 J/kg k

Molecular Weight–350 Kg/ K Mol

At 30℃, the Dynamic Viscosity (μ) of Synthetic Fluid is 0.01062 Kg/m s

The Kinematic Viscosity (ν) is 1.322E-05 m^2/s

$$Re = \frac{V\,D}{\nu}$$

Re = (0.0010448 x 0.1616) / 1.322E-05

Re = 12.77

Prandtl number can be calculated using the below formula,

$P = \frac{\mu\, C_P}{\lambda}$ = (0.01062 X 2165.9) / 0.13787

P= 166.837

Table 9-7 Change in properties of Synthetic Fluid due to Temperature

Temperature (℃)	Dynamic Viscosity (kg-m/s)	Kinematic Viscosity (m^2/s)	Density (kg/m^3)	Specific Heat (J/kg-K)	Thermal Conductivity (W/m-K)	Reynold's Number	Prandtl Number
30	0.01062	1.322E-05	803.78	2165.9	0.13789	12.77	166.837
40	0.00767	9.63E-06	796.98	2203.2	0.13730	17.53	123.077
45	0.00662	8.34E-06	793.58	2221.9	0.13702	20.24	107.349
50	0.00576	7.29E-06	790.18	2240.5	0.13673	23.16	94.385

Reynolds number is less than 2000 for both White Mineral Oil and Synthetic Fluid. So Laminar model is used to solve the naiver stoke equation. CFD results documented by Chinmay Bhatt are compared with the experimental results documented by Trevor Mc.Williams for Validation.

Table 9-8 Validation of an Oil Cooled CFD Model

Flow Rate (LPM)	Experimental Results	CFD Results	Error Percentage
0.3	70	71.23	1.72
0.4	68.74	68.86	0.174
0.5	67.43	66.87	-0.83

9.4 Form Factor Study

9.4.1 Definition of Form Factor

In Computers, the form factor is the size, configuration or physical arrangement of a computing device, a computer case or chassis or one of its internal components. When used to

refer to the size of a free-standing computer or other device, its close in meaning to footprint. Here, Form factor defines the height of the server. In the data center industry, U is considered as standard rack unit, but we are considering the open rack unit for our study. It has the value of 48mm.

9.4.2 Rack unit and Open Rack Unit

A rack unit is a unit of measure defined as 44.50mm. It is most frequently used as a measurement of the overall height of 19in or 23in rack frames, as well as the height of equipment that mounts in these frames, whereby the height of the frame or equipment is expressed as multiples of rack units. A typically full-size rack size is 42U high while equipment is typically 1U, 2U, 3U or 4U high.

Open rack is a mounting system designed by the Facebook's open compute project that has the same outside dimension as typical 19inch racks. It has 21inches out of the 24inches available for 87.5% space efficiency.

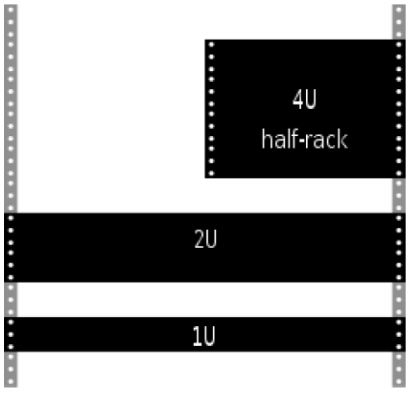

Figure 9-8 Rack Unit Comparison

9.4.3 Parametric Study of Form Factors

The server is basically designed for air cooling application and it has by default form factor as 2U. Ansys ICEPAK has the provision to change the parameters and solve the naiver stoke equations. Two major parameters have been considered are inlet oil temperature and oil

flow rate. Inlet oil temperature has been varied from 30℃ to 50℃. This range has been selected from the previous research experiment carried out on oil immersion cooling. Volume flow rate range for an incoming oil is kept from 0.5 lpm to 2.5 lpm. Maximum value of Reynold's number for this study is 656 obtained at the volume flow rate of an oil as 2.5 lpm. It can be concluded that even at maximum volume flow rate of 2.5 lpm Reynold's number does not exceed 2000 hence, laminar model is used for solution of parametric trails.

Similar procedure repeated for form factor 1.5U and 1U. The Cabinet height is changed according the value of form factor. The major purpose of the study is to get an insight to increase the existing rack density by reducing its form factor. This study is very useful to predict the behavior of cooling fluid at various form factor. Small improvement at server level cooling can be useful for a significant amount of savings at the facility level.

9.5 Thermal Shadowing

Thermal shadowing is the phenomenon in which temperature of a cooling medium increases by carrying heat from one power source and results in decreasing its heat carrying capacity due to a reduction in the temperature difference between the maximum junction temperature of successive heat sinks and incoming fluid. Thermal shadowing causes the localized increase in temperature of an object (heat sink and CPU) that stays in thermal shadow of the other object. Below figure shows the concept of Thermal Shadowing.

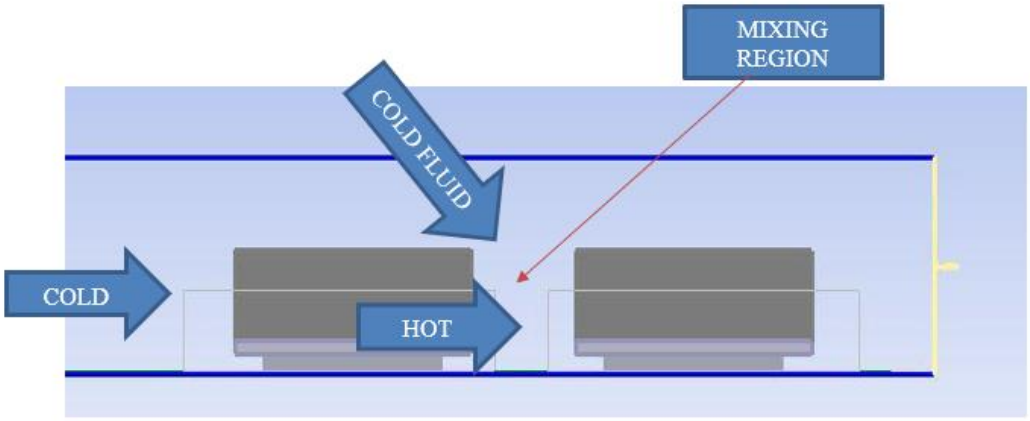

Figure 9-9 Thermal Shadowing Phenomenon

The cold fluid enters from one end of the server, some amount of fluid come across the first heat sink and carries the heat. This increases the temperature of the cold fluid. Some amount of fluid will bypass the first heat sink. The tip clearance and span wise spacing are the major factors of server design, which govern the flow bypass around heat sink. Tip clearance is the space between maximum heat sink height and the top of the server ceiling. The hot fluid that carries the heat from first heat sink mixes with the bypass cold fluid. The mixed fluid stream then enters to the second heat sink. Due to increased inlet temperature of fluid for second heat sink, reduces the temperature difference with downstream temperature and that also reduces heat transfer. Basically, it causes a localized increase of junction temperature of an object which stays in thermal shadow.

This phenomenon can be explained using energy balance equation

$$M_1h_1 + M_2h_2 = M_3h_3$$

Where,

M_1 = mass of cold fluid

h_1 = enthalpy of cold fluid

M_2 = mass of hot fluid

h_2 = enthalpy of hot fluid

M_3 = mass of mixed fluid

h_3 = enthalpy of mixed fluid

To find the temperature of mixed air that enters in the second het sink, enthalpy will be taken as product of heat capacity and temperature.

$$M_1CpT_1 + M_2CpT_2 = M_3CpT_3$$

$$T_3 = (M_1T_1 + M_2T_2) / M_3$$

The temperature after mixing of fluid stream is T_3. Temperature of mixed fluid stream T_3 is higher than the inlet fluid temperature ($T_3 > T_1$). In air cooled servers, to reduce the impact of thermal shadowing, ducting system has been designed so that it can direct the bypass flow towards the shadowed object and minimize the impact of thermal shadowing. In this study, to compare the impact of thermal shadowing, non-directed flow is considered. This research has been done to analyze the parameters like Maximum Junction Temperature, Thermal Resistance.

9.6 Optimization Of Heat Sinks

9.6.1 Types of Heat Sinks

Heat sinks are passive components those are used for heat transfer. The major three types of heat sinks are Parallel plate heat sink, pin fin heat sink and extruded cut plate fin heat sink. The baseline model with the parallel plate heat sink was used in this study.

Parallel Plate Heat Sink

Plate Fin Heat Sink

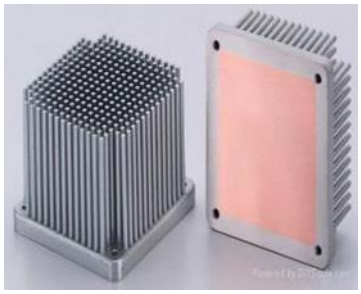

Pin Fin Heat sink

Figure 9-10 Types of Heat Sinks

Heat sinks are designed to increase the heat transfer area between heat producing component and the cooling medium. To increase the efficiency of heat sinks, heat spreaders are used between heat source and secondary heat exchanger. Heat spreader is the heat exchanger that transfers the heat with the more favorable surface area and geometry than the source. Heat spreader is made of very high thermal conductive material so that maximum heat can be transferred. Generally, copper or aluminum is used for heat spreader. Parallel Plate type heat spreaders are popular and readily available in the market. Heat sinks are also built from the materials having high thermal conductivity. Copper and aluminum alloys have favorable heat transfer characteristics, including good thermal conductivity and thermal performance. Hence they are most widely used materials for heat sink manufacturing. At present, research work is going on in customization of heat sinks. Nowadays, it is possible to develop the customized heat sinks depending upon your thermal performance and its applications. The performance of parallel plate heat sink has been studied and validated. So, this study includes thermal performance and optimization of Pin fin and extruded cut plate fin heat sinks for the server under study. The results of these Pin fin and Plate fin are then compared with the existing Parallel plate heat sink. To evaluate the thermal performance of the heat sinks, dimension less numbers like Reynold's number and Prandtl number are obtained. These two

numbers are driving parameters to decide the boundary condition and thermal performance of the heat sinks.

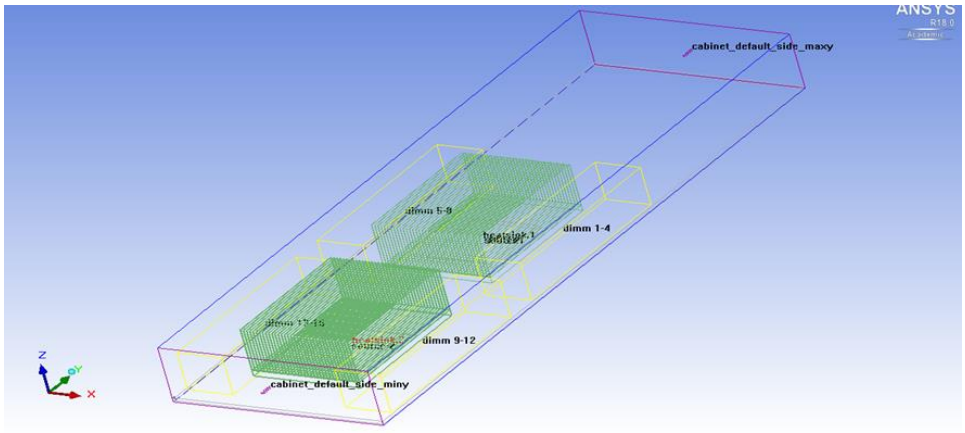

Figure 9-11 Baseline Parallel Plate Heat Sink Server

To evaluate the thermal performance, Ansys ICEPAK is used. CFD model has been developed for plate and pin fin and then using multiparameter optimization, geometry of the heat sinks has been optimized. In this study, server form factor has been taken as 1U. The flowrate of an oil is kept at 1 lpm and inlet oil temperature is taken as 30℃ and mass fix mass flowrate technique is applied.

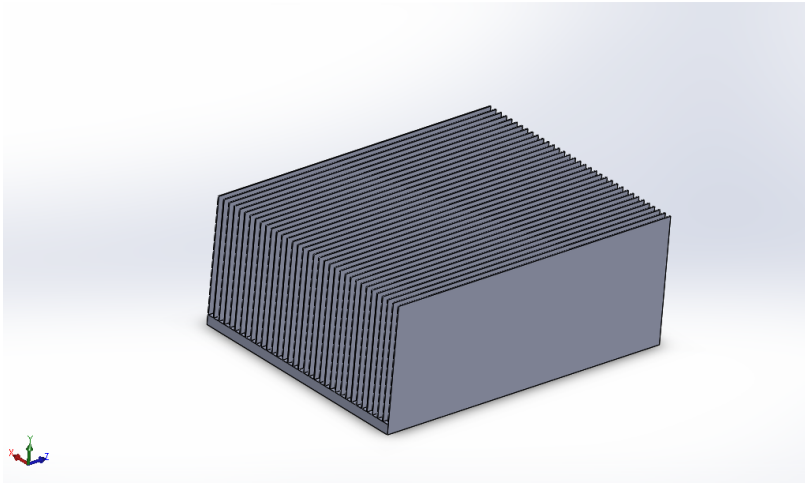

Figure 9-12 CAD model of existing Parallel Plate Heat Sink

Table 9-9 Specifications of existing parallel plate heat sink

Thickness	0.3 mm
Height	41 mm
Length	110 mm
Number of fins	35

Volume of this heatsink can be calculated using the formula,

Volume = Thickness x Height x Length

Volume = 0.3 x 41 x 110 = 1353 mm^3

For 35 fins,

Volume = 35 x 1353

= 47355 mm^3

9.6.2 Modification of Baseline Server

To develop the CFD model of the server having plate fin and pin fin heat sinks respectively, the base line server design needs to be modified. In this optimization study, for all the simulations, we consider 1 Open Rack Unit Server at 30℃ and the Power of the CPU is considered as 65W. The existing parallel plate heat sink has 35 fins which is complex. So, the existing parallel plate heat sink is modified, and the Fin count is reduced to 15. Parametric study was conducted on this optimized model to validate the results with existing baseline server model.

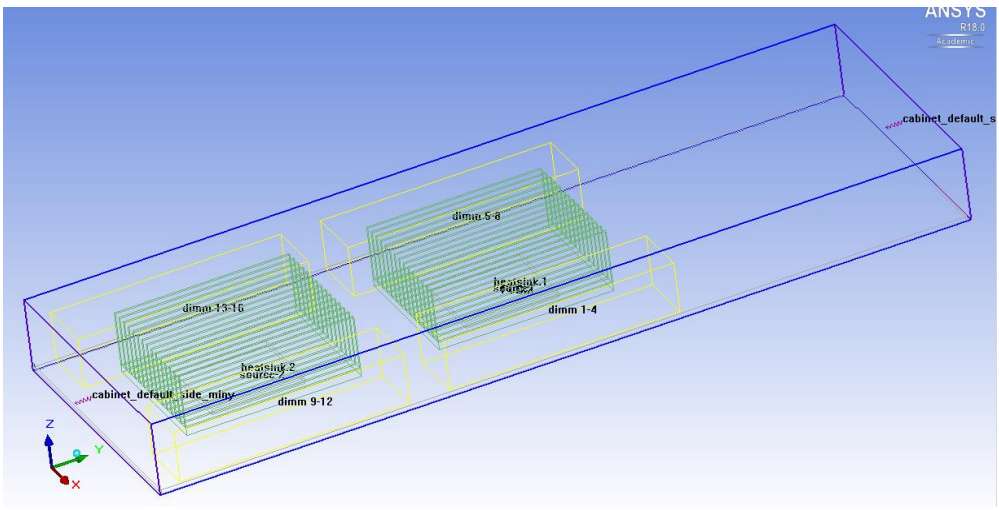

Figure 9-13 Optimized Parallel Plate Heat Sink Server

Similarly, the parallel plate heat sink is replaced with cut plate fins and pin fins. For cut plate fins, fin count is kept constant as 42 and the parametric study is conducted by varying the plate height and plate thickness. For pin fin heat sink, parametric study is conducted by varying pin radius and pin height by keeping the number of fins constant as 25. The same boundary conditions are used for this study.

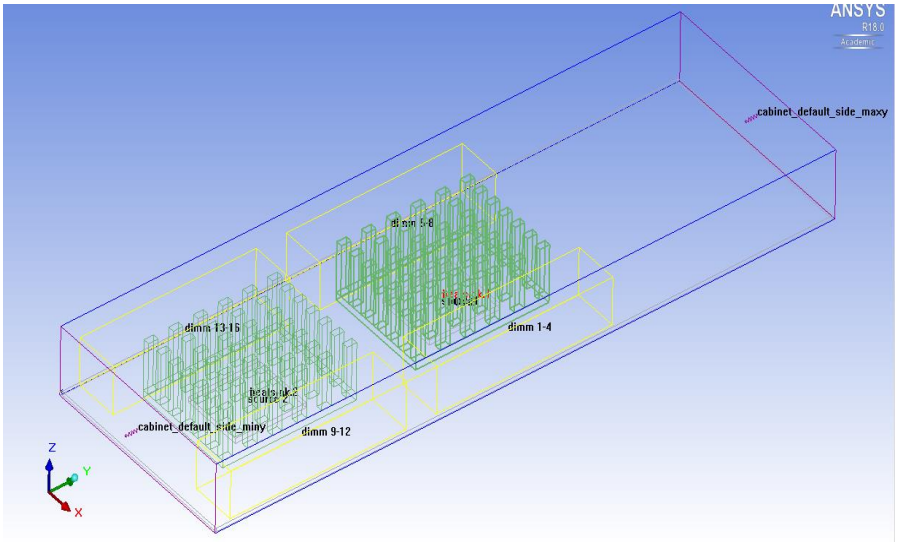

Figure 9-14 Extruded Cut Plate Fins Heat Sink

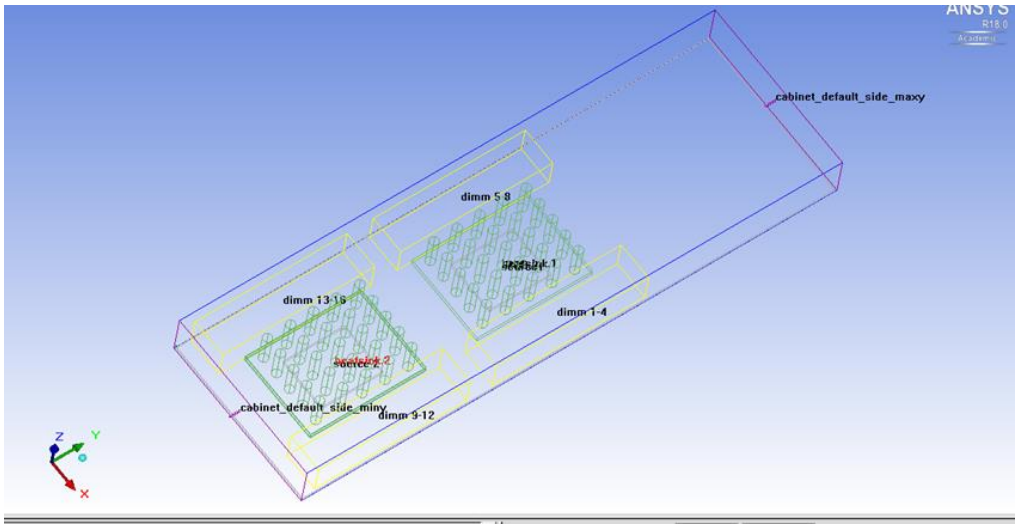

Figure 9-15 Pin fin Heat Sinks

The grid independent study has been carried out for accuracy of the result for optimization.

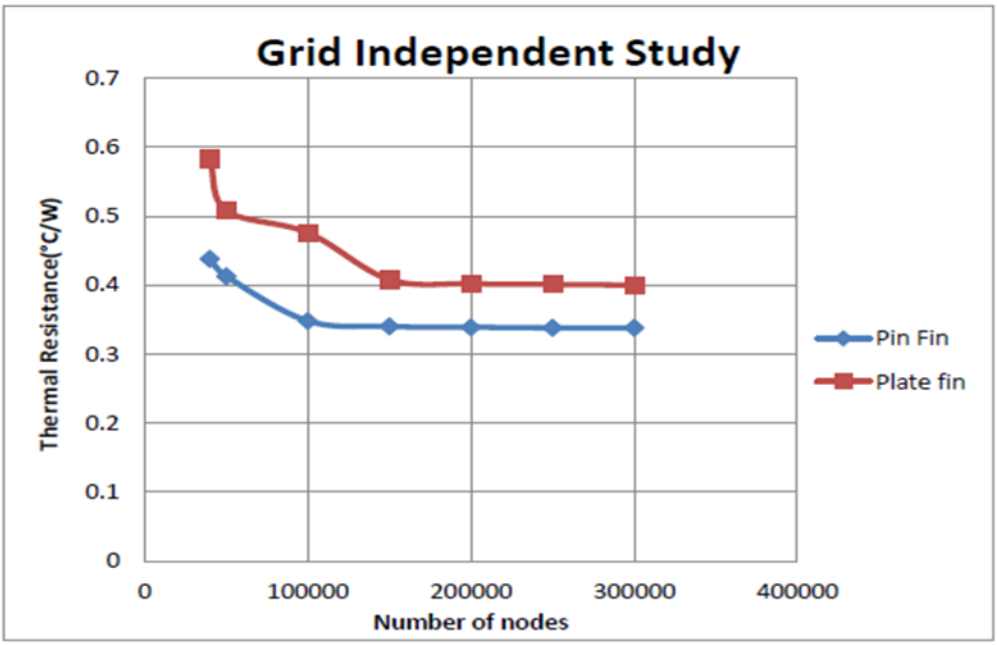

Figure 9-16 Grid independent study for plate fin and pin fin heat sink

Thermal resistance is the driving parameter for the thermal performance of the heat sink. To assure the accuracy of the results, grid independent study is carried out and from Figure 16, it can be said that for both plate fin and pin fin heat sinks, thermal resistance remains constant once the total number of nodes reaches to 150000. Total number of the study for the optimization is taken between 150000 to 250000. The inlet oil flow rate is kept as 1 lpm and temperature as 30℃.

9.7 Results And Conclusions

9.7.1 Form Factor study of 2U server

A series of simulations has been performed by changing the properties depending on the temperature and velocities when height of the server is changed. Form Factor study of Facebook's third generation open compute server includes comparison of thermal resistance and maximum junction temperature of 2U,1.5U and 1U for low velocity oil cooled severs. This study shows the change in trend of thermal performance the server with variation in inlet boundary condition. Purpose of this study is to analyse the change in maximum junction temperature and thermal resistance when form factor of the server is reduced. The simulation run for the 2 open rack unit server using mineral oil can be seen in the following figure,

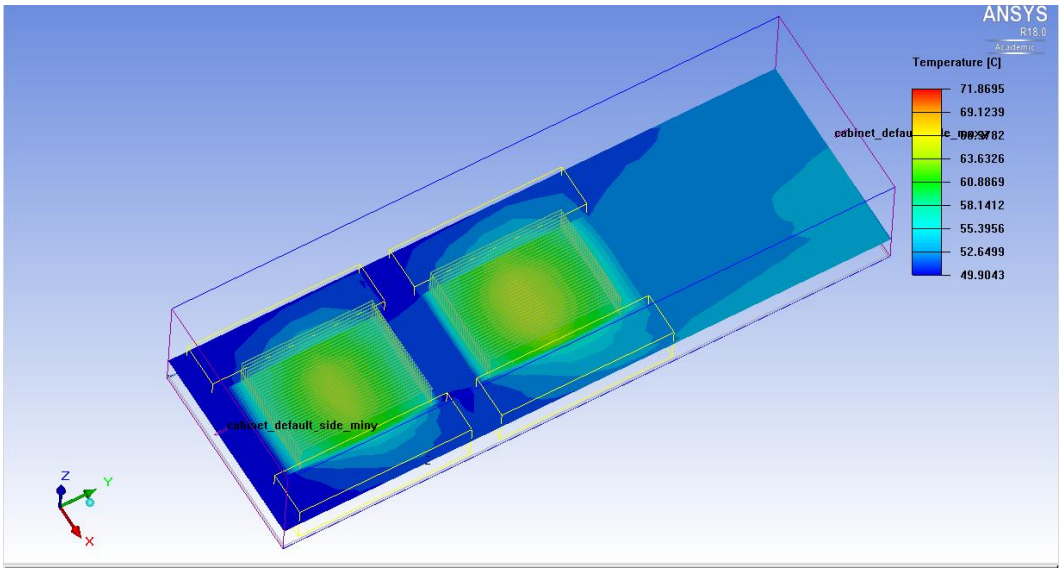

Figure 9-17 Open Rack Unit Server with mineral oil as cooling fluid

The data obtained through the simulations has been tabulated for white mineral oil and EC100. A comparison of the thermal efficiency has been done between white mineral oil and synthetic fluid. The thermal properties are changed depending on the fluid used and the inlet conditions.

9.7.2 Comparison of Mineral oil and Synthetic Fluid For 1 Open Rack unit server

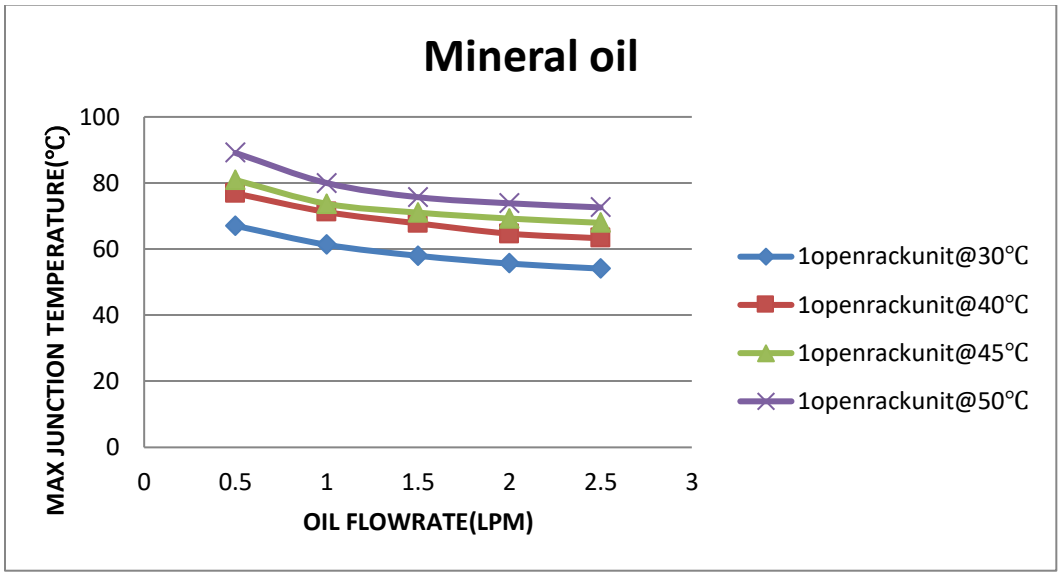

Figure 9-18 Max Junction Temp Vs Oil Flow rate at source 2

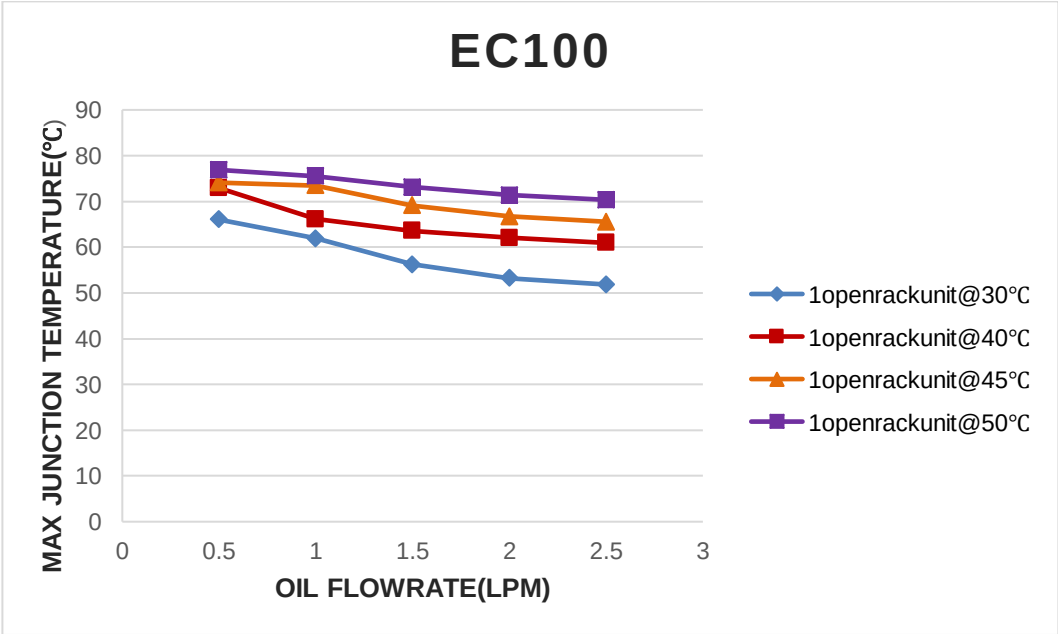

Figure 9-19 Max Junction Temp Vs Oil Flow rate at source 2

We can see from the both the graphs that the temperatures for the source 2 is less when synthetic fluid is used as cooling liquid rather than the mineral oil

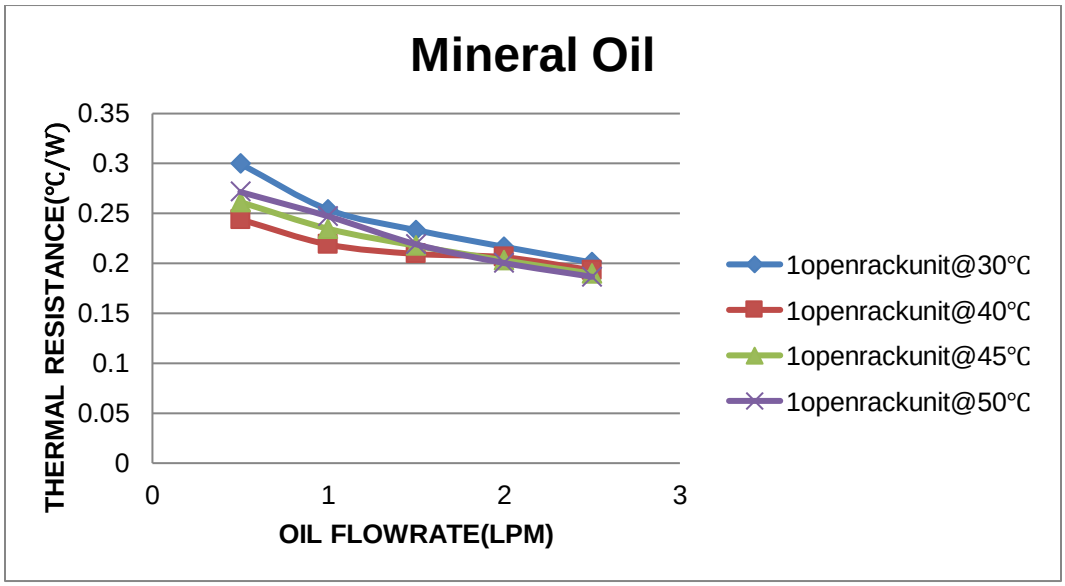

Figure 9-20 Thermal Resistance Vs Oil Flow rate at source 2

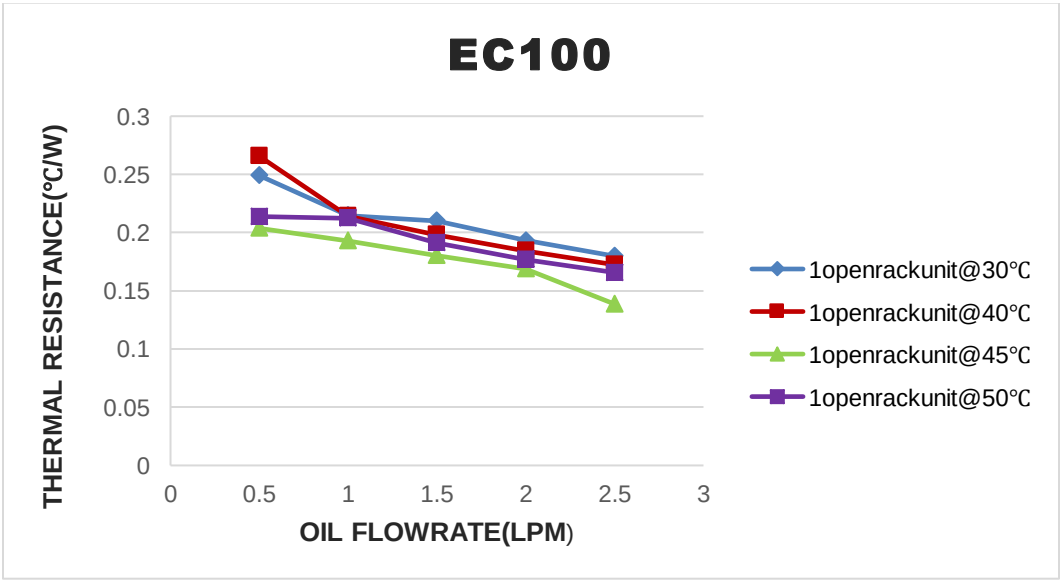

Figure 9-21 Thermal Resistance Vs Oil Flow rate at source 2

Here also we can see that there is an noticeable change in the values of thermal resistance. There is an enhancement in the thermal efficiency when synthetic fluid is used as the cooling liquid.

9.7.3 Comparison of Mineral oil and Synthetic Fluid for 1.5 Open Rack unit server

Similarly, the simulations has been performed for the 1.5 open rack unit server by changing the inlet conditions and properties of the fluids.

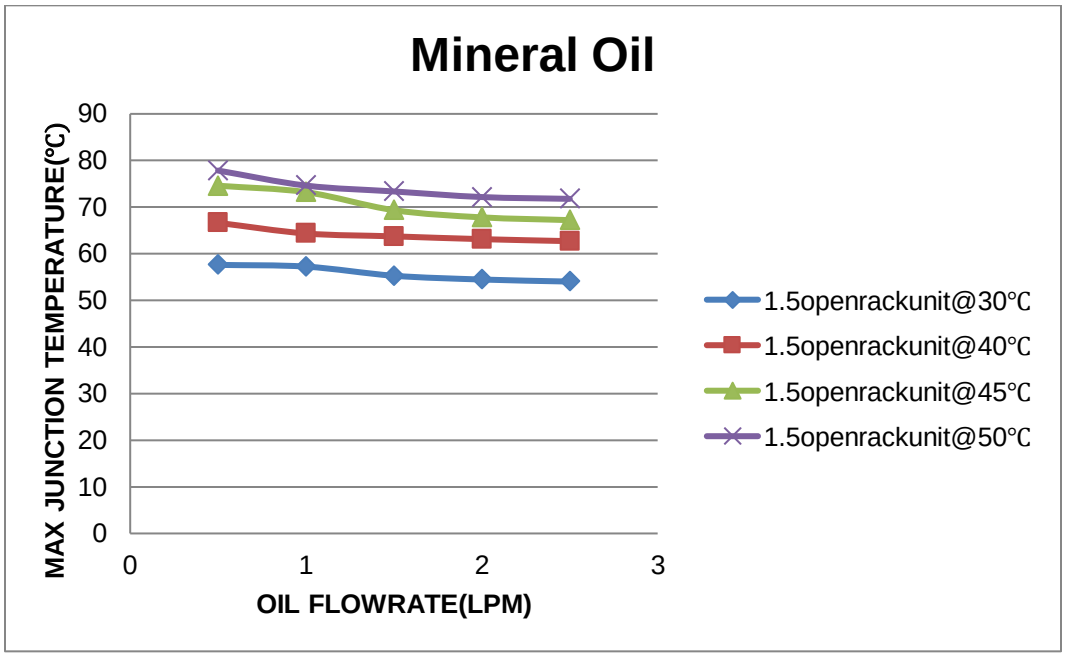

Figure 9-22 Max Junction Temp Vs Oil Flow rate at source 2

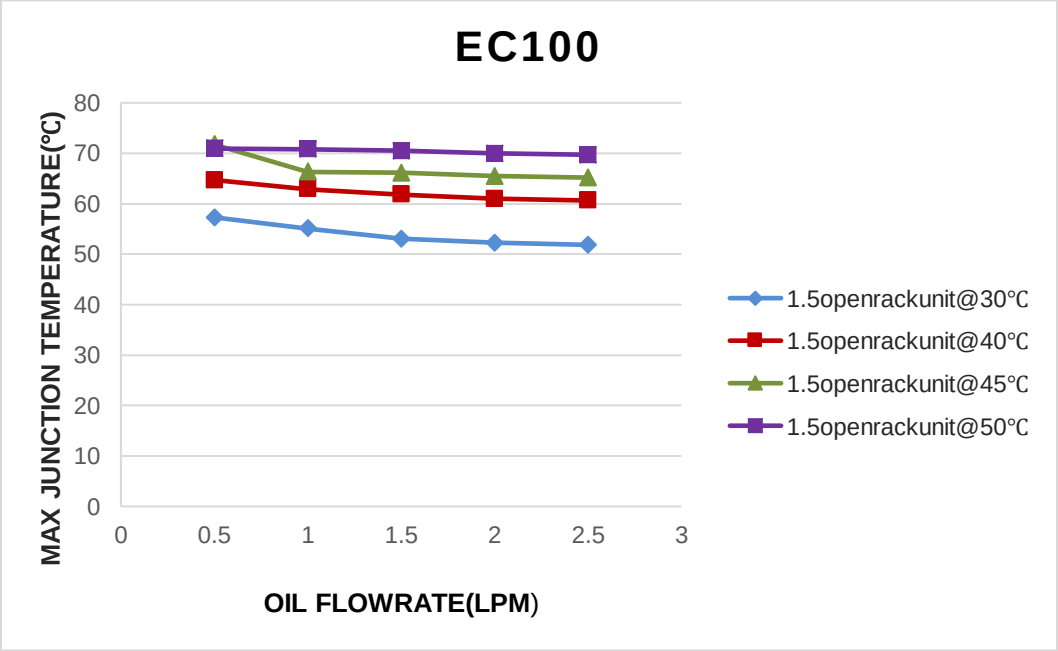

Figure 9-23 Max Junction Temp Vs Oil Flow rate at source 2

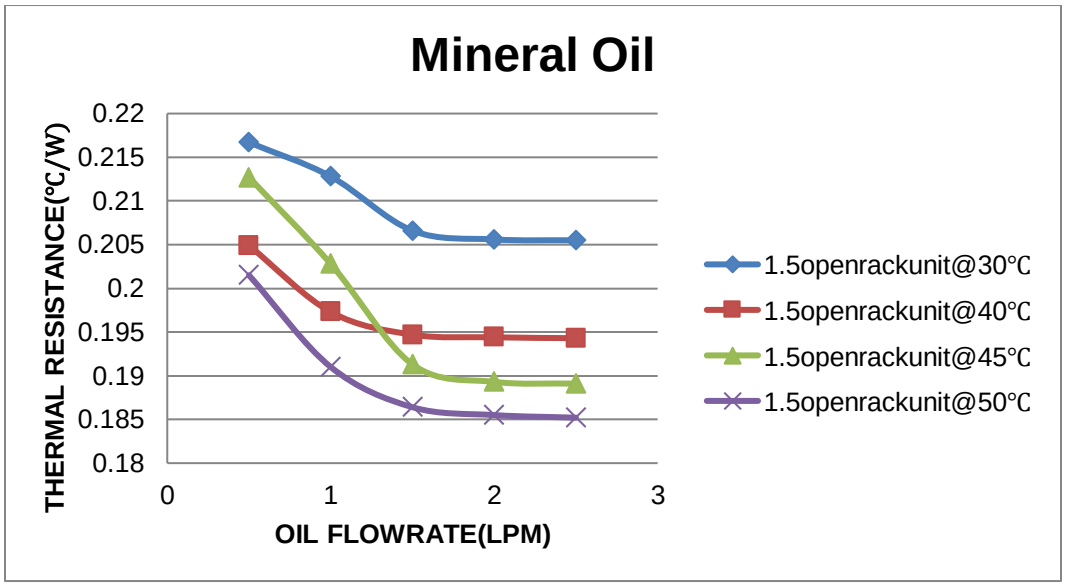

Figure 9-24 Thermal Resistance Vs Oil Flow rate at source 2

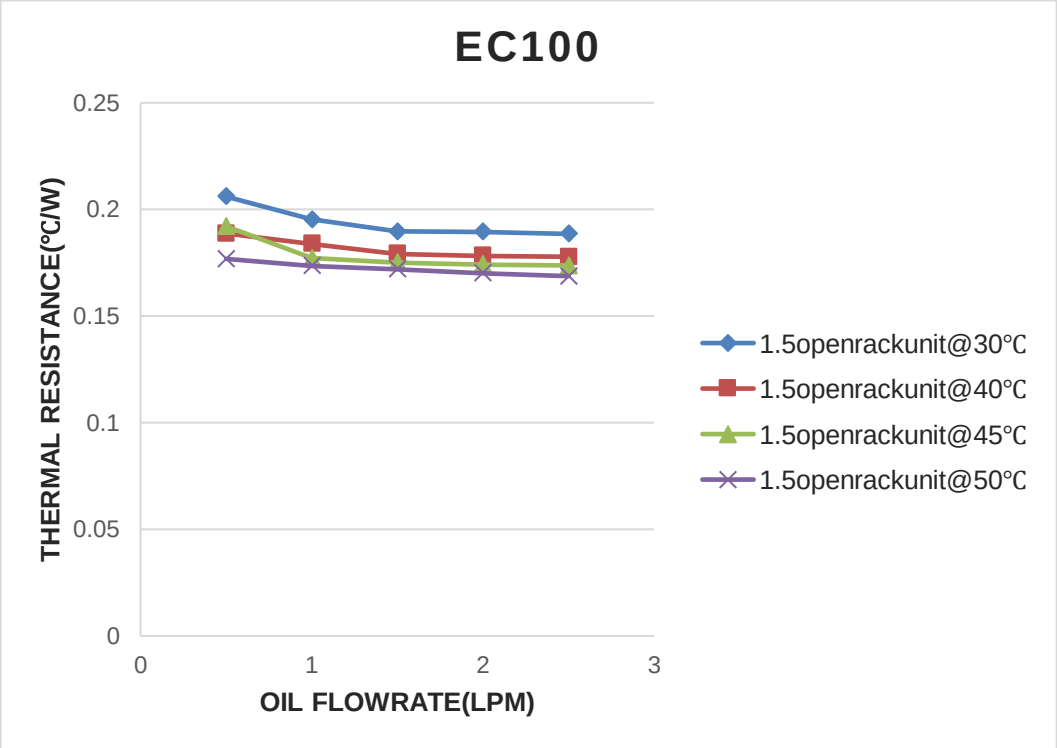

Figure 9-25 Thermal Resistance Vs Oil Flow rate at source 2

For the 1.5 Open rack unit server also, we can see that there is an decrease in the maximum junction temperature and thermal resistance values using the synthetic fluid.

9.7.4 Comparison of Mineral oil and Synthetic Fluid for 2 Open Rack unit server

The data obtained from the simulations is used to tabulate and represented in the graphs for easy understanding.

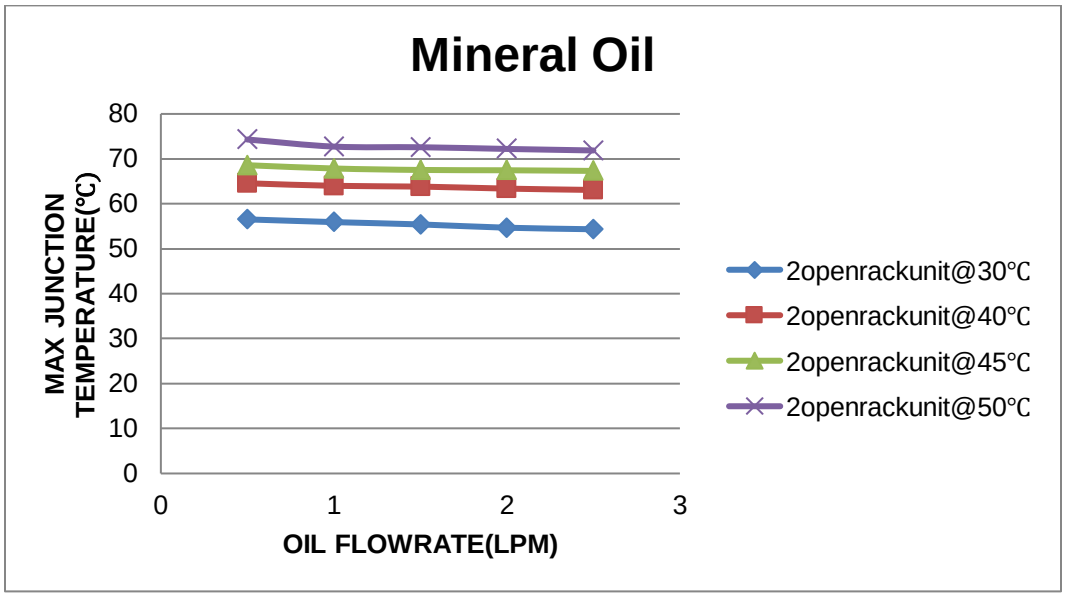

Figure 9-26 Max Junction Temp Vs Oil Flow rate at source2

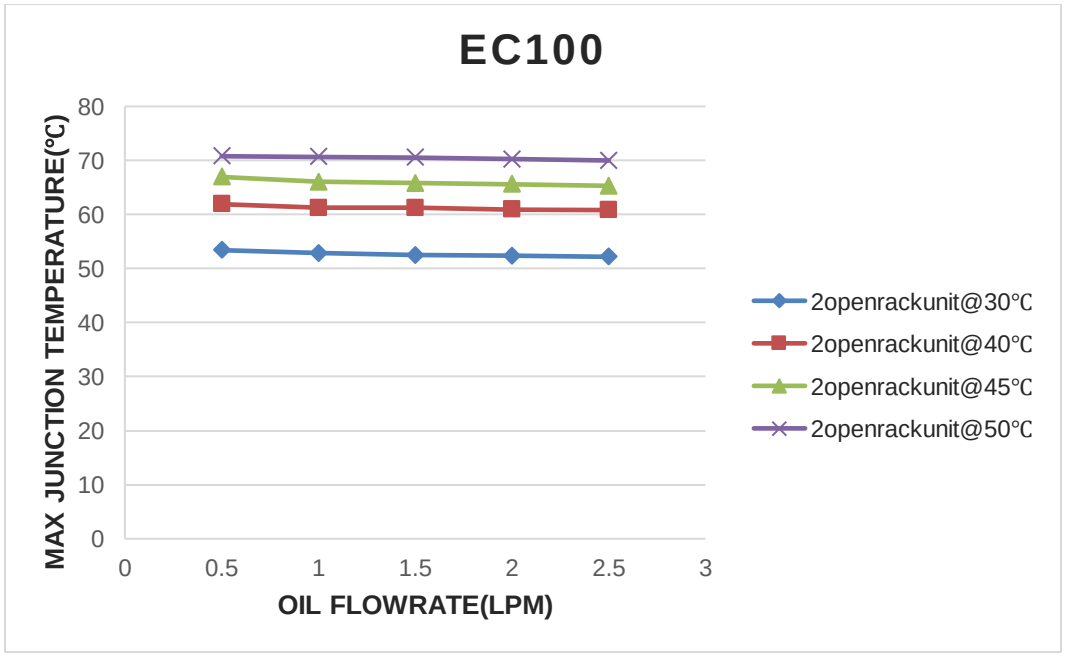

Figure 9-27 Max Junction Temp Vs Oil Flow rate at source2

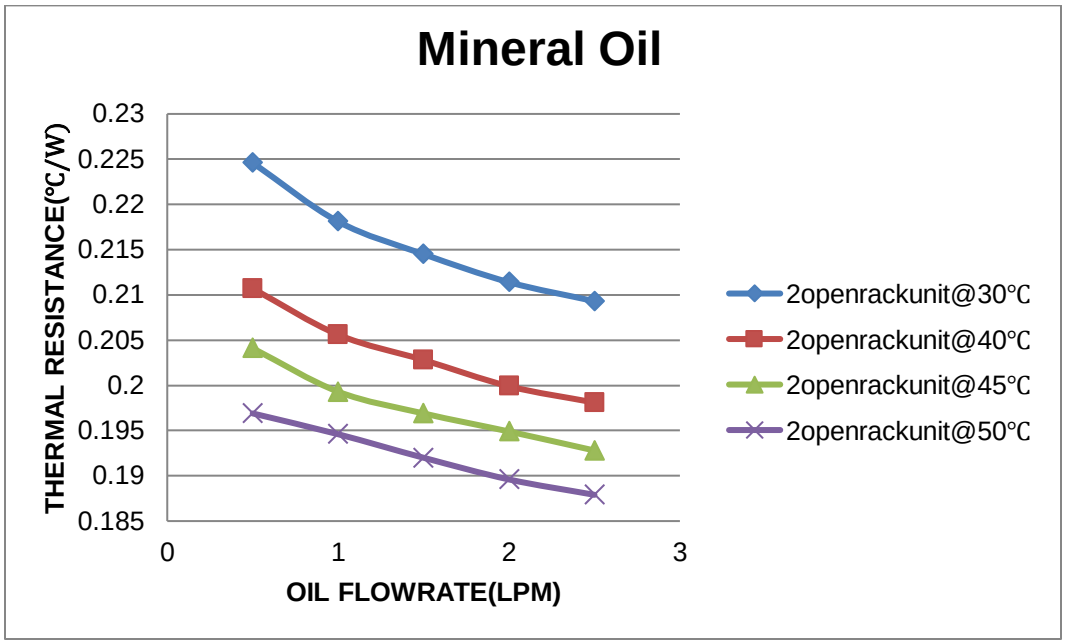

Figure 9-28 Thermal Resistance Vs Oil flow rate at source2

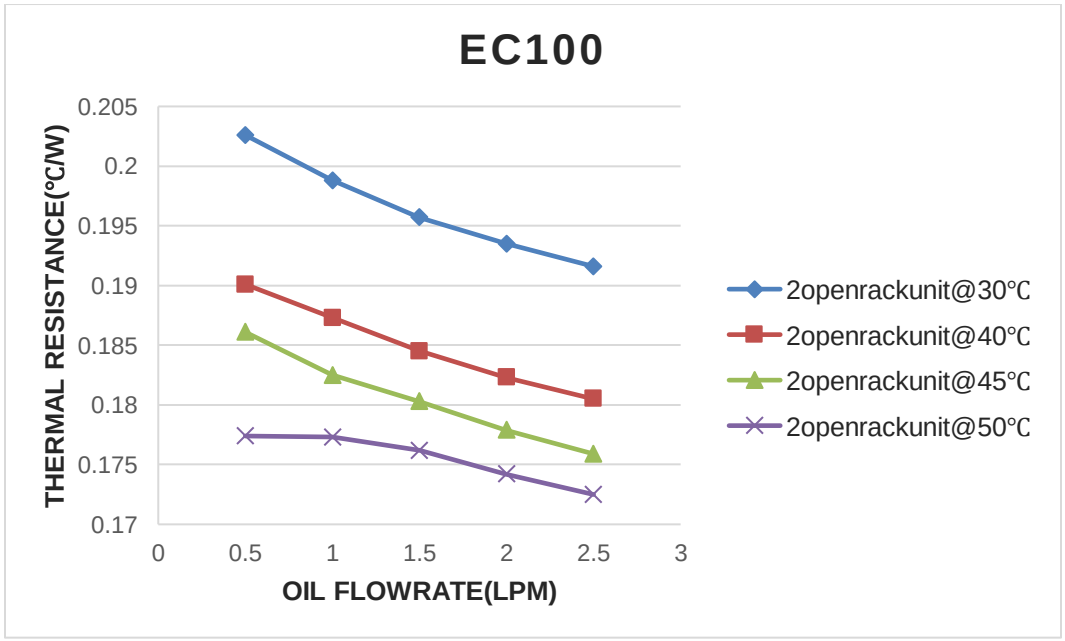

Figure 9-29 Thermal Resistance Vs Oil flow rate at source2

As the size of the server is high and also the inlet temperatures, we can see a lot of difference between the maximum junction temperature and thermal resistance values.

9.7.5 Best Result

Of all the simulations run on the server for different inlet temperatures, we have obtained the best results for 1.5 Open rack unit server @40℃ and a flowrate of 1LPM using synthetic fluid(EC100). It is advisable to keep the oil flow rate in the range of 1 to 2.5 lpm for effective cooling of servers especially with 1.5 Open rack unit server form factor.

Table 9-10 For Source 1 @40℃

1.5openrackunit@40℃	
Temperature	Thermal resistance
60.68	0.2256
60.23	0.2086
59.7	0.199
59.6	0.1906
59.54	0.1875

Table 9-11 For Source 2@40℃

1.5openrackunit@40℃	
Temperature	Thermal resistance
64.69	0.1887
62.9	0.1838
61.84	0.1792
60.94	0.1783
60.63	0.1778

9.7.6 Impact of Thermal Shadowing in Air and Oil Cooled Servers

9.7.6.1 Thermal Shadowing in Air Cooled Server

Inlet temperature is considered as 25℃ and Flow rate as 1LPM. These results are documented by Divya Mani. These are used for our validation with an oil cooled server.

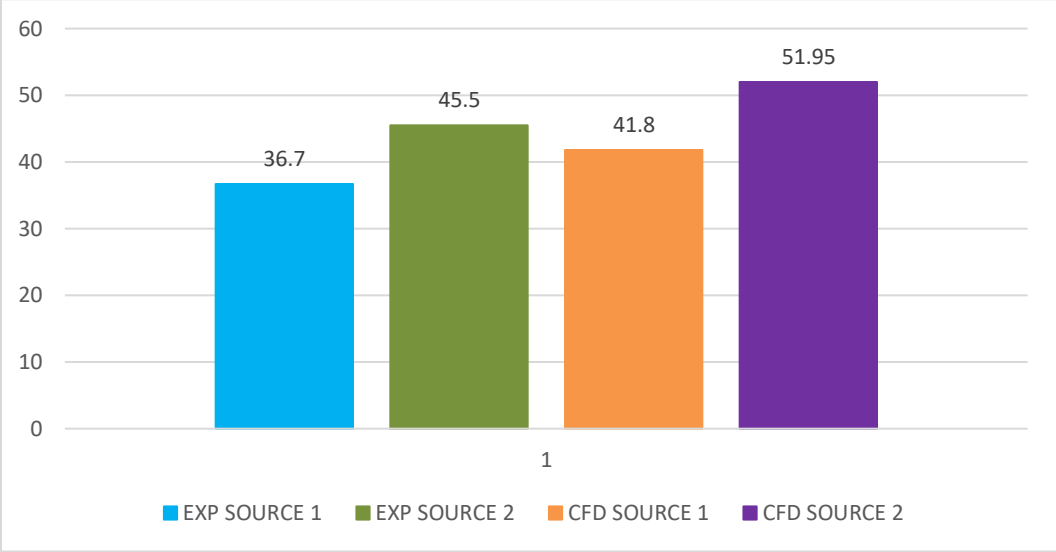

Figure 9-30 Experimental and CFD results of an Air-Cooled Server

From the above figure 30, it can be clearly seen that for experiment, the temperature of source 1 is 36.7℃ and the temperature of source 2 is 45.5℃. The temperature difference between source 1 and source 2 is 8.8℃. If we consider CFD results, the temperature of source 1 is 41.8℃ and the temperature of source 2 is 51.95℃. The temperature difference between source 1 and source 2 is 10.15℃.

9.7.6.2 Impact of Thermal Shadowing in Oil Cooled Server

9.7.6.2.1 Thermal Shadowing in 2 Open Rack Unit Server using White Mineral Oil

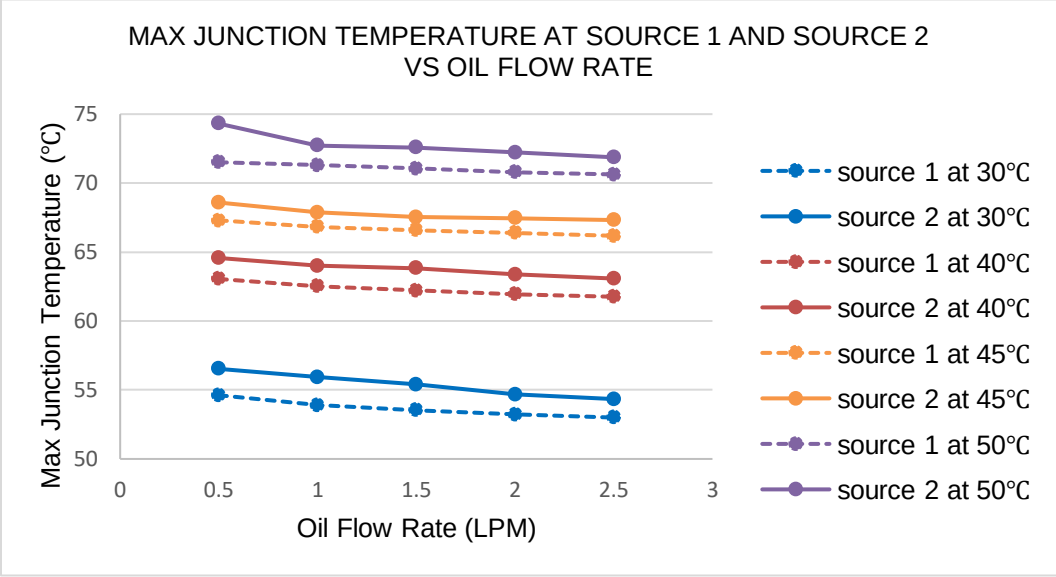

Figure 9-31 Maximum Junction Temperature at source 1 and source 2 vs Oil flow rate for 2 Open Rack Unit Server using White Mineral Oil

Table 9-12 Temperature difference between source 1 and source 2 for 2 Open Rack Unit Server at different temperatures for 1LPM using White Mineral Oil

	Temperature at Source 1 (℃)	Temperature at Source 2 (℃)	Temperature Difference (℃)
At 30℃	54.62	56.53	1.91
At 40℃	63.05	64.57	1.52
At 45℃	67.3	68.59	1.29
At 50℃	71.51	74.31	2.8

It is clear from the above Table 12 that the temperature difference between source 1 and source 2 is less than 3℃. Whereas the temperature difference in an air-cooled server is 10.15℃. So, the impact of thermal shadowing in an Oil Cooled Server using White Mineral Oil can be neglected.

9.7.6.2.2 Thermal Shadowing in 2 Open Rack Unit Server using Synthetic Fluid

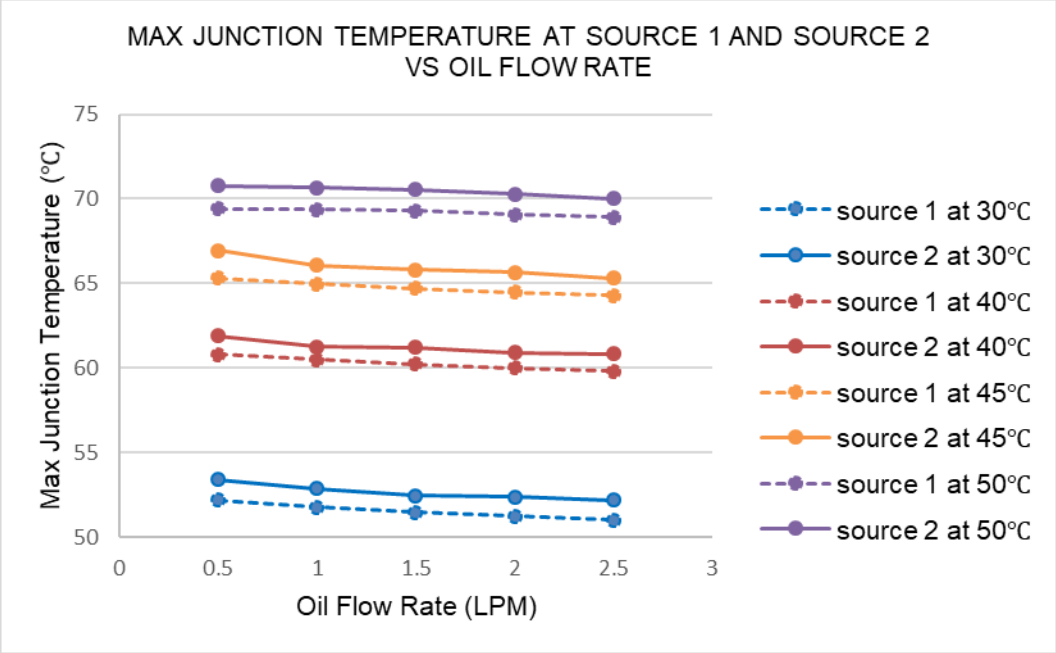

Figure 9-32 Maximum Junction Temperature at source 1 and source 2 vs Oil flow rate for 2 Open Rack Unit Server using Synthetic Fluid

Table 9-13 Temperature difference between source 1 and source 2 for 2 Open Rack Unit Server for 1LPM at different temperatures using Synthetic Fluids

	Temperature at Source 1 (℃)	Temperature at Source 2 (℃)	Temperature Difference (℃)
At 30℃	52.18	53.4	1.22
At 40℃	60.78	61.91	1.13
At 45℃	65.32	66.95	1.63
At 50℃	69.41	70.79	1.38

It is clear from the above Table13 that the temperature difference between source1 and source2 is less than 2℃. Whereas the temperature difference in an air-cooled server is 10.15℃.

So, the impact of thermal shadowing in an Oil Cooled Server using Synthetic Fluid can be neglected.

9.7.6.2.3 Thermal Shadowing in 1.5 Open Rack Unit Server using White Mineral Oil

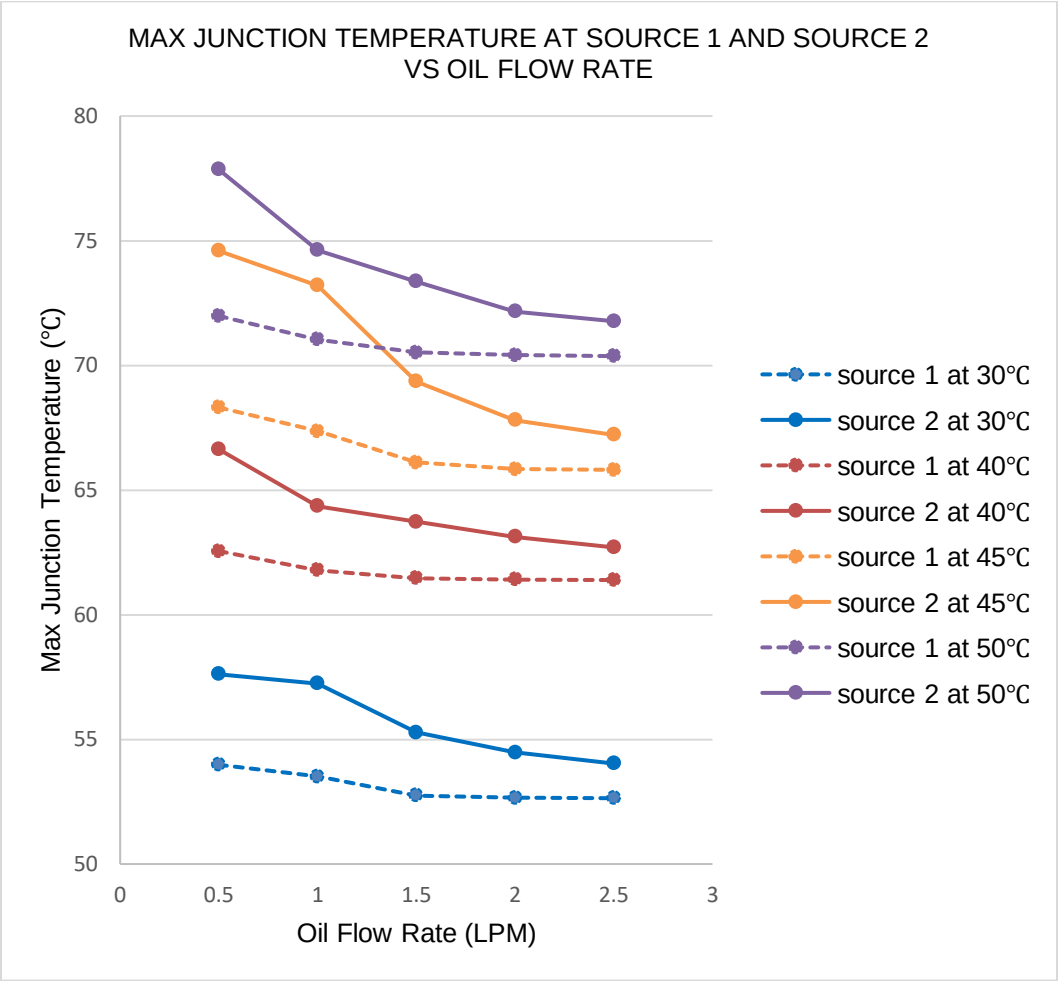

Figure 9-33 Maximum Junction Temperature at source 1 and source 2 vs Oil flow rate for 1.5 Open Rack Unit Server using White Mineral Oil

Table 9-14 Temperature difference between source 1 and source 2 for 1.5 Open Rack Unit Server for 1LPM at different temperatures using White Mineral Oil

	Temperature at Source 1 (℃)	Temperature at Source 2 (℃)	Temperature Difference (℃)
At 30℃	53.98	57.61	3.63
At 40℃	62.55	66.63	4.08
At 45℃	68.31	74.59	6.28
At 50℃	71.98	77.85	5.87

It is clear from the above Table 14 that the temperature difference between source 1 and source 2 is less than 7℃. Whereas the temperature difference in an air-cooled server is 10.15℃. So, the impact of thermal shadowing in an Oil Cooled Server using White Mineral Oil can be neglected.

9.7.6.2.4 Thermal Shadowing in 1.5 Open Rack Unit Server using Synthetic Fluid

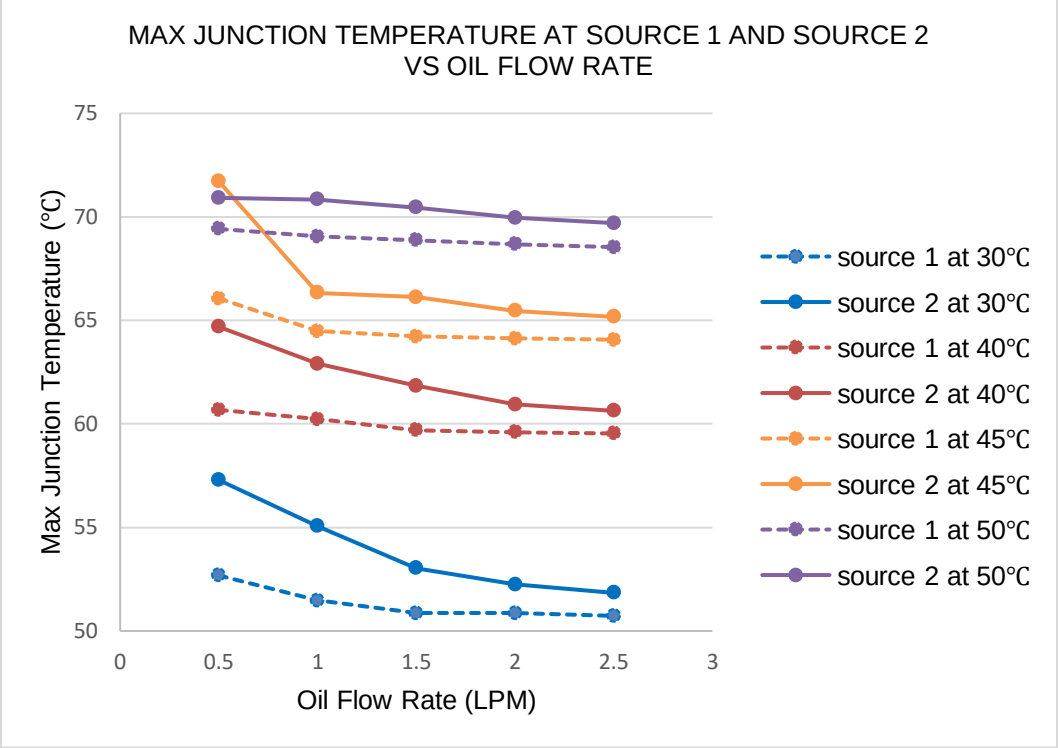

Figure 9-34 Maximum Junction Temperature at source 1 and source 2 vs Oil flow rate for 1.5 Open Rack Unit Server using Synthetic Fluid

Table 9-15 Temperature difference between source 1 and source 2 for 1.5 Open Rack Unit Server for 1LPM at different temperatures using Synthetic Fluid

	Temperature at Source 1 (℃)	Temperature at Source 2 (℃)	Temperature Difference (℃)
At 30℃	52.68	57.29	4.61
At 40℃	60.68	64.69	4.01
At 45℃	66.06	71.71	5.65
At 50℃	69.42	70.92	1.5

It is clear from the above Table 15 that the temperature difference between source 1 and source 2 is less than 6℃. Whereas the temperature difference in an air-cooled server is 10.15℃. So, the impact of thermal shadowing in an Oil Cooled Server using Synthetic Fluid can be neglected.

9.7.6.2.5 Thermal Shadowing in 1 Open Rack Unit Server using White Mineral Oil

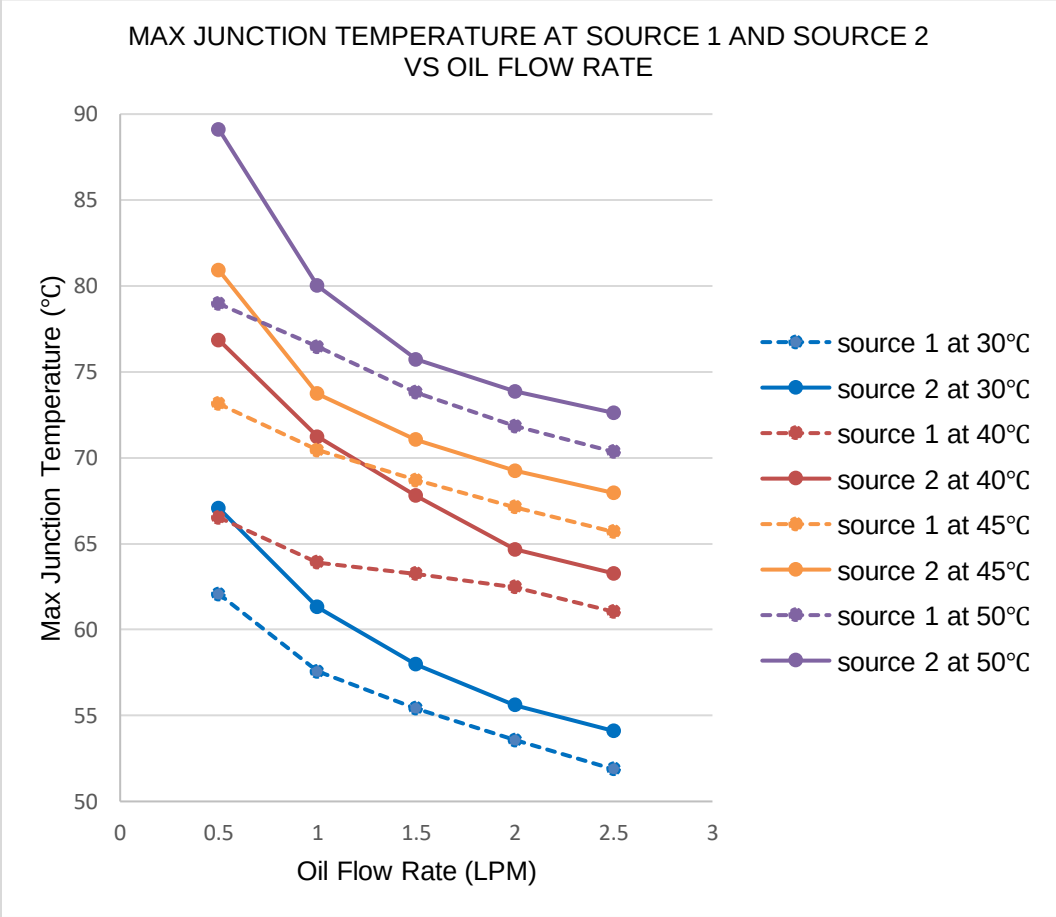

Figure 9-35 Maximum Junction Temperature at source 1 and source 2 vs Oil flow rate for 1 Open Rack Unit Server using White Mineral Oil

Table 9-16 Temperature difference between source 1 and source 2 for 1 Open Rack Unit Server for 1LPM at different temperatures using White Mineral Oil

	Temperature at Source 1 (℃)	Temperature at Source 2 (℃)	Temperature Difference (℃)
At 30℃	62.07	67.06	4.99
At 40℃	66.52	76.85	10.33
At 45℃	73.13	80.91	7.78
At 50℃	78.96	89.11	10.15

It is clear from the above Table 16 that the temperature difference between source 1 and source 2 is less than 10.3℃. Whereas the temperature difference in an air-cooled server is 10.15℃. So, the impact of thermal shadowing in an Oil Cooled Server using White Mineral Oil can be neglected as it is similar to that of an air-cooled server having directed flow using ducting system.

9.7.6.2.6 Thermal Shadowing in 1 Open Rack Unit Server using Synthetic Fluid

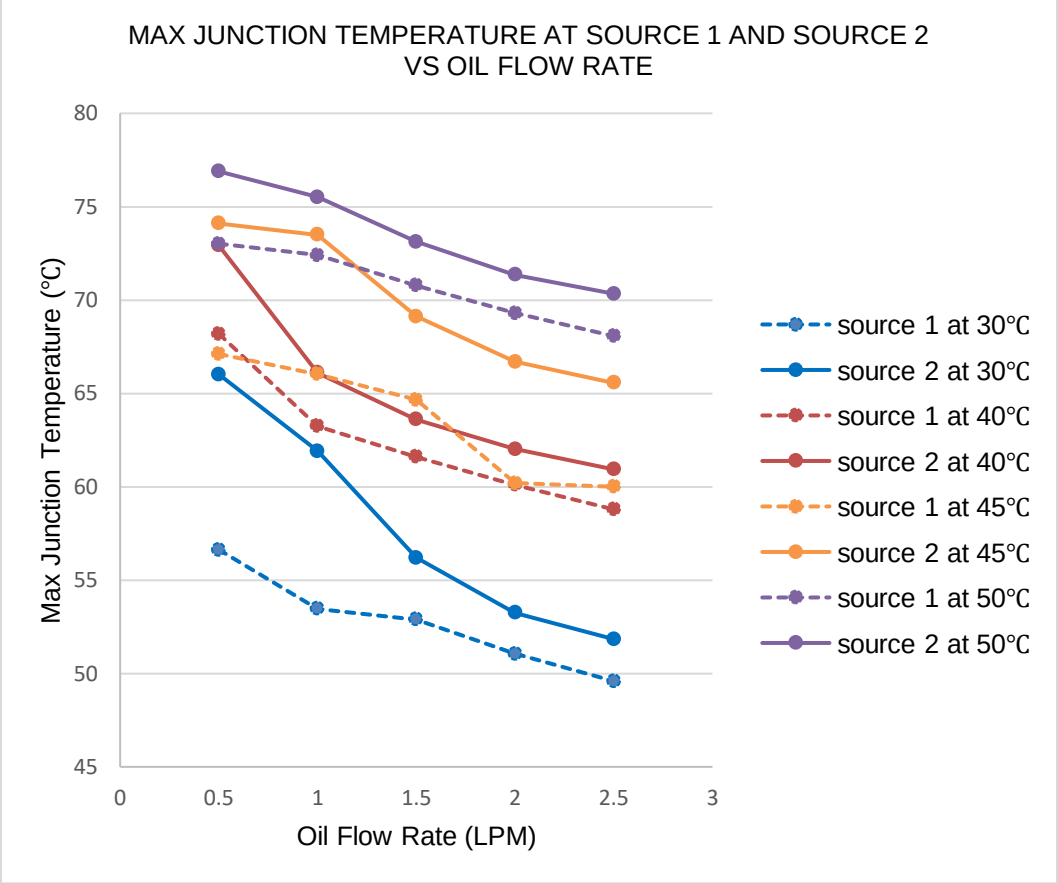

Figure 9-36 Maximum Junction Temperature at source 1 and source 2 vs Oil flow rate for 1 Open Rack Unit Server using Synthetic Fluid

Table 9-17 Temperature difference between source 1 and source 2 for 1 Open Rack Unit Server for 1LPM at different temperatures using Synthetic Fluid

	Temperature at Source 1 (℃)	Temperature at Source 2 (℃)	Temperature Difference (℃)
At 30℃	56.63	66.02	9.39
At 40℃	68.19	72.92	4.73
At 45℃	67.11	74.1	6.99
At 50℃	73.02	76.89	3.87

It is clear from the above Table 17 that the temperature difference between source 1 and source 2 is less than 9.39℃. Whereas the temperature difference in an air-cooled server is 10.15℃. So, the impact of thermal shadowing in an Oil Cooled Server using Synthetic fluid can be neglected as it is like that of an air-cooled server having directed flow using ducting system.

9.7.6.3 Comparison of Impact of Thermal Shadowing in 1 Open Rack Unit, 1.5 Open Rack Unit and 2 Open Rack Unit Servers at 30℃ using White Mineral Oil and Synthetic Fluid

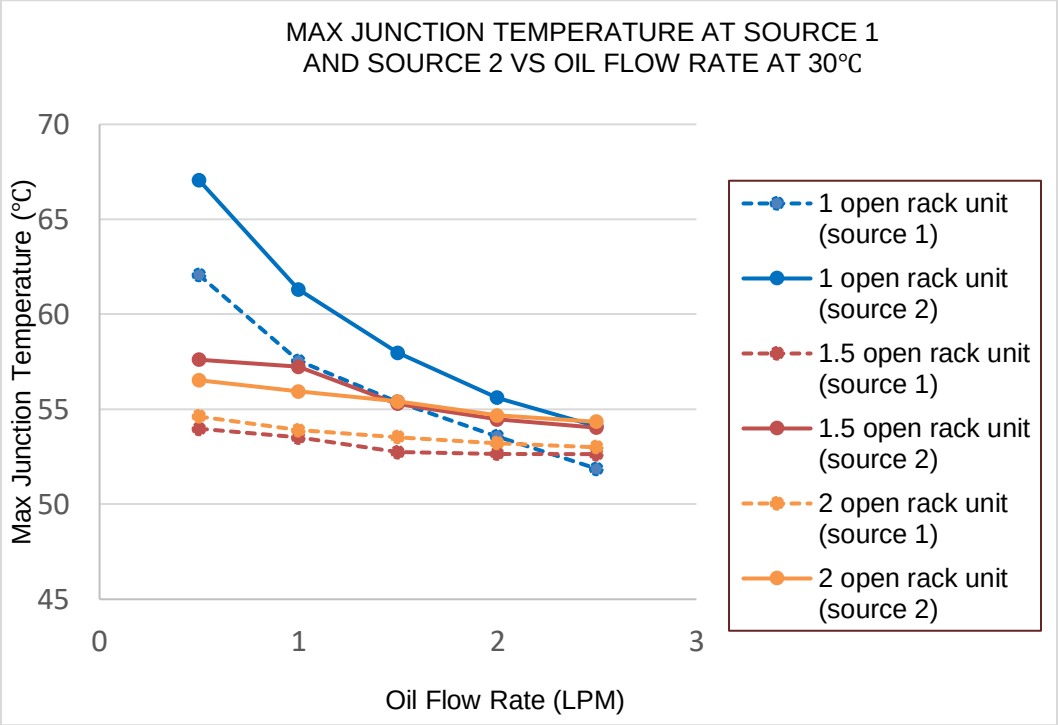

Figure 9-37 Maximum Junction Temperature at source 1 and source 2 vs Oil flow rate for different Open rack unit servers at 30℃ using White Mineral Oil

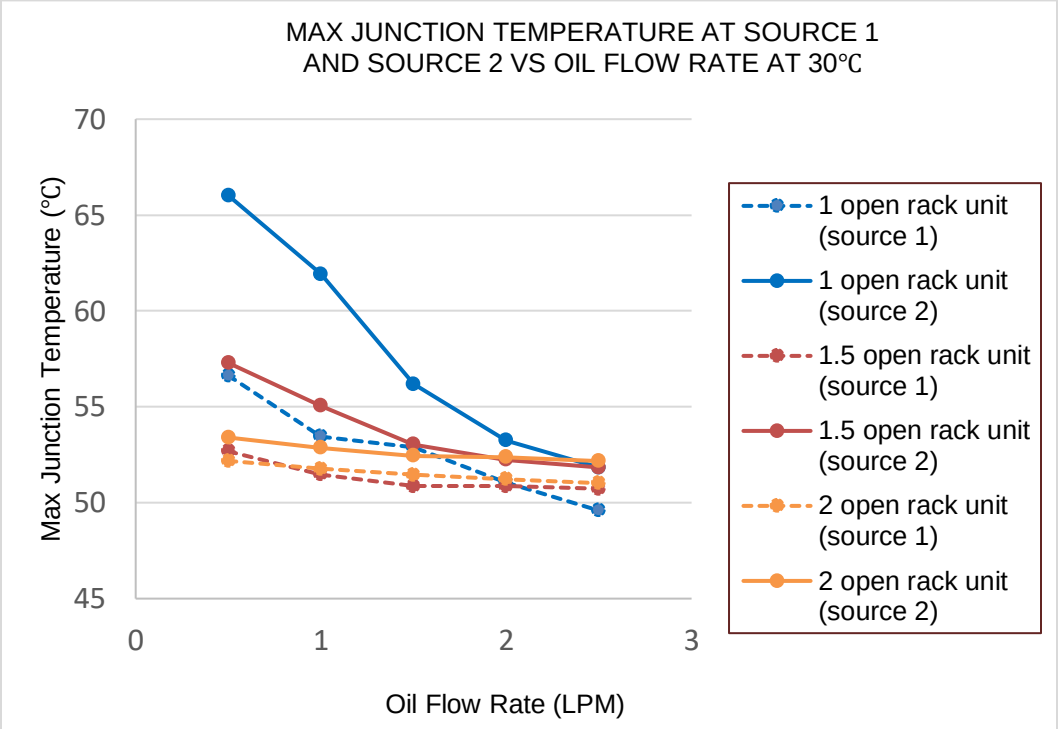

Figure 9-38 Maximum Junction Temperature at source 1 and source 2 vs Oil flow rate for different Open rack unit servers at 30℃ using Synthetic Fluid

Using White Mineral Oil, From the figure 37, the Impact of thermal shadowing can be neglected for all kinds of Open Rack Unit Servers. We can observe that the temperature difference between the source 1 and source 2 for 2 Open Rack Unit Server is less compared to that of 1.5 Open Rack Unit Server and 1 Open Rack Unit Server.

Similarly using Synthetic Fluid, From the figure 38, the Impact of thermal shadowing can be neglected for all kinds of Open Rack Unit Servers. We can observe that the temperature difference between the source 1 and source 2 for 2 Open Rack Unit Server is less compared to that of 1.5 Open Rack Unit Server and 1 Open Rack Unit Server.

Table 9-18 Temperature difference for Air cooled server and Oil Cooled Server using different fluids at 30℃, 1LPM of 2 Open Rack Unit Server

Server	Temperature Difference (℃)
Air cooled Server	10.15
Oil Cooled Server using White Mineral Oil	1.91
Oil Cooled Server using Synthetic Fluid	1.22

From table 18, the impact of thermal shadowing can be neglected for Oil cooled servers when compared to that of an air-cooled server. It is also clear that the temperature difference is even lesser for Synthetic Fluid when compared to White Mineral Oil.

9.7.7 Optimization of Heat Sinks

9.7.7.1 Results with Existing Parallel Plate Heat Sink

For 1 Open Rack Unit Server, at 30℃, 1LPM, with power 65W, with fin count 35 and Thickness of 0.3mm, the Temperature and Thermal Resistance are as follows.

Table 9-19 Temperature and Thermal Resistance of Source 1 and Source 2 for Mineral Oil and Synthetic Fluid with an existing parallel plate Heat Sink

	Temperature at Source 1	Temperature at Source 2	Thermal Resistance at Source 1	Thermal Resistance at Source 2
Mineral Oil	49.19	48.82	0.3093	0.3181
Synthetic Fluid	46.86	46.67	0.2736	0.2792

From the above data, we can calculate the volume by

Volume = Thickness x Height x Length

Volume = 0.3 x 41 x 110 = 1353 mm^3

For 35 fins,

Volume = 35 x 1353

= 47355 mm^3

9.7.7.2 Results with Optimized Parallel Plate Heat Sink

The number of fins is reduced to 15, with the same boundary conditions as that of the existing parallel plate heat sink. The fin count is kept constant as 15 and the height is kept constant as 41mm, the dimension of the baseline model. The plate thickness is varied from 0.25mm to 3.25mm. After conducting parametric study for this condition, we get Thermal resistance as follows.

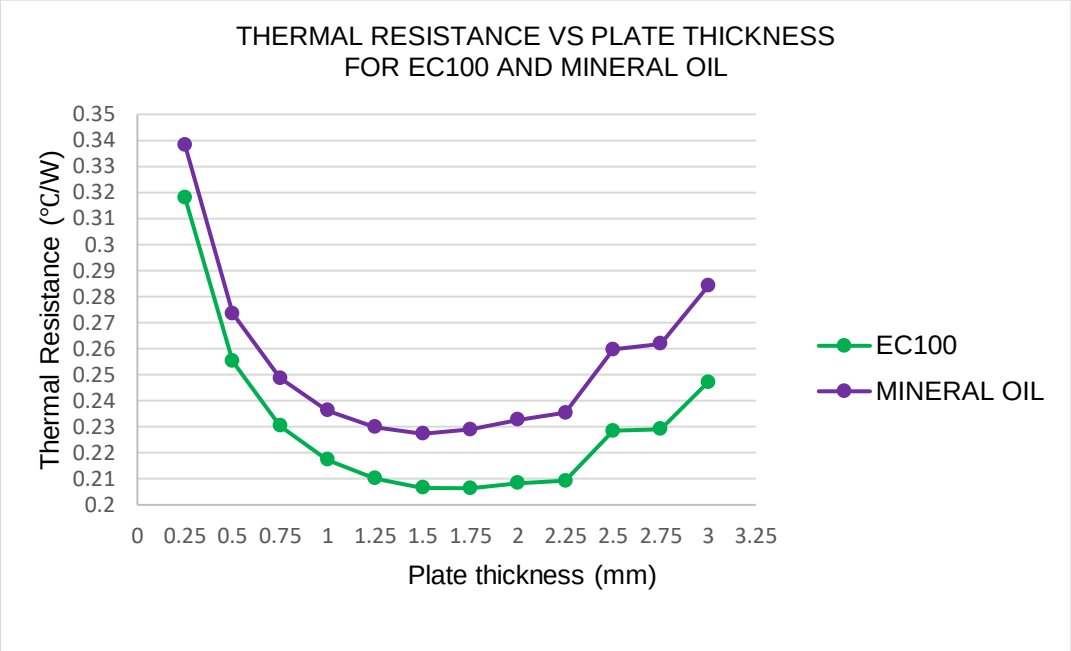

Figure 9-39 Graph of Thermal Resistance vs Plate thickness for Mineral Oil and Synthetic Fluid of an Optimized Parallel Plate Heat Sink

It is clear from the Figure 39 that the Thermal Resistance decreases for both White Mineral Oil and Synthetic Fluid when the thickness is from 0.25mm to 1.5mm. So, any thickness in between 0.25mm to 1.5mm can be considered for the study. In this study, the thickness of 0.25mm is considered. Now keeping the plate thickness 0.25mm as constant, the plate height is

varied from 20mm to 41mm. The thermal resistance curve for this height parametric study is shown below.

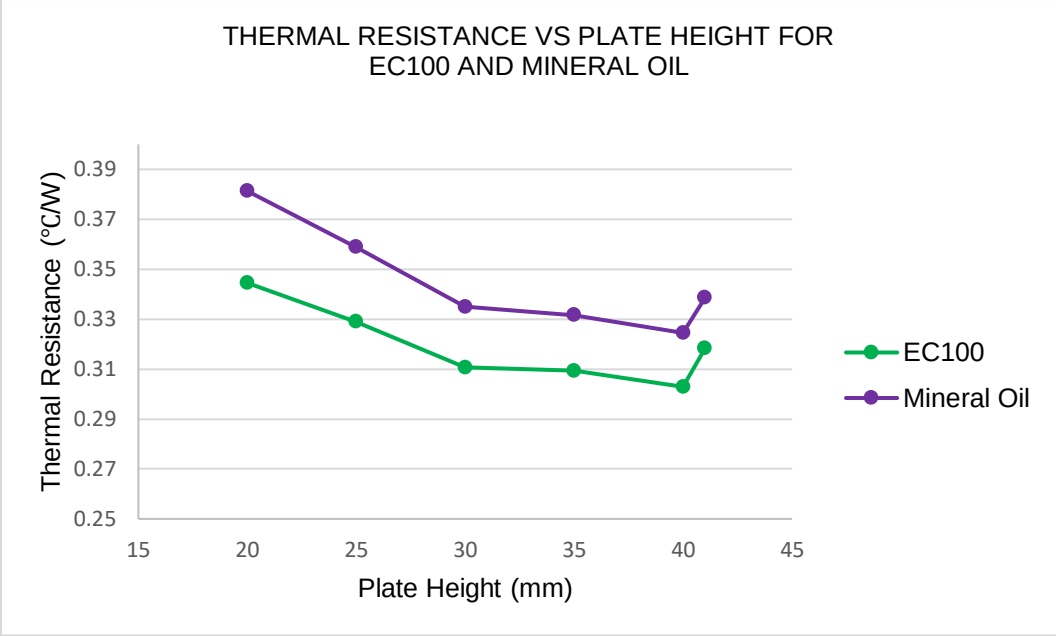

Figure 9-40 Graph of Thermal Resistance vs Plate height for Mineral Oil and Synthetic Fluid of an Optimized Parallel Plate Heat Sink

It is clear from the Figure 40 that the Thermal Resistance decreases for both White Mineral Oil and Synthetic Fluid when the height is from 20mm to 40mm. So, any height in between 20mm to 40mm can be considered for the study. In this study, the height of 20mm is considered. Now the simulation is performed for this optimized model of plate thickness 0.25mm and plate height 20mm and is compared with the results of an existing parallel plate heat sink.

Table 9-20 Temperature and Thermal Resistance of Source 1 and Source 2 for Mineral Oil and Synthetic Fluid with an optimized parallel plate Heat Sink

	Temperature at Source 1	Temperature at Source 2	Thermal Resistance at Source 1	Thermal Resistance at Source 2
Mineral Oil	51.63	52.57	0.3813	0.3659
Synthetic Fluid	49.99	50.32	0.3445	0.3303

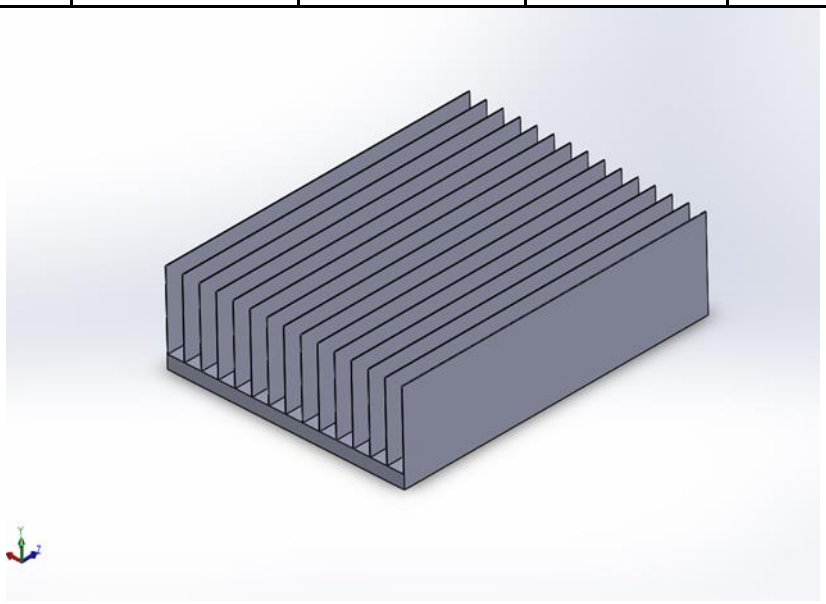

Figure 9-41 CAD model of an optimized parallel plate heat sink

Table 9-21 Volumetric comparison of existing parallel plate heat sink and optimized parallel plate heat sink

	Existing Parallel Plate heat sink dimensions	Optimized Parallel Plate heat sink dimensions
Thickness	0.3 mm	0.25 mm
Height	41 mm	20 mm
Length	110 mm	110 mm
Volume	Thickness x Height x Length =1353 mm^3	Thickness x Height x Length =550 mm^3
Number of fins	35	15
Volume for total fins	35 x 1353 =47355 mm^3	15 x 550 =8250 mm^3

It is clear from the Table 21 that the volume of the optimized model is very less when compared with the base model. The volume is almost decreased by 5 times, which implies that the material used is reduced by 5 times. So, the material cost can be reduced significantly. Also, from Table 20, It is clear that the temperature and thermal resistance are within the specified range.

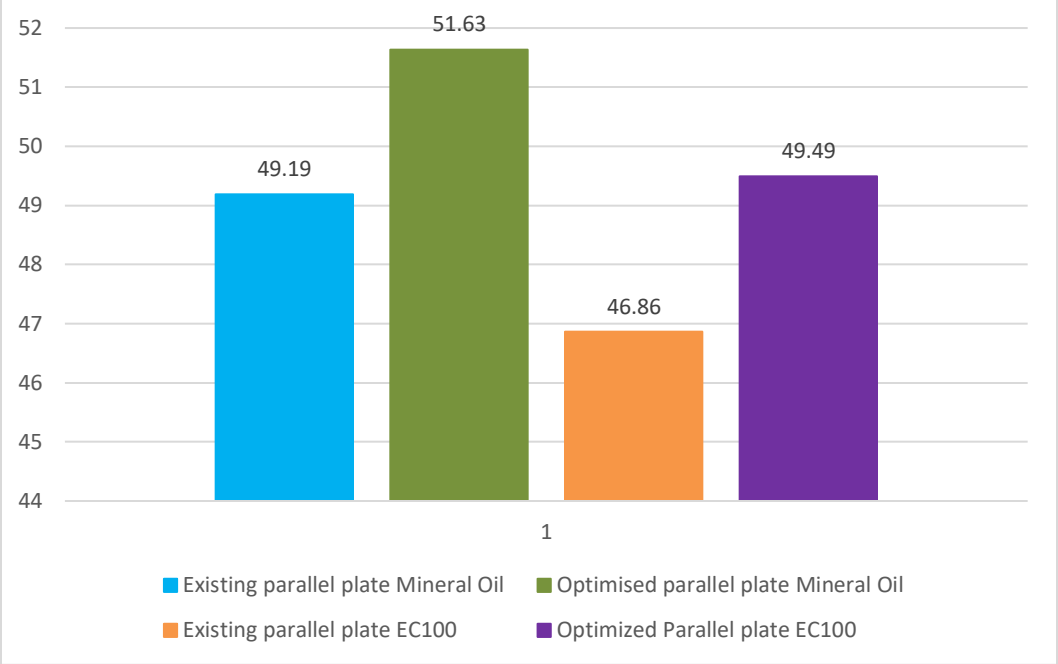

Figure 9-42 Comparison of Temperature at Source 1 for an existing and optimized parallel plate model using white mineral oil and synthetic fluid.

From Figure 42, It can be seen that there is very less variation in Temperature. Although there is increase in temperature of Optimized model, the rise of temperature is less than 5℃. This can be neglected as the temperature is less than the Max Junction Temperature specified by INTEL for 65W power. So, the optimized heatsink has better thermal performance and the material cost can be reduced.

9.7.7.3 Results with Optimized Plate fin Heat Sink

The parallel plates are replaced with plate fins in this study. The boundary conditions are kept same as that of the existing parallel plate heat sink. The plate fin count is kept constant as 42 and the height is kept constant as 41mm, the dimension of the baseline model. The plate

thickness is varied from 4mm to 10mm. After conducting parametric study for this condition, we get Thermal resistance as follows.

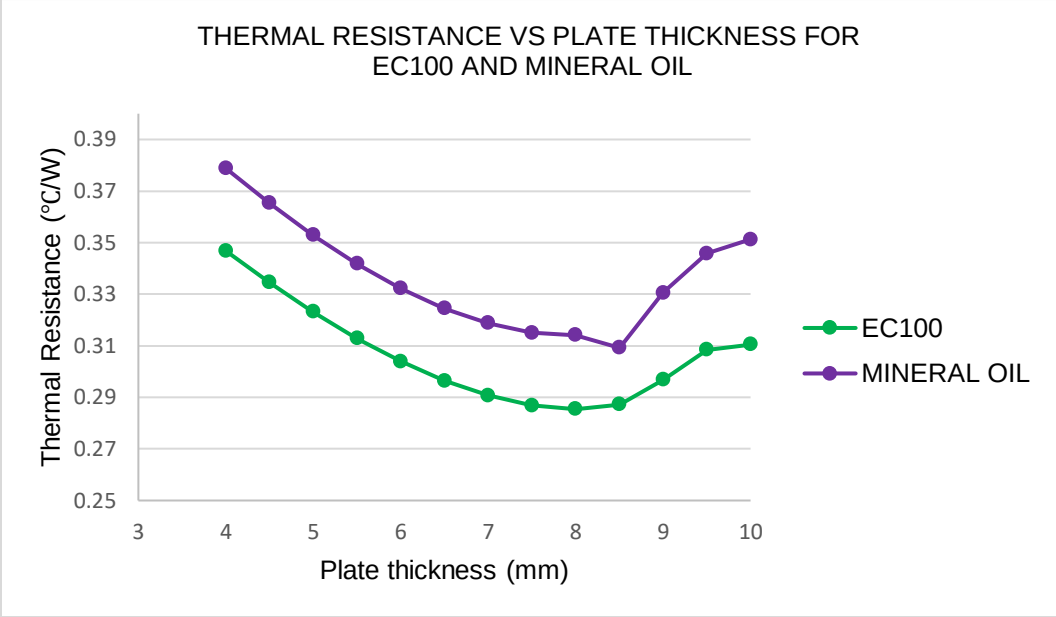

Figure 9-43 Graph of Thermal Resistance vs Plate thickness for Mineral Oil and Synthetic Fluid of an Optimized Plate Fin Heat Sink

It is clear from the Figure 43 that the Thermal Resistance decreases for both White Mineral Oil and Synthetic Fluid when the thickness is from 4mm to 7.5mm. So, any thickness in between 4mm to 7.5mm can be considered for the study. In this study, the thickness of 4mm is considered. Now keeping the plate thickness 4mm as constant, the plate height is varied from 20mm to 41mm. The thermal resistance curve for this height parametric study is shown below.

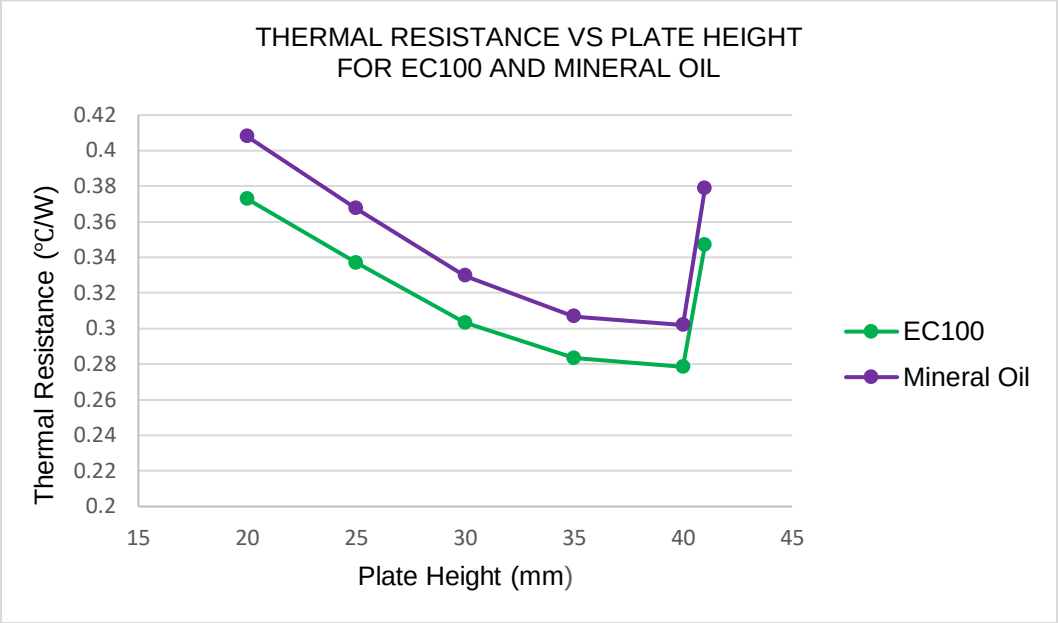

Figure 9-44 Graph of Thermal Resistance vs Plate height for Mineral Oil and Synthetic Fluid of an Optimized Plate fin Heat Sink

It is clear from the Figure 44 that the Thermal Resistance decreases for both White Mineral Oil and Synthetic Fluid when the height is from 20mm to 40mm. So, any height in between 20mm to 40mm can be considered for the study. In this study, the height of 20mm is considered. Now the simulation is performed for this optimized model of plate thickness 4mm and plate height 20mm and is compared with the results of an existing parallel plate heat sink.

Table 9-22 Temperature and Thermal Resistance of Source 1 and Source 2 for Mineral Oil and Synthetic Fluid with an optimized plate fin Heat Sink

	Temperature at Source 1	Temperature at Source 2	Thermal Resistance at Source 1	Thermal Resistance at Source 2
Mineral Oil	54.14	53.51	0.4079	0.428
Synthetic Fluid	51.79	51.38	0.3728	0.3878

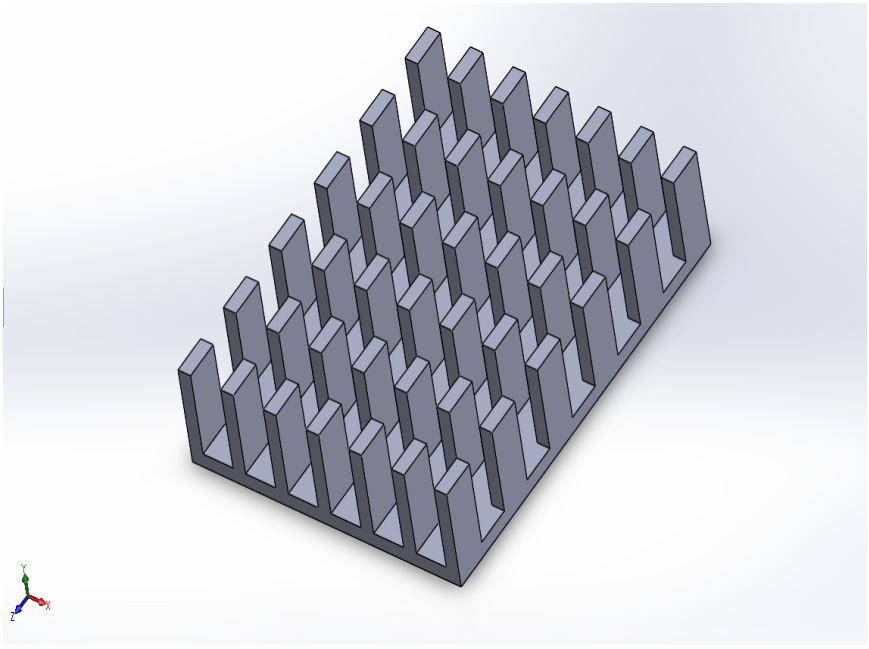

Figure 9-45 CAD model of an optimized plate fin heat sink

Table 9-23 Volumetric comparison of existing parallel plate heat sink and optimized plate fin heat sink

	Existing Parallel Plate heat sink dimensions	Optimized Plate fin heat sink dimensions
Thickness	0.3 mm	4 mm
Height	41 mm	20 mm
Length	110 mm	10 mm
Volume	Thickness x height x length =1353 mm^3	Thickness x height x length =800 mm^3
Number of fins	35	42
Volume for total fins	35 x 1353 =47355 mm^3	42 x 800 =33600 mm^3

It is clear from the Table 23 that the volume of the optimized model is very less when compared with the base model. So, the material cost can be reduced significantly. Also, from Table 22, It is clear that the temperature and thermal resistance are within the specified range.

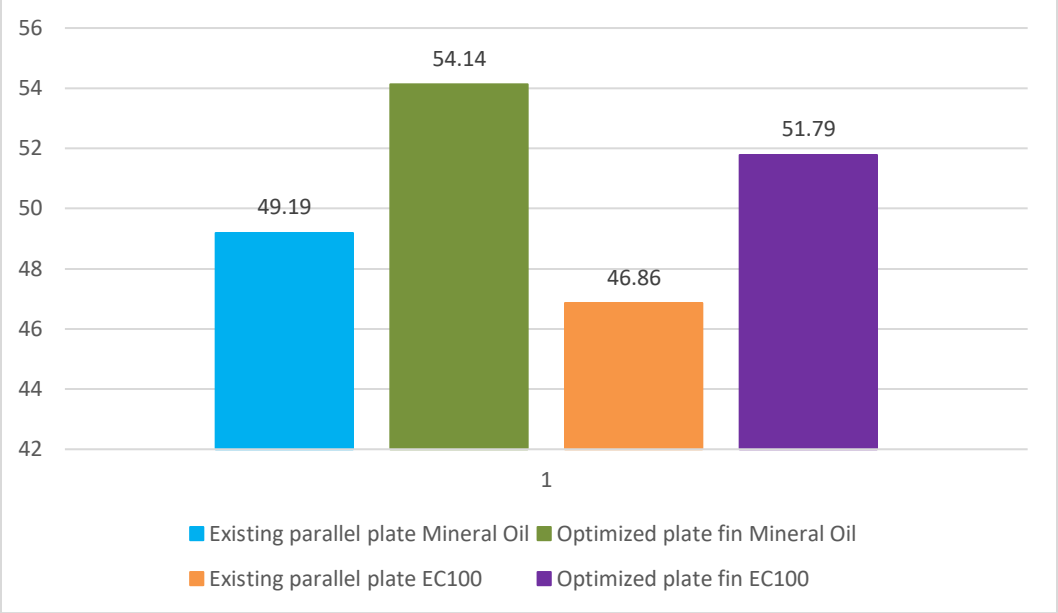

Figure 9-46 Comparison of Temperature at Source 1 for an existing and optimized plate fin model using white mineral oil and synthetic fluid.

From Figure 46, It can be seen that there is very less variation in Temperature. Although there is increase in temperature of Optimized model, the rise of temperature is less than 7℃. This can be neglected as the temperature is less than the Max Junction Temperature specified by INTEL for 65W power. So, the optimized heatsink has better thermal performance and the material cost can be reduced.

9.7.7.4 Results with Optimized Pin Fin Heat Sink

The parallel plates are replaced with pin fins in this study. The boundary conditions are kept same as that of the existing parallel plate heat sink. The pin fin count is kept constant as 25 and the height is kept constant as 41mm, the dimension of the baseline model. The pin radius is varied from 2.5mm to 8mm. After conducting parametric study for this condition, we get Thermal resistance as follows.

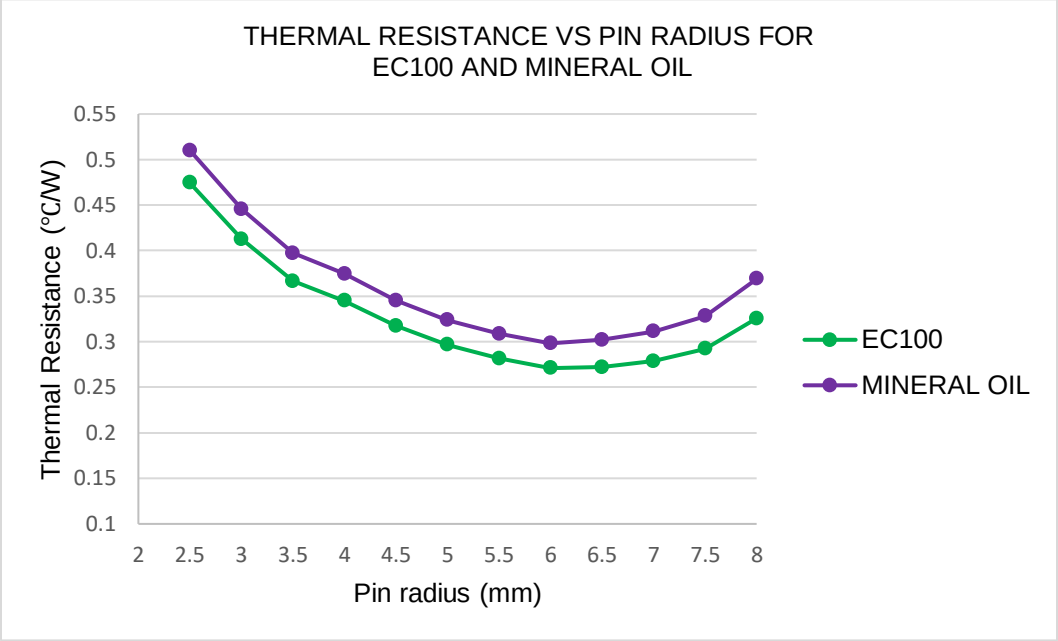

Figure 9-47 Graph of Thermal Resistance vs Pin radius for Mineral Oil and Synthetic Fluid of an Optimized Pin fin Heat Sink

It is clear from the Figure 47 that the Thermal Resistance decreases for both White Mineral Oil and Synthetic Fluid when the radius is from 2.5mm to 6mm. So, any radius in between 2.5mm to 6mm can be considered for the study. In this study, the radius of 3mm is considered. Now keeping the pin radius 3mm as constant, the pin height is varied from 20mm to 41mm. The thermal resistance curve for this height parametric study is shown below.

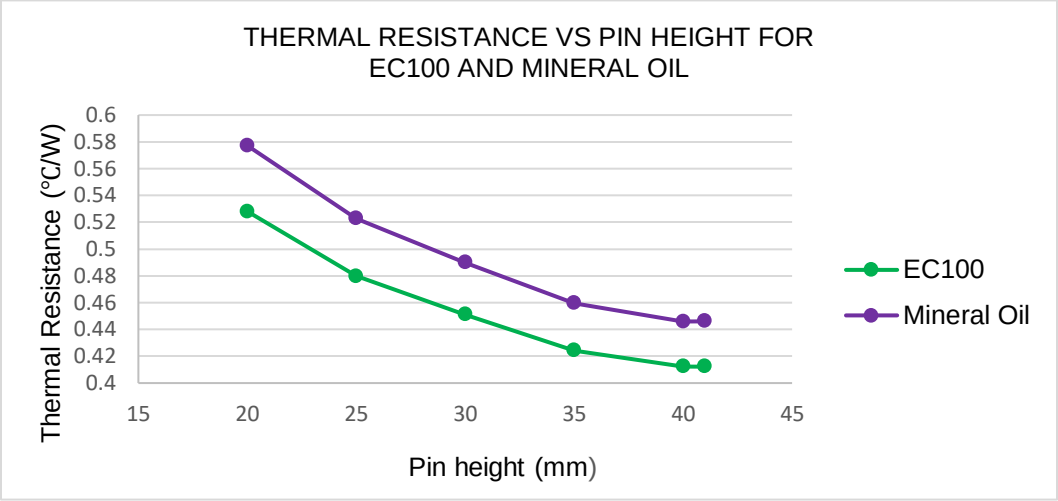

Figure 9-48 Graph of Thermal Resistance vs Pin height for Mineral Oil and Synthetic Fluid of an Optimized Pin Fin Heat Sink

It is clear from the Figure 48 that the Thermal Resistance decreases for both White Mineral Oil and Synthetic Fluid when the height is from 20mm to 40mm. So, any height in between 20mm to 40mm can be considered for the study. In this study, the height of 20mm is considered. Now the simulation is performed for this optimized model of pin radius 3mm and pin height 20mm and is compared with the results of an existing parallel plate heat sink.

Table 9-24 Temperature and Thermal Resistance of Source 1 and Source 2 for Mineral Oil and Synthetic Fluid with an optimized pin fin Heat Sink

	Temperature at Source 1	Temperature at Source 2	Thermal Resistance at Source 1	Thermal Resistance at Source 2
Mineral Oil	61.31	60.94	0.5772	0.6022
Synthetic Fluid	58.36	58.1	0.5281	0.5488

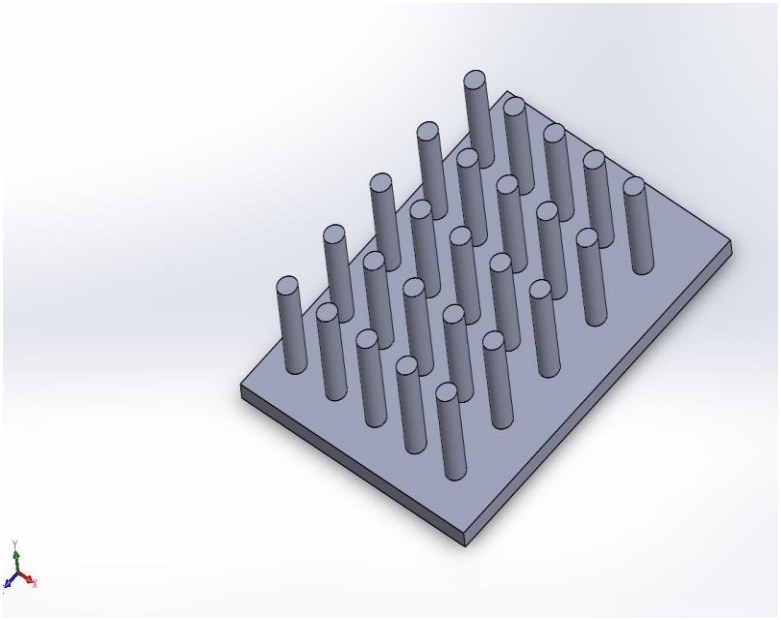

Figure 9-49 CAD model of an optimized pin fin heat sink

Table 9-25 Volumetric comparison of existing parallel plate heat sink and optimized pin fin heat sink

	Existing Parallel Plate heat sink dimensions	Optimized Plate fin heat sink dimensions
Thickness	0.3 mm	-
Height	41 mm	20 mm
Length	110 mm	-
Radius	-	3 mm
Volume	Thickness x height x length =1353 mm^3	Π x $radius^2$ x height =565.2 mm^3
Number of fins	35	25
Volume for total fins	35 x 1353 =47355 mm^3	25 x 565.2 =14130 mm^3

It is clear from the Table 25 that the volume of the optimized model is very less when compared with the base model. So, the material cost can be reduced significantly. Also, from Table 24, It is clear that the temperature and thermal resistance are within the specified range.

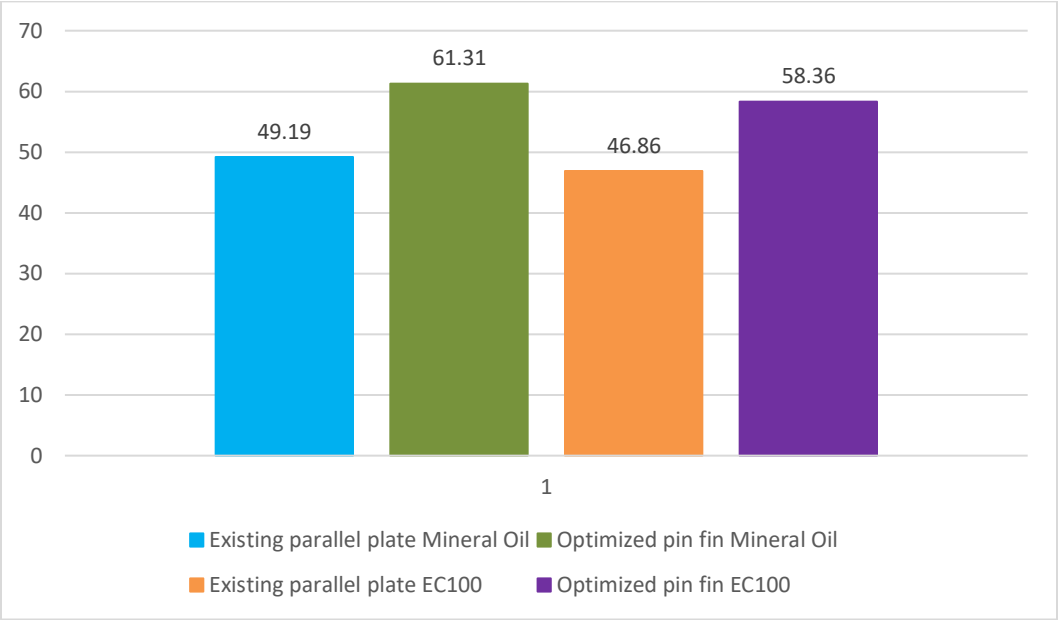

Figure 9-50 Comparison of Temperature at Source 1 for an existing and optimized pin fin model using white mineral oil and synthetic fluid.

From Figure 50, It can be seen that there is very less variation in Temperature. Although there is increase in temperature of Optimized model, the rise of temperature is less than 10℃. This can be neglected as the temperature is less than the Max Junction Temperature specified by INTEL for 65W power. So, the optimized heatsink has better thermal performance and the material cost can be reduced.

9.8 Conclusions

- Ducting system can be removed completely as the fluid flow need not be guided to the second heatsink.
- The comparative study carried out for white mineral oil and synthetic fluid shows an enhancement in thermal management for synthetic fluid (EC100) mineral oil for the same inlet temperatures.
- This study clearly indicates that the single-phase immersion cooling is efficient and capable to accommodate high thermal mass.
- By using single phase immersion cooling we can cool the server at low flowrate and high inlet temperatures.

The study carried out here, opens new vision to improve the cooling system of highly demanding data center technology. The major conclusion and findings are summarized below

- It is clear from the study that the Impact of Thermal Shadowing of the Oil Cooled Server can be neglected as the Temperature difference between Source 1 and Source 2 is 3℃ or lesser which can be neglected when compared to Air Cooled Server.
- So, we can conclude that the ducting system can be removed in Oil Cooled Server.
- Savings in power consumption by the server can be achieved as fans are removed which is an essential part of air cooling system and are replaced with pump for circulation of cooling oil.
- Also, the Impact of Thermal Shadowing of the EC100 is even lesser compared to White Mineral Oil.
- There is no significant Temperature change for Pin fin heat sink and Plate fin heat sink when compared with the existing parallel plate heat sink.

Chapter 10

Reliability Considerations for Oil Immersion Cooled Data Centers

Jimil M. Shah[1*], Richard Eiland[1], Pavan Rajmane[1], Ashwin Siddarth[1], Dereje Agonafer[1] and Veerendra Mulay[2]

[1]University of Texas at Arlington, P.O. Box 19023, Arlington, TX, United States, 76013

[2]Facebook Inc., Menlo Park, CA, United States, 425081

[1*] Corresponding Author: Email: jimil.shah@mavs.uta.edu

Abstract

The improved efficiency of mineral oil may offer simplicity in facility design compared to traditional air cooling and provide a means for cost savings. Despite its improved cooling efficiency and cost savings, a mineral oil immersion cooling technique is still not widely implemented and Original equipment manufacturers (OEMs) are reluctant to jeopardize sales of existing air-based cooling system equipment. Only compelling physics regarding thermal performance of direct immersion cooling is not enough for data center operators. Many uncertainties and concerns persist regarding the effects of mineral oil immersion cooling on the reliability of information technology (IT) equipment both at the component and chassis level. This paper is a first attempt at addressing this challenge by reviewing the changes in physical and chemical properties of IT equipment materials like polyvinyl chloride (PVC), printed circuit board (PCB) and capacitors and characterize the interconnect reliability of materials. The changes in properties of a mineral oil like kinematic viscosity and dielectric strength are also cited as important factors and discussed briefly. The changes in mechanical properties like elasticity, hardness, swelling, and creep are being shown in the paper for thermoplastic materials. The chemical reaction between material and mineral oil as a function of time and temperature is also conferred. The literature gathered on the subject and quantifiable data gathered by the authors provide the primary basis for this research document.

10.1 Introduction

Submerging servers and IT equipment in a mineral oil, a dielectric liquid, enables substantial energy savings today and accommodates growing load densities of future facilities. The existing proprietary submersion cooling solutions [1-4] and numerous case studies [3-6] have established the effectiveness and energy savings for a new construction or a retrofit from device to the facility level. For mission critical operations of a data center, a comprehensive study of reliability and availability is necessary for widespread adoption of any disruptive technology [7,8].

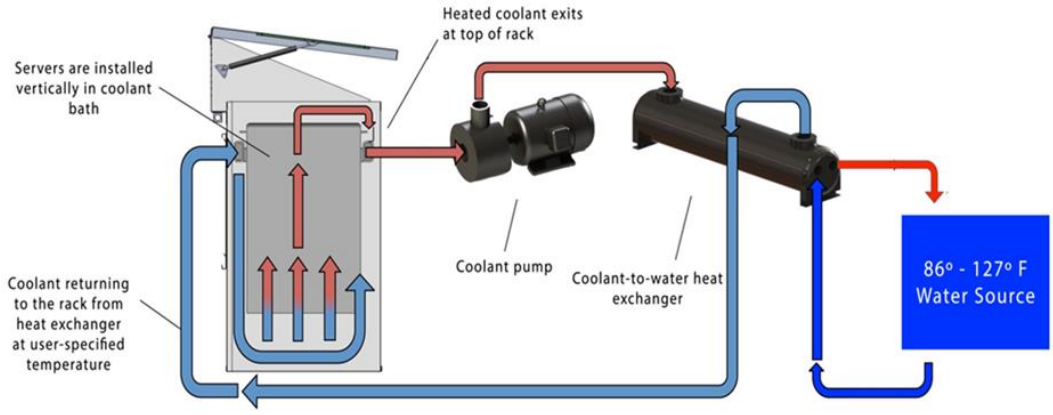

Figure 10-1 Schematic of an oil cooled data center [9]

Figure 1 provides the overview of the working of oil cooled data centers [9], which eliminates the root causes of failures, improves the operating conditions and reliability and advances in cooling technology for data center industries. This technology paves the path for the retrofitting of air cooled data centers and efficient performance with high load capacities.

Oil immersion cooling technology of data centers extends the prospects for improved reliability in operations as it minimizes common operational issues and eliminates the root causes of failure like reduction in solder joint failures, lower operating temperatures for board & components, no oxidation/corrosion of electrical contacts, no moving parts, like fans, within the

device enclosure, no exposure to electrostatic discharge (ESD), no sensitivity to ambient particulate, humidity, or temperature conditions. The reliability advances include a reduction in corrosion & electrochemical migration, lessening of environmental contamination like dust, debris, and particulates, and mitigation of tin and zinc whiskers [10-11].

Electrochemical Migration is a movement of metal through an electrolytic solution under an applied electric field between conductors which are insulated. Electrochemical migration (ECM) is a common reliability issue that can be found in the electronic packaging industry, including different materials and components like dies surface, epoxy encapsulates, PCB and passive components etc. The major ECM drivers are temperature, moisture, contamination and voltage/electrical field. Immersion oil cooling reduces and/or eliminates temperature, moisture, and contamination aspects. The main sources of contamination are storage and environment. The concerns of storage include cleaning chemicals, outgassing and polymeric materials. Operating environments include dust, debris, zinc whiskers, moisture, evaporated sea water and industrial pollutants like sulfur, etc. Oil immersion cooling prevents contamination accumulating. Efficient handling methods and cleanliness should be implemented and filtration of oil lessens the risk of particulate and dust contaminants. The constant operation proves the thermal stability of oil cooled data centers. It is expected to see a hot spot reduction and improved thermal uniformity using immersion oil cooling. Tin whiskers are hair-like single crystal metallic filaments that grow from Tin films. The potential failure modes are direct contact that causes an electrical short (arching) and requires growth of adequate length and in the correct direction. Electro-magnetic (EM) Radiation which releases or receives EM signal and noise at higher frequencies and deterioration of signal for frequencies above 6 GHz, which is independent of whisker length and debris like whisker breaks off and shorts two leads (primarily during handling). These can be mitigated by immersion oil cooling [10].

The problem in immersion cooling is when the whiskers break free, they become airborne and can circulate freely throughout the facility and get blown into the equipment, causing absolute mayhem without you even knowing. By using the pump system that has a layered filtering system, these little whiskers can be captured. Filtering in fluids is far easier than in air as the fluid restrains the filaments from floating free and the filaments are drawn into the circulating pumps and can be filtered in one location.

Another important advantage of oil immersion cooling is that this form of cooling offers the opportunity to remove heat directly from the chip(s) and all other components with no intervening thermal conduction resistance, other than that between the device heat sources and the chip surfaces in contact with the liquid as the fluid is dielectric unlike indirect cooling which can only be used to those components where CDUs are attached and the server cannot be completely immersed to cool all the components as it uses conductive water as a working fluid.

A primary concern by data center industry professionals regarding mineral oil immersion techniques is the impact of the fluids on the long-term reliability of components and systems. By fully immersing a server in oil, a company may be voiding the warranty on their equipment, and expose themselves to potential failure costs. Current industry data regarding the reliability of server systems after immersion in mineral oil suggest that there is no detrimental impact to components [2-4,8]. However, the remarks made in literature are anecdotal, not providing detailed information or data, limiting their utility to the industry at large.

This study focuses on the reliability of servers and IT equipment when submerged in a mineral oil at the device level. Prolonged immersion of servers in mineral oil will onset a wear-out mechanism and upon cumulative damage can lead to component failure. Degradation of material property or component functionality is a result of fundamental mechanical, chemical, electrical and thermal phenomena introduced due to changes in the typical operating environment. The superior heat carrying capacity of a mineral oil compared to air eliminates hot

spots and produces less variation in temperature spatially and in time. The chemical interactions between the coolant and various components for an extended amount of time introduce lifecycle loads which are not observed in traditional air cooling.

The components considered in this investigation are cables, printed circuit boards, packages and passive components. Complete immersion of a server is responsible to the device and component level reliability. With the concern of critical performance, cost, safety and operating environment, the study of the reliability of these four categories of components becomes significant. The study of the change in the properties of a mineral oil like kinematic viscosity, flash point, and dielectric strength is also the subject of anxiety for the data center operators. These properties have the direct relation with the coolant efficiency, servicing costs, pumping power, operating cost and facility design. It becomes critical to know about these changes as it keeps data centers functioning. Some standard methodologies have already been derived to measure the changes in properties of important components submerged in a mineral oil. But sometimes, it becomes hard to follow those standards because of their limitations as they are designed to test the reliability of the materials in air-cooled environment [12-14].

This paper also leaves a scope for instituting design of experiments for determination of modeling parameters and a methodology which should be analogous to accelerated thermal cycling and accelerated thermal aging, so that it can be accepted as a standard methodology to provide the reliability analysis of oil cooled data center components and the coolant. The methodology should be proposed and adopted which can provide the reproducible results to determine the failure in oil cooling technology. The assumptions should be made for all the parameters which are important in the case of oil immersion cooling. The parameters like heat load, flow rate, inlet temperature, and placement and power levels of the components and volume of the oil should be considered to fix the temperature for the thermal overstress experiment.

10.2 Setup and Approach

The study undertaken and discussed below presents a look at the impact of mineral oil on server components. This includes high-level visual observations, microscopic observations made by sectioning server components, and a more detailed study of the change in material properties that result from exposure of printed circuit boards (PCBs) to mineral oil. Similar observations of air cooled servers were taken as a basis for comparison.

10.2.1 Effect of A Mineral Oil On Active Components Like Printed Circuit Boards and Packages

A sample of three servers that were immersed in a mineral oil for a six-month period during thermal testing were taken apart, photographed and sectioned for imaging to document the effects of oil on server components. Figure 2 shows the fading of oil immersed screen-printed component markings on the memory chips of the DIMM modules. Although not a direct impact on mechanical reliability, this fading of markings may impact identification of components when servicing is needed [15-17].

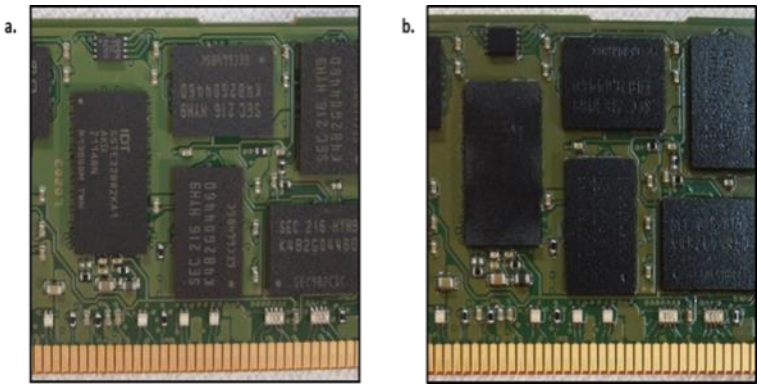

Figure 10-2 Fading component identifies because of oil exposure was seen in (a) an air-cooled server and (b) an oil immersed server

A more detailed visual study was carried out by taking cross sections of various components to determine the microstructure of electronic packages. Key components were placed in molding compound, sectioned, and polished. Control samples of servers that were not

exposed to oil and used in traditional air-cooled based testing underwent the same testing. The details of the package structure were observed under microscopes.

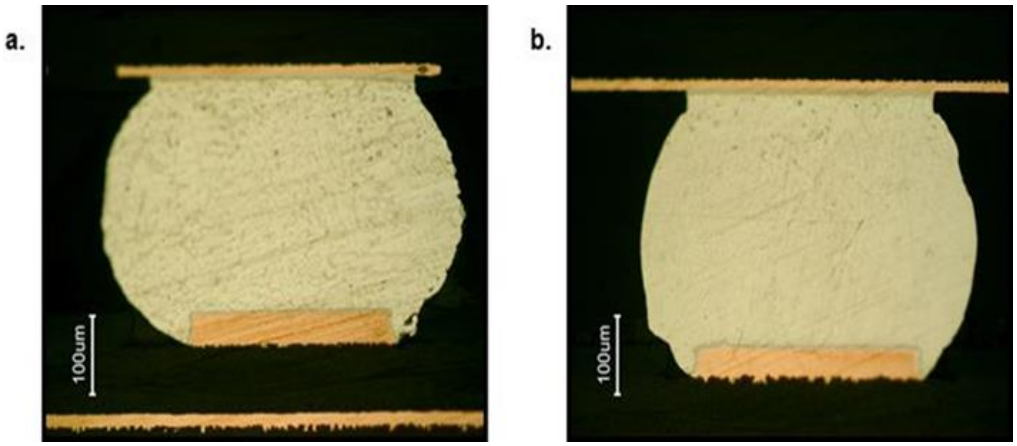

Figure 10-3 Comparison of microstructure of solder balls taken from (a) an air-cooled server and (b) an oil immersed server

Figure 3 offers a comparison of solder balls from the backside of the memory module attached to the DIMMs. As can be seen, there are no noticeable deformations, change in size, or cracking of solder balls. In addition, the intermetallic compound (IMC) layers which provide the mechanical and electrical connection between PCB-solder balls and solder ball-substrate interfaces showed no change in thickness between air cooled and oil cooled samples. The chip under fill material, which strengthens the mechanical connection between a flip chip package and substrate, also showed no detectable variation between air and oil cooled samples. In Figure 4, it is seen that there are no size variations in the metal layers of the packaging substrate. The trace thickness does not change or alter after exposure of the server in an immersive environment.

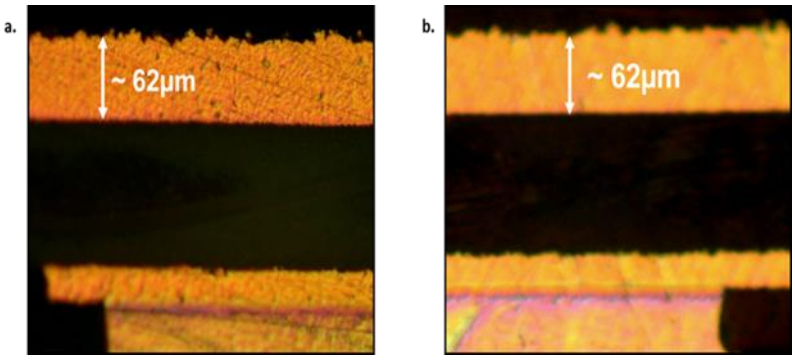

Figure 10-4 Comparison of substrate layer of BGA package taken from (a) an air-cooled server and (b) an oil immersed server

Figure 10-5 Cross section of PCB plated through-hole on oil exposed server

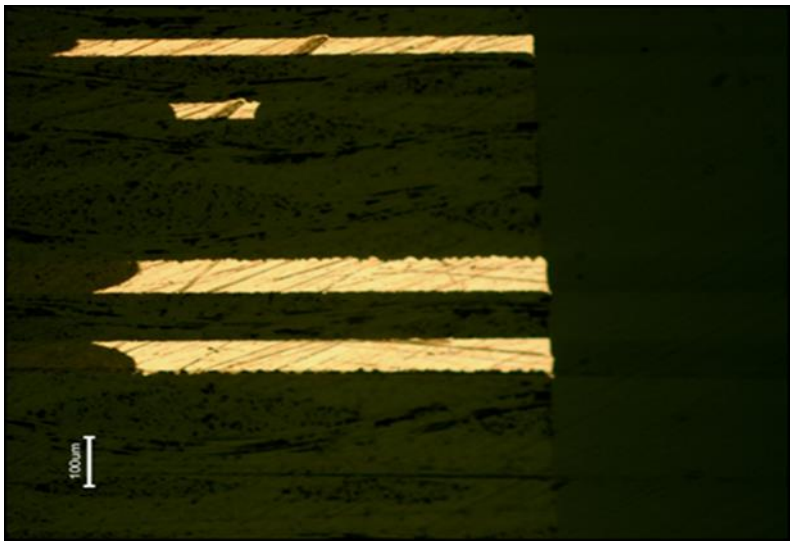

Figure 10-6 Edge of oil exposed PCBs maintain structural integrity and show no indication of delaminating

Additional samples of PCB boards showed no delaminating, swelling, or warpage of layers after extended periods of submersion in mineral oil. In Figure 5, a cross section at a plated through hole location on the motherboard has maintained its structural integrity. Similar observations can be made from Figure 6 at an edge location on the PCB.

The images and results gathered here provide a more detailed account to support the anecdotal claims made in the literature. In terms of component reliability, when submerging servers over the six-month duration, there is not any indicated reason for concern. However, typical servers operate in a data center for longer durations, anywhere from three years up to 10 years. A larger sample size of components and materials tested over extended periods or with the aid of accelerated thermal testing can help strengthen the conclusions made here.

10.2.2 Dynamic Mechanical Analysis of a PCB Material

A study was initiated to determine the extent to which oil exposure alters the material properties of PCBs. Dynamic Mechanical Analysis measures the mechanical properties of

materials as a function of time, temperature, and frequency. The term is also used to refer to the analyzer that performs the test (figure 7). DMA is also called DMTA for Dynamic Mechanical Thermal Analysis. DMA works by applying a sinusoidal deformation to a sample of known geometry. The amount of deformation is related to its stiffness. 10mm*50mm sample size was taken to measure Elastic modulus from a temperature range from 15°C to 120°C. Samples were taken from oil cooled server as well as air-cooled server. The DMA measurement was performed at 1 Hz, 2 Hz, 5 Hz, and 10 Hz for both types of samples.

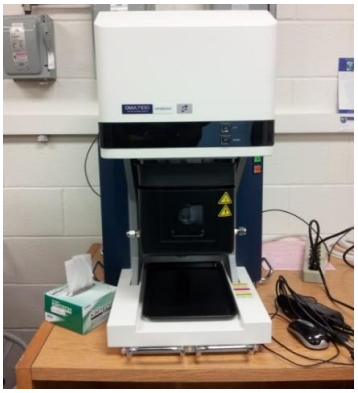

Figure 10-7 Dynamic Mechanical Analyzer

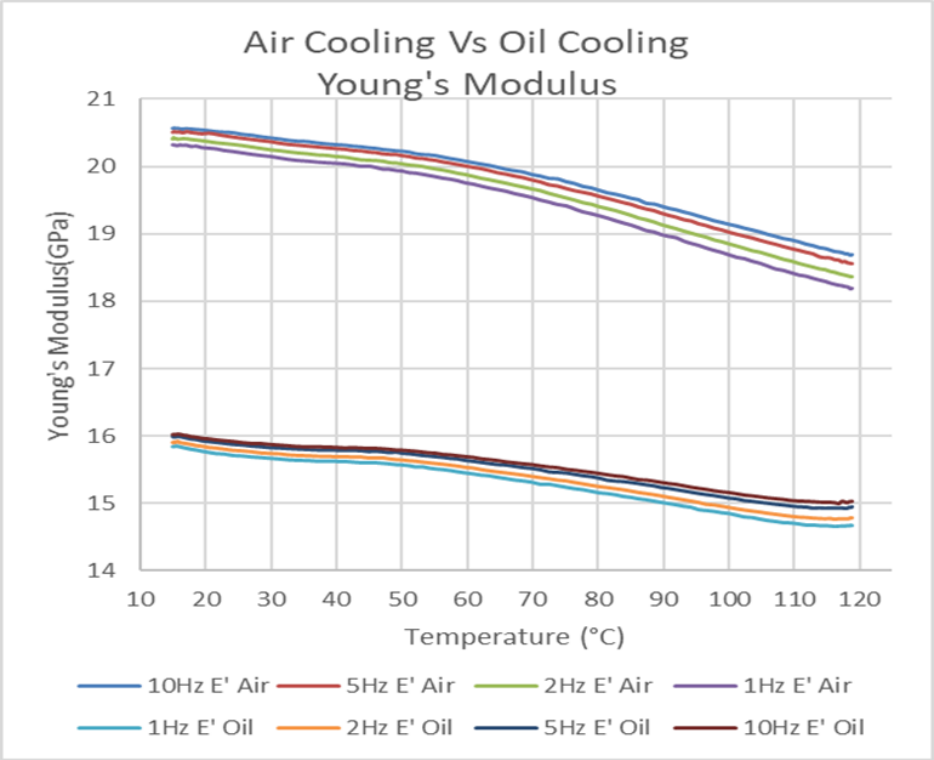

Figure 10-8 Dynamic Mechanical Analyzer: PCB Testing Results

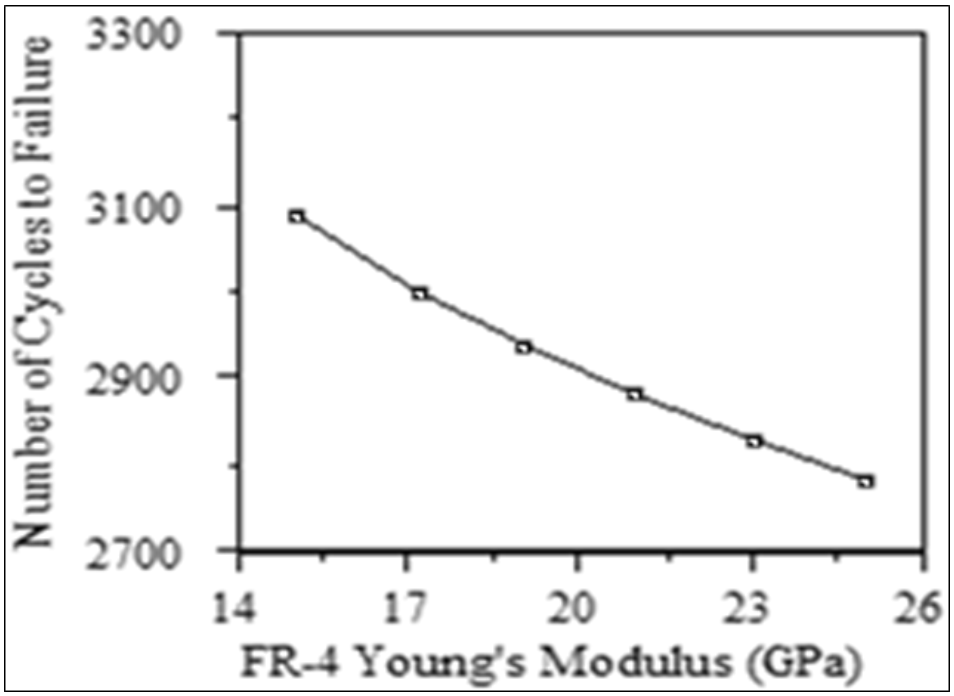

Figure 10-9 Typical relationship between circuit board stiffness and cycles-to-failure [18]

Preliminary strain measurements showed a significant decrease in the Young's modulus of PCB material for servers that had been immersed in oil for an eight-month period as compared to an air-cooled sample as shown in figure 8. A decrease of this type may severely improve the reliable life of a motherboard based on the trend discussed by Cheng et. al. [18] and shown in Figure 9. The results from this study may be input to Finite Element Models (FEA) to further simulate the impact of changes in material properties on the component and solder ball fatigue life [19]. The regression model can be created [20].

10.2.3 Digital Image Correlation (DIC) with Oven testing for Coefficient of Thermal Expansion of PCB

A DIC technique was used to measure in-plane and out-of-plane coefficient of thermal expansion (CTE) of PCB. The samples were cut from the PCBs and then painted with white spray to get a good clear white background followed by black speckled spray paint which

created several black dots on white paint as shown in Figure 10. The working principle of DIC is that the cameras capture the movements of these black dots and measure the deformation in the specimen. Several readings were taken at different temperatures i.e. 25°C, 50°C, 75°C, 100°C and 125°C. 5MP cameras were used with a Digital Image Correlation (DIC) technique to monitor strain in the sample as it was heated from 25°C to 125°C. Sample was baked 6-7 hours before the experiments to remove the moisture.

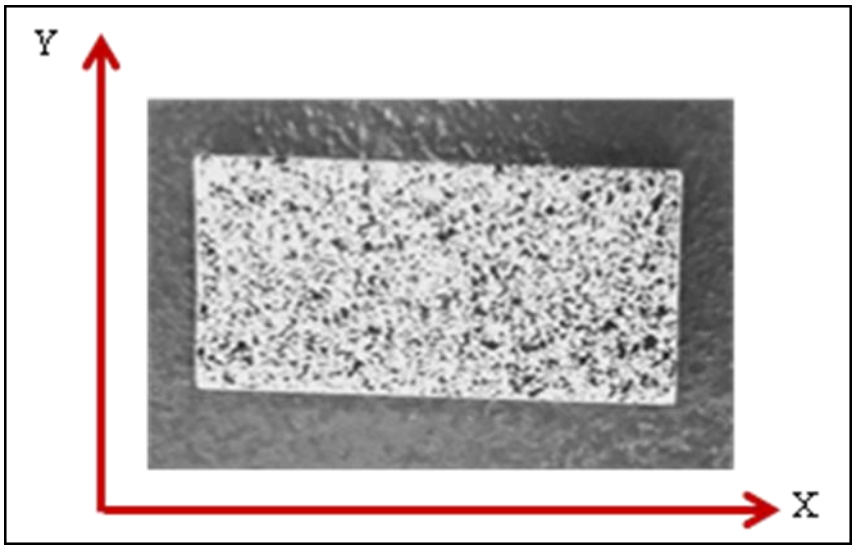

Figure 10-10 Specked Sample used for CTE

Thermocouples were attached to the dummy sample which was kept near to original sample to monitor temperature of the sample at various locations. Since the thermocouples are attached to the sample using thermal tape, there is a possibility that the tape might restraint the sample from free expansion during heating. Therefore, a JEDEC standard was followed and thermocouples were attached to the dummy sample and not on the test sample. The test setup is shown in the figure 11 below.

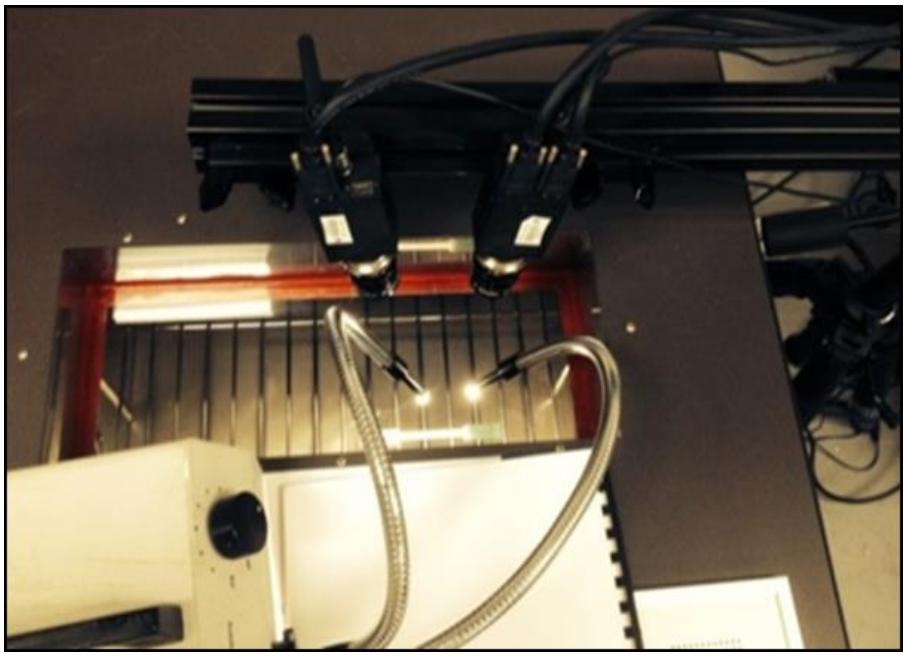

Figure 10-11 DIC Setup

The 20 channel Data Acquisition System (DAQ) was used to collect temperature data from the thermocouples. Images at every 25°C were captured using VicSnap software provided with DIC system. 5MP high speed cameras captured minute deformation in the specimen. From figures 12 and 13, we can see that there is no significant change in the values of CTE of air cooled sample and 8 months oil immersed sample respectively.

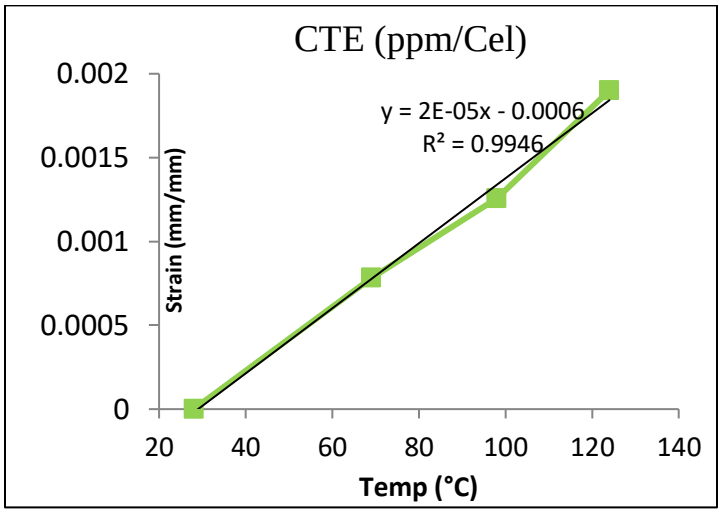

Figure 10-12 CTE in an air-cooled sample

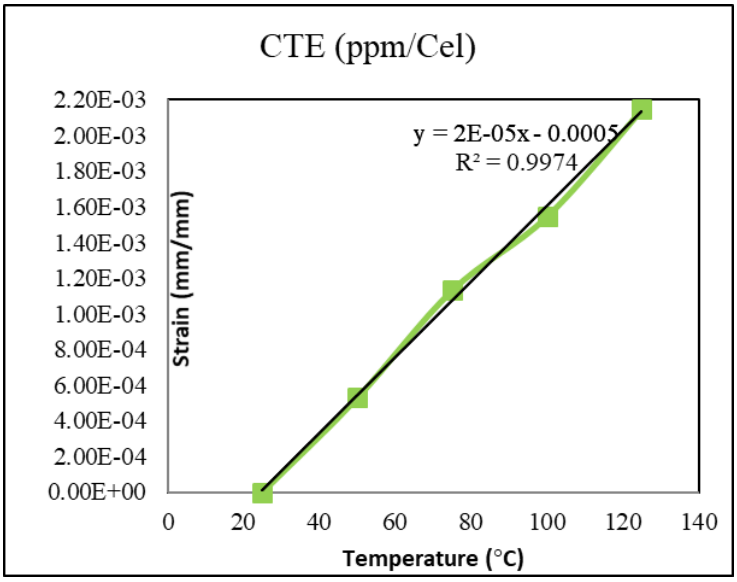

Figure 10-13 CTE in an oil immersed sample

10.2.4 PCB dielectric constant and dissipation factor

The properties those define any dielectric material of PCB epoxies that influence high-speed circuit design, in terms of signal propagation delay and dissipation factor are

- Dielectric constant and
- Dissipation factor or loss tangent [21].

The propagation delay in ns/m is given in terms of effective dielectric constant by the relation:

$$t_{pd} = 1.017\sqrt{\varepsilon_{eff}} \quad (1)$$

where, ε_{eff} is the effective dielectric constant of the PCB epoxy. The increase in the dielectric constant due to water (available in the form of relative humidity, water and gas contamination in a mineral oil) absorption increases propagation delay, that is, it slows down the speed at which the signal travels down the wire.

Dissipation factor or loss tangent tan(δ) affects the insertion loss (attenuation) α, in terms of dB/inch, of the signal as per the following relation:

$$\propto = 2.3 * f * \tan(\delta) * \sqrt{\varepsilon_{eff}} \quad (2)$$

Where, f = frequency (GHz)

As the frequencies rise the GHz scale, more consideration must be paid to dielectric constant and the dissipation factor of the PCB epoxies. The PCB epoxies absorb moisture and will lead towards an increment in the values of both the dielectric constant and the dissipation factor, degrading signal speed and increasing the insertion loss. An oil immersion cooling technology provides more protection to the PCBs from the direct exposure to humidity in the atmosphere [21].

10.2.5 Effect of A Mineral Oil on Passive Components Like Capacitors

Electrolytic capacitors, prominently the Aluminum Conductive polymer capacitors, are generally used in servers. Degradation of performance in electrolytic capacitors can be caused by various factors like electrical, thermal and environmental stresses. Upon electrical overstress, the increase in internal temperature in turn increases the electrolyte evaporation

rate. Similarly, when the capacitor is operating or is stored in the high-temperature environment the heat travels from the body of the capacitor thereby increasing the internal temperature. Figure 14 describes capacitor degradation data in a thermal overstress experiment at 105°C and humidity factor of 3.4% for 3500 hours shown below. Electrolytic capacitors and Polymer capacitors are mainly used in the data center industry and should be tested in Mineral oil at elevated temperatures as provided for air cooling testing in Figure 12 [22].

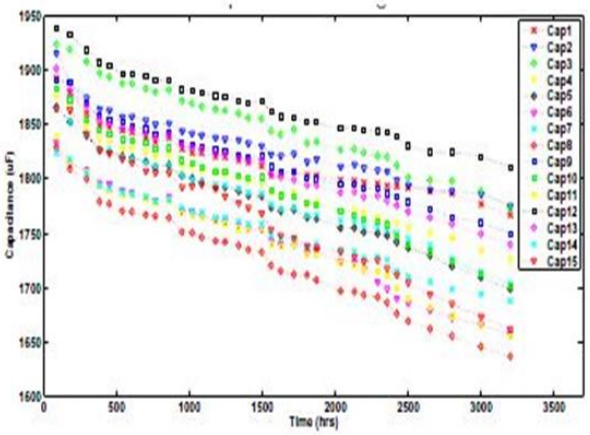

Figure 10-14 Capacitor degradation data in a thermal overstress experiment from air cooling testing [22]

Degradation of Capacitors in turn leads to an implication in two main electrical parameters of the capacitor:

1) Equivalent Series Resistance (ESR), and
2) Capacitance (C).

The temperature profile of a server, when immersed in mineral oil, reduces hot spots and ΔT across the servers and, therefore, provides a better operating environment for capacitors. The concern in mineral oil is about the dissolution of the electrolyte in mineral oil causing degradation in performance. Rubber bungs at the bottom and plastic capacitor sleeve should be avoided due to incompatibility with mineral oil. A degradation of capacitance should

indicate any decrease in electrolyte volume of the capacitor. Liquid electrolyte capacitors that produce hydrogen gas when it fails due to the chemical reaction inside can be a cause of concern as well.

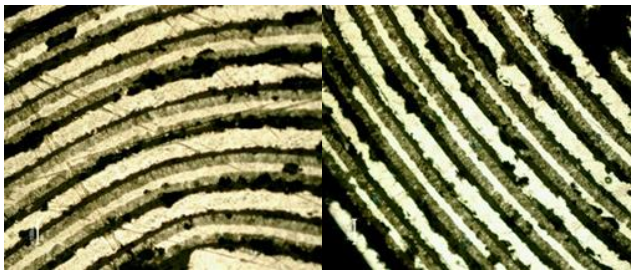

Figure 10-15 Comparison of microstructure of Capacitors taken from (a) an air-cooled server and (b) an oil immersed server

Figure 15 offers a comparison of microstructure of Capacitors. As can be seen, there are no noticeable deformations and/or changes between an air-cooled server sample and an oil-immersed server sample.

10.2.6 Effect of A Mineral Oil on Cables and Switching Devices

An observation made when handling servers after submersion in mineral oil for extended periods is that some materials become noticeably stiffer. This includes the plastic and insulating materials used for connection cords for power, networking, and hard disk drives (HDD). A concern amongst industry professionals is that this hardening may lead to cracking of insulators, exposing wiring or full failure of connectors.

The properties of insulation materials can be characterized as extruded primary insulations, which are applied directly over the conductor and are also used for jackets. As shown in figures 16 and 17, those are mainly polyvinyl chlorides (PVCs), polyethylene, fluorocarbons, and silicones. While PVC insulation has desired mechanical and electrical properties and low cost, those make it a stronghold of the wire and cable industry, it presents environmental concerns. PVC contains halogen. PVC releases toxic gasses, smoke, and acids

while burning that can be harmful to health and equipment. XLPE is halogen-free but is not highly recyclable. These two materials are abundantly being used in the cable industry. Using newly developed polyphenylene ether [mPPE] alloy insulating material is halogen-free and recyclable, yet remains cost-effective and robust. [23].

Figure 10-16 Electrical Cables and Wiring

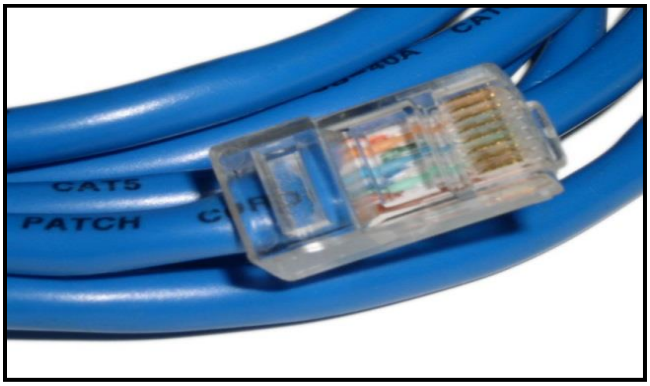

Figure 10-17 Network Cables

There are different formulations of Polyvinyl chloride which show extremely high or low-temperature properties of PVC. Some PVC formulations have –55°C to 105°C rating. The regular PVCs have –20°C to 60°C. The dielectric constant is in between 3.5 to 6.5. XLPE has 150°C ratings. Cross-linking converts polyethylene to a thermosetting material which enhances the properties of a material.

Rubber can be categorized as natural rubber and SBR compounds. These materials can be used for both insulations and jackets purposes. Some formulations are suitable for 55°C minimum, while others are suitable for 75°C maximum.

Table 1 provides information regarding the properties of general insulation and jacket materials like oil resistance, resistant to heat and dielectric strength based on the test results provided by different esteemed laboratories.

Table 10-1 Rating chart

Properties	**PVC**	**PE Cable**	**XLPE**	**mPPE**	**Rubber**
Oil Resistance	Fair	Excellent	Excellent	Excellent	Poor
Heat Resistance	Good	Poor	Good	Good-Excellent	Fair
Dielectric Strength (kV/mm)	15-20	20	20	Not Available	Not Available

For a Mineral oil immersed rack or tank, the cabling architecture could comprise of a top of rack or end of row design like all modern data centers [24]. The servers are connected to the switch generally by an unshielded twisted pair (UTP) cable for up to 10 GB/s for short distances. Off the shelf Category 5E, 24 AWG UTP local area network cable was considered for testing the impact of mineral oil. The cable is plenum rated and has a low smoke PVC jacket and FEP insulation. As the thickness of the jacket specimen was less than 0.76mm, tubular specimen was prepared and tested in accordance with UL 2556. The specimen was 6 cm long and immersed in mineral oil for 48 hours at 100°C. The mechanical testing of the cable jacket specimen (the test setup has been shown in Figure 18) was performed to determine the percentage change in elongation and to compare the change in Young's Modulus.

Figure 10-18 Test setup to measure mechanical properties of cable specimen

From Figure 19, it can be inferred that there is a drastic increase in Young's Modulus. Due to aging in mineral oil the specimen shrunk in length and loss of plasticizers could be attributed to its reduction in weight. No performance impact of a mineral oil on RF components and switching devices has been found yet. No considerable analysis has been carried out yet. Operators have not detected any issues, but to predict the life of materials and performance, the study should be acted upon.

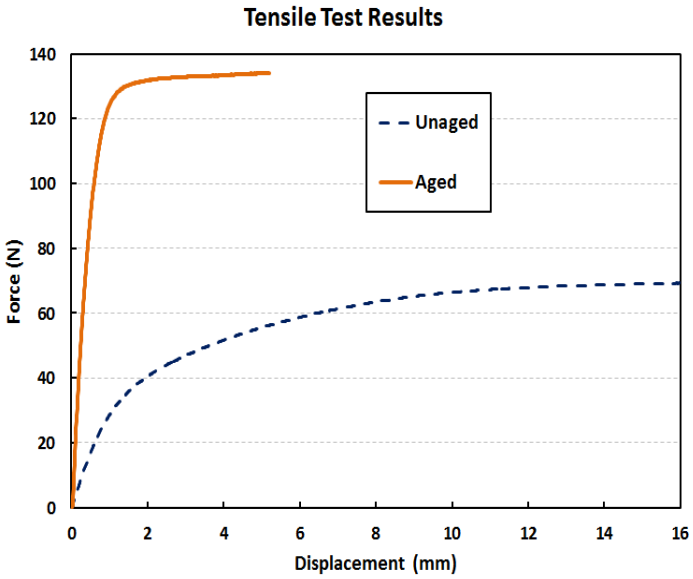

Figure 10-19 Load versus extension for a Low smoke PVC jacket tubular specimen without aging and aged in mineral oil

An evaluation on optics in an oil immersed server should also be carried out. How does oil impact signal and communication to and from a server? How would optics need to be packaged if oil is found to be a problem?

10.3 Changes in Properties of a Mineral Oil

The standard properties of mineral oil as per Data sheets/MSDS from STE Oil Company Crystal Plus Tech Grade Mineral Oil are:

- Density (kg/m3) : 849.3
- Specific Heat (kJ/kg·K) : 1.670
- Thermal Conductivity (W/m·K) : 0.13
- Thermal Expansions Coefficient (1/K) : 0.0007
- hermal Diffusivity (m2/s) : 9.166E-08
- Prandtl Number (at 40°C) : 134.4 [25,26]

NOTE: Some of these properties may be temperature dependent (i.e. density). The changes in properties of a mineral oil are mainly concerned with the changes in kinematic viscosity and dielectric strength [25,26].

The viscosity of oils has a relationship with temperature and time and it affects system pressure directly. So that pumping power becomes critical. A standard correlation between viscosity and temperature for transformer oils is given in [25,26] as:

$$\mu = C_1 * Exp\left[\frac{2797.3}{T + 273.2}\right] \quad (3)$$

Where, μ = dynamic viscosity (centipoise),

T = temperature (°C), and C_1 = coefficient for scaling'

Table 10-2 Analytical calculation of Viscosity with respect to Oil Temperature [25,26]

Oil Temperature (°C)	***Dynamic Viscosity μ (kg/m·s)***	***Kinematic Viscosity v (m^2/s)***
30	**0.01405**	**1.65E-05**
35	**0.01209**	**1.42E-05**
40	**0.01046**	**1.23E-05**
45	**0.00909**	**1.07E-05**
50	**0.00794**	**9.35E-06**
55	**0.00696**	**8.19E-06**

The direct proportionality of viscosity with Reynolds Number (Re) [27], Reynolds number with friction factor (f), and friction factor with pressure drop (Δp) for laminar flow is given below as [25,26],

$$\mu \, \alpha \, \frac{1}{Re} \, \alpha \, f \, \alpha \, \Delta p \tag{4}$$

That results in the relation with the pumping power,

$$P_{pump} = \Delta p * \overline{V} \tag{5}$$

where, $\bar{V}$= volumetric flow rate [25,26].

Figure 20 shows the experimental results which infer that the change in viscosity has the direct impact on pumping power. That may be useful to derive the flow rate and operating conditions. It has a direct relation with operating cost too.

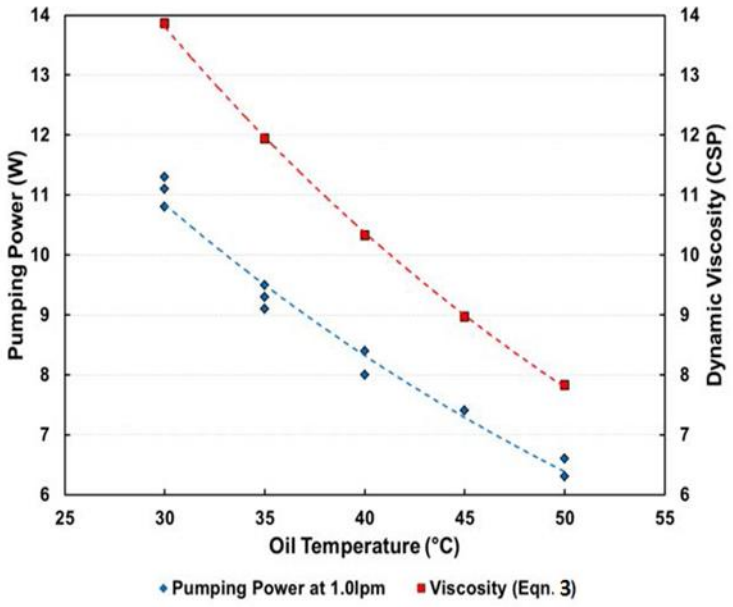

Figure 10-20 The relationship between pumping power and temperature dependent dynamic viscosity [25,26]

Since pumping power and flow rate are directly related to the operating cost, critical performance and efficiency of facility equipment, to study the phenomena regarding the change in viscosity of a mineral oil for data center operators becomes significant.

Temperature, oxygen availability, and presence of a catalyst (Thermal Aging) are the main factors that influence the chemical stability of oil. The hydrocarbon molecules in oil start to decompose at high temperature and that may cause the oil degradation process. The oxygen contents in cooling oil might lead to a rise of the acidity number and to sludge formation [28].

During an accelerated thermal aging process, it is also important to analyze the dielectric properties of mineral oil, such as the breakdown voltage, dielectric losses (tan A), and relative permittivity. There is some analysis carried out for transformer oil. The study of aging test and dielectric property analysis for the transformer (mineral) oil concludes that there is a chance of a leak during the operation and its less biodegradable property leads towards pollution; it has a low flash point and high pour point for transformer operations. At the end of the aging process, the mineral oil demonstrated lower breakdown voltages rather than at the starting. The tanδ of the mineral oil showed the significant variation during the different stages of aging test process. The effect of humidity should also be considered during the oil aging test [28].

Figure 21 indicates the dielectric strength of transformer oil (mineral oil) remains almost consistent across the temperature range of interest for data center applications (30°C-50°C) and Figure 22 shows the study of change in the dielectric property of oil in transformers which shows some degradation over time. The literature states breakdown voltage depends on water content, suspended particles, and cleanliness [29].

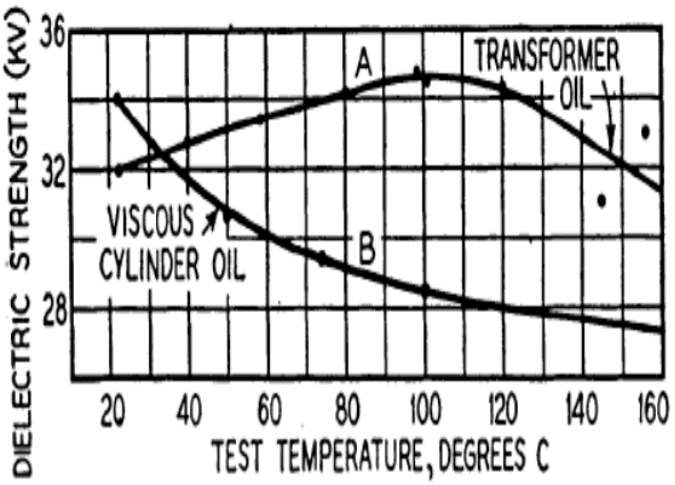

Figure 10-21 Temperature Dependence [29]

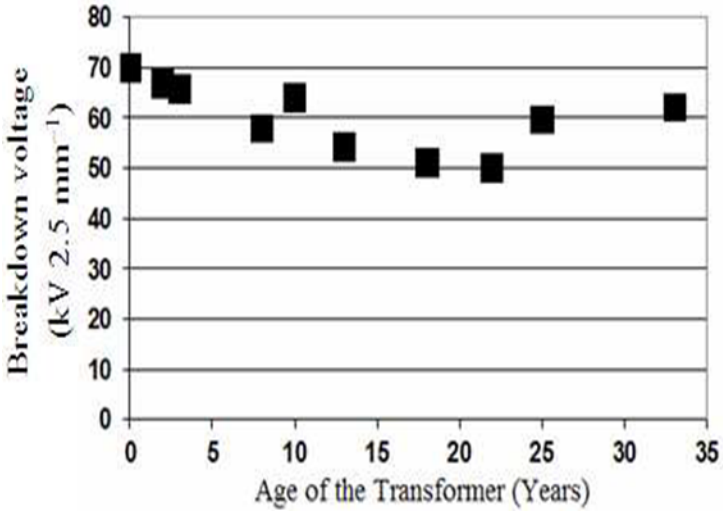

Figure 10-22 Breakdown over Time [29]

Thus, the dielectric property analysis for data center cooling mineral oil should be performed by proposing an aging testing methodology to provide the data for variation in properties to operators for advancements in oil cooling technology and to increase its applicability [29]. It would be an interesting study to observe the change in kinematic viscosity and thermal conductivity of a mineral oil during the actual operation as a function of temperature

and time. The comparative study of different engineered fluids should also be performed to provide more options to industries.

10.4 Accelerated Thermal Cycling (Atc) Trial Testing

The Joint Electron Device Engineering Council (JEDEC) and the American Society of the International Association for Testing and Materials (ASTM) standards won't be relevant due to the significant difference in the ramp rates of air and oil. Failure Mechanisms and Models for IT equipment established by these standards are not directly applicable in the reliability analysis of oil immersed components as oil immersion cooling has different operating conditions than the air-cooled data centers for which these standards have been derived. IEC and ISO test methods might not have the direct applicability to determine the real degradation in the properties of a mineral oil as the oil cooled data center has different parameters affecting the operation such as temperature, flow rate, varied surfaces, different materials etc. The air-cooled system has a high fluctuation in operating conditions such as temperature and relative humidity. The standard also represents such variations in thermal cycling with high temperature differences. In oil cooling, the temperature profile is more stable and even. So, the standard also needs to be developed for such conditions and parameters should be modified accordingly. It is important to provide design of experiment to perform reliability testing and evaluate the life cycle of oil cooled data centers.

The trial experiment (figure 23) was performed to determine feasibility of Accelerated Thermal Cycling (ATC) tests on oil in environmental chamber based on JEDEC standards.

- Cycling test conditions (settings on environmental chamber)
- THI = 100°C
- TLO = 0°C
- Ramp Rate = 10°C/min

- Dwell Time = 1hour
- Oil Volume = 1gallon

Figure 10-23 ATC Trial Testing setup in Environmental Chamber

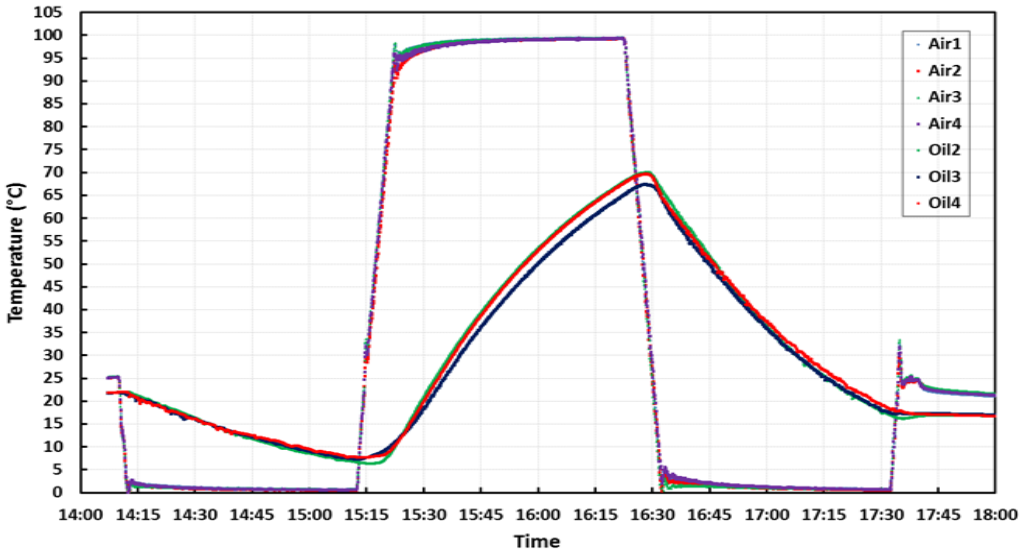

Figure 10-24 ATC Trial Testing results

Figure 24 shows the results of the trial test which was conducted to determine the feasibility of performing ATC tests on oil in the environmental chamber. Clearly, the ramp time and dwell times between air and oil are going to be significantly different. Thus, standards and common assumptions made for air cooling wouldn't apply for immersion cooling lifecycle. Since it seems unlikely that accelerated cycling will be able to be tested in a timely manner, an alternative test is sought. Elevated temperature tests (Thermal Aging) can be used to gather some results for PVC, PCBs, and passive components. In this proposed method, we need to maintain a temperature above typical operating temperature for an extended duration. This type of test is common in capacitor degradation tests.

10.5 Conclusion and Future Work

The information furnished here is based on strong literature review and quantifiable data gathered for validation. The study provides a strong background for direct and indirect reliability concerns related to oil cooling technology. The operators will have trustworthy data to implement this technology.

Oil immersion cooling may offer better practices in some developing countries like India, China, etc. where the environmental conditions for data centers are above ASHRAE G3 severity level and where it is hard to implement airside economizers to derive recommended environmental envelope. With the enhanced reliability, high heat dissipation and performance efficiency, oil cooling technology may serve the data center cooling technology world as a leader in the future.

As we can reiterate that the field of reliability for oil immersion cooling has a lot of scope for future work. The effects of a mineral oil and/or different engineered fluids on major components should be measured. We are currently working with Engineered Fluids, Inc which is a manufacturer of a wide range of dielectric fluids for different applications including EC-100 synthetic fluid for electronics cooling and testing a number of their fluids including EC-100 and

getting great results. The changes in electrical and chemical properties of mineral oil and fluids such as EC-100 should be investigated by aging test. The humidity and contaminant barriers, especially leaching out from plastics of cables and components should be checked. The temperature and heat density optimization should be carried out. Thus, the scope of studying thermal performance and reliability concerns of oil immersion cooling technology is of all data center operators' interest and concern.

10.6 Acknowledgement

This work is supported by NSF I/UCRC in Energy-Smart Electronic Systems (ES2).

10.7 References

1. Green Revolution Cooling (http://www.grcooling.com/)
2. Midas Green Tech (http://www.midasgreentech.com/)
3. http://green.blogs.nytimes.com/2012/09/06/cooling-a computer-server-with-mineral-oil/
4. http://www.liquidcoolsolutions.com/
5. D. Prucnal, "Doing More With Less: Cooling Computers with Oil Pays Off," The Next Wave, vol. 20, no. 2, pp. 20 - 29, 2013.
6. www.dfrsolutions.com
7. Jimil M. Shah, Oluwaseun Awe, Pavan Agarwal, Akhigbe Iziren, Dereje Agonafer, Prabjit Singh, Naveen Kannan and Mike Kaler, “Qualitative Study of Cumulative Corrosion Damage of IT Equipment in a Data Center Utilizing Air-side Economizer”, ASME IMECE 2016, November 11-17, 2016, Phoenix, Arizona, USA.
8. Jimil M. Shah, Oluwaseun Awe, Betsegaw Gebrehiwot, Dereje Agonafer, Prabjit Singh, Naveen Kannan and Mike Kaler, “Qualitative Study of Cumulative Corrosion Damage of Information Technology Equipment in a Data Center Utilizing Air-Side Economizer Operating in Recommended and Expanded ASHRAE Envelope”, ASME J. Electron. Packag 139(2), 020903.

9. Green Revolution Cooling, “Liquid Submersion Cooling Configuration”, http://www.grcooling.com/liquid-submersion-cooling-configuration/
10. C. Tulkoff and C. Boyd, "Improved Efficiency & Reliability for Data Center Servers Using Immersion Oil Cooling," in Electronic System Technology Conference & Exhibition, Las Vegas, NV, 2013.
11. Bergles, A.E., and Bar-Cohen, A., Immersion Cooling of Digital Computers, Cooling of Electronic Systems, Kakac, S., Yuncu, H., and Hijikata, K., eds, Kluwer Academic Publishers, Boston, MA, pp. 539-621, 1994.
12. Jimil M. Shah and Dereje Agonafer, “Issue on Operational Efficiency for Oil Immersion Cooled Data Centers”, Session Co- Chair and Presenter for ASME Panel On "Thermal Management Challenges in Energy Conversion & Conservation", ASME IMECE 2015, November 13-18, Houston, Texas.
13. Jimil M. Shah, Syed Haider I. Rizvi, Indu Sravani Kota, Sahithi Reddy Nagilla, Dhaval Thakkar, Dereje Agonafer, “Design Considerations Relating to Non-Thermal Aspects of Oil Immersion Cooling”, ASME IMECE 2016, Pheonix, AZ.
14. J. Shah, et. al., “Critical non-thermal consideration for oil cooled data-center”, IMAPS ATW 2015, Los Gatos, Ca, 2015.
15. Eiland, R., 2015, “Thermo-Mechanical Design Considerations at the Server and Rack Level to Achieve Maximum Data Center Energy Efficiency”, Ph.D. dissertation, University of Texas at Arlington, Arlington, TX.
16. Shah, J. M., 2016, “Reliability Challenges in Airside Economization and Oil Immersion Cooling,” Master’s thesis, University of Texas at Arlington, Arlington, TX.
17. Jimil Shah, Richard Eiland, Ashwin Siddharth, Dereje Agonafer, UT-Arlington, “Effects of Mineral Oil Immersion Cooling on IT Equipment Reliability and Reliability

Enhancements to Data Center Operations," IEEE ITherm Conference, May 2016, Las Vegas, NV.

18. H. Cheng, et. al. "Parametric Analysis of Thermally Enhanced BGA Reliability Using Finite Volume Weighted Averaging Technique" ASME IMECE, 1998
19. P. Rajmane et al., "Failure mechanisms of boards in a thin wafer level chip scale package," 2017 16th IEEE Intersociety Conference on Thermal and Thermomechanical Phenomena in Electronic Systems (ITherm), Orlando, FL, 2017, pp. 1099-1105.
20. Foad Rahimidehgolan, Gholamhossien Majzoobi, Farhad Alinejad, Jalal Fathi Sola, "Determination of the Constants of GTN Damage Model Using Experiment, Polynomial Regression and Kriging Methods", Applied Sciences 2017, 7(11), 1179; doi:10.3390/app7111179
21. Singh, P., Klein, L., Agonafer, D., Shah, J. M., and Pujara, K. D., 2015, "Effect of Relative Humidity, Temperature and Gaseous and Particulate Contaminations on Information Technology Equipment Reliability," ASME Paper No. IPACK2015-48176.
22. Kulkarni, et. al., "Physics Based Electrolytic Capacitor Degradation Models for Prognostic Studies Under Thermal Overstress", European Conference of the Prognostics and Health Management Society, 2012.
23. http://www.ecswire.com/tools/insulation_jackets/characteristics/#CSPE
24. http://www.thefoa.org/tech/ref/appln/datacenters.html
25. R. Eiland, J. Fernandes, M. Vallejo, D. Agonafer and V. Mulay, "Flow Rate and Inlet Temperature Considerations for Direct Immersion of a Single Server in Mineral Oil," in IEEE ITHERM, Lake Buena Vista, FL, 2014.
26. Eiland R, Edward Fernandes J, Vallejo M, Siddarth A, Agonafer D, Mulay V. Thermal Performance and Efficiency of a Mineral Oil Immersed Server Over Varied

Environmental Operating Conditions. ASME. J. Electron. Packag. 2017;139(4):041005-041005-9. doi:10.1115/1.4037526.

27. Behzad Ghadiri Dehkordi, Saleh Fallah, and Amirreza Niazmand, “Investigation of harmonic instability of laminar fluid flow past 2D rectangular cross sections with 0.5–4 aspect ratios”, Proceedings of the Institution of Mechanical Engineers, Part C: Journal of Mechanical Engineering Science, Vol 228, Issue 5, pp. 828 – 839, First Published June 26, 2013, https://doi.org/10.1177/0954406213491906
28. Endah Yuliastuti, “Analysis of dielectric properties comparison between mineral oil and synthetic ester oil”, Delft University of Technology, June 2010.
29. Clark, F. M., “Dielectric Strength of Mineral Oils” Electrical Engineering, Volume: 54, Issue: 1, 1935, pages 50 -55, DOI: 10.1109/EE 1935.6539592

Chapter 11

Design Considerations Relating to Non-Thermal Aspects of Oil Immersion Cooling

Abstract

Full submersion of servers in dielectric oils offers an opportunity for significant cooling energy savings and increased power densities for data centers. The enhanced thermal properties of oil can lead to considerable savings in both the upfront and operating costs over traditional air cooling methods. Despite recent findings showing the improved cooling efficiency and cost savings of oil as a cooling fluid, this technique is still not widely adopted. Many uncertainties and concerns persist regarding the non-thermal aspects of an oil immersion cooled data center. This paper presents useful information regarding a variety of factors related to the operation of an oil cooled data center. Pertinent material property considerations such as the chemistry, flammability, material compatibility, human health effects, and sustainability of mineral oil are discussed. A general introduction as to the chemical composition and production of mineral oil is provided. A discussion of the trade-offs in thermal performance and cost of the mineral oil is presented. The dielectric nature of oils is critical to their success as a cooling fluid for electronic applications. Factors such as temperature, voltage, and age that affect this property are reviewed. Flammability of oils is a valid concern when immersing costly IT equipment and the pertinent concerns of this aspect are reviewed. The evaporation loss of oil is also mentioned as refueling and safety are important parameters in the establishment of any facility. Leeching of materials, especially plastics, is a reoccurring concern expressed regarding mineral oil immersed IT equipment. Mineral oils are by-products of petroleum refining processes and as such may bring forth sustainability concerns associated with their use and disposal. The long term stability and performance of key physical and material parameters of oils used in applications such as high voltage power are typically monitored. The similarity and implications of the longevity of oils, when used for data center applications, will be examined. Other issues

related to the design, operation, and serviceability of submerged IT equipment and racks will also be addressed. Switching to an oil immersion cooled data center typically brings about several designs and operational changes compared to a typical air-cooled approach. A critical element of oil cooling often cited by opponents of the technology is the issue of serviceability of IT equipment. This paper will discuss some of the additional features a data center may need in place to help alleviate these concerns, as well as, best practices based on experience and observations by the authors. This paper also includes Cup Burner Experiment as per ISO 14520/NFPA 2001 standard to determine the minimum design concentration of fire extinguishing agent for the class B hazard of heavy mineral oil and the class C hazard of electronic equipment as a part of the safety concerns for oil cooled data centers. The visual observations of the servers after immersion in oil for 8 months are also explained for a better view of the system related issues. The discussion presented here is based primarily on literature gathered on the subject and quantifiable data gathered by the authors.

11.1 Introduction

With the fast growth of Information Technology Equipment, the concern for removing heat out is constantly increasing. The world is looking for cheaper and reliable sources to meet the need [1] [2]. In the vast expansion the use of Mineral Insulating oil for cooling IT equipment expanded a lot and now it becomes essential to monitor and maintain the reliability of cooling oil along with the durability concerns. To explore and develop a deeper understanding with the concept of oil Immersion cooling this paper provides the insight for current challenges.

The reason in choosing mineral oil for cooling purpose is its production and availability at a cheaper cost throughout the world. Also to mention here oil immersion cooling has an edge over water or air in terms of thermal properties which is the key in cooling microelectronics. The main resource of mineral oil is fossil fuel which contributes to 85% of the energy used in the world as shown in Figure 1.

Ever since we now have set up that mineral oil would have been a lot more effective to use for eliminating temperature by personal computers. It is also important to know about the operational efficiency with respect to the properties of fluid, compatibility of components, safety and serviceability.

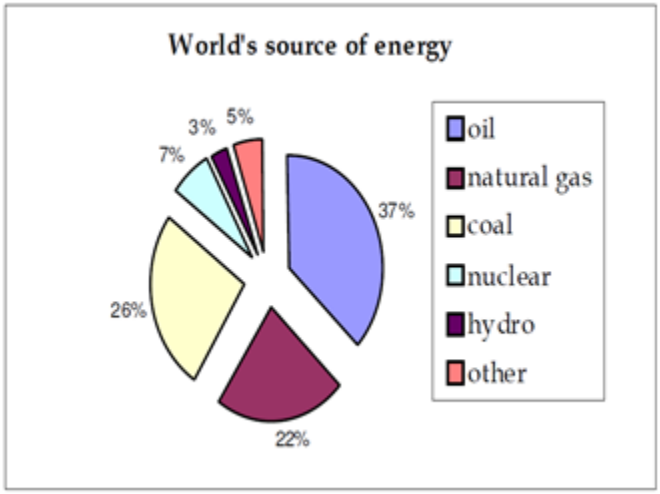

Figure 11-1 World's source of energy [11]

11.1.1 Oil Emersion Cooling System

The machine will be comprised of some sort of tank loaded with mineral oil that supports the computers and a pump element that contains a good oil-to-water temperature exchanger and oil circulation pump. With this installing, the warmth exchanger will be linked with the facility's cold water never-ending loop; on the other hand, this may not be required, because will be mentioned afterward. The actual oil will be circulated relating to the tank along with the temperature exchanger by way of a little pump. The actual pump swiftness will be modulated to help keep a consistent temperature inside the tank. That fits the air cooled water offer straight away to force. The style with the tank inner surface will be such that the neat oil coming from the temperature exchanger will be led to ensure the vast majority of this ought to pass through the computers before the time for the warmth exchanger. The actual combination of pump

swiftness modulation and oil ducting ensures that the air cooled water is used really proficiently. The machine solely sends the total required fulfilling the load, and the majority of what on earth is pumped goes by throughout the load [4].

There are three useful part benefits to immersion oil cooled besides their productivity. The program is designed to maintain a consistent temperature within the tank. Since the pump will be modulated to help keep a collection place temperature no matter what changes with server workload, the computers reside in a good isothermal environment. Among the factors that cause enterprise, motherboard downfalls are because of the mismatch inside the coefficients associated with cold weather expansion, as well as CTEs. The actual CTEs with the silicon, precious metal, solder, plastic-type material, and fiberglass utilized in some sort of enterprise motherboards are all different, meaning that these supplies expand and deal on different premiums with respond to temperature changes.

Within an environment in which the temperature will be transforming often as a result of heap changes, this particular variation with CTEs can easily at some point produce hardware downfalls about the enterprise motherboard. Oil immersion lowers this challenge simply by setting up a temperature-stable environment.

The 2nd part advantage will be server personal hygiene. Air-cooled computers are fundamentally facts heart fresh air purifiers. Even though facts are reasonably clean situations, there exists even now some dust and dirt found. A standard server holder will be drawing inside a big workplace full of fresh air every minute. Just about any dust as well as dirt because fresh air does accumulate inside the chassis with the computers.

The final part advantage of immersion cooled will be peace and quiet. Immersion cooled techniques to make almost no noise. This is not a good minor advantage, as numerous modern day air-cooled facts center operates around as well as earlier mentioned the

Occupational Security and Health and fitness Administration's allowed restricts intended for ability to hear security.

Along with effective by using air cooled water along with the part benefits mentioned above, there exists yet another edge to immersion cooled server solidity. A standard air-cooled server holder uses with regards to 10 kW. In certain cautiously engineered HPC shelves, 15–20 kW associated with load could be cooled down with fresh air. When compared, the typical off-the-shelf immersion air cooled program will be scored to support 40 kW associated with server load without unique architectural as well as working factors [4] [5].

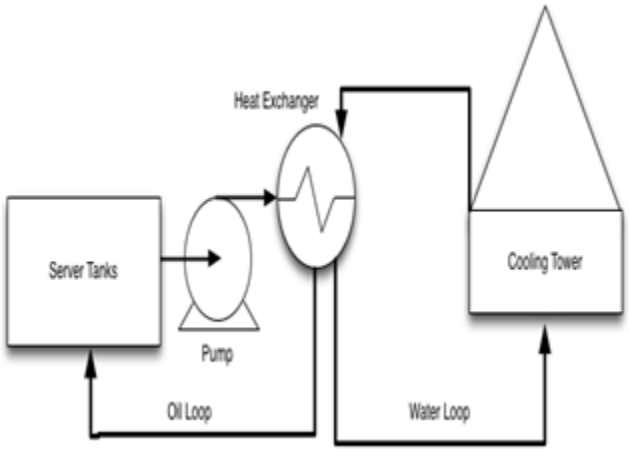

Figure 11-2 Schematic of oil cooled system [7] [8]

11.1.2 Lower Capital Cost

The infrastructure requirement of immersion cooling is much less compared to air cooling so, building an immersion cooling dedicated data center is considerably less expensive. Cooling an infrastructure requires a large portion of construction prices. Data centers with high reliability/availability, it's not uncommon for the cooling infrastructure to account for 50% of the construction price. According to the American Power Conversion Data Center Capital Cost Calculator, cooling infrastructure accounts for forty-third of the data center construction cost [4].

When the technical loads are high in large DATA centers around sixty MW, construction prices might rise abruptly to one billion dollars. About half of it is being spent on cooling infrastructure per data center. The major benefit of immersion-cooled systems is, they don't need chillers, CRAC units, temperature & humidity controls, high raised flooring etc., and hence there is a considerable reduction in financial expenditures over air-cooled systems [4] [5].

11.1.3 Lower Operating Expenses

Oil immersion cooling in comparison with air cooling has many advantages. The energy savings of the former is greater than the latter as much of energy in air cooling is taken up in cooling the fluid which is fan power and in circulating it. Approximately fan power takes up to 0.13W of power to move 1W of waste heat into chilled water loop. The technical load to power fan at 100 percent for fan powered air is 10.5 percent more than oil immersion. Refrigeration of 285tons is required by 1MW of technical load data centers. Usually, air cooling takes up to 600KW to cool 1MW of the technical load at 2.1KW per ton, whereas this taking up of energy is eliminated in immersion cooling using the oil as the server fans, chillers, etc., are not utilized on oil immersion cooling mechanism. Oil takes away approximately 1200 times more heat by volume when compared to air [4] [5].

Oil has higher performance and is readily available and lower in cost. This immersion cooling has the capability of cutting the construction costs of data centers in future in half. Oil immersion cooling can cool the high-density servers for only a small percentage of that of costs of air cooling. Also, it can support up to 30KW per rack of loads in comparison to the latter whose load support is limited to 15KW per rack. About 500 million dollars is spent in the construction of cooling infrastructure per data center and this cost doesn’t arise in the case of oil immersion cooling [5] [6].

11.2 Mineral Oil: Chemistries/ Properties

11.2.1 History

First in 1982, General Electric introduced Mineral oil as a dielectric coolant. Its high flash point and widespread production around the world were the key reasons for its selection. Mineral oil is a good insulating material as it has good electrical properties, aging behavior, low viscosity and low relative permittivity and can easily be refined from petroleum [10] [11].

The modern history of oil started in the nineteenth century with the refining of paraffin from unrefined petroleum. The Scottish scientist James Young in 1847 saw characteristic petroleum drainage in the Ridding's colliery at Alfreton, Derbyshire from which he refined light thin oil suitable for use as lamp oil, in the meantime, getting thicker oil suitable for greasing up apparatus. In 1981, petroleum oil as a use for transformer oil was discovered by Sebastian de Ferranti [11].

11.2.2 Mineral Oil: Chemistry

Crude petroleum acts as a source of extraction of petroleum oil, which contains hydrocarbons along with a little proportion of Sulphur and Nitrogen [11]. The molecules of hydrocarbons are mainly composed of Paraffin, Naphthenes, and Aromatics. Methane as a gas, normal butane and isobutane come under the group Paraffin, whereas Naphthenes contain ring structures which can be either with 6 carbons atoms within six-membered rings or 14 carbon atoms within three-membered rings. Aromatics also fall under the category of six-membered ring structures, monoaromatic meaning single ring and polyaromatic which refers to two or more rings [11].

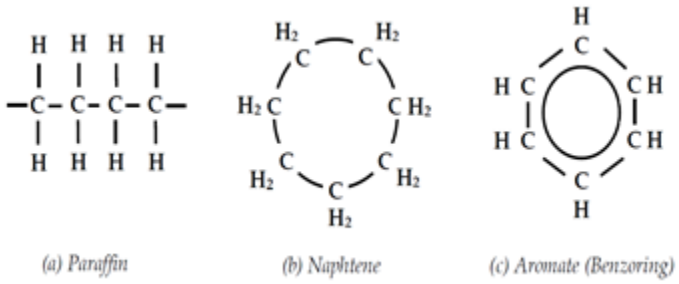

Figure 11-3 Hydrocarbons in the mineral oil [11]

On refining crude petroleum, useful products like gasoline, kerosene, lubricating oils, LPG (liquid petroleum gas), and so on are obtained. In this process, various steps like Sulfuric acid extraction, selective solvent extraction, earth filtration, hydrogenation, re-distillation, filtration, dehydration are followed and this process also consists of a vacuum distillation unit [11].

11.2.3 Mineral Oil: Chemical Stability

Factors that influence the chemical stability of oil are:

- Temperature
- Oxygen availability
- Catalyst presence

Extreme temperature can be a significant reason in the decomposition of the hydrocarbon molecules. This may lead towards the degradation of the mineral oil. Contents of Oxygen in insulating oil might lead to a rise of the acidity number and sludge formation. As per the standards, Copper and iron (Catalysts) should be dissolved in oil during aging process and might accelerate the aging process [11].

11.2.4 Mineral Oil: Desired Characteristics

Oil insulation has two important purposes in the data center operation, as the insulation material and the cooling medium. There are several other requirements for data center insulating oil:

- To act as a coolant, the main task of absorbing the heat from the package and the system and then transmitting it to the outer surface of the equipment. At higher temperatures, the viscosity of the oil decreases indeed facilitating the circulation of the oil. It is important to keep the pour point low so the oil is capable at any visible flow.
- Oil makes a good contribution to insulate different parts at different electrical potential by penetrating into and filling the spaces between insulation layers.
- Oil temperature in service should be maintained below its flash point and also to minimize the evaporation losses the volatility of the oil should remain low.
- In order to safety, it should not be a hazardous material [11].

11.3 Life Cycle of Oil

When the oil is in the process of extracting heat out of a chip in PCB which is a part of Information Technology Equipment, there are several processes which occur some of them are oxidation, contamination by; moisture, particles or fiber; overheating and electrical leakage [12]. The stability/ longevity of mineral oil depend on following factors:

11.3.1 Oxidation Stability:

The strength of mineral oil to withstand oxidation under thermal stress and in the presence of oxygen and copper catalyst is known as oxidation stability. Since almost all the oil submerged equipment are exposed to air so there is a wide chance of oil to get oxidized. Time being the critical factor in deciding the oxidation stage of the oil, as the sludge formation is an indication of oxidation in oil. Sludge can be soluble in oil depending upon the oil type; generally naphthenic oil accommodates sludge and keeps it soluble until saturation point reaches.

Another type is Paraffinic oil; they resist the solubility of sludge. Either way sludge plays an important role in the cooling operation of the equipment, once it starts accumulating in the corners and across the boundaries of pipes making the flow slow down causing an overheat. An early indication of oil oxidation can be done by monitoring color, appearance, moisture level and acidity level tests. Oxidation stability measures the expected life cycle of oil under service with electrical equipment. This factor becomes extremely important in data centers where the environment is contained and room for service is limited. There exist natural compounds in oil that inhibits oxidation known as oxidation inhibitors along with those synthetic inhibitors are also available to increase the stability of the oil. To calculate remaining lifetime of oil in operation or unused one there is test specified in IEC 61125 method (B) and IEC 61125 method (C) [20].

11.3.2 Interfacial Tension (IFT):

Interfacial Tension is used to provide a mean for detecting degradable products and soluble polar contaminants. A sudden decrease in IFT indicates non-compatibility and degradation between the components of server and oil. It's a good practice to measure IFT between oil and water prior to operation and during operation to get comparative results [20].

11.3.3 Particle count:

Particle count is the factor that directly affects other properties of the oil in the operation like dielectric strength, Viscosity, flash point and thermal efficiency of the oil. It defines the number of particles present in the oil while it is in operation. The particles can be from oil as well as from the equipment it is cooling. For instance, metallic, fiber, sludge etc. So a continuous filter system must be attached to oil chamber so that on every cycle it runs doesn't affect the performance of oil [21].

11.3.4 Flash Point:

The most important concern with the oil immersion cooled data center is ignition point of the oil since Flash point is the lowest temperature of the oil at which it can form an ignitable

mixture with air and can be hazardous for the whole facility. Low molecular hydrocarbons that cause lowering in flash point of oil are produced by either overheating or electrical discharge in the oil compartment which results in the breakdown of oil [22].

11.3.5 Viscosity:

Viscosity in oil has direct relation with the heat dissipation from ITE and is dependent upon the aging of the equipment, oxidation stability and temperature of the oil. Normal operation of the oil in given range of temperature doesn't alter the viscosity effectively except for extreme conditions of corona discharge and oxidation [23].

Viscosity is temperature dependent and should follow the relation:

$$\mu = C_1 * \mathrm{Exp}\left[\frac{2797.3}{T + 273.2}\right] \quad (1)$$

Where, μ is the dynamic viscosity in centipoise, T is the temperature in °C, and C1 is a coefficient for scaling (a value of 0.001383 was determined using the 40°C value from STE Oil data sheets as a reference point)

Table 11-1 Analytical calculation of Viscosity with respect to Oil Temperature [6]

Oil Temperature (°C)	Dynamic Viscosity μ (kg/m·s)	Kinematic Viscosity v (m^2/s)
30	0.01405	1.65E-05
35	0.01209	1.42E-05
40	0.01046	1.23E-05
45	0.00909	1.07E-05
50	0.00794	9.35E-06
55	0.00696	8.19E-06

11.3.6 Break Down Voltage:

The energy supplied to the insulation material decides its breakdown capabilities. Moisture can be the main factor which can affect the electrical stability of oil. The tendency of a mineral oil to attain water contaminates the mineral oil. In areas where oil is used for cooling of

ITE, the measurement of breakdown voltage tells the presence of particle and water in it. The low value of breakdown voltage shows free water and solid particles. But the absence of contaminants cannot be directly related to the high value of breakdown voltage [24].

11.3.7 Pour Point:

This property is a measure of oil flow at relatively low temperature. It is of immense importance where the data centers are located in cold regions and with the need to maintain the average temperature of oil in the compartment. To overcome the decrease in pour point oil toppings are added to get multivariate results [25].

11.3.8 Density:

Just like pour point, Density of white mineral oil is extremely important in cold climates when it comes to data center use. Density is not affected by the normal oil deterioration and it doesn't impact when it comes to comparing the quality of different oils. It helps in deciding oil with respect to climate condition for optimum operation. For instance, in a case of moisture formation in oil compartment the water crystals will float on the top of high-density oil while sink down in case of a low-density oil [26]. Also, the leaching out of materials from ITE would play a significant role in the difference of density which can be responsible in the variance of pumping power as well as thermal efficiency of the system.

11.3.9 Corrosive Sulfur:

Sulfur is an essential part of oil and it depends on the degree of refining, type of refining and the quality of crude oil used. The present Sulfur contents may disturb the oxidation stability of oil since more percentage of Sulfur compound in oil less will be the oxidation stability of oil. Corrosive Sulfur imparts oxidation so it is very necessary to know the percentage of Sulfur in provided oil before using since most specification needs oil free of corrosive Sulfur. At elevated temperature Sulfur on top of a hot metal surface can form metal Sulfides which eventually can disturb the electrical equilibrium of the oil [27].

11.4 Serviceability, Safety and Health Hazards

11.4.1 Serviceability

Sometimes, oil is prone to heat, water, oxygen and other catalysts which are harmful to its properties. So as to keep its quality, sampling and analysis regularly is recommended. Deterioration of oil can be known by just observing the color and its clarity through conservator's visor. This inspection can also be used to monitor leakage and spills of oil too [14]. Some serviceability issues may arise like systems must drain before removing to avoid slip/fall hazards. [15] [16]

Mineral oil is a dielectric fluid, so that there will be no circuit breakdowns [17]. To determine the serviceability of the oil, some parameters must be taken into consideration, [18]

- Electrical parameter
- Physical parameter
- Chemical parameter

In order to reach factory heat, run performance, the oil should maintain its dielectric performance, age very slowly and to have sufficient heat dissipation and desired viscosity properties. The quantity of acidic materials present in the oil determines its acid number. As the oil ages in service increases the acid number that the oil is oxidized or contaminated with foreign matter. Dielectric losses in oil insulation are determined by the dissipation factor also called as oil power factor. Contamination and deterioration can be evaluated with this factor [17]. For the oil to be in service, it should be as non-volatile as possible and must possess a higher viscosity at the working temperature and should be of lower carbon content [18].

11.4.2 Spill and Disposal:

11.4.2.1 Prevention

The spilling of a material asks for special precautions in order to prevent fatal accidents. As its less biodegradability, it should be prevented entering sewers or water streams in the case if spillage has occurred. The further spill may create slipping hazards and evacuation of all non-essential personnel from the spill area should be the first step. As the oil floats on water, absorbent material and pads are useful. Spills may need to be reported to the national response center (800/424-8802) [13].

11.4.2.2 Waste Disposal Methods

The mineral oil can be hazardous waste without proper handling and disposing of oil as per federal law guidelines. To increase the recycling and reuse of the material, the federal law approved treatment and special disposal sites should be followed. The exposure of spillage can be hazardous for a waste water treatment system and may demand for chemical and biological oxygen. Spill material may show some biodegradability if gradually exposed to microorganisms. Land farming, incineration, and land disposal are potential treatment and disposal methods [13].

11.4.3 Flammability

The liquids which have a flash point below 100 deg., those are called as “Flammable Liquids”. The flash point of a mineral oil is 388 F (197.7C) and a boiling point is of around 590F (310C). That proves that mineral Oil is not a flammable liquid. It is a Class IIIB Combustible Liquid which means that to make it burn, it must be exposed to high heat before it will sustain a flame [13].

11.4.4 Health Hazards:

The handling of mineral oil must be considered with great importance in regard to personal hygiene.

- Direct contact may result in irritation.

- Much care must be taken in the case of prevention of release of mineral oil into the environment. [13]
- Short-term exposure does not signify health hazard.
- Inhalation for a short period of time also does not affect much.
- Eye contact, skin absorption and skin irritation are not observed for short-term exposure.
- Ingestion will cause a cathartic (Laxative) effect and the digestive tract may experience some irritation.
- Aspiration into lungs may cause Lipoid Pneumonia. [13]

11.4.5 Safety Concerns

The major safety concerns and recommendations are listed below:

- How the oil is handled in a data center depends on its flash point, the rate of evaporation and density.
- If the oil evaporates significantly at the bath operating temperatures then the vapor has to be continuously vented so as not to accumulate in the tank or in the room and increase the risk of a fire or explosion.
- In production environments, the tanks would need to be installed in a separate room with fire doors and away from other IT equipment. This is so that if there is a fire, it won't spread easily to the rest of the data center. Extra fire suppression would be installed in this room.
- For oils with a high flash point (>500F), water suppression may be sufficient even if the oil floats as the goal is to cool the oil quickly using water. However, if the oil is denser then it is even better as the water can form a layer above the oil and act as an oxygen barrier.

- High flow water sprinklers and higher density of sprinkler heads are generally recommended near and above the oil tanks.
- Installation on a raised floor requires sprinklers to be installed in the underfloor region.
- For oils with a lower flashpoint, evacuation of the oil away from the computer room and use of gas fire suppressant may be necessary.
- 8. Tanks need to be installed with mechanical thermal safety switches so that power to the IT equipment and oil tank is cut in case the oil temperature gets too high.
- 9. Tanks and oil circulating equipment and plumbing need to be made of fire resistant materials such as stainless steel or rolled steel. Plastics should be avoided. The tanks must have a lid that is kept closed during normal operation, and be made strong enough to protect the tank in case of falling burning debris. Aluminum could be used for secondary containment but not for the tank or the plumbing as it can deform at high temperatures and there is a risk of oil leaking out of the tank and adding fuel to the fire.

The fire tests that might be needed to run would be to build an approximation of an immersed server inside the oil and see a few things:

1. What are the ways that we can get the server container to burn? This would be to document the likely failure modes.
2. Document temperatures of server or power supply components which caused ignition.
3. What is the heat release rate of a server container when allowed to burn? A cone calorimeter is the test apparatus to capture this.
4. What is the extinguishing concentration of various clean agents for the oil being used?
5. Can the fires spread to other containers once the initial one starts to burn?

In short, it is necessary to determine at what the flash point of the oil, which is being used and then determine what the required extinguishing concentration will be to extinguish the fire should one start.

It is very essential to obtain various properties of petroleum oil for using it in any manufacturing process. In this regard the comparative determination of Volatility of various oil samples becomes very important.

The tests which are being used to determine volatility of mineral oil do not provide such information regarding the indication of what may be expected when these mineral oils are exposed to oxidation and evaporation under certain conditions. It had been observed that under certain conditions the evaporation and oxidation rates were accelerated which were totally different from the results obtained while conducting the tests under A.S.T.M designation D 6-30.

11.4.6 Minimum Extinguishing Concentration [MEC]

11.4.6.1 Objective

The test method involves the determination of flame extinguishing concentration of 3M™ Novec™ 1230 Fire Protection Fluid by cup burner experiment that is in line with the NFPA standard 2001.

11.4.6.2 Guidelines:

The following guidelines for FK- 5-1-12 (chemical notation for Novec™ 1230 fluid) mentioned in NFPA standard 2001 (Flame extinguishing concentration for class B fuels as described in Annex B section 5.4.2) were taken into account [33]:

1. The flame extinguishing concentration for class B fuels shall be determined by the cup burner method described in Annex B.

   Caution: Under certain conditions, it can be dangerous to extinguish a burning gas jet. As a first measure, the gas supply shall be shut off.

2. Measurement equipment used in applying the cup burner method shall be calibrated.
3. The flame extinguishing concentration for Class A fuels shall be determined by test as part of a listing program. As a minimum, the listing program shall conform to ANSI/UL 2127 or ANSI/UL 2166 or equivalent.

4. The minimum design concentration for a Class B fuel hazard shall be the extinguishing concentration, as determined in point 1, times a safety factor of 1.3 [33].

11.4.7 Experimental Procedure

This test method covers the procedure for determination of the cupburner extinguishing concentrations for which the ISO 14520-1: 2006 Annex B Determination of flame-extinguishing concentration of gaseous extinguishants by the cupburner method was used [32]. The apparatus consisted of a cylinder filled with saturated Novec™ 1230 fluid vapor placed in a heated bath of 3M™ Novec™ 7500 Engineered Fluid at 90 ºC constantly maintained by the help of a heating tape and a variable transformer. A metering valve with a Vernier handle was introduced at the exit point of the gas column to control the flow of saturated Novec™ 1230 vapor into the air stream. The air flow rate was controlled with a manostat rotameter [35].

The air/agent mixture was made to converge in a common stream and was passed

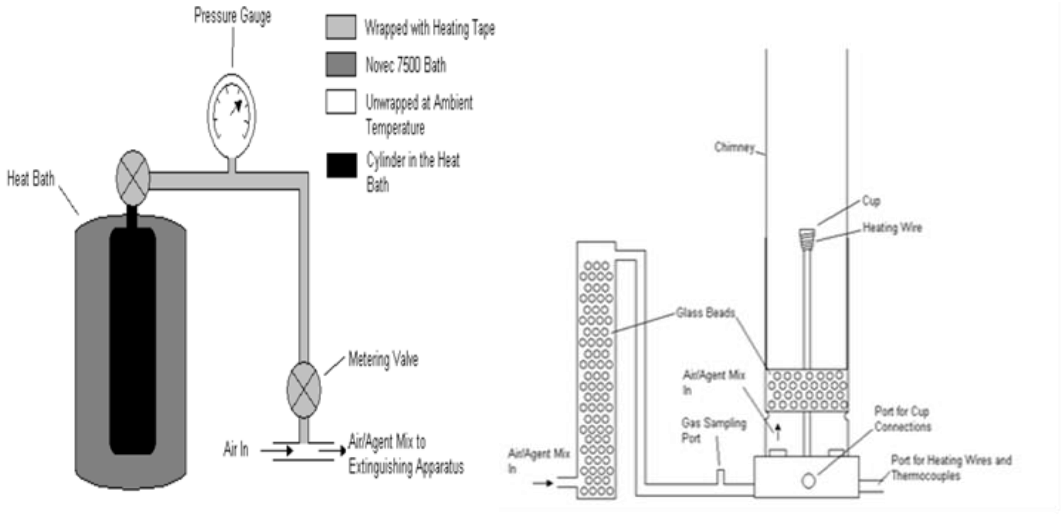

Figure 11-4 Supply Apparatus to Air Flow [34] [36]

through a column filled with glass beads to achieve uniformity in the gas mixture before the gas sampling port [36].

11.4.8 Results:

The cupburner extinguishing concentration for Light Mineral Oil as determined in the test phase was 5.24 ± 0.19 percent concentration by volume (ideal gas assumption). The complete Light Mineral Oil test results are shown in Table 2.

Table 11-2 Light Mineral Oil Summary of Experimental Results

	Average Value	Standard Deviation	Number of Values	Error +/-
[g/cm^3]	6.880E-04	2.914E-05	5	2.554E-05
[vol %]	5.24	0.22	5	0.19

The cupburner extinguishing concentration for Heavy Mineral Oil as determined in the test phase was 5.38 ± 0.20 percent concentration by volume (ideal gas assumption). The complete Heavy Mineral Oil test results are shown in Table 3.

Table 11-3 Heavy Mineral Oil Summary of Experimental Results

	Average Value	Standard Deviation	Number of Values	Error +/-
[g/cm^3]	7.063E-04	2.931E-05	5	2.569E-05
[vol %]	5.38	0.22	5	0.20

11.4.9 Conclusions:

The final recommended extinguishing concentrations with Novec 1230 fluid for the Light Mineral Oil and Heavy Mineral Oil fuels are shown below in Table 4.

Table 11-4: Recommended Novec 1230 Fluid Cup Burner Extinguishing Concentration

Fuel	Extinguishing Concentration [vol %]
Light Mineral Oil	5.3
Heavy Mineral Oil	5.4

Extinguishing concentrations are marked up to the design concentrations used in system design. Per the NFPA standard, following is the calculation for minimum design concentration for Novec 1230 for the class B hazard of heavy mineral oil.

$$5.4 \times 1.3 = 7.02$$

This exceeds the minimum design concentration for the class C electrical equipment, so it would both extinguish class B and C hazards.

11.5 Material Reliability and Compatibility

Immersion cooling attacks the device level. The major components which come directly in contact with mineral oil are:

- Printed circuit boards (PCBs)
- Electronic packages
- Insulation (PVCs)
- Passive components (resistors, capacitors, etc.)
- Switching Devices and optic fiber

The impact of mineral oil immersion on the reliability and operability of servers and electronic components becomes significant and should be studied properly before establishing the data center facility. The changes in different properties of components, as well as mineral oil, may cause serious issues during operation. It is important to provide DOE to perform reliability testing and evaluate the life cycle of oil cooled data centers.

The trial experiment was carried out to check the feasibility of Accelerated Thermal Cycling tests so that the material compatibility experiments can be performed.

Figure 5 shows the experiment set up for the initial trial for ATC feasibility. Objective is to determine feasibility of Accelerated Thermal Cycling (ATC) tests on oil in environmental chamber based on JEDEC standards.

Figure 11-5 Environmental chamber and test set up

Cycling test conditions (settings on environmental chamber):

THI = 100°C

TLO = 0°C

Ramp Rate = 10°C/min

Dwell Time = 1 hour

Oil Volume = 1 gallon

Figure 6 concludes that the ramp time and dwell times between air and oil are going to be significantly different. Alternative methods which are analogous to JEDEC and ASTM standards should be developed.

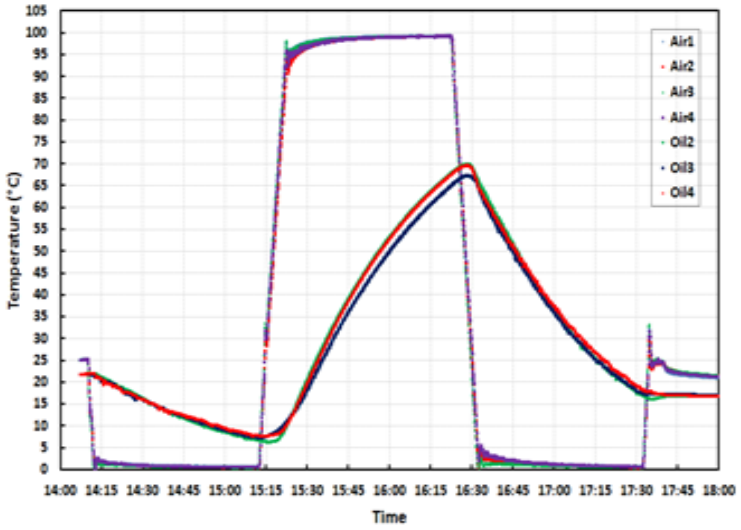

Figure 11-6 Results – ATC Trial Testing [28] [31]

11.5.1 Visual/ Cosmetic Changes:

Figure 11-7 Adhesives concerns

Figures 7 and 8 show some visuals/cosmetic changes observed in the oil cooled test setup after keeping servers immersed in mineral oil for 8 months. Here we can see that barcode sticker was very easily removed by light touch. Pooling of oil under the label is easily seen, too.

That shows the attack of mineral oil on the adhesive. Ink(labeling) can also be the issue for identification at the time of serviceability [29] [30] and [31].

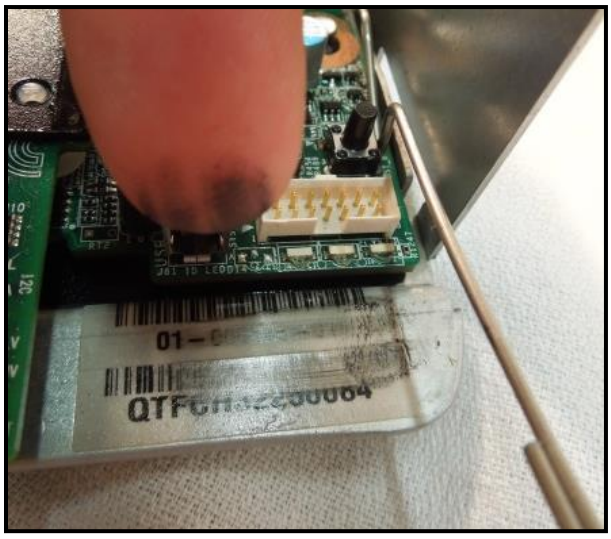

Figure 11-8 Ink/ Labeling issues

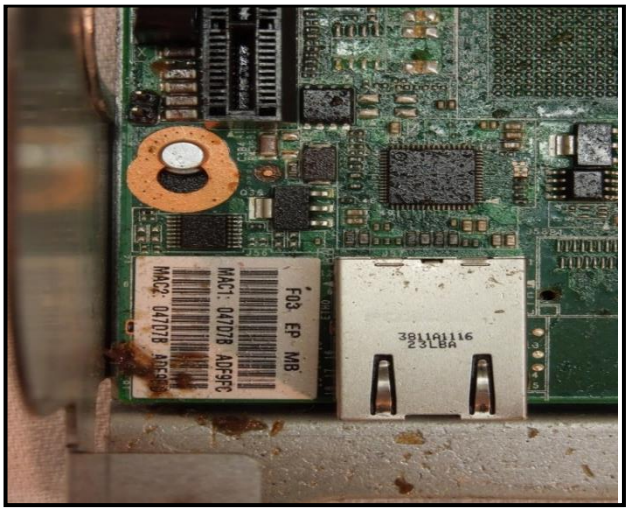

Figure 11-9 Dust and particulates

Picture 9 shows the accumulation of debris and particles because of improper upstream handling makes mineral oil contaminated during the operation and creates the problems in the flow of fluid by clogging or blocking the pipes during circulation. This heavy debris was likely

collected during the shipping process but highlights the residual oil's propensity to collect contaminates [29] [30] and [31].

11.5.2 Potential Failure Modes: Contamination and Cleanliness:

An oil cooled system's biggest impact may be on:

- Serviceability:
    - Dust/contamination issues when removing and replacing servers from oil tanks during servicing
- Inventory tracking of server components:
    - Labels and ink being removed by handling

Possible system clogging/contamination by adhesives, labels, and debris

- Proposed Suggestions:
    - Improved methods of mitigating residual surface oils
    - Possible use of RFID tags instead of label [29] [30] and [31].

11.6 Conclusion and Future Work

Mineral oil should be environmentally sustainable working fluid which cannot differ with respect to its solvency for common system contaminants. The refining process and additives of inhibitors play an important role in the chemical and oxidation stability of mineral oil. For the longevity of mineral oil in operation, it should be equipped with the inhibitors for desired characteristics. Fluid dielectric properties should not affect the signal integrity and dielectric properties of components. Fluid should not affect the reliability and compatibility of components beyond the certain threshold limit which can be responsible for the failure of the system.

The effect of contaminated and degraded mineral oil on the thermal efficiency of the data center should be studied. The improvements to IT equipment (thermal and mechanical design) for more efficient systems should be made in order to achieve optimum cooling efficiencies.

The operational efficiency of oil cooled data center depends on the life of oil, serviceability and safety. The desired properties can be achieved by additives, but chemical stability should be maintained by inspection of oil at regular intervals. The sustainability of the system depends on the longevity of oil and the oil should be prevented from moisture, catalysts and dust contaminants. For that oil should be tested before use, in service and after use. The material compatibility should be determined to predict the life curve of the data center.

The visual observation raises concerns related to the serviceability and inventory control. The proposed solution can be useful for the smoother operation of the data centers.

The oil cooled data center can be cheaper and more efficient as compared to air cooling because of its system requirement over the conventional air cooling unit and reliability enhancements like even and stable temperature environment, noise reduction, corrosion reduction.

11.7 Acknowledgement

We would like to acknowledge Mr. David P. Olds (Fire Suppression Applications | 3M Electronics Materials Solutions Division | 3M™ Novec™ 1230 Fire Protection Fluid (Not an HFC)) from 3M for being the cup burner value source, however this is only part of an entire fire detection and suppression system provided by Kidde Fire Systems and designed and installed by a trained and authorized local representative.

This work is supported by NSF I/UCRC in Energy-Smart Electronic Systems (ES2).

11.8 References

1. Green Revolution Cooling (http://www.grcooling.com/)
2. Midas Green Tech (http://www.midasgreentech.com/)
3. http://green.blogs.nytimes.com/2012/09/06/cooling-a computer-server-with-mineral-oil/
4. D. Prucnal, "Doing More With Less: Cooling Computers with Oil Pays Off," The Next Wave, vol. 20, no. 2, pp. 20 - 29, 2013.
5. Submersion Cooling Evaluation, PG&E's Emerging Technologies Program;
6. R. Eiland, J. Fernandes, M. Vallejo, D. Agonafer and V. Mulay, "Flow Rate and Inlet Temperature Considerations for Direct Immersion of a Single Server in Mineral Oil," in IEEE ITHERM, Lake Buena Vista, FL, 2014.
7. C. Tulkoff and C. Boyd, "Improved Efficiency & Reliability for Data Center Servers Using Immersion Oil Cooling," in Electronic System Technology Conference & Exhibition, Las Vegas, NV, 2013.
8. www.dfrsolutions.com
9. Bergles, A.E., and Bar-Cohen, A., Immersion Cooling of Digital Computers, Cooling of Electronic Systems , Kakac, S., Yuncu, H., and Hijikata, K., eds, Kluwer Academic Publishers, Boston, MA, pp. 539-621, 1994.
10. Shah, J., Eiland R., Rizvi, H., Agonafer, D., "Critical Non-Thermal Factors for Oil Immersion Cooled Data Center", IMAPS ATW 2015, Los Gatos, California.
11. Endah Yuliastuti, " Analysis of dielectric properties comparison between mineral oil and synthetic ester oil," Delft University of Technology, June 2010.
12. "Fluids for electro technical applications - unused mineral insulating oils for transforms and switchgear", international standard, IEC, 3rd edition, 2003-11.

13. "Material safety data sheet" by STE oil company, Inc. “Revised IEC standard for maintenance of in-service insulating oil” by Prof.B.Pahlavanpour, Dr. M. Eklund, Mr. K.Sundkvist, Nynas Naphthenic
14. “HPC cooling: liquids and systems” by Phil Hughes, CEO, Clustered Systems Company, Inc
15. www. Energymangertoday.com
16. ”Analysis of transformer oil with the help of image processing” by Mr. A shish S.Waychal, Prof.Y. N. Bhosale, Mr. Shruhari Kulkarni, dept of EE, MSEDCL
17. “Transformer failure rate prediction based on condition assessment”, by M.Ahfaz khan, Dr. A.K.Sharma.
18. “Electrical world”, volume 67, Mc Graw-Hill,1916.
19. “Standard Test Method for Oxidation Stability of Mineral Insulating Oil”-Active Standard ASTM D2440
20. Electrical Power Equipment Maintenance and Testing, Second Edition by Paul Gill
21. IEC 60970 Insulating liquids – “Methods for counting and sizing particle”
22. ISO 2719:2002 – “Determination of flash point”
23. ISO 3104 Petroleum products -- Transparent and opaque liquids – “Determination of kinematic viscosity and calculation of dynamic viscosity”
24. IEC 60156 Insulating liquids – “Determination of the breakdown voltage at power frequency”
25. ISO 3016 Petroleum products – “Determination of pour point”
26. ISO 3675 Crude petroleum and liquid petroleum products – “Laboratory determination of density”
27. DIN 51353 Testing of insulating oils “detection of corrosive sulfur; silver strip test”

28. Jimil M. Shah and Dereje Agonafer, “Issue on Operational Efficiency for Oil Immersion Cooled Data Centers”, Session Co- Chair and Presenter for ASME Panel On "Thermal Management Challenges in Energy Conversion & Conservation", ASME IMECE 2015, November 13-18, Houston, Texas.
29. Jimil M. Shah, “Reliability challenges in airside economization and oil immersion cooling”, The University of Texas at Arlington, May 2016.
30. Richard Eiland, “Thermo-Mechanical Design Considerations at the Server and Rack Level to Achieve Maximum Data Center Energy Efficiency”, The University of Texas at Arlington, May 2015.
31. Jimil M. Shah, Richard Eiland, Ashwin Siddharth, Dereje Agonafer, “Effects of mineral oil immersion cooling on IT equipment reliability and reliability enhancements to data center operations”, ITHERM 2016, Las Vegas, NV.
32. The ISO 14520-1: 2006 Annex B Determination of flame-extinguishing concentration of gaseous extinguishants by the cup burner method
33. NFPA 2001: Standard on Clean Agent Fire Extinguishing Systems
34. Brian P. Carnazza, John G. Owens PE, Paul E. Rivers PE, Justin S. Schmeer, “FK-5-1-12 PERFORMANCE CHARACTERISTICS: RECENT DEVELOPMENTS”, 3M Industrial Chemicals Laboratory, 2011.
35. ISO 14520-1:2000(D) © ISO 2000, Method of evaluating inerting concentration of fire extinguishing vapour, ISO copyright office, Case postale 56 CH-1211 Geneva 20.
36. Robin, Mark, et al, US Patent No. 6112822, Method for Delivering a Fire Suppression Composition to a Hazard …, September 5, 2000.

Chapter 12

Accelerated Thermal Degradation of Printed Circuit Board, Passive Components and Fiberoptic Cables for Single Phase Immersion-Cooled Data Centers

12.1 Introduction

Cooling of high-power IT equipment is not a problem without a host of solutions. Non-traditional methods like water-cooling and rack-mounted cooling have been adopted by operators in an effort to push power-densities. One such practice is the immersion cooling of IT equipment. It proves to be a powerful and cost-efficient technique as it eliminates the need for server fans, elevated flooring and a Computer Room Air Conditioning (CRAC) unit. In an immersion cooling system, the hardware enjoys a few benefits like having lower junction temperature, no temperature swings or hot spots, and it generally runs more reliably with improved performance [1]. It is the practice of immersing the servers in a dielectric coolant. The fluid utilized must have adequately low electrical conductivity so as not to interfere with the usual operations of the device. In the event that the fluid is, to some degree, electrically conductive, it becomes crucial that the vulnerable parts of the equipment be protected from electromagnetic interactions. Hence, it is desirable that the fluid be dielectric [2].

Submerging the majority of a server's heat generating components in a dielectric fluid engenders dependability issues at the gadget level [3], and this paper reports on the authors' attempts to explore those issues and whether they warrant special preventative care. Dielectric fluids are not only used in computing and electric power applications, but also in medical and domestic applications. In single phase immersion cooling, the dielectric fluid coolant dependably remains in liquid state (as opposed to the two-phase coolants that change state from liquid to gas and back). The coolant fluid is in contact with the equipment submerged in the bath and is pumped through the equipment towards a heat exchanging system that extracts the heat gathered by the coolant. This heat exchanging system allows for the rejection of the coolant's

heat to a water-cooled circuit. Thus, overall, single phase immersion-cooled data centers would observe lower maintenance cost, lower coolant cost, absence of coolant evaporation and reduction in noise compared to air cooled ones [2,4].

There is a need for a framework for testing IT equipment cooled by means of oil-immersion, as there is a lack of an established methodology or industry standard for the same. Such a framework for the maintenance and serviceability of immersion-cooled data centers can be based on the ideas and recommendations put forth in, “Design Considerations Relating to Non-Thermal Aspects of Oil Immersion Cooling”. This paper reviews the changes brought about by oil-immersion in the physical and electrical properties of three types of essential data center server components: printed circuit boards, electrical components, and fiberoptic data cables.

To comprehensively understand the effects of aging components in oil-immersed environments, the testing was divided into three parts:

I. Assessing the change in material properties, specifically Young’s modulus
II. Measuring changes in electrical properties
III. And lastly, the visual as well as micrographic analysis of the components

ASTM D3455 is an industry standard available for testing compatibility of various materials with mineral oil. With necessary modifications made for server components, it is possible to devise a method for testing compatibility with both mineral and synthetic dielectric fluids. The modifications that were implemented in this experiment were as follows:

- The dry run cycle was reduced to 8 hrs at 30^{o}C and 10% RH
- The baking time of the sample was reduced to 4 hrs at 45^{o}C and 35% RH
- And the cycle time was reduced from 164 hrs at 100^{o}C to 72 hrs at 45^{o}C [5].

Accelerated Thermal Cycle (ATC) testing, especially the 'ATC JEDEC' standard, which is utilized for air-cooling has a crucial limitation. Due to vastly different heat capacities, there is a

considerable difference in the ramp rate of air and oil, making the JEDEC standard redundant for oil-immersion testing.

Printed circuit board serves a basic but essential function in servers. In order for them to perform satisfactorily when immersed in oil, their mechanical and electrical reliability has to be. An accelerated thermal cycling test would enable us to establish, if any exists, a correlation between aging time (number of cycles) and an ideal indicator of mechanical performance. Since in this case, the main constituents are polymeric and metallic in nature, a good test for mechanical performance would be one based on change in elastic modulus of the PCB sample, as a whole, with time. In order to gauge if any aging phenomena are triggered, in addition to the mechanical analysis, a close inspection of formation of cracks and/or ingress of dielectric fluid in the PCB is necessary. Any distinctly high variations in Young's modulus, outer appearance, or surface morphology would warrant a deeper investigation, and as such, this study serves to form the foundation upon which further research on the reliability of using oil-immersion as a viable alternative to air-cooling can be performed.

In the case of passive components, a careful inspection of any microstructural cracks, which decide the mechanical and electrical execution of key server functions is of prime importance. The study attempts to analyze the change in the electrical properties. The electrical properties such as resistance, capacitance etc. are measured using the multimeter and the microstructure imaging is performed using the Scanning Electron Microscope (SEM). By investigating any trends in resistance or capacitance change over thermal cycles against the normal or standard performance of pristine passive components, significant information about the compatibility and reliability considerations of single-phase oil-cooled systems can be acquired.

Optical cables are employed in systems that require higher data transmission rates, thus enjoying vast use in data center intra and inter-rack connections. Maintaining the integrity

of the transmitted signal is critical, and to this end, it is necessary to test if there is increased diminution in the mechanical and optical performance, over time, of oil-immersed interconnections as compared to traditionally air-cooled ones. Extensive ingress of oil can lead to structural or optical changes at the core-cladding interface, leading to increased attenuation. Extant and even the most recent literature on mechanical testing of water-immersed optical fibers reveals that the effect of diffusion of water into the cable structure is the dominant factor in mechanical degradation, as attested by Glaesemann [12] and Dwivedi [13]. However, there does not exist any documented testing of optical cables by high-temperature aging upon immersion in mineral or synthetic oil. The analysis done in this research serves to fill that gap in knowledge by testing certain assumptions about the extent of change in thermomechanical behavior of thermally aged IT hardware components immersed in single-phase oil, with the fundamental assumption concerning optical cables being that they would stiffen (increased elastic modulus) with aging time.

12.1.1 Aim and Objective

The primary objective of this work is to quantitatively ascertain and characterize the potential degradation of operability of single-phase oil-immersed components. It is an exercise in elucidating the reliability concerns of active and passive server components, and optical data cables due to the possible physical or chemical action of dielectric fluid. The objectives are stated below:

1. To expand the scope of hardware components that can be reliably cooled by means of oil immersion to include PCBs, passive components and fiberoptic data cables
2. To outline a comprehensive methodology for testing these components, and develop an understanding of the impact of oil immersion cooling on reliability of data center components

3. To conceive and execute a well-designed experiment that can be used as a general approach for testing the performance of IT equipment immersed in dielectric coolants
4. To track the evolution of material properties (Young's modulus) of PCBs and optical cables with time and compare against the pristine as-received components, which could reveal potential for modeling lifetime estimates
5. To record the electrical performance of the passive components over various thermal aging cycles
6. To compile a body of information to enable industry to make more educated decisions for mechanical and functional robustness of IT hardware, based on the results of compatibility with dielectric oil
7. To make necessary comparisons between results of testing on mineral oil-immersed, synthetic oil-immersed against air-exposed control specimens, in order to evaluate the ideal candidate for choice of coolant.

12.2 Methodology

12.2.1 Sample Preparation

The samples were prepared and baked in accordance with the ASTM D3455. After each cycle, the specimens were taken out and the experiments were performed to record the changes in material properties, electrical performance, and visual as well as micrograph analysis for any cracks. The results of the experiments are discussed in this paper.

12.2.2 Printed Circuit Board

A printed circuit board is composed of a flat sheet of insulating material and a layer of copper foil, laminated to the substrate. Samples of PCB were prepared using Isomet 1000 precision cutter. The IsoMet 1000 is a precision segmenting saw intended for cutting different kinds of materials with negligible deformation. This accuracy cutting machine is perfect for fragile parts by just utilizing gravity fed force [6]. Its extraordinary flexibility in chucking allows

into consideration holding a wide range of test shapes and configurations giving the present lab an exactness cutting machine fit for sectioning practically any material including fragile or ductile metals, composites, cements, laminates, plastics, electronic gadgets, and bio materials. Samples prepared using the cutter, have a dimension of 50mm*10mm. The unknown elastic modulus of the sample was tested using the DMA machine. For the sample dimensions when using a hard sample, thin out the thickness (for bending measurement) and make the cross-section area smaller (for tension measurement). PCBs have an average stress/strain ratio of 12 GPa to 19 GPa depending on the board manufacturers. They can operate between temperatures of -50^{o}C to 110^{o}C.

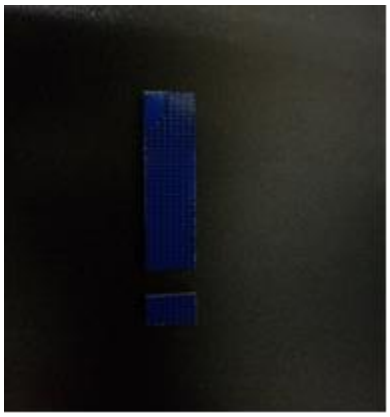

Figure 12-1 Printed circuit board

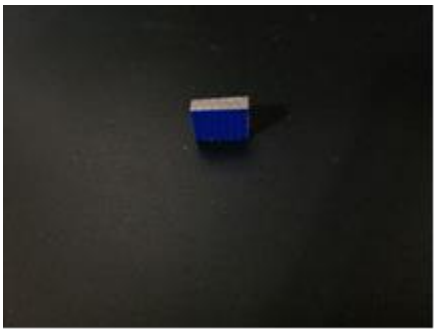

Figure 12-2 Cut section image of PCB for SEM

12.2.3 Passive Components

The passive components were procured based on the surface mount components used in the servers. The list of components used for the experiment are Thick Film Resistor, Polymer Capacitor, Electrolytic Capacitor, Transistors and Printed circuit boards. A thick film resistor is generally a Surface Mount Device (SMD) and typically called as chip resistor. Thick film resistor is widely used in electrical and electronic industry and it is cheaply available [7]. The thick film resistor used in this experiment as a resistance of 1 k ohms and can be operated at a maximum temperature of 105^{o}C.

Figure 12-3 Thick Film Resistor

The electrolytic capacitor is a form of polarized capacitor. This type of capacitor is constructed using two thin films of aluminium foil, one layer being covered with an oxide layer as an insulator. The term aluminium electrolytic capacitor refers to the capacitor used along with the aluminium foil. A paper sheet soaked in the electrolytic solution is placed between them and then the plates are wound around one another and placed into a can [8]. The electrolytic capacitor used in this experiment as a capacitance of 100 µF and 470 µF and can operate in a temperature range of -55^{o}C to 105^{o}C.

Figure 12-4 Electrolytic Capacitor

The polymer capacitor is similar to aluminium electrolytic capacitor in construction, it as anode foil, cathode foil and different paper separator in between. Instead of a liquid electrolyte, the polymer capacitor will have a solid polymer [9]. The polymer capacitor used in this experiment as a capacitance of 270 µF and 560 µF and can operate in a temperature range of -55^{o}C to 105^{o}C.

Figure 12-5 Polymer Capacitor

A transistor is a miniature electronic component that can do both different tasks like an amplifier and can also act as a switch. Depending on the material used for doping in transistor we can classify the terminal as N-type and P-type. The NPN and PNP junction transistors are quite commonly used in the electronic appliances. We have used both NPN and PNP transistors in this experiment. The transistor can operate without flaw till the temperature range of 150^{o}C.

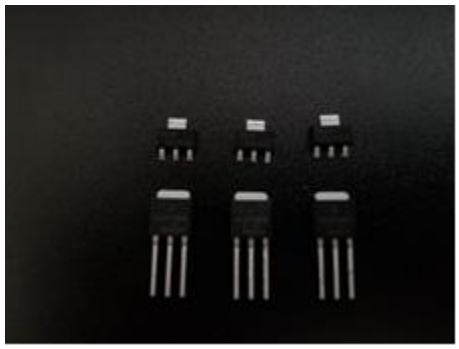

Figure 12-6 NPN and PNP Transistor

Printed circuit boards produce the electronic circuits ordinarily used in the industry. Glass reinforced plastic (FR4 type) produces the boards with the help of copper tracks in the place of wires. Active and passive components are settled in position by penetrating openings through the board, finding the parts and then fastening them in place. The copper tracks connect the components together, framing a circuit. Mounting the electrical parts on the printed circuit boards require an assembly process. This procedure should be possible by hand or through specific apparatus. The assembly process requires the utilization of solder joint to put the components on the board.

12.2.4 Fiberoptic Cable

Active optical cables (AOCs), a relatively new choice for data transmission networks, are enjoying growing use in data centers. They are a variant of standard multimode fiber that is preferable for short reach interconnections. The AOC tested in this work was a standard OM2 category Silica-based two-circular-core multimode fiber (MMF) cable.

Since the cable was the primary focus of this study, samples were cut out only from the cable part of the equipment, and not the transceivers. Three, approximately 50 cm-long sections were cut out from the 3 meters of active optical cable used in this test. To gauge the effect of immersion on aging of fiber coating, the ends of said sections were kept open and immersed to enable entry of oil. This was connected with the possibility that due to the eventual ingress of

the dielectric oil through the cable jacket, there would be physical contact with the cladding coating, which protects the central part of an optical cable, the core. Thus, assessing the impact of that on the mechanical function of the cladding coating would be integral to the experiment.

Figure 12-7 Air-Exposed Fiberoptic Cable Sample

50 cm long sections of the as received, pristine cables were cut to be placed in an environmental chamber for thermal aging tests. As explained in the following section, the experiment was divided into four cycles, and after each of the cycles ended, 15 cm sections were cut out of the longer 50 cm sections of cables from each jar. Subsequently, three specimens were cut from said 15 cm sections, and immense care was exercised while cutting to make sure that no yellow yarn strands (the strength or strain relief member in the cable) were pulled out, so that both the fibers were intact, and any possible inaccuracy was avoided. The circular cable specimens were each approximately 5 cm in length, and had an average outside diameter of about 2.9 mm.

Figure 12-8 Oil-Immersed Sample

12.2.5 Experimental Set up and Procedure

Accelerated aging conditions were achieved by immersing the component samples in a zero-stress condition in jars containing mineral oil and commercial synthetic engineered fluid placed in a climatic chamber at an elevated temperature for a total duration of 288 hours. The environmental chamber used for this experiment was Thermotron SE-600-10-10. Initially, the environmental chamber underwent a dry run, immediately followed by the baking cycle. During the baking cycle, all the components placed inside the chamber had minimal contact with each other. 5 1L Borosilicate glass jars were used, wherein two were filled with mineral oil, another two with synthetic fluid and one jar was exposed to the air at the temperature and RH setpoint in the environmental chamber, to serve as a control for the effect of immersion. The jars containing the fluids were each filled up to the 800 ml mark. Subsequently, the samples of active, passive components, and optical cable were submerged in each of the dielectric fluids. The specimens were divided into three sets, wherein one of the sets was placed in the synthetic oil jars, the second in the mineral oil jars, with both of the jars were closed tightly, and the third in the air-exposed jar, which had no cover placed on it. Out of the two jars containing the same fluid, PCB samples and passive components were placed in one jar and optical fibers in the second one to eliminate even a remote effect of the materials of different components on each other.

Figure 12-9 Environmental chamber containing the synthetic and mineral oil jars with components

Following that, all five jars were placed in the environmental chamber and a 72-hour cycle was initiated.

Figure 12-10 Thermotron display with environmental chamber conditions

Upon completion of the first 72 hours, a set of samples from all five jars was taken out using tongs and stored in airtight aluminum packets after which the next cycle for the period of 72 hours was started. This was done for 4 cycles, thus totaling an aging duration of 288 hours. This entailed a ramp time of approximately 1 hour and dwell time of between 70-71 hours for each cycle. The choice of 45 °C temperature and 35% RH setpoints closely resembled the

choice of aging conditions in literature. 35% RH corresponding to a 30°C dew point in 45°C dry bulb chamber temperature is low enough to remove moisture as a variable, and is relatively close to realistic air-cooled data center operating conditions. Once the samples were extracted from the jars, they were put through the relevant mechanical and electrical tests. For active components and fiberoptic cable, the Young's modulus was experimentally determined using the DMA 7100 machine, and its evolution with time was plotted in a graph. Elastic modulus is an ideal indicator of changes in mechanical properties of polymeric materials immersed in oil. This is substantiated by results reported by A Leal-Junior et al. Data generated by the software for elastic modulus facilitated the characterization of frequency and temperature-dependent viscoelastic properties of the polymeric materials in the optical cable and PCB, under sinusoidal excitations [10,11]. The data for the cable samples was recorded at two different frequencies – 1 Hz and 5 Hz. A small sinusoidal force amplitude of 100 mN was applied by the machine on the sample with a strain amplitude of 20 μm (0.1% strain). For passive components, the change in electrical properties such as capacitance, resistance, and barrier voltage were recorded, and the material characteristics were recorded for capacitors and resistors by making a cross-section and performing SEM imaging. The results are discussed in the next section.

Figure 12-11 Cut section image of Electrolytic Capacitor, Polymer Capacitor and Thick Film Resistor respectively for SEM

12.3 Results and Discussion

12.3.1 Printed Circuit Board

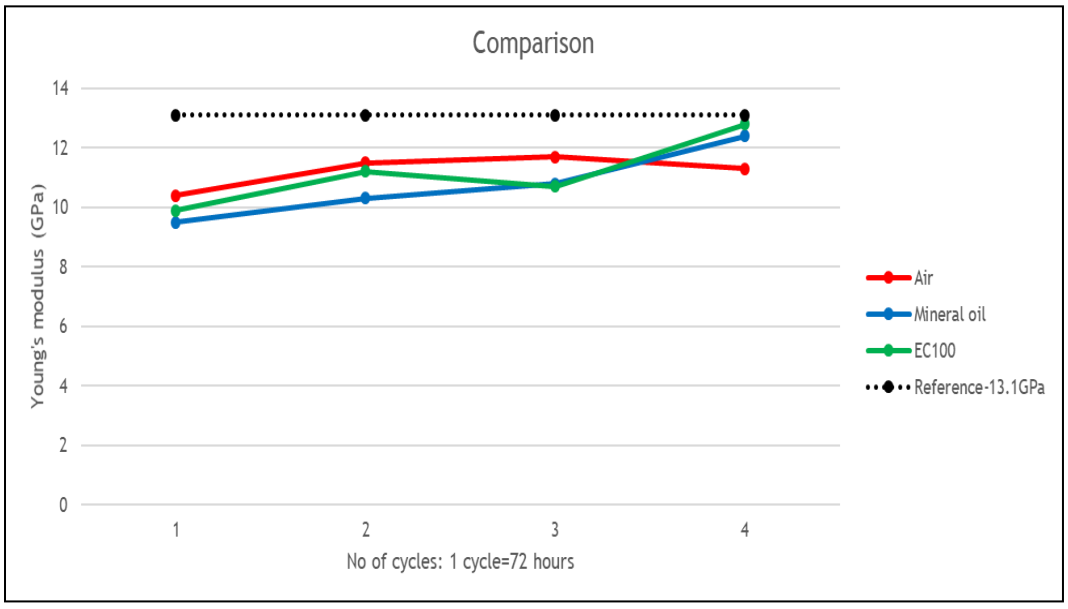

Figure 12-12 Comparison of Young's Modulus of PCBs: exposed to Air vs Immersed in Mineral Oil vs Immersed in Synthetic Fluid

The brittleness of the component increases with increase in Young's Modulus. In our experiment, it is evident that the Young's Modulus of the specimens is well below the reference value of 13.1 GPa. The PCBs are well reliable to use for Immersion Cooling application.

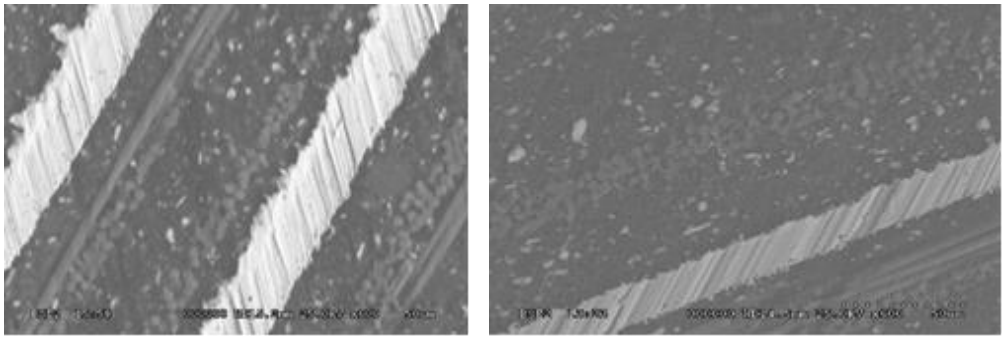

Figure 12-13 SEM Analysis for Mineral oil and Synthetic fluid immersed PCBs

Figure 13 shows SEM analysis for mineral oil and synthetic fluid immersed PCBs. This analysis was performed on the samples after the 4th cycle (288 hours) of thermal aging. In both cases, there is no sign of crack formation or oil penetration on the components. There is no deformation and the structural integrity was maintained.

12.3.2 Passive Components

The electrical property of the passive components from each of the medium are measured after each thermal cycle of 72 hours. The measured results along with the SEM Imaging are discussed in this section:

Using the trend data of the electrical properties measured we have created graphs to show the comparative variation in the electrical properties of the samples exposed to air vs samples Immersed in Mineral Oil vs Synthetic Fluid. The change in resistance of the Thick Film Resistor tested in 3 different mediums is represented below.

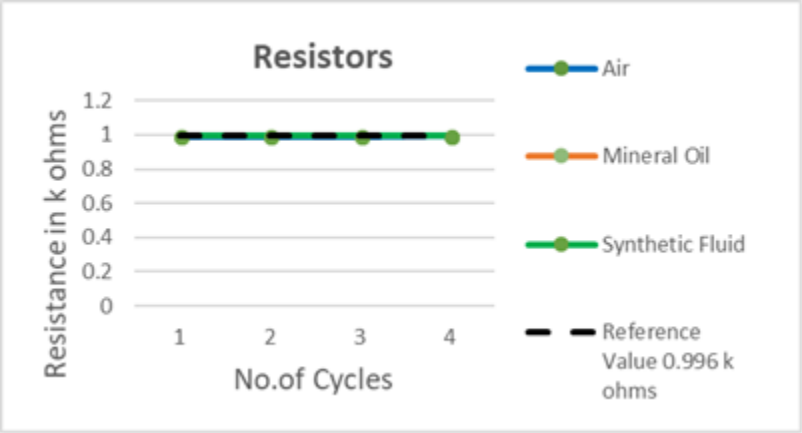

Figure 12-14 Change in resistance of samples exposed to various medium vs no. of thermal cycles

From the Graph above it is evident that the resistance is maintained constantly at the reference value for all the 3 conditions during the thermal cycling. It states that the thick film resistors are as reliable to use in Immersion Cooling as used in the Traditional cooling method. The authors have taken 2 different electrolytic capacitors for the experiment and their recorded value of the electrical properties are recorded and plotted as a graph which is illustrated below.

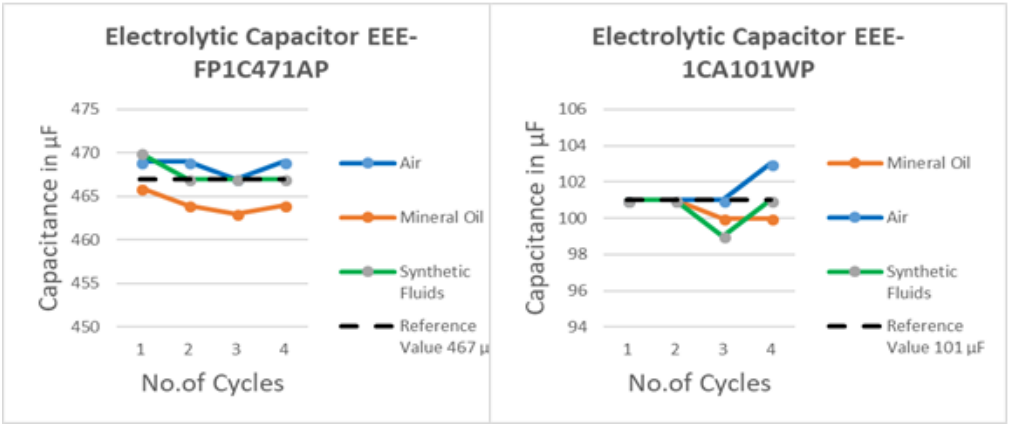

Figure 12-15 Change in capacitance of the Electrolytic Capacitor exposed to various medium vs no. of thermal cycles

The allowable tolerance of the electrolytic capacitor is 20% of its original or reference value. From the above graph it is evident that the variation in the capacitance is well within the allowable range and hence it is safe and reliable to use in Immersion Cooling.

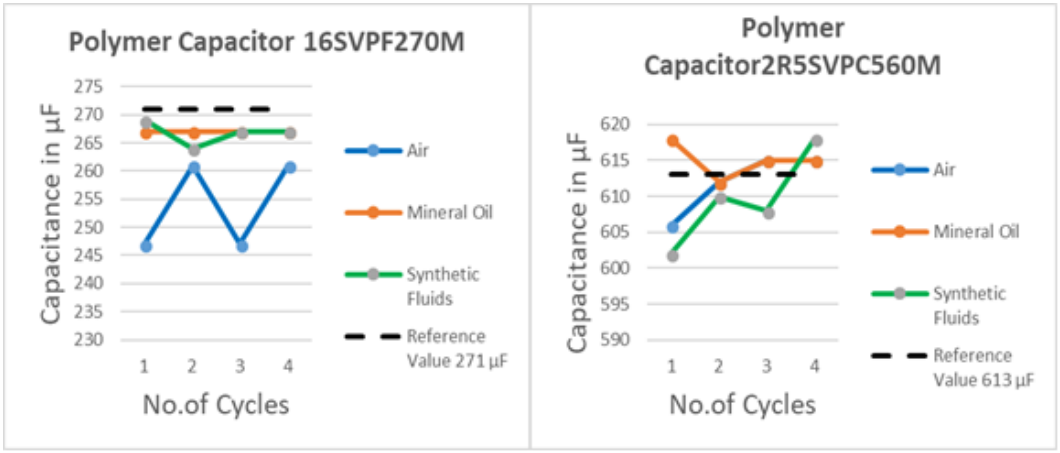

Figure 12-16 Change in capacitance of passive capacitors exposed to various medium vs no. of thermal cycles.

The allowable tolerance of the polymer capacitor is 20% of its original or reference value. From the above graph it is evident that the variation in the capacitance is well within the allowable range and hence it is safe and reliable to use in Immersion Cooling.

Table 12-1 Air-Exposed vs Mineral oil immersed vs Synthetic Fluid immersed PNP Transistor

PNP		BASE TO EMITTER	BASE TO COLLECTOR	EMITTER TO BASE	COLLECTOR TO BASE	COLLECTOR TO EMITTER
Test 1 (72 hour Cycle)	Air Exposed	OL	OL	0.671	0.67	OL
	Mineral Oil Immersed	OL	OL	0.671	0.67	OL
	Synthetic Fluid Immersed	OL	OL	0.671	0.669	OL
Test 2 (144 hour cycle)	Air Exposed	OL	OL	0.671	0.67	OL
	Mineral Oil Immersed	OL	OL	0.671	0.67	OL
	Synthetic Fluid Immersed	OL	OL	0.671	0.669	OL
Test 3 (216 hour cycle)	Air Exposed	OL	OL	0.671	0.669	OL
	Mineral Oil Immersed	OL	OL	0.671	0.669	OL
	Synthetic Fluid Immersed	OL	OL	0.669	0.669	OL
Test 4 (288 hour cycle)	Air Exposed	OL	OL	0.671	0.669	OL
	Mineral Oil Immersed	OL	OL	0.667	0.667	OL
	Synthetic Fluid Immersed	OL	OL	0.671	0.669	OL

Table 12-2 Air-Exposed vs Mineral oil immersed vs Synthetic Fluid immersed NPN Transistor

NPN		BASE TO EMITTER	BASE TO COLLECTOR	EMITTER TO BASE	COLLECTOR TO BASE	COLLECTOR TO EMITTER
Test 1 (72 hour Cycle)	Air Exposed	0.575	0.556	OL	OL	OL
	Mineral Oil Immersed	0.57	0.554	OL	OL	OL
	Synthetic Fluid Immersed	0.571	0.552	OL	OL	OL
Test 2 (144 hour cycle)	Air Exposed	0.574	0.557	OL	OL	OL
	Mineral Oil Immersed	0.574	0.556	OL	OL	OL
	Synthetic Fluid Immersed	0.575	0.557	OL	OL	OL
Test 3 (216 hour cycle)	Air Exposed	0.576	0.557	OL	OL	OL
	Mineral Oil Immersed	0.573	0.556	OL	OL	OL
	Synthetic Fluid Immersed	0.574	0.556	OL	OL	OL
Test 4 (288 hour cycle)	Air Exposed	0.574	0.556	OL	OL	OL
	Mineral Oil Immersed	0.573	0.556	OL	OL	OL
	Synthetic Fluid Immersed	0.571	0.554	OL	OL	OL

As shown in Tables 1 and 2, for both the PNP and NPN transistor the values of the voltage across the terminals for all the thermal cycles are within the range specified which means they are reliable to use with the immersion cooling technique.

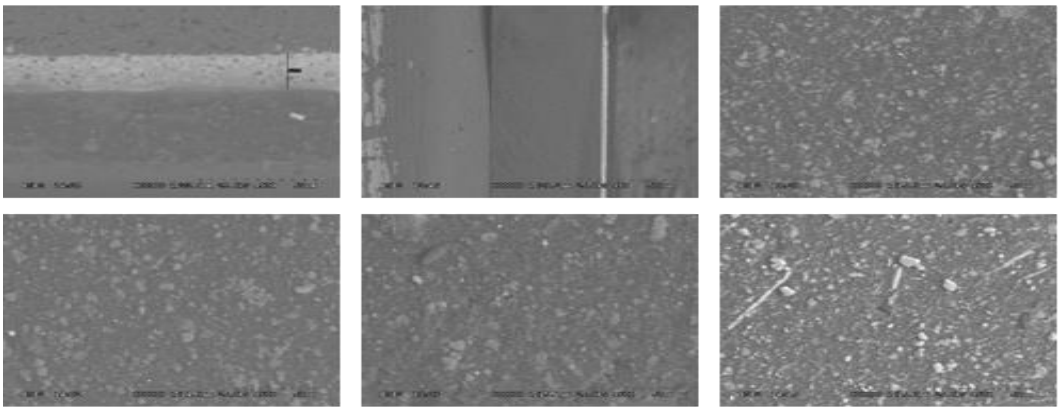

Figure 12-17 SEM Images of Components taken from 4th Thermal Cycle. (from top left) Thick Film resistor immersed in mineral oil, (2nd from top left) Thick Film Resistor immersed in Synthetic Fluid, (top right) Rubber Sealing (EPDMS) of Electrolytic capacitor immersed in Synthetic Fluid, (2nd from bottom left) Rubber Sealing of Polymeric capacitor immersed in Mineral Oil, (bottom right) Rubber Sealing of Polymeric capacitor immersed in Synthetic Fluid.

From the SEM images, we can infer that the structural integrity of all the components was maintained. There is no formation of crack or penetration of fluid on the surface of the components. The Rubber sealing used in the Electrolytic capacitor is Synthetic Rubber {Ethylene propylene diene monomer (EPDMS)}. These results show that there is no effect of dielectric fluids on the material property of rubber sealing.

12.3.3 Optical Cable

The DMA test results of 2-3 specimens after each of the four thermal cycles were recorded and studied. For convenience and consistency, the results reported are the ones observed for the 1 Hz frequency. The results of the DMA tests at the DMA furnace temperatures of 40 °C and 22 °C have been presented in Figures 18 and 19 respectively. Numerical values are in Tables 3 and 4 respectively. Changes in the viscoelastic properties indicate changes in the macromolecular polymer chain structure of either the jacket or the cladding coating or both.

Table 12-3 Numerical values of DMA results at 40 °C

E (Mpa)				
Cycle	**Air-exposed**	**Mineral oil**	**EC-100**	**Baseline**
1	22.9	84.5	144	28.57
2	30.7	149.2	253	28.57
3	38.9	294	311	28.57
4	35.9	316.9	321.8	28.57

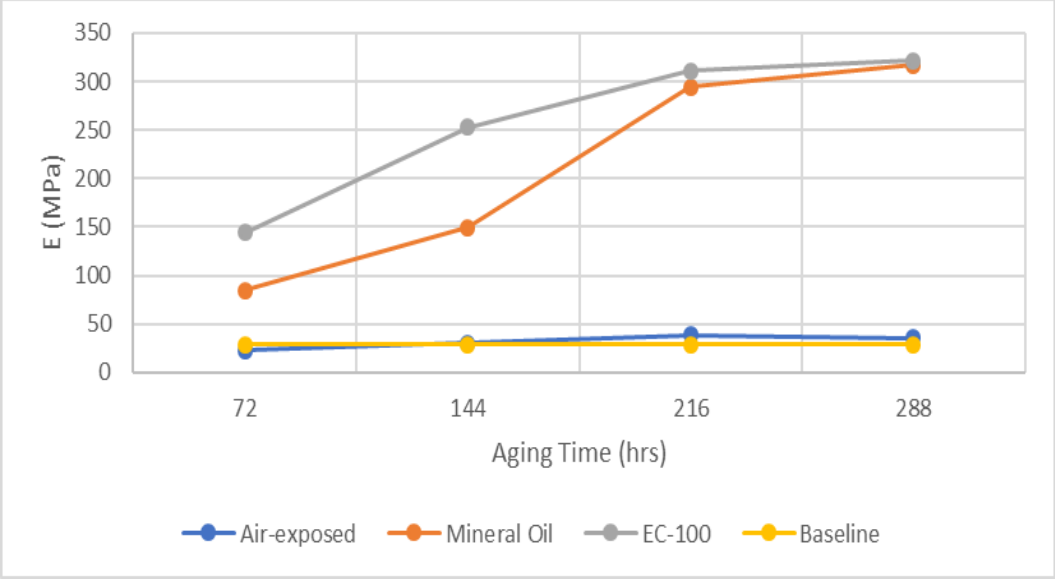

Figure 12-18 Evolution of complex/elastic modulus over aging time at DMA furnace temperature of 40°C

Table 12-4 Numerical values of DMA results at 22 °C

E (Mpa)				
Cycle	**Air-exposed**	**Mineral oil**	**EC-100**	**Baseline**
1	120	484	676.6	101.35
2	100	653.8	860	101.35
3	102.5	950	945.5	101.35
4	108.3	901.5	930.6	101.35

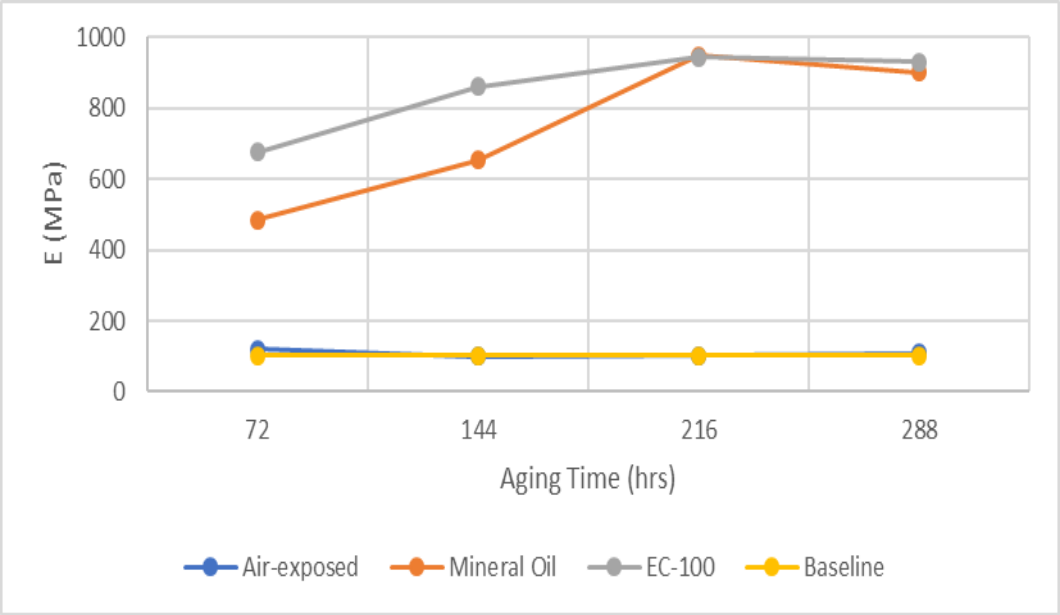

Figure 12-19 Evolution of complex/elastic modulus over aging time at DMA furnace temperature of 22°C

To better understand the underlying mechanism of the elastic modulus changes in the thermoplastic PVC jacket due to aging by immersion in high-temperature oil, the Young's modulus (E) vs. time results may prove sufficient. The rate of change of elastic modulus, which is a strong indicator of thermomechanical behavior, undergoes a reduction by the third cycle. Logarithmic trends fitted to the data in the graphs bolster the hypothesis that the effect of aging is self-limiting and slows down after the first few cycles. PVC jacket hardness is increasing due to plasticizers leaching out and/or ingress through diffusion of oil. Coating toughness rose in magnitude and may contribute to increase in the fiber mechanical strength. Stiffness and Young's modulus of cable increased with aging time, as hypothesized, and this was in agreement with recent and extant literature. Reduction in elastic modulus change over aging time is proposed to be due to two competing phenomena:

1) Increased initial diffusion of oil molecules through PVC jacket, and loss of plasticizers due to elevated aging temperature increasing diffusion coefficient, and aggregation of the PVC molecules increasing microvoids. The loss of plasticizer is causing PVC molecules to aggregate and allow for more voids for the oil-ingress. High temperatures damage acrylate coatings, which might deteriorate its adhesion to the fiber, causing delamination and exposing the bare fiber to undergo cracking/fractures.
2) Increased thermal degradation of fiber coating entails stiffening, reduced ductility, and increased net strength resulting in reduction in diffusion of oil molecules, as evident from tanδ peak shifts.

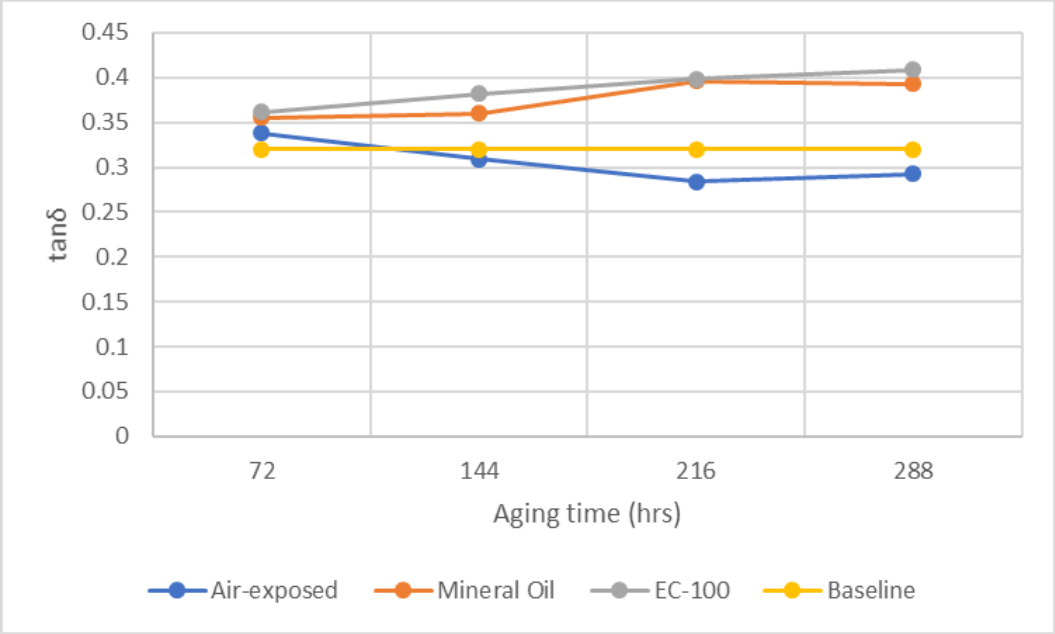

Figure 12-20 Tanδ peak shifts with aging time

The effect of immersion on loss tangent (ratio of storage modulus(E') to loss modulus(E'')) for all samples is tabulated in table 5. The upward trend in tanδ peaks, as seen in Figure 20 is indicative of elevation in glass transition temperature (Tg), and since it is strongly

dependent on the content of plasticizer and general polymer chemical state [14], it is reasonable to conclude that some plasticizer leached out into the oil as a result of aging.

Table 12-5 The effect of immersion on loss tangent (ratio of storage modulus (E') to loss modulus(E''))

Cycle	**Air-exposed**	**Mineral oil**	**EC-100**	**Baseline**
1	0.33830526	0.35529798	0.361604	0.319697
2	0.30887017	0.35970908	0.382362	0.319697
3	0.28423888	0.39612275	0.398727	0.319697
4	0.29276326	0.39275625	0.408451	0.319697

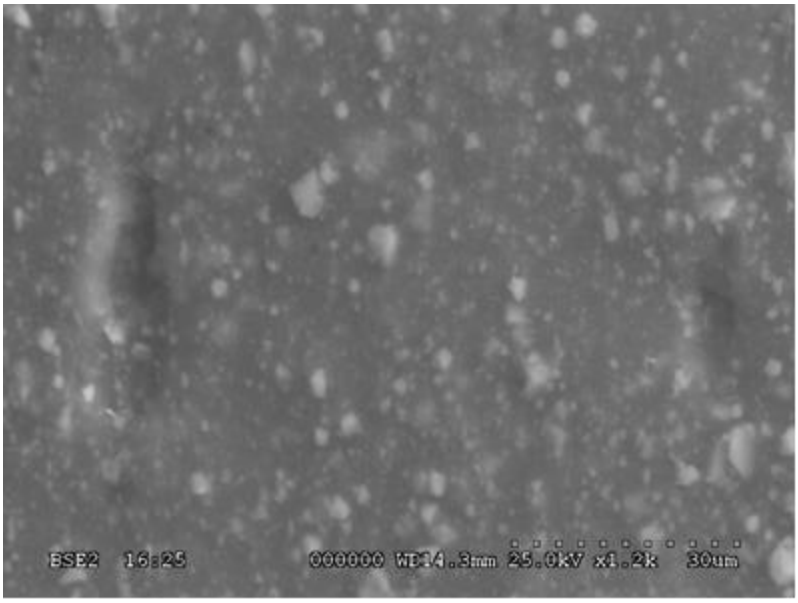

Figure 12-21 SEM micrograph of air-exposed sample after third cycle

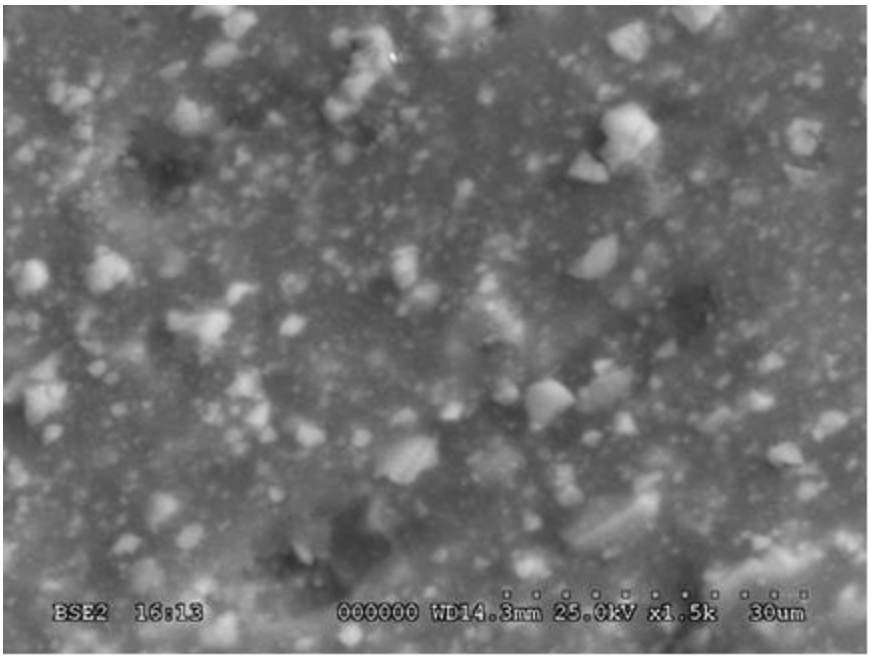

Figure 12-22 SEM micrograph of oil-immersed sample after third cycle

An inspection of the SEM micrographs shown in Figures 21 and 22 reveals small inorganic filler molecules, plasticizer and microvoids on the PVC surface. When we compare micrographs of the mineral-oil immersed sample surface morphology with that of the air-exposed, increased microvoids and aggregation of PVC molecules is readily visible, which are potentially causing the coating to toughen.

Nevertheless, the coating becoming stiffer is actually a positive outcome as it minimizes transmission losses due to microbending. However, this needs corroboration by optical loss testing. Similar tests need to be repeated at higher aging temperatures, so as to determine an oil-PVC interaction dependent phenomenological exponential Arrhenius model, based on chemical reaction kinetics of the interaction. Since this testing was performed at a single aging temperature of 45°C, there are not nearly enough data points to develop a first order Arrhenius-type model to the temperature-dependence of cable performance.

Nonetheless, owing to the plateauing of elastic modulus values after longer aging durations as observed in this experiment, it is reasonable to assume that with the choice of a cable with an oil-resistant jacket material, there is considerable scope for immersion-cooling optically interconnected servers without significant changes in mechanical reliability and operability of the system.

References

1. Jimil M. Shah, Richard Eiland, Ashwin Siddarth and Dereje Agonafer “Effects Of Mineral Oil Immersion Cooling on IT Equipment Reliability and Reliability Enhancements to Data Center Operations” 10.1109/ITHERM.2016.7517566.
2. https://submer.com/what-is-immersion-cooling/
3. http://www.allied-control.com/immersion-cooling
4. J. Shah et al., "Critical non-thermal consideration for oil cooled data-center" in IMAPS ATW 2015, Los Gatos, Ca, 2015.
5. ASTM D 3455-02 “Standard Test Method for Compatibility of Construction Material with Electrical Insulation Oil of Petroleum Origin”
6. https://www.buehler.com/isoMet-1000-precision-cutter.php
7. http://www.resistorguide.com/thin-and-thick-film/
8. https://www.electronicsnotes.com/articles/electronic_components/capacitors/electrolytic.php
9. http://www.weonline.com/web/en/passive_components_custom_magnetics/blog_pbcm/blog_detail_electronics_in_action_105536.php
10. Nilesh R. Bhavsar, H. P. Shinde, Mahesh Bhat. “Determination of Mechanical properties of PCB.” IJMER ISSN (Print): 2321-5747, Volume-2, Issue-4,2014.
11. Unique Rahangdale, R Srinivas, S Krishnamurthy, Pavan Rajmane, Abel Misrak, Dereje Agonafer “Effect of PCB thickness on solder joint reliability of

Quad Flat no-lead assembly under Power Cycling and Thermal Cycling” SEMI-THERM, 33rd Symposium 2017.

12. Glaesemann, G. S., S. T. Gulati, and J. D. Helfinstine. "Effect of strain and surface composition on Young's modulus of optical fibers." Optical Fiber Communication Conference. Optical Society of America, 1988.
13. Dwivedi, Anurag, G. Scott Glaesemann, and C. K. Eoll. "Optical Fiber Strength, Fatigue and Handleability After Aging in a Cable." IWCS Proc. 1994.
14. Crawford, Dawn M., Robert G. Bass, and Thomas W. Haas. "Strain effects on thermal transitions and mechanical properties of thermoplastic polyurethane elastomers." Thermochimica Acta 323.1-2 (1998): 53-63.

Chapter 13

Conclusions

With the continued increase in demand for information technology (IT) applications and services, there are growing energy requirements to sustain their operation. The studies reported here offer insight into new, energy efficient methods for cooling data centers starting at the server, rack; and facility level. The principle results and conclusions of these findings are outlined below.

13.1 Characterizing Contamination to Expand ASHRAE Envelope in Airside Economization

The rapid expansion of the IT equipment business and increasing pressure to reduce energy consumption, data centers with specific applications, and specific geographies should move their operating conditions up to ASHRAE A1 allowable environment

considering the danger of short-circuit failure mode due to particulate matter. The weather data bin analysis provides the opportunity of utilizing free air cooling for the maximum hours during a year. The correlation of historical environmental trend data with its implications supports the usage of air-side economizers for a certain period with proper measures of contamination. From an industry perspective, it should be noted that in the four years of operation in the hot and humid Dallas climate using only evaporative cooling or fresh air cooling, we have not seen a single server failure in our research pod. That performance should highlight an opportunity for significant energy savings for data center operators in a much broader geographic area than currently envisioned with evaporative cooling. It is required to determine the chemical composition and temporal and spatial variation of the gaseous contamination in real-world data centers with ANSI/ISA standard 71.04-2013 severity level G2. Gas analyzers should be used to predict the gaseous composition of the air and simulating the same conditions in the laboratory to understand the parameters affecting the corrosion rate in depth. The test can be conducted by using copper and silver corrosion coupons and state-of-the-art

test PCBs in experimental data centers with ISA severity level G2 or G3. The accelerated testing on real computers considering the self-heating effect should be carried out to understand the reliability degradation of actual equipment due to corrosion. It is essential to manufacture hardware robust against PCB creep corrosion/short circuits caused by settled particulate matter in humid environments and surface mount resistor open circuits by gaseous contamination. The corrosion testing should be done in real-world field conditions with larger data as laboratory testing facility do not represent the environment in data centers. It is necessary to develop a corrosion reliability model to determine an end of life of servers.

13.2 Thermal and Reliability in Immersion Cooling of Data Centers

Immersion cooling system is capable enough to keep the system temperature below permissible limit of temperature. For an effective cooling of server having the form factor of 1U and 1.5U, it is advisable to maintain the oil flow rate greater than or equal to 1 lpm depending upon power density of server. Rack density can be increased by replacing 2U servers with 1U servers. Instead of white mineral oil, low viscosity other engineered fluids like EC 100 can be used to achieve reduced pumping power and circulation cost. The volume of the optimized pin fin heat sink is very less compared to the existing heat sink and there is very less variation in temperatures. So, the optimized heatsink can reduce the material cost significantly.

The issues associated with the mechanical reliability and operational service impact of adopting single-phase immersion cooing strategy must be addressed before the technology will see widespread adoption. The visual studies presented here indicate that certain compromises or adjustments in data center operation, such as inventory tracking and servicing procedures, will need to be made for this technology. From a structural point of view, no damage or alterations to components were observed from both the macro and microscopic views. However, changes in mechanical properties due to exposure of dielectric fluids may alter the length of the useful life of components in fluids. Studies with an increased sample size and over

multiple time durations help strengthen the findings presented above. Understanding the rate of change of material properties over extended service times may help build industry confidence in this technology and promote future adoption.

Appendix A

Arduino Code for the Current Sensor

```
#include <Wire.h>
#include <Adafruit_INA219.h>
Adafruit_INA219 ina219;

void setup(void)
{
  Serial.begin(115200);
  while (!Serial) {
      // will pause Zero, Leonardo, etc until serial console
opens
      delay(1);
  }

  uint32_t currentFrequency;

  Serial.println("Hello!");

  // Initialize the INA219.
  // By default the initialization will use the largest range
(32V, 2A).  However
  // you can call a setCalibration function to change this range
(see comments).
       ina219.begin();
  // To use a slightly lower 32V, 1A range (higher precision on
amps):
```

```
        //ina219.setCalibration_32V_1A();
        // Or to use a lower 16V, 400mA range (higher precision on
volts and amps):
        ina219.setCalibration_16V_400mA();

        Serial.println("Measuring voltage and current with INA219 and
to determine the DRH of Pure Salts");
      }
      void loop(void)
      {
        float shuntvoltage = 0;
        float busvoltage = 0;
        float current_mA = 0;
        float loadvoltage = 0;
        float power_mW = 0;

        shuntvoltage = ina219.getShuntVoltage_mV();
        busvoltage = ina219.getBusVoltage_V();
        current_mA = ina219.getCurrent_mA()+0.1;
        power_mW = ina219.getPower_mW();
        loadvoltage = busvoltage + (shuntvoltage / 1000);

      //Serial.print("Bus Voltage:   "); Serial.print(busvoltage);
Serial.println(" V");
```

```
       //Serial.print("Shunt Voltage: "); Serial.print(shuntvoltage);
Serial.println(" mV");
       Serial.print("Load Voltage:  "); Serial.print(loadvoltage);
Serial.println(" V");
       Serial.print("Current:       "); Serial.print(current_mA);
Serial.println(" mA");
        // Serial.print("Power:         "); Serial.print(power_mW);
Serial.println(" mW");
        Serial.println("");
        Delay(1500);
}
```

Biographical Information

Jimil recently received his PhD in Mechanical Engineering at The University of Texas at Arlington under the guidance of Professor Dereje Agonafer. He has also received his MS from the University of Texas at Arlington in May 2016. He received his Bachelors' degree with honors in Mechanical Engineering from Gujarat Technological University, India in June 2012. Jimil's research at UTA is in the area of Data center cooling. He also has interest in the general area of electronic Packaging and Internet of Things. Currently, he is working on "An In-depth understanding of Single-Phase Immersion Cooling strategies for data centers" and "Impact of particulate and gaseous contamination on IT equipment where air side economizers are implemented." He has also interest in environmental effects on the reliability of wearables.

Jimil is a student member of ASHRAE and ASME. He recently received "2018 ASME Electronic and Photonic Packaging Division (EPPD) Student Member of the Year Award". He is the recipient of College of Engineering Summer Dean's Dissertation Fellowship, Summer 2018 and I-Engage Mentoring Program Scholarship, Spring 2018 at UTA. He has received the "Best Student Abstract Award" at IMAPS 2015, Los Gatos, CA. He has also been the recipient of the 2015-2016 Electronic, MEMS and Nanoelectronics Systems Packaging Center Scholarship Award at UTA. He has publications on Contamination and Corrosion of IT Equipment and Reliability of Oil Immersion Cooling including a paper on contamination that has appeared on a special issue of ASME Journal of Electronic Packaging. He has three applied Patents while in India and has received "Innovative Project Award" during his Bachelors' by GTU Innovation Council. He has an industrial experience in production at FIAT India Limited, Pune and as a lecturer at Parul University, Vadodara in India.

Coming from a business background, Jimil was always aspired to be an entrepreneur in the field of mechanical engineering. He would like to use this knowledge in mechanical engineering for the good of mankind and help all the public equally.